Institut de Géologie
Université de Neuchâtel

NEOGENE TECTONICS AND THERMAL MATURITY OF SEDIMENTS OF THE EASTERNMOST SOUTHERN ALPS (FRIULI AREA, ITALY)

A thesis in Geosciences presented to the faculty of Sciences of Neuchâtel University in candidacy for the degree of Doctor of Sciences

by

CHRISTOPHE NUSSBAUM

-August 2000-

Board of examiners:

- Prof. Martin Burkhard — Supervisor (Neuchâtel)
- Dr. Greg Schönborn — Co-Supervisor (San Ramon, California, USA)
- Dr. David Ferrill — Examiner (San Antonio, Texas, USA)
- Prof. Karl Föllmi — Examiner (Neuchâtel)

ABSTRACT

The easternmost part of the Southern Alps represent a key area in the Alpine belt where the Paleogene Dinarides intersect with the Neogene Southern Alps. The study area was deformed first by SW-vergent thrusts related to the most external Dinarides during the Paleocene and Eocene and then by S to SSE-vergent "Alpine" thrusting since the Tortonian (late Miocene). The ongoing activity of this deformation phase is documented by uplifted Quaternary terraces and intense seismic activity.

As in the central Southern Alps, transverse structures play a major role in the fold-and-thrust belt of the easternmost part of the Southern Alps. Transverse zones localized along preexisting structures, which are related to Middle Triassic and Early Jurassic extensional faults. The north-south trending aligned Tagliamento and Incaroio transverse zones split the Friuli Alps into two segments of different structures. Consequently, the architecture of the Friuli Alps may be roughly divided into three blocks: a central block formed by the transverse zones, which separates western and eastern blocks. To unravel geometry and kinematics series of large-scale cross-sections from the E-Insubric line to the Friuli plain were constructed. Thanks to kinematic balancing based on surface data, three Alpine thrust systems involving basement slabs could be identified. Each system forms a thrust sheet with its particular basement unit and its sedimentary cover. Retrodeformed state of cross-sections shows that the minimum macroscale shortening since the beginning of Late Miocene amounts to about 50 km in the Friuli Alps. The kinematic evolution is in sequence from north to south, except in the eastern block where an out-of-sequence thrust occurred. Retrodeformation of Alpine thrusting is an essential tool to understand geometry and kinematics of the previous Dinaric and inherited structures.

The Friuli region experienced two destructive earthquakes and numerous aftershocks from May to October 1976. Hypocenters of these recent earthquakes have been projected onto different large-scale cross-sections. A good correlation is found between the hypocenters distribution of the strongest earthquakes of the 1976-sequence and the

geometry in the cross-sections. Spatial distribution and focal mechanisms of aftershock-hypocenters indicate activity along the frontal thrust system. This is in agreement with the southward sequence of thrusting.

At various places Dinaric/Alpine superposed structures have been preserved. The Dinaric WSW to SW vergent thrusts and faults cannot be connected to an overall network. In fact, many of these faults have loose ends since they were cut and dismembered by the subsequently active south-vergent Alpine thrusts. Dinaric structures consists mainly of a décollement in the Upper Permian evaporites and a number of splays with minor shortening that ramp through the Mesozoic sequence. This tectonic style with long detachments and the absence of metamorphism along some 250 km of exposure along the Dinaric strike point to a low critical taper for the frontal part of the Dinaric orogenic wedge.

Thermal maturity of rocks from various stratigraphic horizons and tectonic units has been determined. No data indicate that Alpine thrust sheet emplacement had perturbed the thermal maturity of sediments. One of the main factors controlling the paleotemperature regime, and hence the thermal maturity of sediments, was burial via sedimentary loading. No data supports the existence of an inherited Dinaric metamorphism.

Based on the total shortening of the belt and subsidence curves, geodynamics of the South Alpine orogenic wedge have been roughly estimated. Calculations suggest an average rate of thrust tip propagation of about 5 mm/year and a thrust uplift rate of about 1.25 mm/year. The ratio vertical versus horizontal motions indicate that the thrust advance rate is about 4 times greater than the thrust uplift rate.

ACKNOWLEDGMENTS

I would like to express my gratitude to all those who have helped and supported me. First I would like to thank my principal advisor Gregor Schönborn who introduced me to the fascinating world of cross-section balancing. I am gratful to him for his help, his encouragements and his pertinent comments throughout the course of my study. Many of his ideas and suggestions are incorpotated in the work.

I am indebted to Professor Martin Burkhard, who offered me the opportunity to do this thesis research and who made stimulating comments and suggestions on my work.

A special thank goes to Dr. David Ferrill from the Southwest Research Institute of San Antonio (Texas). I appreciated very much the exchange of ideas, his detailed corrections, and his pertinent comments and suggestions on my manuscript.

I acknowledge Prof. Karl Föllmi for accepting the reading and the correction of my manuscript, and especially for the improvment of the English.

I thank Thierry Adatte who has performed the X-ray diffraction analyses (XRD). He introduced me to the complex world of clay minerals and gave me pertinent information about the illite crystallinity. Sébastien Ryser is thanked for his friendship and for performing the Rock-Eval analyses.

Many colleagues and friends from the Geological Institute of Neuchâtel helped me in providing an open and supporting atmosphere. Among them are noticed especially Marie-Pierre Bolle, Nathalie Challandes, Pierre Dick and Federica Tamburini for their assistance with the computer and continue encouragements.

Finally, I greatly appreciated the ongoing support and encouragements of my wife Marie-Claire and the smile of my son Caryl. I also thank very much my family.

TABLE OF CONTENTS

1. INTRODUCTION

1.1 GENERAL SETTING OF THE STUDY

1.1.1 Plate tectonic setting

The eastern Southern Alps in northeastern Italy form an active fold-and-thrust belt that developed at the northeastern edge of the Apulian (or Adriatic) microplate (Fig. 1). The eastern Southern Alps resulted from the northward motion of the Adriatic indenter. The present-day intricate architecture of this belt is the combined result of (1) Late Carboniferous to Early Permian transtensional faulting, (2) Middle Triassic and Early Jurassic rifting, Jurassic-Cretaceous basin formation, and carbonate platform formation, (3) Jurassic to present plate convergence between Apulia and Europe with major changes in convergence direction over time, and (4) the shape of the indenting Apulian microplate.

Due to the lack of Alpine metamorphism, the Southern Alps have preserved an almost intact cross-section of a Jurassic passive continental margin, where the stratigraphy shows the history of progressive foundering and drowning of the margin as a small oceanic basin was being created in the west (chapter 2). Since Jurassic time, this margin remained a stable block, a quiet tectonic island in the Alpine realm. Nevertheless, this margin suffered southwest-vergent Dinaric deformation since the Paleocene-Eocene (chapter 3), and south-vergent Alpine thrusting from the Tortonian to present (chapters 4 and 5). The ongoing activity of this later deformation phase is testified by uplifted Quaternary terraces and intense seismic activity in the Friuli region (chapter 6). This later deformation phase has largely contributed to the build up of the present-day architecture of the eastern Southern Alps (Fig. 2). The tectonic setting is further complicated by a concomitant transtensional event during Alpine thrusting. This transtensional deformation is limited to a narrow wedge near the E-Insubric line (chapter 7).

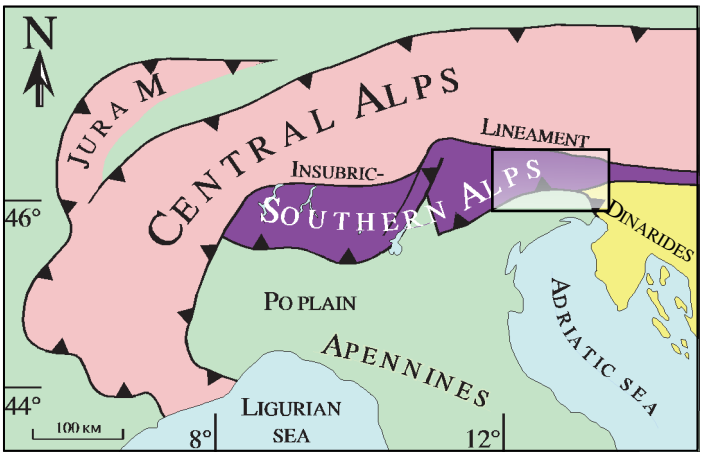

Fig. 1. Location of the study area with respect to the Alps. Note the superposition of Alpine and Dinaric structures in the easternmost Southern Alps. Rectangle corresponds to Fig. 2.

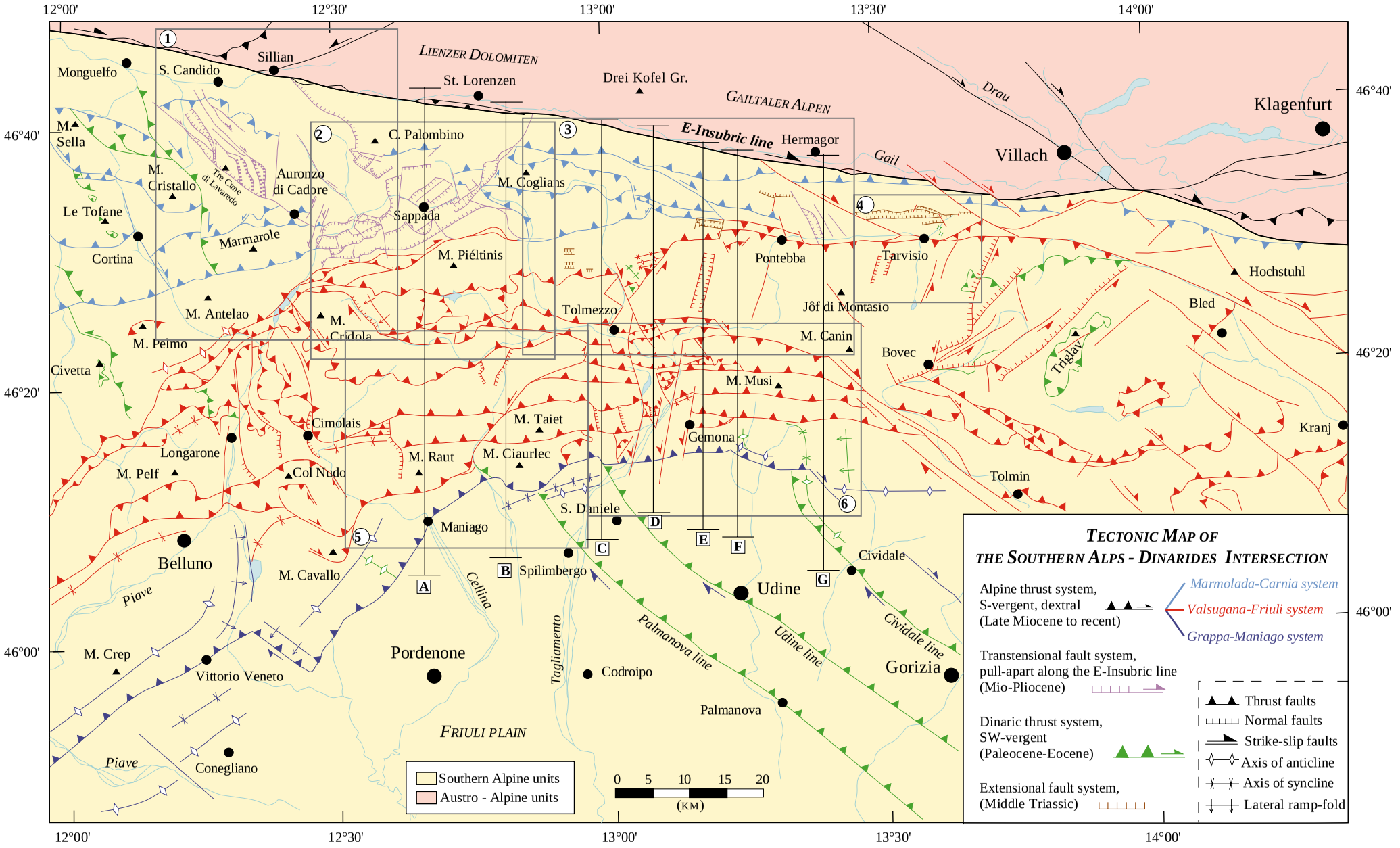

Fig. 2. Simplified tectonic map of the easternmost Southern Alps. Based on new mapping and previous mapping of Castellarin (1981), Bigi *et al.* (1992), and Schönborn (1999).

1.1.2 Geographical localization

The investigated area belongs to the northeastern corner of Italy, located between Austria in the north and Slovenia in the east. This area is part of the eastern Southern Alps which are locally divided in several mountain chains: in the west the Dolomites, in the north the Carnic Alps, in the east the Julian Alps, and in the central part the Friuli Alps (Fig. 3). The Friuli Alps are often termed *Prealps of Friuli, Friuli region* or *Friuli area* in the literature. The Friuli Alps are also called Friulian piedmont arc by Carulli *et al.* (1990). The Friuli Alps includes the Carnia and the Friuli regions, and are bounded in the south by the Friuli plain. The Carnic Alps are located on the border between Austria and Italy, whereas the Julian Alps share the border between Italy and Slovenia. In this study, I focused on the Friuli Alps where I investigated six areas (dashed rectangles in Fig. 3).

1.2 PREVIOUS WORK

A number of previous studies of the eastern Southern Alps have led to an abundance of geological data. To present all important studies that lead to the actual stand of knowledge would be beyond the scope of this work. Many previous works in the easternmost part of the Southern Alps dealt either with relatively restricted areas or with the region-wide tectonic features. Works on Alpine geology were focused on various areas located in the Friuli Alps:

- southern part (*e.g.*, Martinis, 1966, 1975, 1979; Cavallin, 1976; Amadesi, 1968; Amadesi and Lenarduzzi, 1973; Pisa, 1972; Bosellini and Sarti, 1978; Sarti, 1979, 1982, Poli, 1996).
- northern part (*e.g.*, Ferasin, 1958; Ferasin *et al.*, 1969; Assereto, 1963; Ceretti, 1965; Frascari, 1968; Carulli *et al.*, 1982a,b, 1987; Cavallin and Martinis, 1982; Venturini and Delzotto, 1992).

Various works dealt with the regional-scale geology (*e.g.*, Selli, 1963; Zanferrari, 1974, Zanferrari *et al.*, 1982; Frascari *et al.*, 1979, 1980; Carulli *et al,* 1980., Carulli and Ponton, 1992; Castellarin, 1979; Castellarin *et al.*, 1980, 1992; Venturini, 1990c; Venturini and Fontana, 1992). Roeder and Lindsey (1992) have constructed a series of large-scale

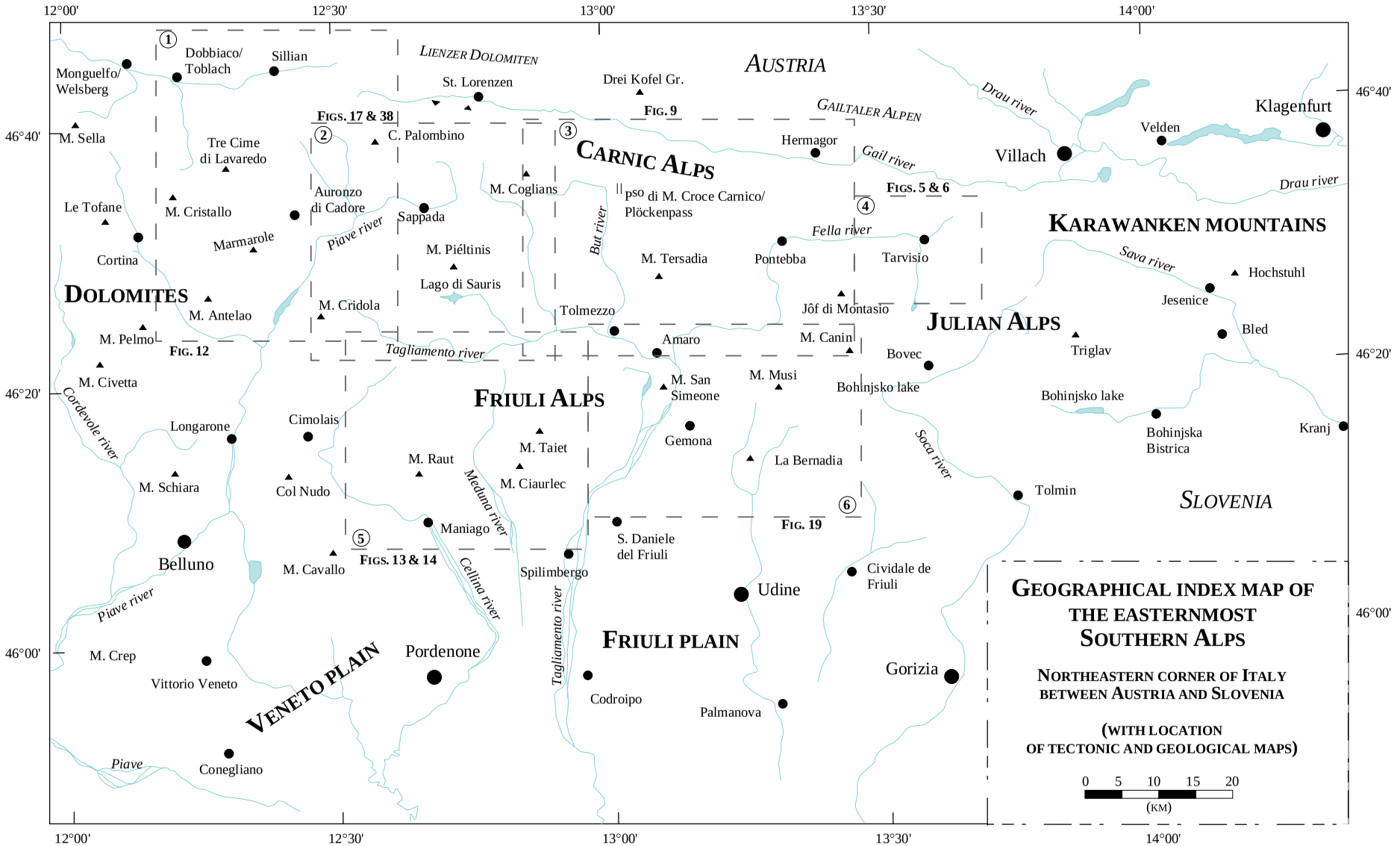

Fig. 3. Geographical index map of the easternmost Southern Alps. The Friuli Alps are commonly termed Friuli Pre-Alps, Friuli area or Friuli region in the literature.

cross-sections in a wide area extending from the Dolomites to the Julian Alps and Dinarides in Slovenia. Their construction style introduces thrusts not visible at the surface and very long décollements, which lead to complex structure and increased shortening. However, the foreland portions of their cross-sections are constrained by deep well data and are therefore more reliable than the more internal parts of the cross-sections.

In the adjoining Dolomites, Doglioni and Castellarin (1985), Doglioni (1987, 1992a) and more recently Schönborn (1999) have contributed to a better understanding of the large-scale structure. Detailed structural analysis of a large sector of the northeastern Dolomites has been carried out by Caputo (1996, 1997).

Much additional work has been done by Italian, Austrian and German geologists, but it concerned mostly the detailed stratigraphy and paleotectonics of the eastern Southern Alps (many authors, citations in chapter 2), and the Alpine and Variscan tectonometamorphic evolution of the Carnic Alps (Venturini 1990b, Läufer, 1996; Hubich and Läufer, 1997; Hubisch *et al.*, 1999; see also citations in chapter 3.1). The thermal history of the Carnic Alps (Rantitsch, 1997) and the thermal histories of Teriary basins situated around and within the Eastern Alps are examined using coalification data (Sachsenhofer, 1992). Various paleomagnetic studies were carried out in the Dolomites on Lower Triassic, Jurassic and Cretaceous samples (Channel *et al.*, 1992; Channel and Doglioni, 1994), and in the Carnic Alps on Upper Carboniferous samples (Manzoni *et al.*, 1989).

1.3 THEMES AND OBJECTIVES OF THIS RESEARCH

This study is part of a project of the Swiss National Science Foundation aimed at a clarification of the deep structure and kinematics of the eastern Southern Alps. Following the destructive earthquakes that hit the Friuli region in 1976, many studies on recent seismotectonics have been carried out. Many publications have dealt with the location and distribution of hypocenters, fault plane solutions (*e.g.*, Console, 1976, Ebblin, 1976;

Müller, 1977; Finetti *et al*., 1979; Siro and Slejko, 1982; Carulli *et al*., 1982c; Barabano *et al*., 1985; Slejko *et al*., 1987), seismic hazard assessment (Slejko and Kijko, 1991) and with others geophysical disciplines as gravimetry, magnetometry, DSS profiles (Cati *et al*., 1987a; Cavallin and Pirini Radrizzani, 1987; Finetti *et al*., 1987) and seismic tomography (Amato *et al*., 1990). Nevertheless, poor constraint on the deep structure has inhibited understanding earthquake sources. Additionally, seismic reflection profiles were carried out only in the Friuli-Veneto plain (Amato *et al*., 1977; Pieri and Groppi, 1981; Cassano *et al*., 1986; Barozzi and Colombi, 1992), and deep well data are scanty in the literature (Cati *et al*., 1987b; Sartorio and Rozza, 1991; Barozzi and Colombi, 1992). Construction of balanced cross-sections should contribute to a better understanding of the Friuli region. Kinematic balancing is a promising tool to constrain the construction of a cross-section. The application of balancing concepts provides a new image of the deep structure and the kinematic evolution of the eastern Southern Alps. Extensive field mapping at 1:10.000 and 1:25.000 of the key zones was carried out to provide detailed constraints for cross-section construction and tectonic interpretation.

The easternmost Southern Alps represent a key area in the Alpine belt where the Paleogene Dinarides intersect with the Neogene Southern Alps. Based on the superposed structures, this study aims at a clarification of geometry and kinematics of the Dinaric deformation phase. Retrodeformation of Alpine thrusting is an essential tool to understand geometry and kinematics of the previous Dinaric and inherited structures.

Finally, this study tries to the determination of the influence of different tectonic styles (Dinaric and Alpine) on thermal maturity, which is assumed to be mainly dependent on temperature and time. This requires analyzing samples from various stratigraphic horizons and tectonic units. Results from section balancing and thermal maturity of sediments allow the calculation of parameters like thrust uplift rate, thrust advance rate and subsidence rate. Based on these values, geodynamics of the eastern South Alpine orogenic thrust wedge are evaluated.

1.4 METHODOLOGY

The large-scale cross-sections of this study (chapter 5) are constructed from the concept of section balancing. The tectonic style of the easternmost Southern Alps is favorable for the construction of balanced cross-sections: there are prominent detachment horizons (Bellerophon, Raibl formations), separated by thick rigid layers with minimal internal shortening (Serla and Schlern formations and Dolomia Principale). Moreover bed thickness in the mainly chevron-type folds is largely preserved.

The techniques of section construction have taken a major step forward over the past three decades. The search for hydrocarbons in the frontal fold-and thrust-belt of the eastern Canadian Rocky Mountains has led to develop a technique which has come to be known as balanced section construction (Bally *et al*., 1966; Dahlstrom, 1969, 1970; Boyer and Elliott, 1982). However, since the beginning of the 20th century some geologists constructed approximatively balanced cross-sections in frontal fold-and-thrust belts. Chamberlin (1919) first introduced the concept of area balancing, and Buxtorf (1916) formulated the principles of line length and area balancing.

The use of the line length balancing concept in its modern form was first restricted to areas with seismic coverage. The formulations of the geometry of fault-related folds by Suppe (1983, 1985), Suppe and Medwedeff (1990) have allowed the application of the balancing concept into areas without seismic data. According to these authors, unexposed faults may be predicted based only on the geometry of the related folds in areas with bedding plane slip and constant thickness of strata. However, there are important restrictions with the application of Suppe' s principles since thinning of beds often is observed in belts deformed under low-tempreature conditions (*e.g*., Ramsay, 1992).

The method of balancing cross-sections is based on the principle of material conservation during deformation. At low P and T conditions, the volume stays largely constant during brittle deformation, except for fluid expulsion (3D). If a cross-section lies exactly parallel to the transport direction ("plane strain"), the principle of mass

conservation may be reduced to that of surface or area preservation during deformation (Goguel, 1962; Laubscher, 1965, 1988). When bedding plane slip (flexural slip) is the dominant type of small-scale deformation, and the thickness of the beds remains constant (no thickening and thinning), a cross-section in transport direction must be line length balanced (Dahlstrom, 1969). According to Elliott (1983) and Woodward *et al*. (1989), a balanced cross-section must be both retrodeformable and admissible. Dave Elliott (1983) said in his paper: "… the structures drawn on the section are those that can be seen in the area in cliffs, road cuts, mountain sides, etc. The use of these structures leads to an admissible cross-section. Additionally a restored as well as a deformed-state cross-section should be constructed at the same time. If a section can be restored to an unstrained state it is a viable cross-section. By definition a balanced section is both viable and admissible..."

Bedding plane slip is systematically observed in chevron type folds. In this study, the method of line length balancing was systematically used for constructing the large-scale cross-sections. The line length balance consists in measuring the lengths of different beds and compares them to each other.

Geiser (1988) proposed to check the "kinematic admissibility", *i.e*. whether a cross-section really can be deformed with the faults indicated in the retrodeformed version. Geiser (1988) showed that many published cross-sections are well-balanced, *i.e*. they are restorable and admissible, but are kinematically not viable. For an overview over balanced cross-sections, the reader is referred to Marshak and Woodward (1985) and Woodward *et al*. (1989).

A balanced cross-section is made up of two parts:

a. Mechanical part (dynamics):

- there must be a mechanically plausible way to get from stage A to B
- angles of thrusts and faults must correspond to Mohr-Coulomb criteria
- the strain of the deformed stage sections must correspond to the observations in the field

b. Geometrical part (kinematics):

- It must be possible to reconstruct a section with intermediate steps of the deformation -> forward modeling
- Each intermediate step must itself be area or line length balanced
- Undeformed geometries of thrusts must be reasonable
- Shortening along different thrusts and splays must be mutually compatible

When deep seismic reflection data are lacking, as it is the case in the easternmost Southern Alps, the following data are absolutely needed to construct balanced cross-sections:

- Tectonic framework (-> cartographic traces of faults, geometry and kinematics of faults and of deformed strata)
- Tectonostratigraphy (-> stratigraphic thickness, décollement levels)
- Paleogeographic and paleotectonic evolution (-> lateral changes of thickness)
- Common sense and sometimes a little bit of imagination…

Finally, it is useful to clarify that construction of balanced sections is made easier when major structures are first taken into consideration. Small-scale criteria (slickensides, stylolites, shear bands, shape fabrics…) should be used statistically to support kinematics of the large-scale structure. As conclusion, the most important benefit of balancing cross-sections in thrust-belts as poorly understood as the Friulian Alps is that they force the geologist to think about the consequences of locally observed structures on the large-scale setting.

1.5 TERMINOLOGY

Some of the more widely used terms in this study are defined here to provide the basis for the following discussion. The brief terminology presented below is mainly inspired from the glossary of thrust tectonics terms (McClay, 1992).

Backthrust: A thrust fault which has an opposite vergence to that of the main thrust system or thrust belt.

Blind thrust: A thrust fault that is not emergent –i.e. it remains buried such that the displacement on the thrust below is compensated by folding or cleavage development at a structurally higher level.

Fault-bend fold: A fold generated by movement of a thrust sheet over a ramp. For more details, the reader is referred to Suppe (1983).

Fault propagation fold: A fold generated by propagation of a thrust tip up a ramp into undeformed strata. For more details, the reader is referred to Suppe and Medwedeff (1990).

Flat: That part of a thrust fault which is bedding parallel.

Imbricate fan: A system of linked emergent thrusts that diverge upwards from a sole thrust.

In sequence thrusing: A thrust sequence that has formed progressively and in order in one direction.

Lateral-ramp: A ramp in the thrust surface that is parallel to the direction of transport of the thrust sheet.

Out-of-sequence thrusting: The opposite to "in sequence thrusting". Thrust faulting which develops in a sequence other than in sequence. Out-of-sequence thrusts commonly cut through and displace pre-existing thrusts. Morley (1988) discuss out-of-sequence thrusting.

Phases: A phase is a time interval of tectonic activity. Three orogenic phases can be distinguished in the easternmost part of the Southern Alps: a Variscan phase of middle Carboniferous age (Visean to Westphalian), a Dinaric phase of Paleogene age (Paleocene to Eocene) and a Neogene Alpine phase (late Miocene to present).

Pin lines: This term is used for line length balancing. During deformation no material transport takes place across this line. Pin lines must have the same geometry in the deformed state as in the undeformed state. If not, the bed lengths do not remain constant.

Ramp: That part of a thrust fault that cuts across bedding. Ramps may be divided into hangingwall ramps and footwall ramps. Ramps commonly have angles between 10° and 30°.

Sole thrust: The lowermost thrust common to a thrust system (may also be termed *floor thrust*).

Splay: Second-order thrust fault (*i.e.* smaller in size and displacement) that emerges from a main thrust fault.

Thrust sheets: A thrust sheet is bounded by major thrust and made up of several units.

Thrust systems: A thrust system consists of a number of corresponding and branching thrusts that are geometrically, kinematically and mechanically linked. The terminology for thrust systems has been discussed by Dahlstrom (1970), Boyer and Elliott (1982), Woodward *et al.* (1989) and others. Based on surface data, the present study has distinguished three thrust systems in the eastern Southern Alps. The three thrust systems developed in sequence from north to south, except in the eastern part of the Friuli Alps where the second thrust system is itself cut by an out-of-sequence thrust (chapter 5).

Thrust vergence: The direction towards which the hangingwall of the thrust fault has moved relatively to the footwall.

Tip line: The edge of a thrust fault where diplacement dies to zero.

Triangle zone: A combination of two thrusts with the same basal detachment and with opposing vergence such as that they form a triangular zone.

Units: A unit is a stratigraphic interval bounded at the base and at the top by décollement horizons. The eastern end of the Southern Alps is made up of three main units; the pre-Middle Permian basement unit, the Lower-Middle Triassic unit and the Upper Triassic-Cretaceous unit (chapter 4.3). Minor décollement levels may subdivide locally these units.

2. PALEOTECTONIC AND PALEOGEOGRAPHIC EVOLUTION

Before constructing cross-sections, the first step consists in drawing up the stratigraphic thickening wedge (chapter 2.5). This is important due to the abundance of lateral changes of facies and thickness variations. Consequentely, a detailed knowledge of the paleogeographic and paleotectonic evolution is required. The paleogeographic evolution presented below is mainly inspired from a set of published data (Cousin, 1981; Bosellini *et al*., 1981; Winterer and Bosselini, 1981; Venturini, 1990a, 1990b; Krainer, 1992, 1993; Schönlaub and Heinisch, 1992; Massari, 1990; Massari *et al*., 1993). The published data concerning the subsurface features of the Friuli-Veneto plain and the Northern Adriatic sea are limited to some wells and seismic sections published by AGIP (AGIP, 1977; Amato *et al*., 1977; Pieri and Groppi, 1981; Cati *et al*., 1987b).

This chapter is mainly a compilation and summary from the literature rounded off by some own observations. The description of the paleotectonic and paleogeographic evolution starts with the late to post-Variscan sequence (Late Carboniferous to Late Permian) following the last Variscan deformations. A synthetic stratigraphic column is presented in figure 4 as reference.

2.1 LATE CARBONIFEROUS-PERMIAN WRENCH-FAULTING TECTONICS

In the eastern Southern Alps, the Variscan basement outcrops in the Dolomites (Trentino-Alto Adige), the Carnic Alps and the southern Karawanken Mountains (Fig. 3). The studied area covers only the Carnic Alps.

In the Southern Alps, Late Carboniferous-Permian molasse sediments lie on the folded Variscan basement with a classical unconformity. This major unconformity separates the Variscan synorogenic sedimentary sequences (**Dimon and Hochwipfel** formations) of Visean to early Westphalian age from the late to post-Variscan molasse sediments. The Variscan basement was folded with a south-vergence, and was in the

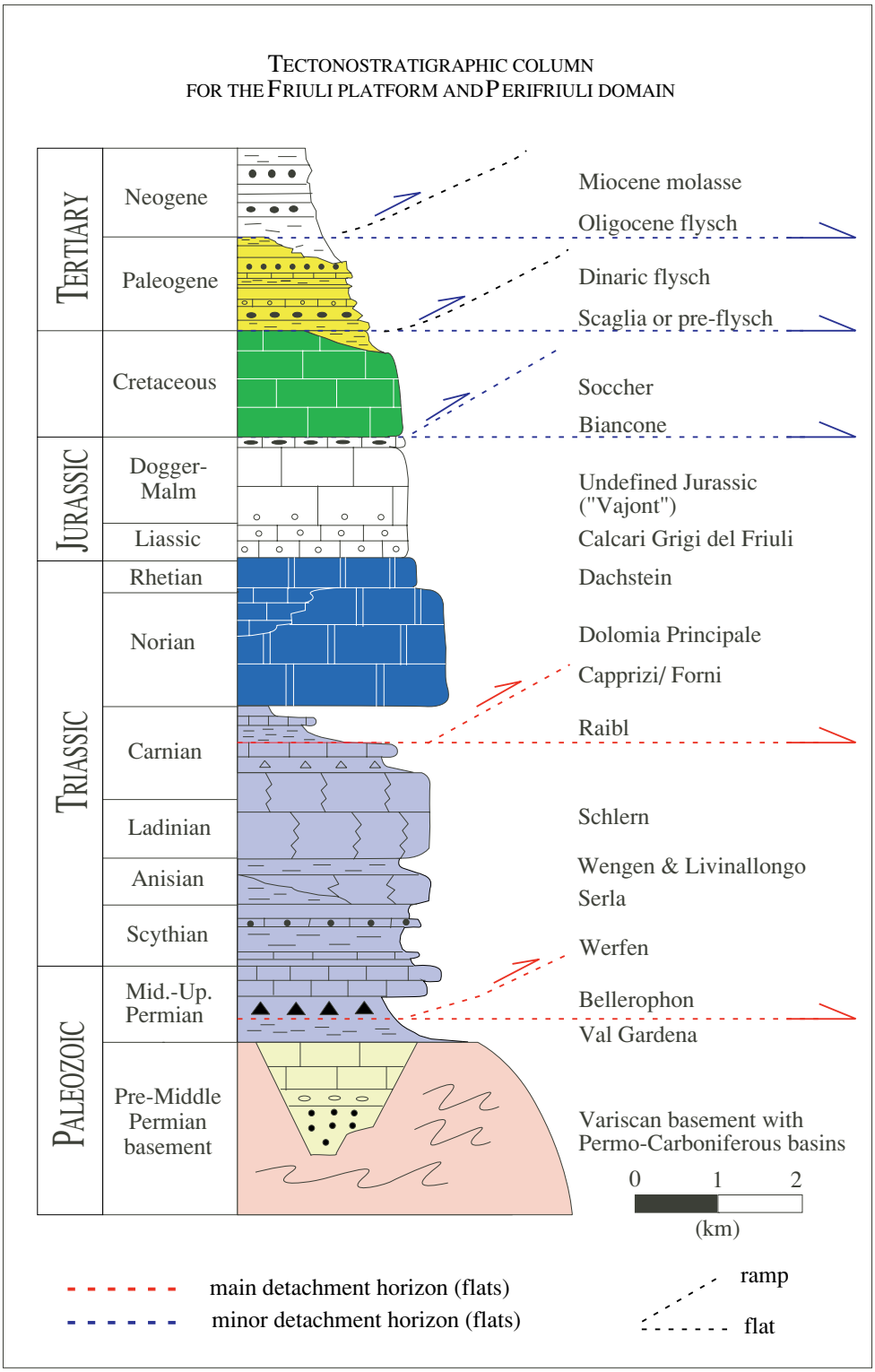

Fig. 4. Tectonostratigraphic column. The main detachment horizons in Bellerophon and Raibl define three major units: a pre-Middle Permian basement, a Lower-Middle Triassic unit and an Upper Triassic-Neogene unit. Minor décollements may locally divide the uppermost unit.

western part of the Carnic Alps, slightly metamorphosed during Westphalian times. After the Variscan orogenic phase, block- and wrench-faulting resulted in the formation of discrete basins mainly oriented WNW-ESE (for example the "Pramollo basin", see Venturini 1982, 1990a,b). These pull-apart basins were filled with the late Variscan molasse sediments constituted of the Late Carboniferous **Bombaso** formation, **Auernig** group and Early Permian **Rattendorf** group (see in Krainer, 1992, 1993). According to Arthaud and Matte (1977) and Matte (1986), the intramontane basins were formed as a result of transtensional and transpressional tectonic processes along megashear zones, due to the eastward drift of the Eurasian plate and the westward drift of the African plate.

The late to post-Variscan sequence of the eastern Southern Alps is divided into two cycles, which are separated by a major intra-Permian tectonic event ("Saalian movements"), characterized by strong block faulting (Krainer, 1992). The boundary is marked by a stratigraphic gap and a significant change in sedimentation, although there is no detectable angular unconformity. The sediments of the upper cycle conformably overlie the sequence of the lower cycle. Strong synsedimentary block faulting is expressed by the huge amount of reworked material from the lower cycle within the sediments of the upper cycle. In parts of the Carnic Alps, the sediments of the lower cycle have been completely reworked due to strong uplifting of discrete crustal blocks, and the basal sediments of the upper cycle (**Tarvisio breccia**) rest upon limestones of Devonian age.

The lower cycle is characterized by Late Carboniferous-Early Permian sediments and volcanic rocks, which were accumulated in intramontane basins formed by block-and wrench-faulting. The sequence of the first cycle is represented by cyclic deltaic and shallow marine clastic and carbonate sediments, the Bombaso formation, Auernig, Rattendorf, and Trogkofel groups, ranging from late Moscovian to late Artinskian. Within the upper part of the Auernig group and the Rattendorf group clastic-carbonate cycles are well developed, caused by eustatic sea-level fluctuations due to the Gondwana glaciation (Massari *et al*., 1991;Venturini, 1990a, p. 81-86).

Middle-Late Permian sediments of the second cycle, which are more widely distributed and not restricted to discrete basins, unconformably overlie Early Permian or even older rocks. With a hiatus due to severe block faulting ("Saalian movements"), the **Tarvisio (Tarvis) breccia** overlies the Trogkofel formation. The thickness of this breccia which is interpreted as a scarpfoot fan deposit and proximal debris flows, ranges from a few metres up to about 200 m (Krainer, 1993). Limestone clasts derived from the Trogkofel formation and the matrix is formed by red and grey shales and marls. The upper cycle continues with continental to shallow marine clastic sediments of the **Val Gardena (Gröden) formation** which repeatedly interfinger with and grade upwards into the shallow marine evaporitic and carbonate sediments of the **Bellerophon formation**. The Val Gardena formation shows abrupt variations in thickness (0-500 m) due to strong synsedimentary tectonics. The Bellerophon formation is formed by carbonatic shales and siltstones with intercalated thin dolomite layers and sandstones. The Bellerophon transgression prograded slowly westwards over a low-gradient or flat landscape. Sabkha sediments formed on this very shallow and wide, evaporitic transition zone. The lower part of the Bellerophon formation comprises a thick sequence of laminated gypsum, which subsequently served as major décollement level during Dinaric and Alpine thrust tectonics. During prograding transgressional events, fossiliferous limestones of open-lagoon shallow water environments were deposited. A significant change in sedimentation is recognized at the Permian/Triassic boundary, caused by a climatic shift (Krainer, 1993). Transgressive-regressive cycles within the Scythian **Werfen formation** are related to eustatic sea-level fluctuations, possibly caused by different spreading rates of mid-ocean ridges (Assereto *et al*., 1973; Brandner *et al*., 1984). The sediments of the Werfen formation were deposited in a shallow shelf environment ranging from subtidal, tidal flat and supratidal mudflat environment. From west to east, the Werfen formation unconformably overlies the Val Gardena sandstone, sabkha facies and shallow shelf limestone facies of the Bellerophon formation.

The reader is also referred to the results presented by the Italian research Group (1986) and to Hallam (1983), Carulli *et al*., (1986); Buggisch and Noè (1986), Brandner

(1988), Massari and Neri (1993), and Haas *et al*. (1995) for a detailed discussion of the Permian-Triassic boundary and Werfen formation.

2.2 MIDDLE TRIASSIC RIFTING PHASE AND RELATED THERMAL SUBSIDENCE

During Middle Triassic times, the eastern Southern Alps underwent a rifting phase. This rifting phase broke the area into several basins with different degrees of subsidence (Viel, 1979). From Anisian to Carnian, the paleogeographic setting was dominated by fast growing carbonate platforms (**Serla and Schlern** formations) with deep, partly anoxic lagoons in between (*e.g*., Leonardi, 1967, Bosellini, 1984, Buser, 1987). Abrupt changes in thickness of Anisian and Ladinian deposits indicate an important synsedimentary tectonic activity during this period of time. The geological map of the eastern and central part of the Carnic Alps (scale 1:20.000) indicates that the **Ugovizza breccia**, supposed to be deposited during the Anisian, in some places (south of the M. Cavallo di Pontebba) directly overlies the Devonian limestones across an angular unconformity (Venturini, 1990b). Additionally, clasts of Devonian have been found in the Ugovizza breccia, suggesting erosion of about 1000 m of sediments (Assereto, 1963; Assereto *et al*., 1968). Ladinian magmatic activity (intrusive and volcanic rocks of the **Livinallongo** formation) is often interpreted as result of the rifting of the future Halstatt-Meliatta ocean (Stampfli *et al*., 1991). In the Dolomites, volcano-tectonic domal uplift and subsequent caldera formation occurred at the same time as the late Ladinian magmatic phase (Doglioni, 1983). Three Middle Triassic magmatic events have been recognized in the Julian Alps (Gianolla, 1992): the first one, late Anisian in age, is documented by ignimbrites and volcanic clasts; the second one is early Ladinian in age while the third one is recorded in late Ladinian basinal tuffitic deposits. The products of the early Ladinian volcanism are known as **Rio Freddo Volcanics** and are to be related to an explosive hydromagmatic activity.

Local contractional tectonic features of Middle Triassic age have been demonstrated in the Dolomites (Pisa *et al*., 1979; Bosellini *et al*., 1982, Castellarin *et al*., 1982). Doglioni (1984, 1987) has interpreted the alignment between the Stava line and the northern limb of

the Cima Bocche anticline as a N70°E trending sinistral transpressive zone of Middle Triassic age. The basement has been strongly deformed by this sinistral transpression forming flower structures along the Stava line-Cima Bocche anticline which now forms a narrow and elongated basement high. According to Doglioni (1987), the maximal stress was oriented N40°E in Middle Triassic. Minor structures in the Marmarole area are also interpreted as being caused by Ladinian compressional tectonics (Picotti and Prosser, 1987). Sinistral transpression of the Stava line in the central Dolomites and coeval subsidence are interpreted as having been generated by early sinistral movements between Europe and Africa (Doglioni, 1984). Therefore, the Middle Triassic rifting phase is assumed to have been controlled by strike-slip faulting.

Triassic normal faults are not easy to recognize in the field, but different thicknesses of the sedimentary cover indicate the presence of buried growth faults that do not cut the overlying sedimentary cover. As these paleofaults are commonly not oriented in an ideal way to the Alpine transport direction, they often are reactivated as transpressive or transtensive faults during subsequent Alpine deformation. When these inherited faults trend at an acute angle to the transport direction, they frequently cut the belt into segments with different structures. The Incaroio transverse zone is interpreted in this way (chapter 4.2). In fact, numerous examples of Middle Triassic synsedimentary faults are well documented in the northern part of the Friuli Alps.

Best records are found north of Tarvisio, where the Ladinian dolomites are dropped down across E-W trending normal faults (Figs. 5 & 6). Based on structural compatibility arguments and sedimentary evidence, these normal faults are suspected to be of Middle Triassic age. The occurrence of an important breccia horizon (Ugovizza breccia) and thickness changes in the Lower-Middle Triassic sequence point to Middle Triassic synsedimentary faults. The tectonic setting shows that these normal faults are located in the footwall of the Alpine north-vergent backthrust (see cross-section in Fig. 7). Both types of faults strike parallel to each other. No criteria indicate that these faults have been reactivated during the emplacement of the backthrust. The orientations, sense of slip, and

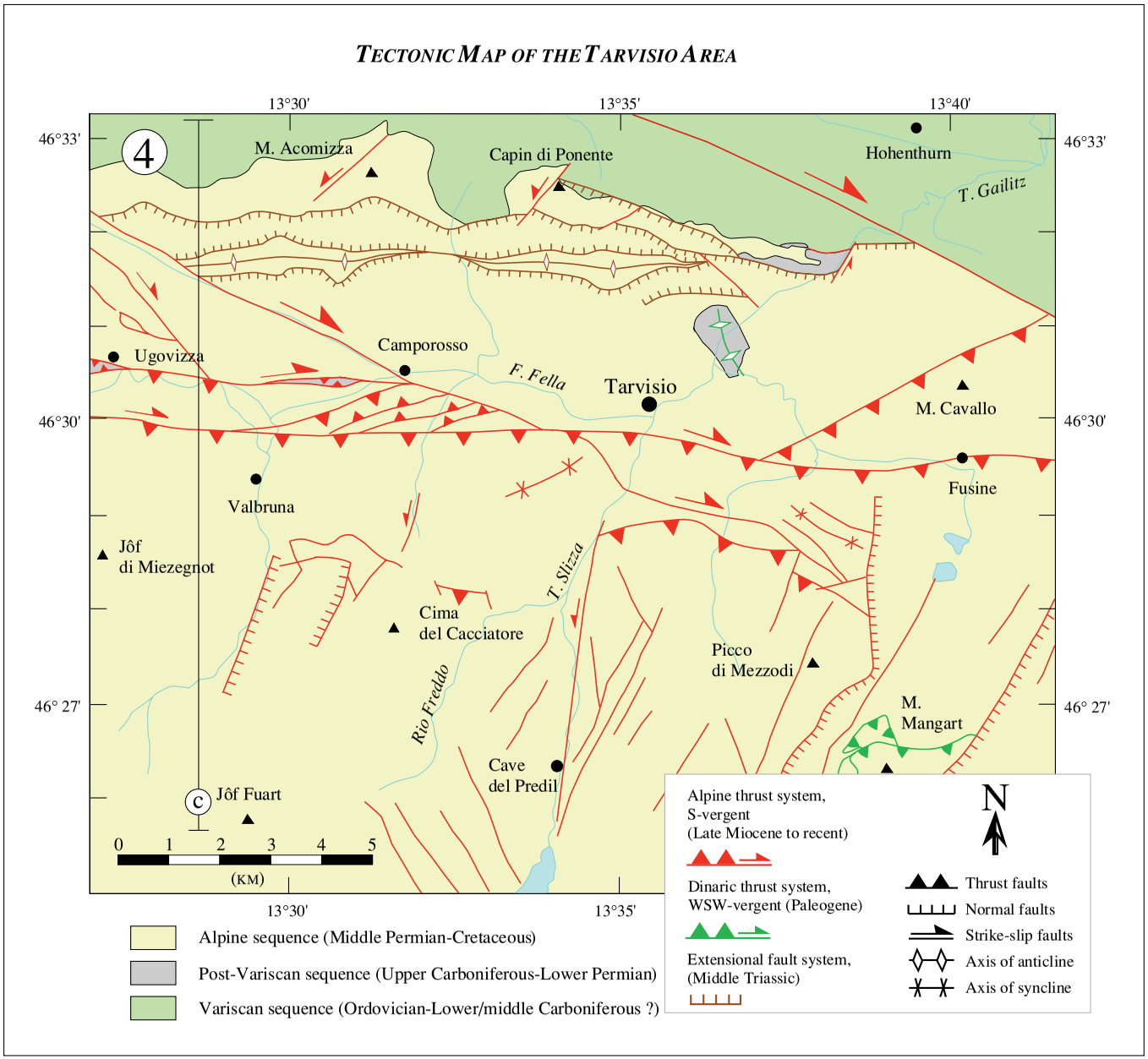

Fig. 5. Tectonic map of the Tarvisio area (n° 4 in Figs. 2 & 3). Based on new mapping at 1: 25.000, and after Venturini (sheet 14a Tarvisio, 1981). Cross-section c refers to Fig. 7.

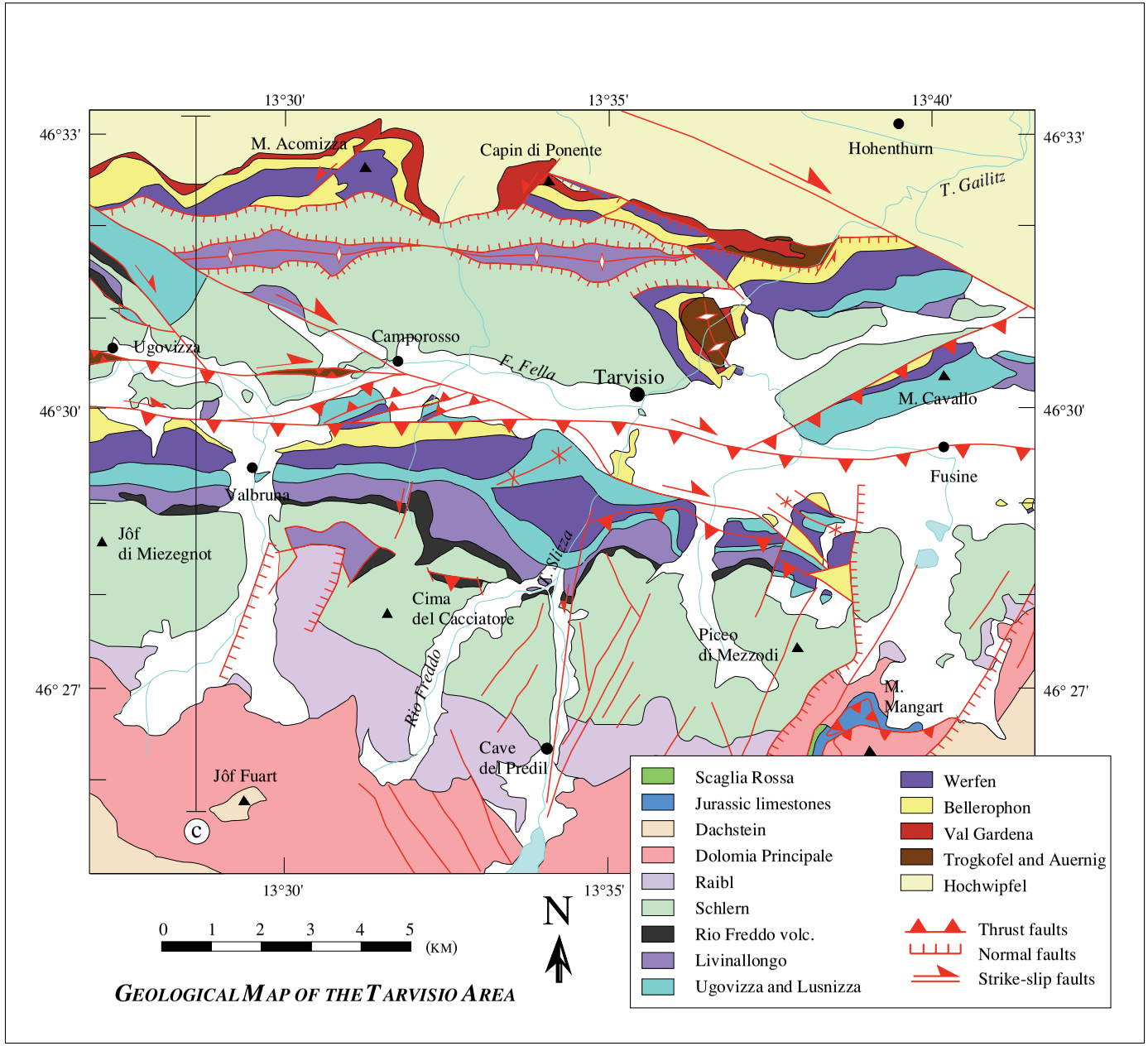

GEOLOGICAL MAP OF THE TARVISIO AREA

Fig. 6. Geological map of the Tarvisio area (n° 4 in Figs. 2 & 3). Based on new mapping at 1: 25.000 and previous mapping of Gortani *et al.* (sheet Tarvisio 14a, 1949), and Assereto *et al.* (sheet Tarvisio 14a, 1967, 1968). Cross-section c refers to Fig. 7.

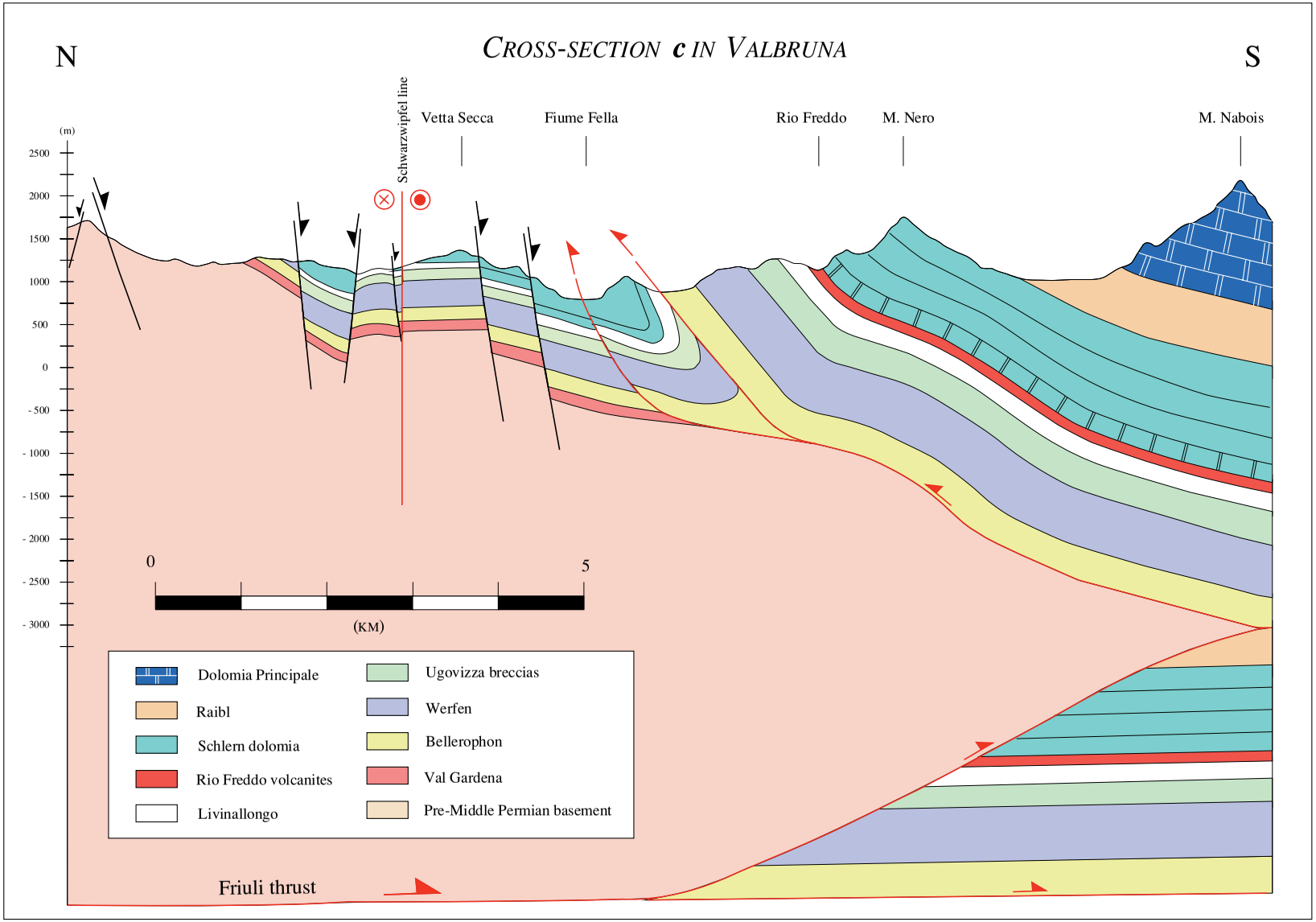

Fig. 7. Cross-section c in Valbruna. Note the preserved Middle Triassic normal faults in the footwall of the Alpine backthrust.

sedimentation patterns associated with these normal faults accomplish a north-south extension phase which has previously been recognized by some authors (Venturini, 1990b; Läufer, 1996). However, until now no Neogene north-south extension has been documented by reliable field data. For these reasons, these faults are assumed to be older than Neogene, probably of Middle Triassic age.

In the northern part of the Friuli Alps, small E-W trending grabens filled with Anisian dolomites and calcareous breccias of the Serla formation have been preserved. Synsedimentary breccia are exposed at several places like in the M. Arvenis graben. (Fig. 8). The photograph in figure 8 shows a dolomitic and calcareous breccia of probably Anisian age. Other grabens are documented at the M. Salinchiet east of the village of Paularo and M. Zoncolan south of the village of Ravascletto (Fig. 9). Gartnerkofel mountain provides a well-preserved Middle Triassic half-graben located at east of the Pramollo basin of Permo-Carboniferous age (Fig. 9, see also Venturini, 1990b). A brown color renders their localization on the tectonic map of the Tolmezzo area easier (Fig. 9). In conclusion, the Middle Triassic evolution, from Anisian to Carnian, is interpreted as the result of the rifting and the passive margin evolution at the edges of the Hallstatt-Meliata and Vardar oceans farther east (Ziegler, 1989; Stampfli *et al*., 1991; Stampfli, 1996).

During the Norian, a huge peritidal platform of some 1000 to 1700 m thick formed. The corresponds to an important rate of sedimentation and may be regarded as the consequence of thermal subsidence that followed the Middle Triassic rifting phase (Stampfli *et al*., 1991). These platform carbonates, called **Dolomia Principale formation**, behaved as rigid layers during subsequent deformation. Due to its rigidity and its large areal distribution, the Dolomia Principale layer may serve as horizontal key bed for the retrodeformation. During the Norian, pelagic facies also developed locally between the platforms, defining three small basins of limited extension (Tolmin, Bled and Carnic basins). Within these basins, anoxic conditions developed, which favored the deposition of bituminous limestones (**Capprizi formation**). In the Friuli plain, the deep wells of AGIP have revealed the existence of another basin: the intra-Friuli basin (Cati *et al*., 1987b). In

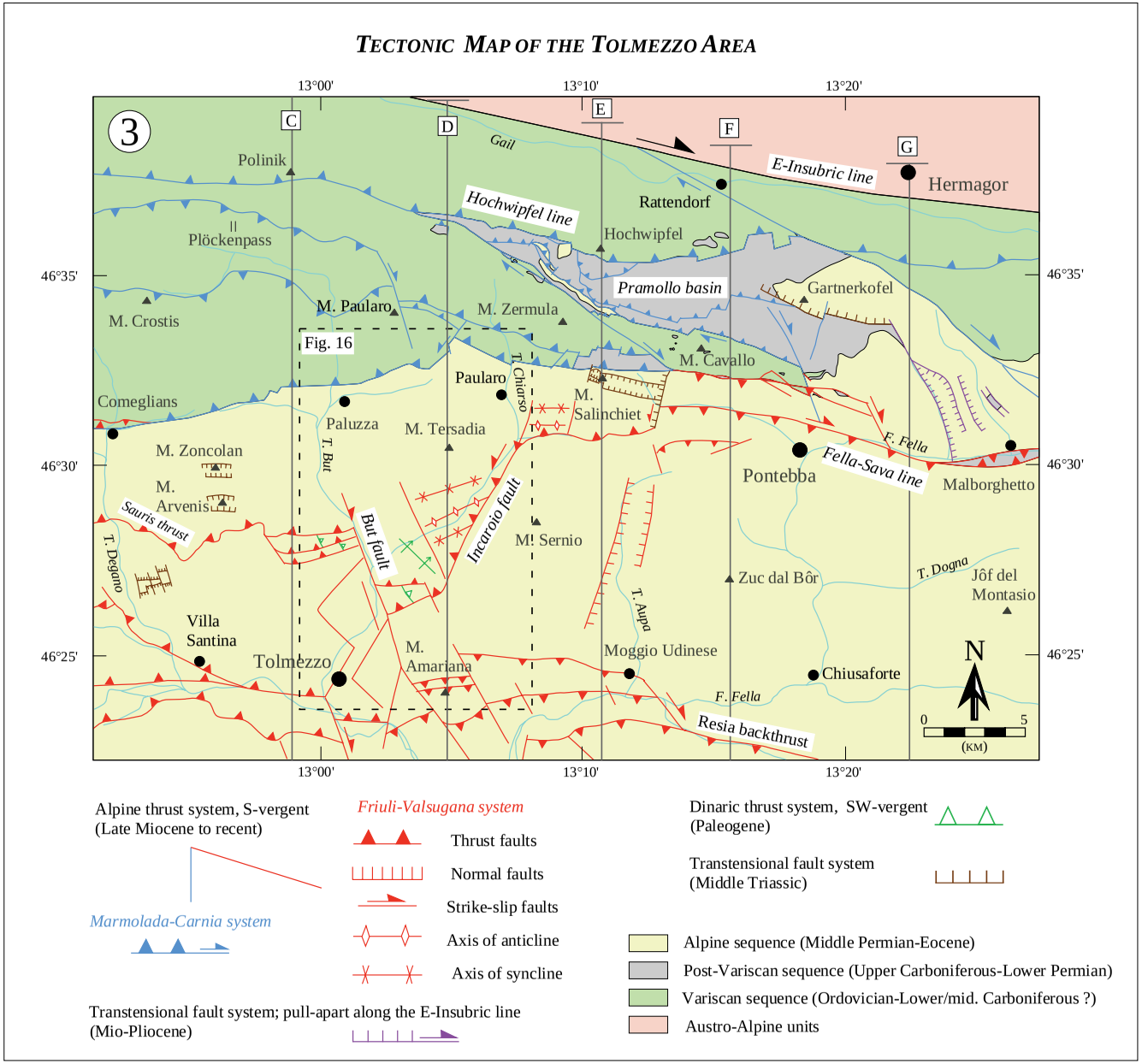

Fig. 9. Tectonic map of the Tolmezzo area (n° 3 in Figs. 2 & 3). This area is located in the Carnic Alps in the north (Paleozoic basement) and the northern part of the Friuli Alps. Based on new mapping at scale 1: 25.000, and after Gortani and Desio (sheet 14 Pontebba, 1925, 1927), Bianchin (1980), Frascari *et al*. (1981), and Carulli *et al*. (1982b). The Pramollo basin is drawn according to Venturini (1990b). Cross-sections C, D, E, F and G refer to Figs. 25, 26, 27, 28 and 29. The tectonic map of the Incaroio transverse zone is located by a dashed rectangle (Fig. 16). The Fella-Sava line was termed by Carulli *et al*. (1990). The other faults such as Sauris thrust, Resia backthrust, But fault, and Incaroio fault are informally called in this study. Note the preservation of E-W trending grabens of Middle Triassic age (M. Zoncolan, M. Arvenis and M. Salinchiet grabens) and the half-graben of Gartnerkofel. Photograph of a Middle Triassic synsedimentary breccia (Fig. 8) was taken in the M. Arvenis graben

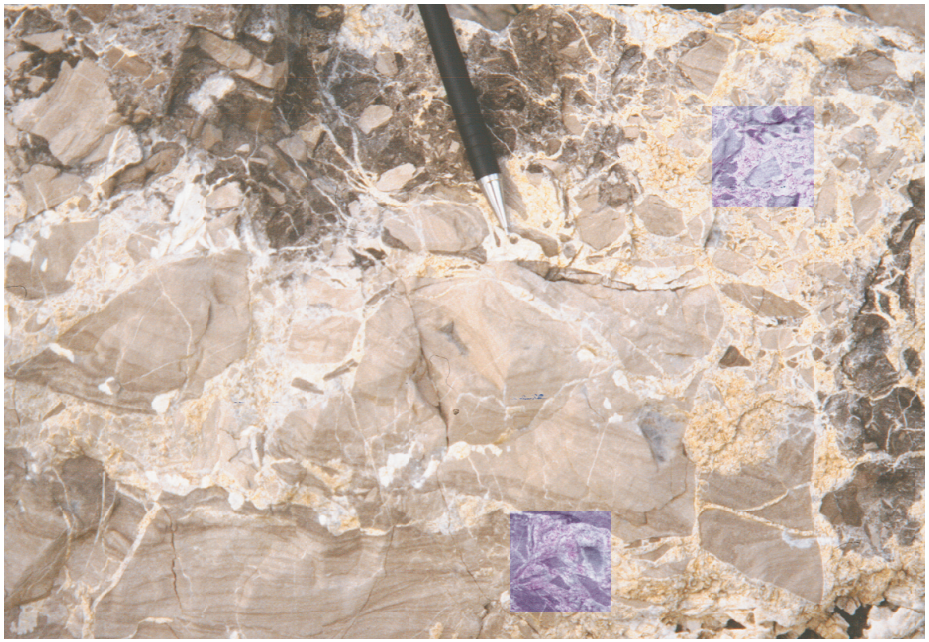

Fig. 8. Dolomitic and calcareous breccia (Serla formation) from the Middle Triassic M. Arvenis graben. Location in Fig. 9.

this case, the sedimentary strata have been called differently (**Forni formation**). These four areas of pelagic sedimentation extended during the Jurassic. They represent the onset of the main pelagic domains that grew during the Jurassic and partly during the Cretaceous. So in Late Triassic, the facies distribution predetermines the zonation of wide paleogeographic domains (alternation of basin-shallow platform) for Jurassic and Cretaceous times. The Rhetian and the Hettangian are characterized by the persistence of carbonate platform environment with the sedimentation of the **Dachstein formation**. The total thickness of Dolomia principale and Dachstein together may locally exceed 2000 m. Consequently they have largely contributed to the current architecture of the eastern Southern Alps.

The reader is referred to De Zanche (1990) for a complete review of the Triassic stratigraphy and paleogeography of the eastern Southern Alps.

2.3 Early Jurassic rifting and Jurassic-Cretaceous basin-shallow platform evolution

Since the Early Jurassic, extensional tectonics and subsidence were driven by the rifting and opening of the Alpine Tethys (Piemont-Ligurian ocean) farther west. During the Early Liassic, the widespread Upper Triassic carbonate shelf broke up into two large platforms with a deeply incised basin in between, the **Belluno basin**. The western platform (**Trento high**) drowned in the late Liassic, and subsequently experienced deep water sedimentation, whereas the eastern platform (**Friuli platform**) remained shallow-water shelf during the whole Mesozoic (Fig. 10). According to seismic-reflection data, an intermediate basin (**Friuli basin**) separated the Friuli platform into a southwestern and a northeastern part (Cati et *al.,* 1987b). The northern border of the northeastern Friuli platform outcrops in the frontal part of the Friuli Alps. The Belluno trough filled up with debris, and the end of Middle Jurassic time, it was no longer a submarine depression but a gentle slope connecting the Friuli platform to the deep pelagic Trento plateau (Winterer and Bosellini, 1981). After maximal transgression during the Oxfordian (Cousin, 1981),

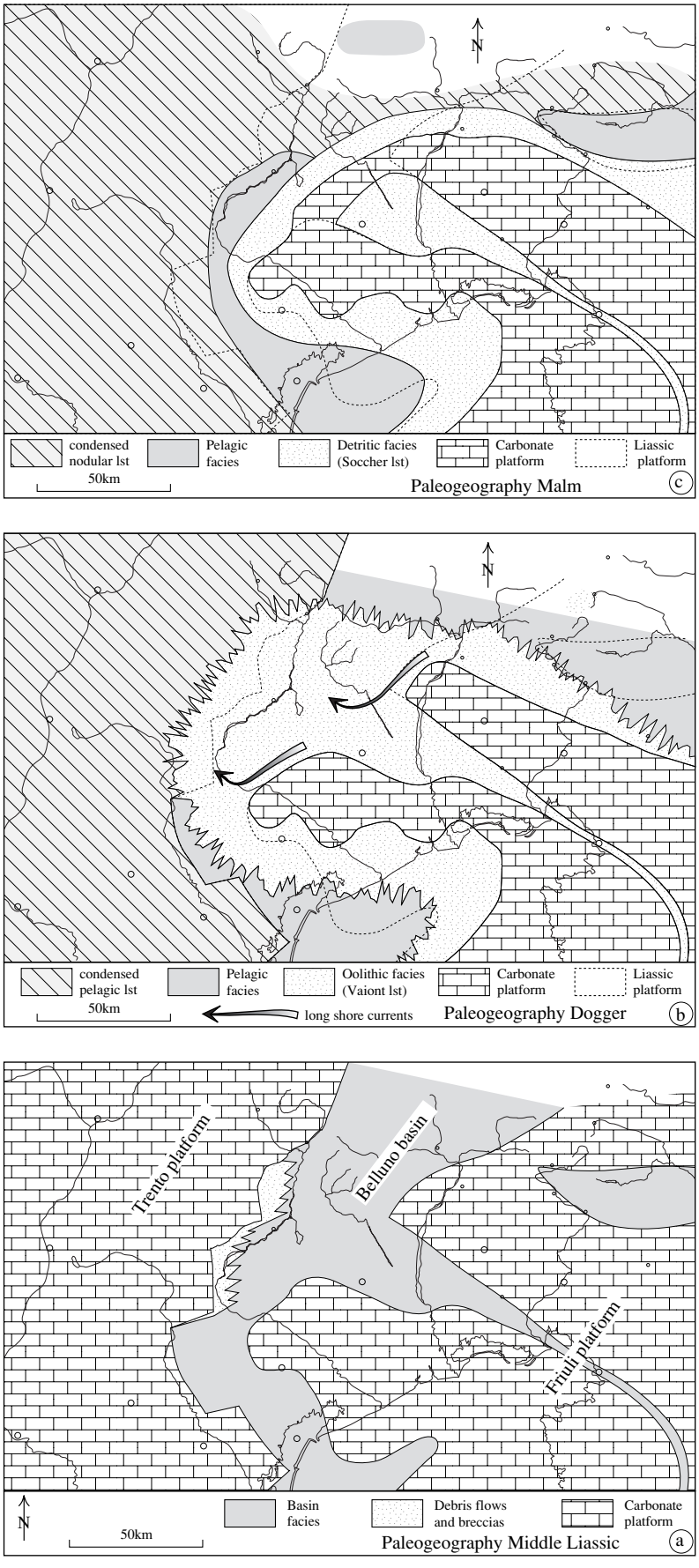

Fig. 10. Paleogeographic evolution of the Jurassic passive continental margin of the eastern Southern Alps. (a) Rifting led to the Trento and Friuli platforms with the Belluno basin in between during early Liassic. (b) The Trento platform drowned during late Liassic, but remained a submarine high, while currents deposited thick oolithic sequences (Vaiont limestones) in the Belluno basin during the Middle Jurassic. (c) The Friuli carbonate platform persisted until it was covered by flysch during the early Eocene (situation during the Upper Jurassic). An intermediate basin (called Friuli basin by Cati *et al.*, 1987) separated it into a northeastern, a southwestern, and a northwestern part. The northwestern part grew after the Oxfordian transgression and reached its maximum extension during the Cenomanian (Cousin, 1981). Subsequent thrusting is not back stripped. Taken from Schönborn (1999).

the Friuli platform prograded into the basin (Fig. 10). During the Kimmeridgian and the lower Tithonian, Ellipsactinies limestones built up a barrier reef on the Friuli platform and red and nodulous pelagic calcareous were deposited on a shoal (**Ammonitico Rosso** facies). At the end of the Cretaceous, the sediments of the typical pelagic **Scaglia formation** were deposited. Sedimentation of the Scaglia lasted until the Paleocene.

The Early Jurassic rifting phase is well documented by breccia deposition that are readily observable in the field. Synsedimentary faults are generally evidenced by abrupt lateral thickness changes in Lower Jurassic sedimentary strata. The occurrence of sedimentary breccia is also a good indicator of synsedimentary fault activity. In many cases, these paleofaults are reactivated during subsequent deformations as steep transpressional faults or as pure strike-slip faults. These inherited faults also localize lateral or oblique ramps in transverse zones and they serve as such as transfer zones for shortening.

2.4 Evolution of the Veneto Basin during the Cenozoic

The Cenozoic sedimentary evolution has been marked by the development of flysch and molasse basins, linked to the Dinaric and Alpine orogenies. Sedimentation of the Paleogene flysch formations was mainly influenced by the Mesozoic paleogeography and by the westward approaching Dinaric chain. Since the Late Oligocene, the first molasse accumulated in the Veneto basin between Belluno and the eastern Friuli (Cousin, 1981; Figs. 2 & 3).

2.4.1 Paleogene evolution

Two types of formations dominate the Paleogene deposits: the Eocene flysch of the external Dinarides and the Oligocene molasse of the Veneto basin.

Since the Late Paleocene and throughout the Eocene, the flysch deposits invaded the Friuli platform and its northwestern border. The first appearance of the flysch varied in time, from Thanetian (in NE) to the uppermost Lutetian (in SW). Consequently, the depot-centers in the north are more advanced than those farther south (Cousin, 1981). Schönborn (1999) interpreted this pattern by sinistral transverse zones that follow approximatively the edges of the northwestern part of the Friuli platform (Fig. 11). The Dinaric orogeny transformed the paleogeographic zones defined in the Mesozoic.

The first molassic deposits appeared in two different basins during the Oligocene. At this time, the newly formed Dinaric chain separated the foredeep basin (Veneto basin) from the internal basin (Sava basin, Central Slovenia). The Oligocene is characterized by isolated outcrops of a lagoonal and estuarine environment. Examples are the Oligocene flysch of Peonis (Val Tremugna) and Trasaghis (see Sarti, 1979; Venturini and Tunis, 1991).

The Dinaric flysch formations were deposited transgressively on Cretaceous limestones of the Friuli platform. The age of the top of these Rudist limestones varies from the Cenomano-Turonian to the Campanian. At some places, the base of the flysch overlies an additionnal horizon, the Scaglia formation of Maastrichian-Thanetian age.

In conclusion, the Dinaric flysch formations are mainly Eocene, whereas the Dinaric molassic deposits are mainly Oligocene.

2.4.2 Neogene evolution

During the Neogene, sandy and marly molasse-type deposits were accumulated in the same area of sedimentation, the Veneto basin. This basin was first part of the Dinaric foredeep and an eastward thickening sequence was deposited from the Late Oligocene to the Early Miocene. Since the Middle Miocene, the area of sedimentation was integrated into the newly formed Alpine foredeep and a northward thickening sequence developed.

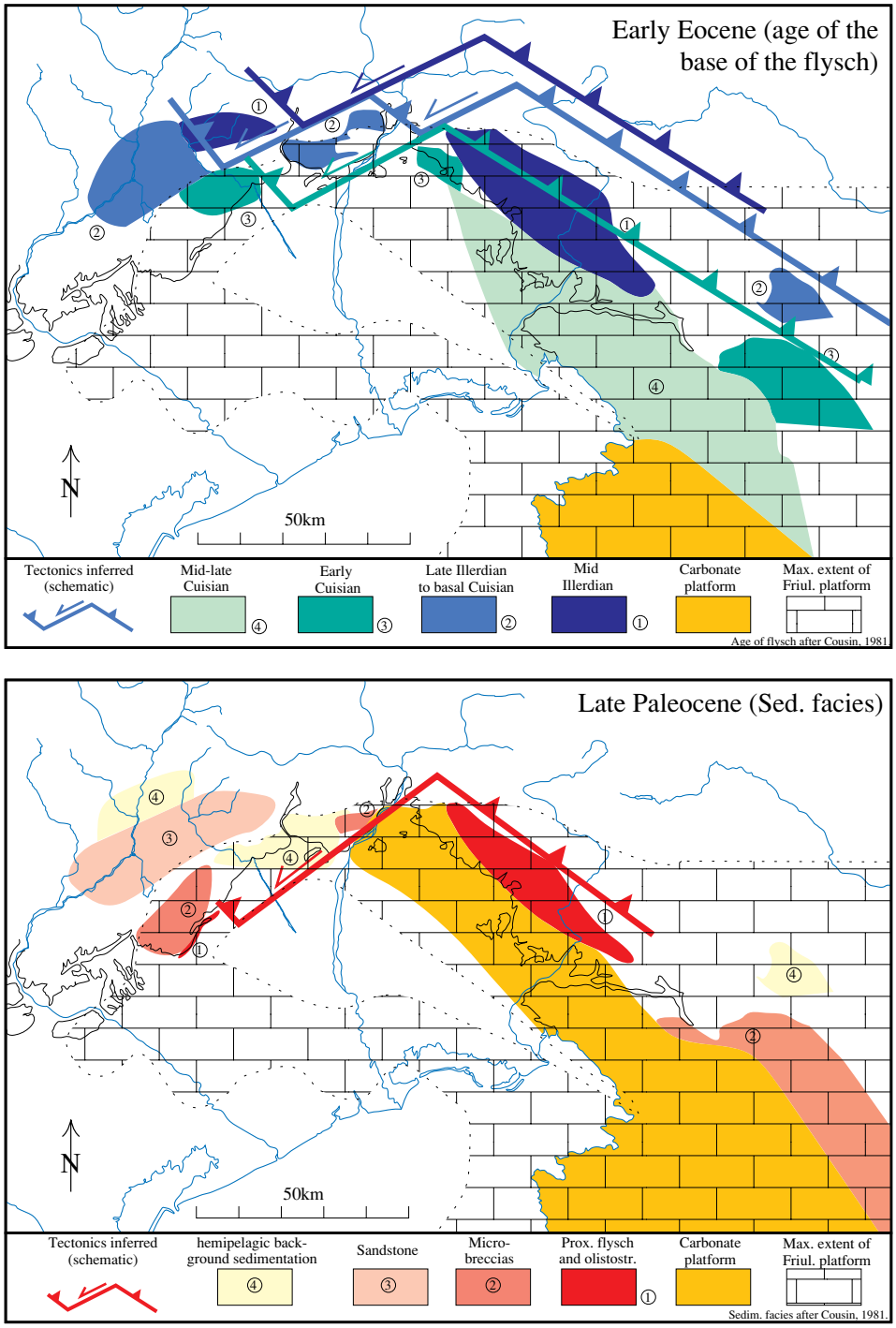

Fig. 11. Flysch sequences date the Dinaric deformation as mainly late Paleocene to early Eocene in northeastern Italy. The irregular age pattern of beginning flysch deposition suggests sinistral strike-slip zones following the limits of the northwestern Friuli platform. Subsequent thrusting is not back stripped. Age and distribution of flysch are according to Cousin (1981). Taken from Schönborn (1999).

Neogene molasse of the Veneto basin outcrops today from Belluno and Vittorio Veneto (west) until Ragogna in Friuli (east).

Since the Burdigalian, an eastward, marine transgression across the Veneto basin was completed. Transition from a marine, gritty and glauconitic molasse to a marly molasse in middle Miocene indicates increase in water depth. From the Late Miocene, sedimentation is dominated by continental and brackish facies, indicating emergence. The first conglomerates appear in the Tortonian (~ 10 Ma). These conglomerates are interpreted to be formed by uplifted mountains, and indicate the onset of Alpine uplift on the border of the sedimentation area. On the Friuli plain, alluvial sediments continued to accumulate until Quaternary times (Amato *et al*., 1977).

Dating of conglomerates is always a difficult exercise: the example of the "Conglomerato di Osoppo" illustrates well this problem. During summer 1994, mammalian (*Hipparion: bovide and rhinoceros*) trackways were identified on a bedding surface exposed at the top of the Colle di Osoppo (Osoppo hill), on the east bank of Tagliamento River. The exposure was created as part of excavations made during the restoration of the old fort damaged by the earthquake of 1976. These trackways permit dating of the upper part of the "Conglomerato di Osoppo" on a biostratigraphic basis (Dalla Vecchia and Rustioni, 1996). Their results give a post-evaporitic Messinian age for the deposition of these conglomerates, whose age was subject, until now, to various interpretations (Tortonian age after C.Venturini, 1992; early Pleistocene age after S. Venturini and Tunis, 1992). Recently, Viaggi and S. Venturini (1995) found ostracods that give and confirm a post-evaporitic Messinian age for these conglomerates.

Significant contributions dealing with several aspects of the Veneto-Friuli basin molasse were given by Cousin (1981), Stefani (1984), Massari *et al*. (1986a,b, 1993), Grandesso *et al*. (1992), and Venturini and Tunis (1992).

2.5 THE STRATIGRAPHIC THICKENING WEDGE OF THE EASTERNMOST SOUTHERN ALPS

This chapter aims at the reconstruction of various local stratigraphic columns. The stratigraphic sections are largely inspired from Winterer & Bosellini (1981), Cousin (1981) and Cati *et al.,* (1987b). These data are very helpful for the construction of cross-sections and subsidence curves.

The Friuli Alps may be divided into western and eastern parts along the Tagliamento River. The Tagliamento River follows an important N to NNE trending normal fault of Early Jurassic age (chapter 4.2) which subdivides the Friuli Alps in the eastern and western parts.

2.5.1 Eastern part of the Friuli Alps

Important aspects of the paleogeographic evolution in the eastern part of the Tagliamento valley are:

- Transgression of an Upper Campanian-Maastrichian pre-flysch or Scaglia facies
- Pre-late Cretaceous erosional phase
- E-W thickness changes in Liassic deposits (from 50 to 500 m)

Along a north-south profile, the Jurassic-Cretaceous paleogeographic setting may be divided in two main domains: in the north the "Perifriuli" domain, mainly dominated by pelagic sequences since the Early Jurassic, and in the south the Friuli carbonate platform. The "Perifriuli" domain itself may be divided in two parts, a deep part near the Friuli platform and a shallow part to the north. The deepest part constitutes a shoal (called the Perifriuli shoal by Cousin, 1981) between the Belluno trough to the west and the Tolmin trough to the east. Due to this complex paleogeographic setting, the eastern part of the Friuli Alps must be described by at least five different stratigraphic sections. Thickness changes in Jurassic-Cretacous sediments are abundant and pre-Santonian erosional phase

reworked Upper Triassic rocks. The four first sections are located in the "Perifriuli" domain and the last one is located farther south on the Friuli platform.

a. Northwestern part (M. Forcella):

- Lutetian: at least 50 m, eventually more since sediments are cut by the Resia backthrust.
- Hiatus from Hettangian (200 Ma) to Lutetian (45 Ma).
- Upper Triassic (Norian-Rhetian): 1800 m.

At M. Forcella, a Middle Eocene alternance of marls, of calcareous breccias, and paraconglomerates lies with an angular unconformity directly on top of the dolomitic limestones of the Dachstein formation (Rhetian-Hettangian?). The surface of the carbonates has been eroded during an important karstification phase, with the karsts being infilled with Middle Eocene calcarenites. The faunal association is predominantly constituted by macroforaminifera like Nummulites, characteristic of the lower Lutetian (for more information, refer to Carulli *et al*., 1982a; Cousin, 1981).

b. Western part (M. Plauris, M. Cumieli, M. Chiampon, M. Cuarnan):

- Upper Cretaceous Scaglia (Cenomanian to Campanian): 300 m.
- Hiatus from Berriasian to Cenomanian
- Middle-Upper Jurassic: 200 m.
- Lower Jurassic: 300-500 m.
- Upper Triassic (Norian-Rhetian): 1200 m -1800 m (increasing northward).

c. Eastern southern part (M. Musi, M. Zaiavor, M. Stol):

- Upper Cretaceous flysch (upper Campanian-Maastrichtian): 250 m
- Hiatus from upper Berriasian-lower Valanginian to upper Campanian.
- Middle-Upper Jurassic: 200 m.
- Lower Jurassic: 50 m.
- Upper Triassic (Norian-Rhetian): 2000 m.

d. Eastern central part (Val Uccea, M. Urazza):

- Upper Cretaceous Scaglia (Santonian): 250 m.
- Hiatus from the base of Hettangian to Santonian.
- Upper Triassic (Norian-Rhetian): 2000 m.

e. Southern part (La Bernadia)

This area belongs to the Friuli carbonate platform. Reefal and neritic limestones with rudists were deposited at least until 90 Ma (Turonian). From 80 Ma, Scaglia (red clay rich limestones) or a flysch were deposited: they are transgressive on top of the reefal limestones. These transgressive sequences of upper Campanian-Maastrichtian age may overly a substratum eroded as deep as Upper Triassic sediments (M. Matajur). What happened in the time interval between 90 and 80 Ma? An aerial erosion event occurred, but when did it start exactly and when did deposition of the reefal limestones stop? In the western part, the Cretaceous is formed by a complete sequence until Maastrichtian (M. Jouf and M. Cavallo), but there, the Scaglia facies is younger (Paleocene). The Dinaric flysch overlies the upper Campanian-Maastrichtian Scaglia or flysch with an unconformity. The base of the Dinaric flysch was dated as late Thanetian (~ 55 Ma) by Cousin (1981). Nevertheless, the transition to the Scaglia or flysch may be absent, and the Dinaric flysch directly overlies the Cretaceous reefal limestones (i.e. in the transverse valley of Torre). The stratigraphic column for the eastern southernmost part of the Friuli Alps may be summarized as follows:

- Dinaric flysch from upper Thanetian (~ 55 Ma) to upper Lutetian (~ 40 Ma): 2500-3000m.
- Hiatus between 65 and 55 Ma ?
- Scaglia facies or flysch from upper Campanian (~ 80 Ma) to Maastrichtian (~ 65 Ma): 20-50 m.
- Hiatus between 90 and 80 Ma ?
- Cretaceous reefal limestones at least until Turonian (~ 90 Ma): 950-1150 m.

- Middle-Upper Jurassic: 700-750 m (extrapolated from the western Friuli Alps because of lack of exposure).
- Lower Jurassic: 50-100 m (extrapolated from the western Friuli Alps).
- Upper Triassic: 1900-2000 m.

2.5.2 Western part of the Friuli Alps

East-west lateral variation in sedimentation is less important in the western part than in the eastern part, consequently only two stratigraphic sections are described. The first one is located in the "Perifriuli" domain and the other one in the Friuli platform farther south.

- Perifriuli domain: (M. Naiarda, M. Verzegnis)
- Dinaric flysch fromYpresian to lower Lutetian : > 400 m
- Hiatus between 60 to 50 Ma.
- Scaglia facies (upper Campanian-Maastrichtian): 0-50 m.
- Cretaceous: 200 m.
- Middle-Upper Jurassic: 400-500 m.
- Lower Jurassic: 200-700 m.
- Upper Triassic: 1900-2000 m

- Friuli platform: (M. Ciaurlec, M. Jouf, M. Cavallo)
- Pliocene-Pleistocene (3-1 Ma).
- Hiatus from 5 to 3 Ma.
- Miocene molasse from upper Aquitanian-Burdigalian (~ 20 Ma) to Messinian (~ 5 Ma): 2100-2400 m.
- Hiatus between 45 to 20 Ma.
- Dinaric flysch from Ypresian (~ 50-53 Ma) to lower Lutetian (~ 45 Ma): 800-1200 m
- Hiatus between 60 to 50 Ma.
- Scaglia facies (Paleocene): 0-50 m.

- Cretaceous reefal limestones until Turonian with hiatus or until Maastrichtian times: 1200-2000 m.
- Middle-Upper Jurassic: 700-750 m.
- Lower Jurassic: 50-100 m.
- Upper Triassic: 1900-2000 m

The thickness of the Cretaceous limestones shows a wide range, from 1200 m on the M. Ciaurlec to more than 2000 m on the M. Cavallo above Aviano. The thickness of the limestones increases at the west. The reasons for this are probably an erosional phase that occurred before 80 Ma in the east, and also the nature of these limestones which are formed by reef-forming organisms such as rudists. The thickness of the Dinaric flysch reaches only 1000 m in this area, in contrast to the 2500-3000 m-thick deposits to the east.

3. VARISCAN AND DINARIC TECTONICS

In this chapter, the characteristics of pre-Alpine contractional structures are described. It is necessary to separate Alpine structures from the older ones in order to unravel and quantify the degree of Alpine deformation. Before being affected by the Alpine deformation, the easternmost part of the South Alpine realm underwent the Variscan deformations during the middle Carboniferous times and the Dinaric deformations during the Paleogene. Field work was carried out in the Variscan basement in order to identify Alpine structures. Consequently, this study does not aim at a new interpretation of the Variscan tectonic evolution. The review below is extracted from the literature.

3.1 VARISCAN DEFORMATION

South of the E-Insubric line, the Variscan basement is represented in the Carnic Alps and Karawanken Alps. Rocks deformed during Variscan deformation are considered as Variscan basement. The Carnic Alps are made up by an Ordivician to mid-Carboniferous Variscan basement and an Upper Carboniferous to Middle Triassic cover sequence. The Variscan basement is exposed due to a basement ramp-fold that produced south-tilting of the Lower-Middle Triassic sequence. This ramp-fold is related to the more internal thust of the belt: the Carnia thrust (chapter 5, see cross-sections in Figs. 23-29).

Studies of the Variscan tectonometamorphic evolution of the Carnic Alps were carried out by various authors (*e.g.*, Castellarin and Vai, 1982; Venturini, 1990b, Läufer, 1996; Hubisch, 1999). The Variscan basement is divided into an epizonal metamorphic part in the western Carnic Alps and an anchizonal metamorphic part in central and eastern Carnic Alps. The boundary between these two units is located approximatively in the area of the Val Bordaglia fault zone. Due to very low-grade metamorphism, the central and eastern Carnic Alps represent one of the few places in the world in which an almost continuous fossiliferous sequence of Paleozoic age is preserved. The oldest fossiliferous

rocks are Caradocian in age (upper Ordovician) and comprise thick acidic volcanics named Comelico Porphyroid and volcaniclastics of the Fleons formation. The Devonian reefal limestones make up most of the summits of the Carnic Alps. Main reef builders were stromatoporoids, tabulate corals and calcareous algae (see in Kreutzer, 1990). Detailed information about the stratigraphic and facies succession and the general geological framework of this mountain chain is found in Schönlaub (1979), Tolmann (1985), Venturini (1991), Schönlaub and Heinisch (1993) and others.

According to Hubich and Läufer (1997) and Hubich *et al*. (1999), Variscan deformation produced stacking of three nappes: the Fleons nappe in the western Carnic Alps, the Cellon-Kellerwand nappe and the Hochwipfel nappe in the central Carnic Alps. These authors have recognized two Variscan deformation phases. A first ductile deformation event (presumably Visean/Namurian) under epizonal metamorphic conditions (Tmax: 300-450°) was followed by a second deformation phase (presumably Namurian/Westphalian) under higher anchizonal conditions (Tmax: 260-300°C). Kinematic indicators such as shear bands or slickensides, indicate top-to-south thrusting during the first deformation phase and top-to-SSW for the second phase. The first deformation phase was recognized only in the Fleons nappe. Both deformations are assumed to be of Variscan age, because their style and metamorphic grades differ from the ones in the less intensely deformed post-Variscan sequence.

3.2 Paleogene (Dinaric) deformation

3.2.1. Introduction (literature)

In this paragraph, I describe and explain structures of the key-area where the Paleogene Dinarides intersect with the Neogene Southern Alps. The easternmost part of the South Alpine belt built up on an area that had been deformed by the northwest external Dinarides during the Paleogene (Laubscher, 1971b; Doglioni and Bosellini, 1987). Therefore, this area underwent two different contractional events. Deformation began

probably in the Paleocene with the first appearance of flysch in the Thanetian (Cousin, 1981). The westward extension of the Dinaric belt reached the central Dolomites, where Dinaric thrusts are well preserved today (Doglioni, 1987). Kinematic criteria such as slickensides and shape fabrics show that the external Dinarides were translated in a southwesterly direction. But as Dinaric structures were strongly dismembered by subsequent Alpine tectonics, some blocks were locally rotated by strike-slip movements, indicating an apparent transport direction to the west. However, the Dinaric thrusts are more easily recognizable in the central Dolomites where they doubled the Dolomia Principale unit (Fig. 12). Several examples of Dinaric thrusts are well preserved on different famous summits of the Dolomites as La Civetta, La Croda Rossa, Le Tofane, and La Rochetta, where these thrusts verge toward the west-southwest. Further informations about Dinaric thrusts in the Dolomites are available in the literature (Doglioni, 1985, 1987; Doglioni and Bosellini, 1987; Doglioni and Siorpaes, 1990).

3.2.2 Dinaric/Alpine superposed structures (data and observations)

Dinaric/Alpine superposed structures are identified at different scales and places in the Friuli Alps. Nevertheless, the Dinaric sructures cannot be connected to an overall network. Many of these faults have loose ends since they were dismembered by the south-vergent Alpine thrusts. Field observations suggest that the superposed Paleogene-Neogene structures are characterized by three different geometries:

- cross-cutting thrusts
- superposed folds
- Dinaric thrusts cross-cut by Alpine normal faults

Cross-cutting thrusts. The major part of the Friuli Alps is characterized by a lack of large-scale superposed structures, except in the frontal part of the belt, where Dinaric structures are recognized (as examples: M. Bernadia, M. Ciaurlec and M. Jouf). In the Maniago area, the NW-SE trending ramp-folds of Cretaceous limestones and Eocene

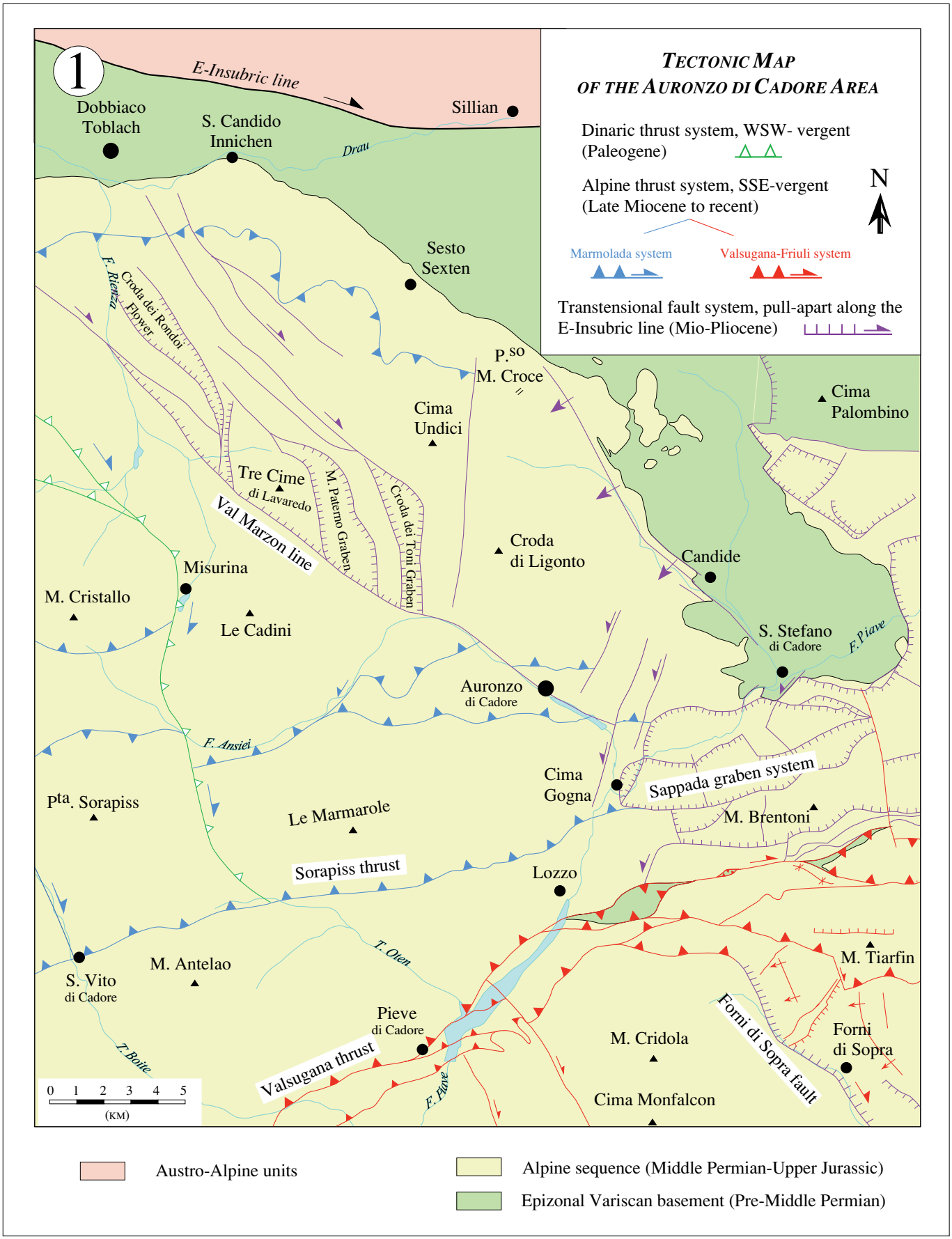

Fig. 12. Tectonic map of the Auronzo di Cadore area (n 1 in Figs. 2 & 3). Based on new mapping at 1: 25.000, and on previous mapping of Castiglioni *et al*. (sheet 12 Pieve di Cadore, 1940), Semenza (sheet 12 Cortina d'Ampezzo, 1981), Caputo (1997), and Schönborn (1999).

flysch are cross-cut by E-W Alpine thrusts (Figs. 13 & 14). The geometry of the frontal part of the Friuli arc suggests a Dinaric tectonic style involving detachment folds, and fault-propagation folds with the décollement level located in the Lower Cretaceous Biancone formation (Fig. 15). The stratigraphic layers below the Biancone horizon seem not to be implied in the folding. Forelimbs of these SW-vergent folds are not overturned and dip at 30° or less suggesting the presence of a blind thrust at depth.

In the northern part of the Friuli Alps, some evidence for small-scale Dinaric thrusts is locally preserved. North of Tolmezzo, a west-vergent thrust is cut and transported southward by an Alpine thrust (Figs. 9 and 16). At Zuglio, small-scale west-vergent thrusts (Fig. 16) have transported Ladinian Schlern dolomites onto the Carnian hemipelagic sequence. In each observed case, the Dinaric thrusts imply minor shortening (Carnian onto Ladinian and Anisian onto Ladinian).

Superposed folds. Superposed folds are mainly observed in Upper Permian evaporitic horizons of the Bellerophon formation. Various outcrops show superposed folds. Near Dierico along the Chiarzò River, small-scale SW-vergent folds are refolded by SSE vergent folds (see stereoplot Dierico in Fig. 16). The SW-vergent folds (F1) are interpreted as Dinaric and the SSE vergent folds (F2) as Alpine. Between Sutrio and Arta Terme along the right bank of the But River, similar superposed folds are observed. The fold size is of metric to decametric scale. North of the Forni Avoltri village, Upper Permian evaporites are clearly deformed by southwest-vergent folds with wavelengths of about 30-50 m, whereas higher up the Lower Triassic deposits are not folded (Figs. 17 & 18). The SW-vergent folds are cross-cut by Alpine transpressional reverse faults. These different observations suggest that the external Dinarides were transported southwestward above a major décollement horizon located in the Upper Permian evaporites.

Dinaric thrusts cut by Alpine normal faults. South of Tarvisio, the Mangart Mountain is deformed by some complex west-vergent thrusts that are cross-cut by Alpine NNE-

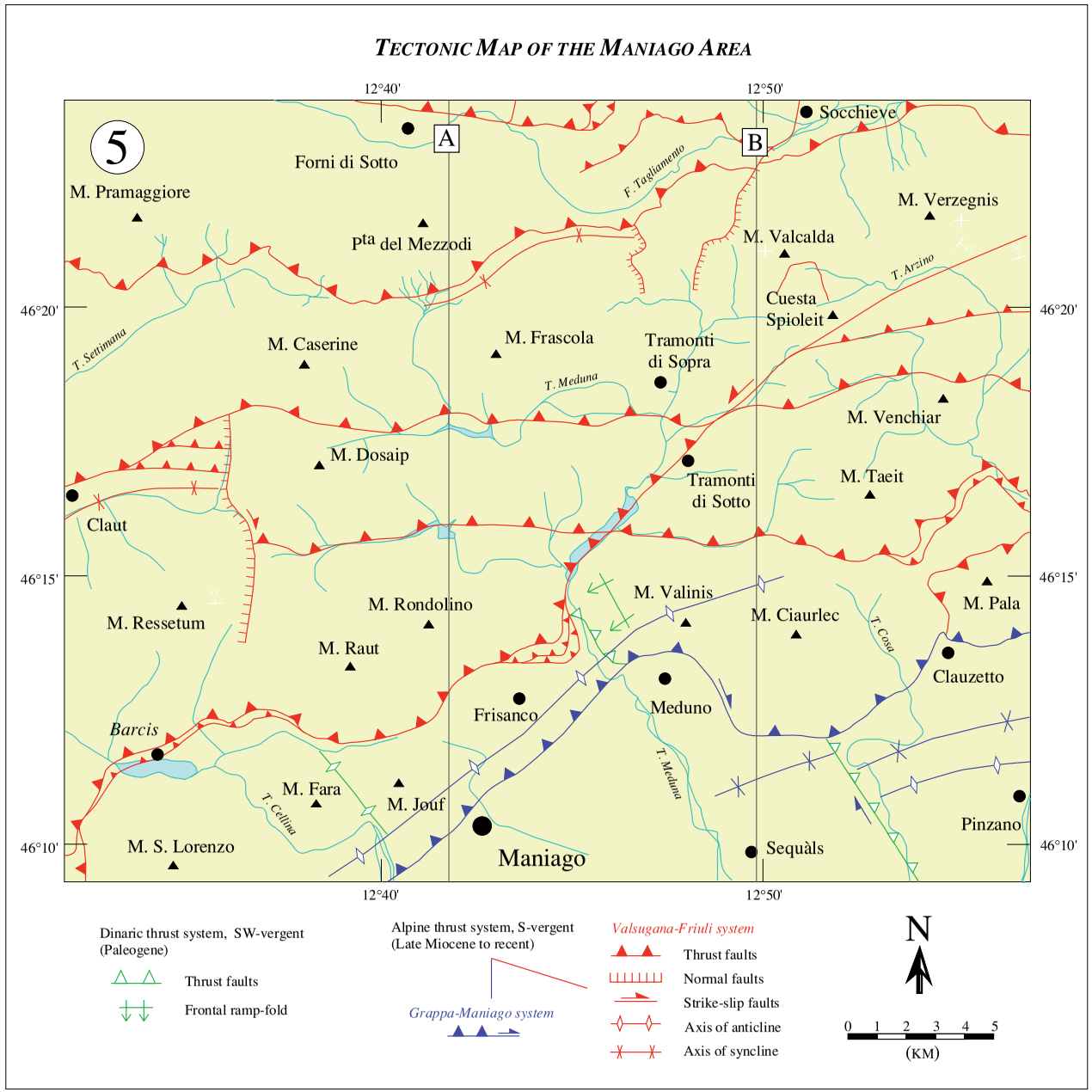

Fig. 13. Tectonic map of the Maniago area (n °5 in Figs. 2 & 3). Based on new mapping at 1: 25.000 and after Cavallin, 1981 (sheets 24 Maniago and 39 Pordenone). Cross-sections A and B refer to Figs. 23 and 24.

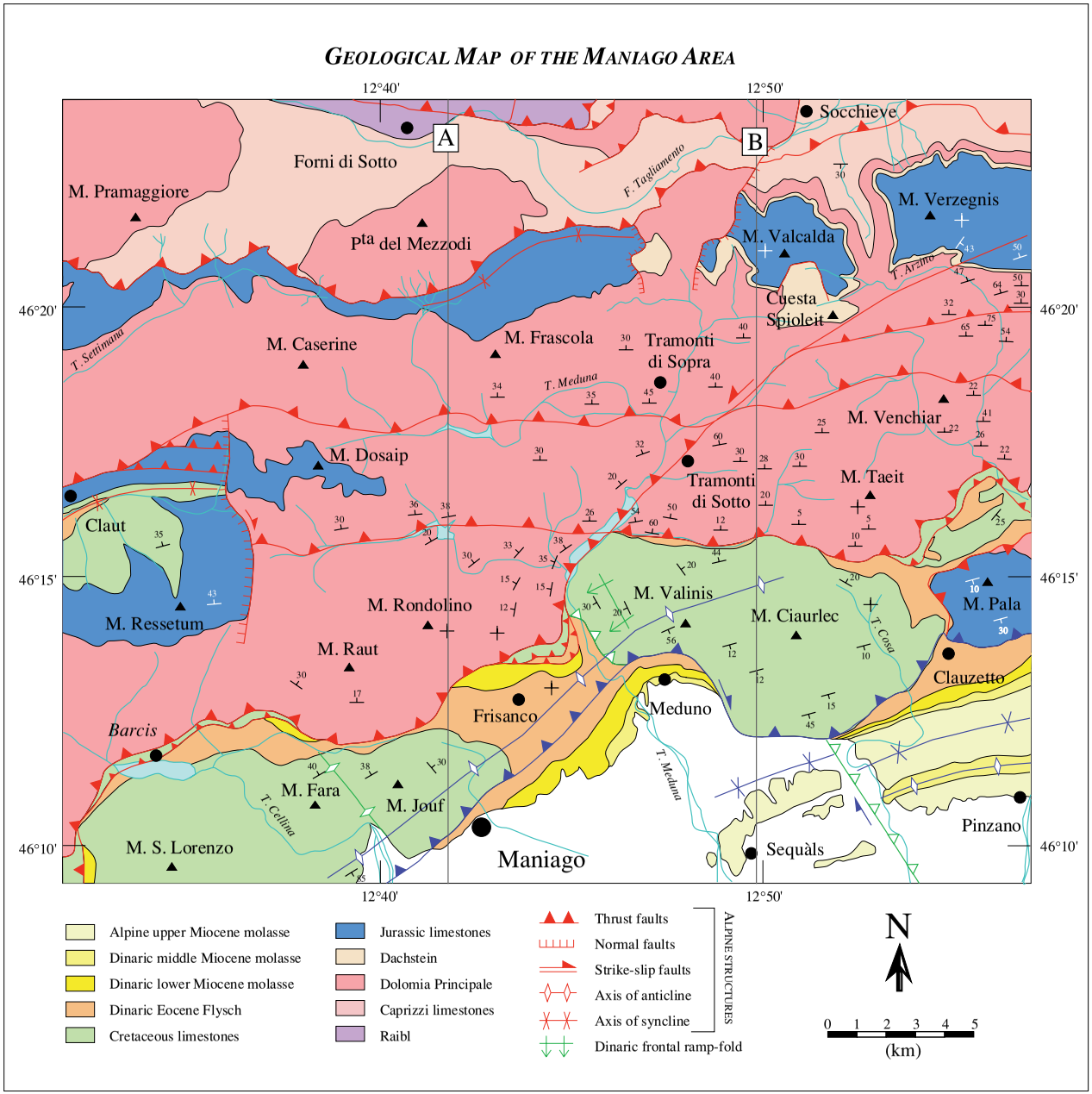

Fig. 14. Geological map of the Maniago area (n° 5 in Figs. 2 & 3). Based on new mapping at 1: 25.000, and on previous mapping of Zenaris (sheet 24 Maniago, 1927), and Comel and Ferasin (sheet Pordenone 39, 1956). Cross-sections A and B refer to Figs. 23 and 24.

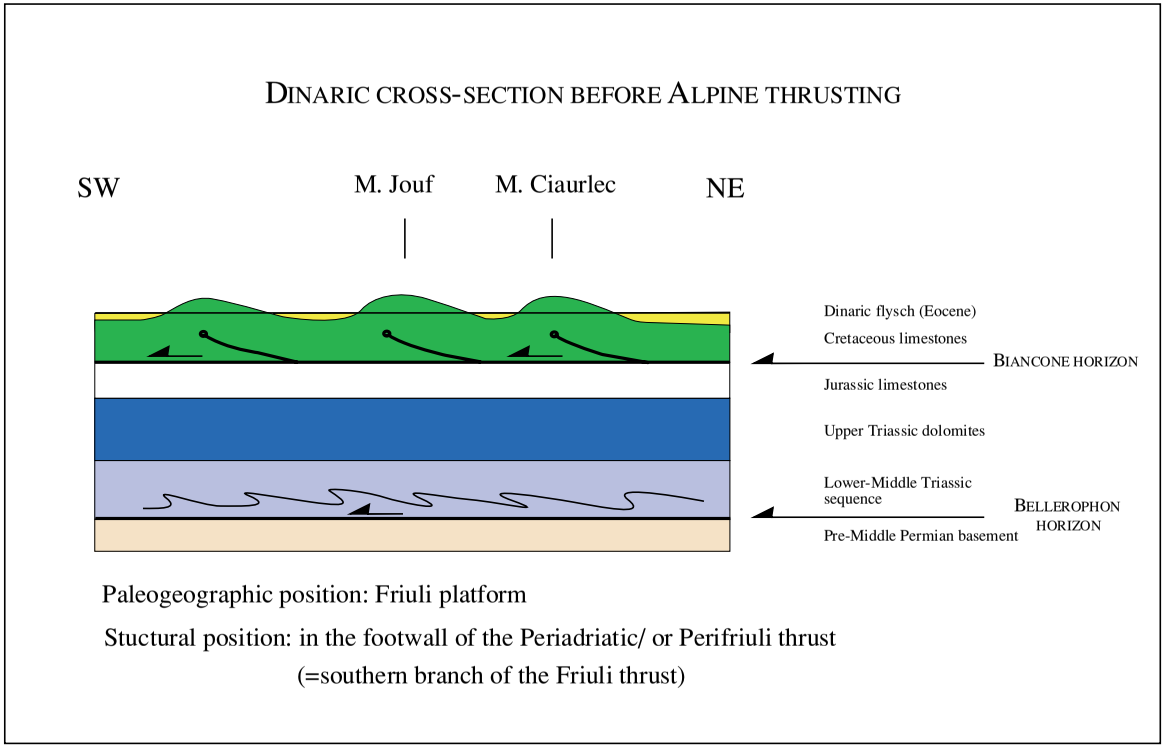

Fig. 15. Schematic Dinaric cross-section before Alpine thrusting. This section is located in the frontal part of the Friuli Alps near Maniago.

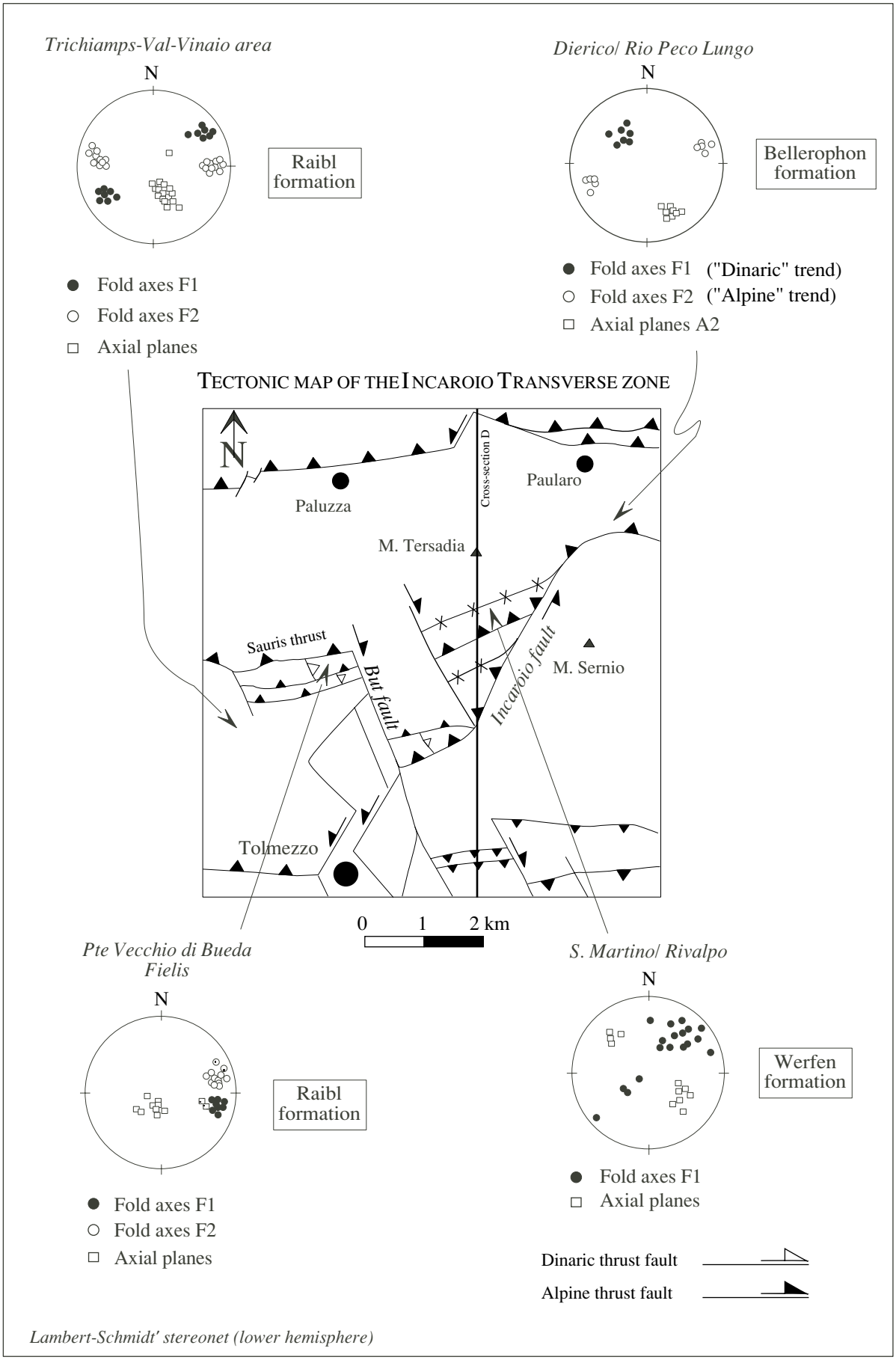

Fig. 16. Tectonic map of the Incaroio transverse zone (location in Fig. 9). Stereoplots show fold axes and axial planes in the incompetent layers.

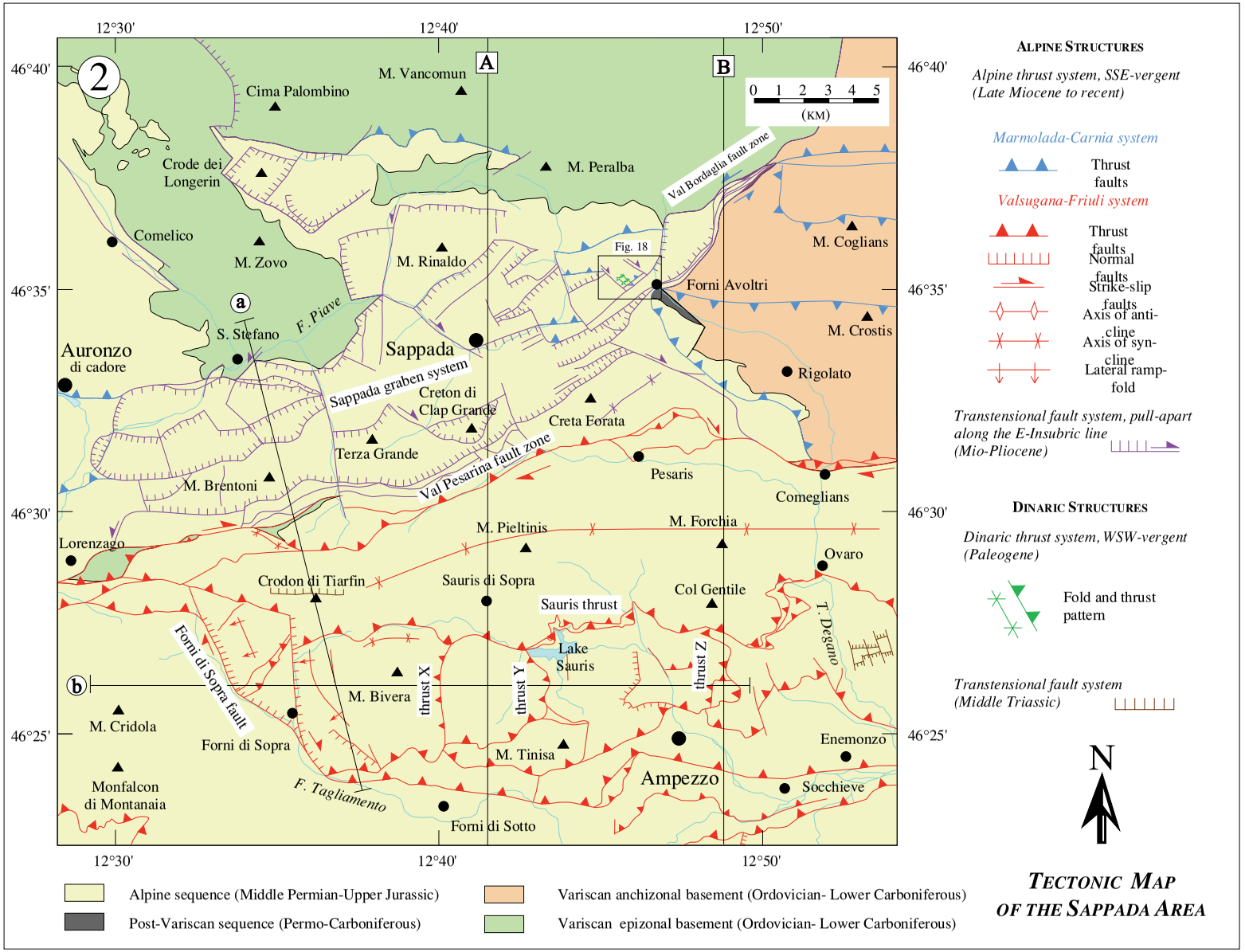

Fig. 17. Tectonic map of the Sappada area (n 2 in Figs. 2 & 3). Based on new mapping at 1: 25.000 and 1: 10.000, and after Frascari and Vai (sheets 4c-13, Monte Cavallino-Ampezzo, 1981). Large-scale cross-sections A and B refer to Figs. 23 and 24. Local cross-sections (a) and (b) refer to Figs. 40 and 41. Geological map of the Avoltri area is located by a rectangle (Fig. 18).

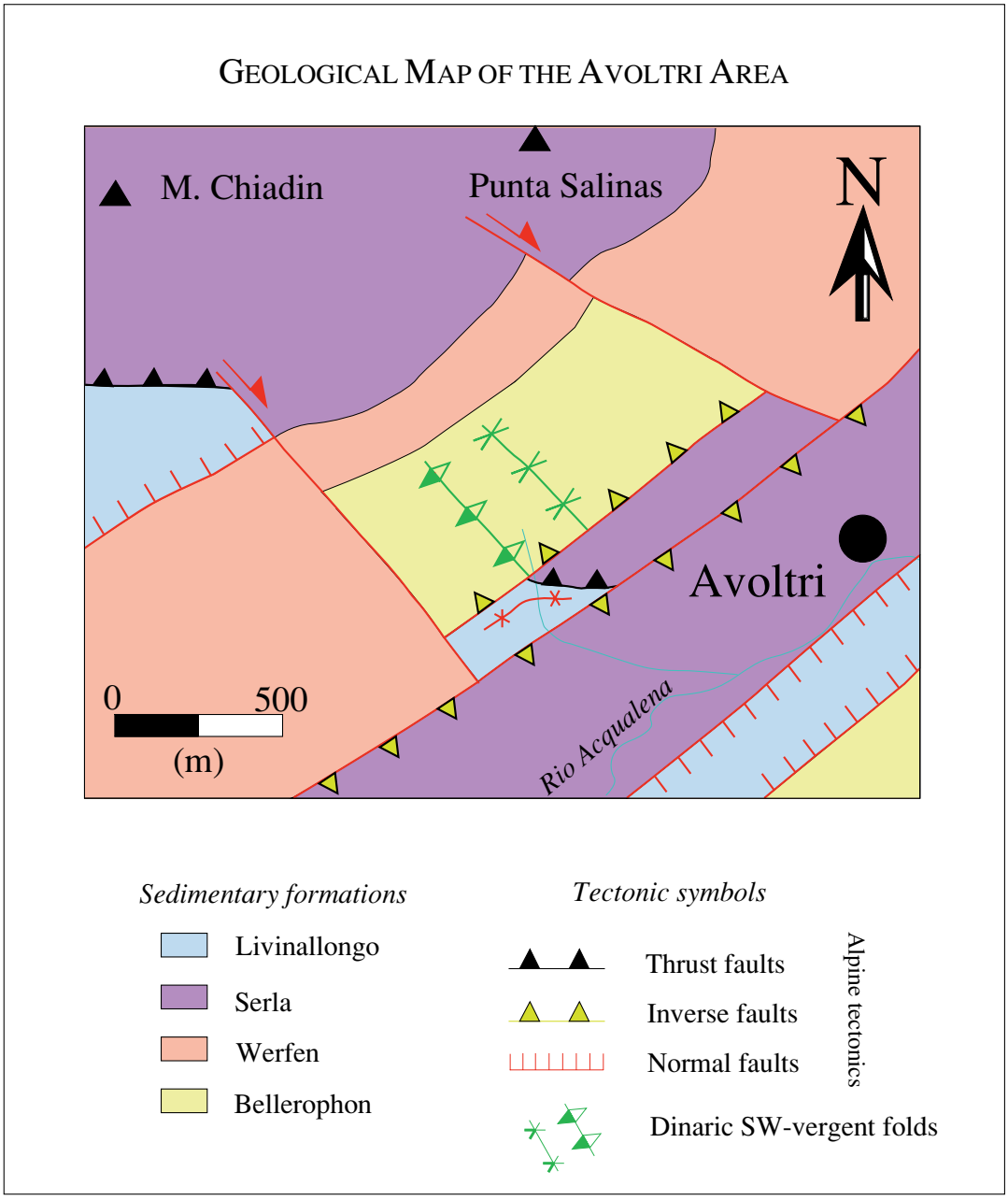

Fig. 18. Geological map of the Avoltri area (location in Fig. 17). Based on new mapping at 1:10.000. Note the cross-cutting relationships between the SW-vergent Dinaric folds and the Alpine reverse faults.

trending normal faults (Fig. 5). This is the only known example of Dinaric thrusts cut by Alpine normal faults.

3.2.3 Main results (interpretation)

Dinaric WSW to SW-vergent thrusts and faults cannot be connected to an overall network. In fact, many of these faults have loose ends since they were cut and dismembered by the younger active south-vergent Alpine thrusts. Nevertheless, the superposed structures have revealed some features of Dinaric deformation. Two décollement levels are recognized as having been active during Dinaric thrusting. The deepest follows the gypsum of the Bellerophon formation of Late Permian age and the second is located within the Biancone horizon at the base of the Cretaceous limestones (Figs. 4 and 15). Other décollement horizons are not excluded, but until now no structures have been identified that would indicate their presence. Accordingly, in the study area, Dinaric deformation consists mainly of a décollement in the Upper Permian evaporites and a number of splays with minor shortening that ramp through the Mesozoic sequence. This tectonic style concerns the northernmost part of the external Dinarides. Thermal data show the absence of metamorphism along some 250 km of exposure across Dinaric strike. In contrast, the central Dinarides (Trnovo-Sava nappe) in Croatia and southern Slovenia were deformed by far traveled thrust sheets (Schönborn, pers. comm.).

This tectonic style that implies long detachments, and the absence of metamorphism across Dinaric strike support the interpretation of a low critical taper. The reader is referred to Chapple (1978), Boyer and Elliott (1982), Davis *et al*. (1983), Woodward (1983), Dahlen *et al*. (1984), and Platt (1988) for explanations about the mechanics of frontal imbrication and details about critical taper models.

4. NEOGENE (ALPINE) TECTONICS

4.1 REGIONAL SETTING

4.1.1 Tectonic setting

The eastern Southern Alps are part of the south-vergent or backthrust part of the doubly vergent Alpine orogen. The eastern Southern Alps form a south-vergent brittle fold-and-thrust belt with flat-ramp-flat thrust trajectories and ramp-folds. The Periadriatic line, which is the eastern segment of the Insubric line, separates the eastern Southern Alps from the Eastern Alps in the north (Figs. 1 & 2). Several local names of valleys are used in the literature to describe different parts of this line (Pusteria, Gailtal). However, Periadriatic and E-Insubric are the most widely accepted names for describing this line or lineament. We have chosen in this study to use the name "E-Insubric" line in order to avoid confusion with the "Periadriatic overthrust" located farther south (this latter name was used by Castellarin, 1981). The E-Insubric line constitutes the present-day plate boundary between the European plate and the Apulian or Adriatic micro-plate. It is a remarkable, several hundred kilometers long, fault system, and which has experienced dextral displacement that has been documented by several authors (e.g. Laubscher, 1971a, 1985a; Rathore and Becke, 1980; Schmid *et al*., 1989, Polinski and Eisbacher, 1992; Fodor *et al*., 1996, 1998, and many others). The model of the lateral escape of the Eastern Alps to the east is mainly based on the dextral strike-slip movement of the E-Insubric line (Ratschbacher *et al.*, 1989, 1991).

In the west, active thrusting ends against the sinistral Schio-Vicenza line (some 50 km west of Venice), where the shortening is transferred southward across the Po plain to the Apennines (Semenza, 1974). In the east, shortening is transferred along the Dalmatian coast to the SE by dextral strike-slip faults. The seismic activity follows the current border to the NE of the Adriatic microplate (Slejko *et al*., 1987).

4.1.2 Structural style

Due to the alternation of various carbonate platform layers and shaly and evaporitic deposits, classical flat-ramp-flat thrust structures developed. Ramps developed through the rigid platform carbonates and flats in the evaporitic and shaly décollement horizons (Fig. 4). Because the exposed basement in the Carnic Alps shows Alpine brittle deformation (*e.g.*, Venturini, 1990b; Läufer, 1996), the flat-ramp-flat concept was also applied for the construction of the deeper parts of the sections. According to large-scale cross-sections (chapter 5), basement rocks were deformed at depths of 12-13 km to the surface and, therefore, deformation may have been ductile.

4.1.3 Map-view information

Maps are an important source of easily accessible information. Construction of tectonic maps is the first step in a process aimed at understanding geometry and kinematics. A tectonic map has to be kinematically admissible. Displacements along faults have to be transferred from one fault to another one in a coherent way, shortening must be compatible along a fault system. Cross-cutting relationships of faults and structures must correlate on sections and maps.

The tectonic map of the Southern Alps-Dinarides intersection is a compilation of published data [Castellarin (Editor), 1981; Ambrosetti *et al*. (1983), Bigi *et al*., 1992, and Schönborn, 1999] and new mapping (Fig. 2). The field area investigated during this study has been divided into six local maps (location in Figs. 2 & 3). The regional tectonic map of the easternmost Southern Alps shows that the Alpine thrusts are generally well aligned in an E-W direction in most of the region, whereas the frontal thrust is slightly curved (Fig. 2). According to the sedimentary sequences decribed in Cousin (1981), the Maniago thrust (called Periadriatic thrust by Castellarin, 1981, or Perifriuli thrust by Cousin, 1981) is suspected to follow the northwestern edge of the Jurassic-Cretaceous Friuli platform. Then the thrust transports the basinal sequences onto the Friuli platform. This case may illustrate

the strong influence of the shape of a paleoboundary on orientation of subsequent thrusting.

4.2 INHERITED FAULTS AND TRANSVERSE ZONES

The Southern Alps are divided by several transverse zones into compartments of different structures. The important role of these transverse structures was first recognized in the central Southern Alps by Laubscher (1985b, 1990) and by Schönborn (1992a, 1992b, 1994). Schönborn proposed quantitatively consistent kinematic models using a series of balanced cross-sections for unravelling these intricate zones. Transverse zones can be initiated along inherited faults or along paleogeographic boundaries such as a platform edge (Thomas, 1990). The origin of the inherited faults may be related to different tectonic events in the past. The paleotectonic evolution presented in chapter 2 describes the different events that produced inherited faults. The paleofaults are not easy to recognize in the field, but they are identified primarily based on abrupt lateral variations in thickness of the sedimentary cover which indicate the presence of buried growth faults. These growth faults are only exposed when they have been reactivated or eroded. Sedimentary evidences such as breccia are needed to prove the presence of synsedimentary fault. In fact, thicknesses may also vary in function of the distance of the depo-center, which may vary as the consequence of sea-level change. In that case, thickness changes are not related to synsedimentary tectonics.

The interference between inherited Mesozoic faults and Alpine structures is dominant in the eastern Southern Alps. Resulted structures are described as well in the central Southern Alps (Bernoulli *et al*., 1992; Schönborn, 1992a, 1994; Bertotti *et al*., 1993) as in the eastern Southern Alps (Bosellini and Doglioni, 1986; Doglioni, 1992b). Middle Triassic and Early Jurassic rifting lead to important normal faulting in the thick passive-margin sequence. These normal faults, preceding the opening of the Halstatt-Meliata ocean in the east and the Alpine Tethys in the west, acted as zones of mechanical weakness and led to segmentation during subsequent thrusting. The Mesozoic platform and

basin distribution also influenced subsequent Dinaric and Alpine tectonics. Subsequent reactivation commonly does not occur on the inherited fault plane, but produces a parallel network of faults (Gillcrist *et al.*, 1987). Fault reactivation depends on orientation of the inherited fault with respect to the main compressive stress. This geometric factor was termed slip tendency (Morris *et al.*, 1996) and calculates the probability of reactivation of faults. When compression occurs, different structures may be initiated depending on the orientation of the inherited faults or paleoboundaries. Paleoboundaries oriented perpendicular to compression generally triggered thrusts. Paleofaults oriented approximately parallel to subsequent compression partly were commonly reactivated as strike-slip faults, often tear faults. Examples are the Dinaric sinistral transverse faults following the edges of the northwestern Friuli platform (Fig. 11). Paleostructures oriented obliquely to subsequent compression tend to give rise to strike-slip faults. Strike-slip reactivation is the case in the Tagliamento and Incaroio transverse zones, as is described in the following.

The eastern Dolomites and the Friuli Alps are divided into different segments by the following major transverse zones (all names are informal):

- the Cimolais-Longarone zone
- the Incaroio zone (along the Chiarso River)
- the Tagliamento zone (between Amaro and Gemona)

4.2.1 The Cimolais-Longarone Transverse Zone

The Cimolais-Longarone transverse zone was not integrated in this study. It is located between the Piave and Cellina Rivers (approx. between the villages of Longarone and Cimolais) and was studied by Schönborn in 1992-1993 (unpublished). The transverse zone is bounded near Longarone by a sinistral strike-slip fault and near Cimolais by a dextral strike-slip fault. The present-day geometry of this zone reflects the reaction of an

Alpine thrust to an inherited superposition of Early Tertiary ramp-folds in the south and Mesozoic faults carried piggy-back on top of them in the north.

4.2.2 The Incaroio Transverse Zone

Previous data. The study of the Incaroio transverse zone is based on various geological maps from Bianchin *et al*. (1980), Frascari *et al*. (1981), and Carulli *et al*. (1982b). Frascari *et al*. (1980) and Roeder and Lindsey (1992) have constructed a cross-section through the Incaroio transverse zone. Stratigraphic data from this area is found in Frascari (1982).

Observations and new data. The northern part of the Friuli Alps is divided by a major N-S striking transverse zone into compartments of different structural style. This transverse zone is located between the Chiarzò and But rivers (Fig. 9). The N020-030° trending Incaroio fault and the NNW-SSE But fault branch together in the south, north of Tolmezzo (Fig. 9). They define a triangular indenter. The internal part of the indenter is deformed by southeast-vergent folds (stereoplot of S. Martino/ Rivalpo in Fig. 16). It is important to note that these folds are oblique with respect to the north-south Alpine transport direction. Kinematic criteria such as slickensides and stylolites indicate sinistral transpressive movements along the Incaroio and pure dextral strike-slip movements along the But fault. The Incaroio fault outcrops well on the left bank of the Chiarzò River in the Incaroio valley. By contrast, the But fault rarly outcrops.

Interpretation. First, the age of the Incaroio and But faults must be debated. Are they inherited or newly formed during Alpine teconics? No direct arguments can be found for inherited structures of Early Jurassic age since all sediments younger than the Middle Triassic have been eroded in the Incaroio area. The But fault separates Carnian beds consisting of deltaic facies sedimentary rocks in the west and lagoonal facies sedimentary rocks in the east (Jadoul and Nicora, 1979; Brusca *et al*., 1981; Frascari, 1982; Carulli *et al*., 1982b). During Middle Triassic times, this whole area (Carnico-Bellunese basin)

underwent continued differential subsidence. Several N-S striking horsts and grabens were distinguished by Viel (1979). Taken together, these structural and stratigraphic observations indicate a Middle Triassic age for the But fault. Mapping of the Incaroio fault has revealed that the Ladinian dolomites (Schlern formation) are lacking northwest of the fault. There, the Carnian Raibl beds directly overly on the Ladinian Wengen formation. Southeast of the Incaroio fault, the stratigraphic pile is complete. So, Middle Triassic synsedimentary tectonics could be also explain the origin of the Incaroio fault. Based on mapping and stratigraphic features, the Incaroio and But faults are suspected to be inherited faults of probably Middle Triassic age.

The geometry of the Incaroio transverse zone may be regarded as a triangular indenter pushed southward during Alpine deformation (Fig. 16). This complex structure was probably initiated along the N020°- 030° trending Incaroio fault (informal name, Fig. 16). This inherited fault is not oriented ideally with respect to the north-south Alpine transport direction and thus becomes reactivated as a sinistral transpressive fault during south-vergent Alpine deformation. This inherited fault plays a very important role: it separates the northern part of the Friuli Alps into two segments of different structures and serves as a transfer zone between the north-vergent Fella backthrust to the east and the south-vergent Sauris thrust to the west (Fig. 9). The sinistral transpressive movement along the Incaroio fault is indicated by striations on fault planes and matches well with the direction of the Incaroio fault with respect to the north-south Alpine transport direction.

An important question must be debated: how can we explain the oblique orientation of the SE-vergent folds in the Incaroio indenter with respect to the north-south Alpine transport direction? Two kind of models are proposed here:

- Deflection of the main compressive stress near the Incaroio fault (local rotation of $\sigma 1$)
- Rotation of sedimentary strata located in the Incaroio indenter above a décollement horizon

The first model is based on the Alpine reactivation of the Incaroio inherited fault. The maximum compressive stress is deflected by the Alpine reactivation of the inherited Incaroio fault as a sinistral strike-slip fault. This interpretation implies an anticlockwise rotation of σ1 from circa N350 (Alpine transport direction) to N320 (inferred from SE-vergent folds). A similar model may be given for explaining the focal mechanism pattern recorded near the inherited Tagliamento fault (details in chapter 6). In this interpretation, the role of the Incaroio fault is dominant, whereas the But fault would have no significant influence.

The second model implies an Alpine reactivation of the inherited But fault. The strain incompatibilities due to the reactivation of both cross-cutting faults (But and Incaroio faults) lead to rotations within the triangular indenter and may explain the obliquity of the southeast-vergent folds with respect to the north-south trending maximum principal shortening direction. Nevertheless, rotation only occurs if the sedimentary strata can be detached above a décollement horizon. In this example, anticlockwise rotation would occur and would be probably limited to one side of the reactivated fault: the dextral But fault which is better oriented (NNW-SSE) with respect to the north-south Alpine transport direction.

According to field observations (reported on cross-section D, Fig. 26), no detachment was identified in the Incaroio area. In conclusion, the interpretation of rotation is not supported by field data. The interpretation of a local deflection of σ1 by the sinistal Alpine reactivation of the inherited Incaroio fault is largely preferred in this study.

4.2.3 The Tagliamento Transverse Zone

Previous data. The study of the Tagliamento transverse zone is based on various works about the geology of the M. S. Simeone-Brancot area (Amadesi, 1968; Amadesi and Lenarduzzi, 1973, Cousin, 1981) and on the tectonic and geological maps of Pontebba

(Frascari *et al*., 1981; Gortani and Desio, 1925, respectively) and Udine (Carobene *et al*., 1981; Feruglio, 1925, respectively). Structure of the M. S. Simeone was integrated in large-scale N-S profiles by Frascari *et al*. (1980) and Roeder and Lindsey (1992).

Observations and new data. The southern part of the Friuli Alps is divided by a major N-S striking transverse zone into compartments of different structural style. This transverse zone extends along the Tagliamento River from Amaro in the north to Osoppo in the south, and is informally called Tagliamento transverse zone in this study (Fig. 19). The Tagliamento transverse zone is formed by a network of parallel, NNE-trending faults. Current activity and kinematics of these faults are also proved by focal mechanisms measured during the recent earthquakes of 1976 and 1980 (chapter 6, see also Slejko *et al.,* 1987). Two cross-sections (d) and (e) have been constructed in the Tagliamento transverse zone (Figs. 20 & 21). Both cross-sections were balanced using GEOSEC-20^{TM}. They have been line-length balanced above the basal detachment within the Carnian evaporites. They show a backthrust in the north and a complex south-vergent thrust with minor splays in the south. A south-vergent out-of sequence thrust cuts between the backthrust and the forethrust. This out-of-sequence thrust continues to the east as is shown on the large-scale cross-sections E, F and G (Figs. 27-29). The cross-section (e) is complicated by a minor backthrust linked to the south-vergent thrust (Fig. 21). Cross-section D goes across the Tagliamento transvers zone (Fig. 26).

The age of the faults that initiated the Tagliamento transverse zone is revealed by significant changes in Early Jurassic deposits. Prominent thickness changes follow an E-W direction. In the west (M. Cuar, M Prat), the Liassic limestones are about 50 m-thick, whereas in the east (near Gemona), Liassic deposits are about 500 m-thick (stratigraphic sections from Cousin, 1981). Additionally, in the west the upper Pliensbachian-Bajocian sequence is lacking, probably linked to emersion. Moreover, pelagic formations were deposited in the same time on the eastern side. The synsedimentary fault strikes N10°, the eastern block has been down thrown. Along Lake Cavazzo further north, another

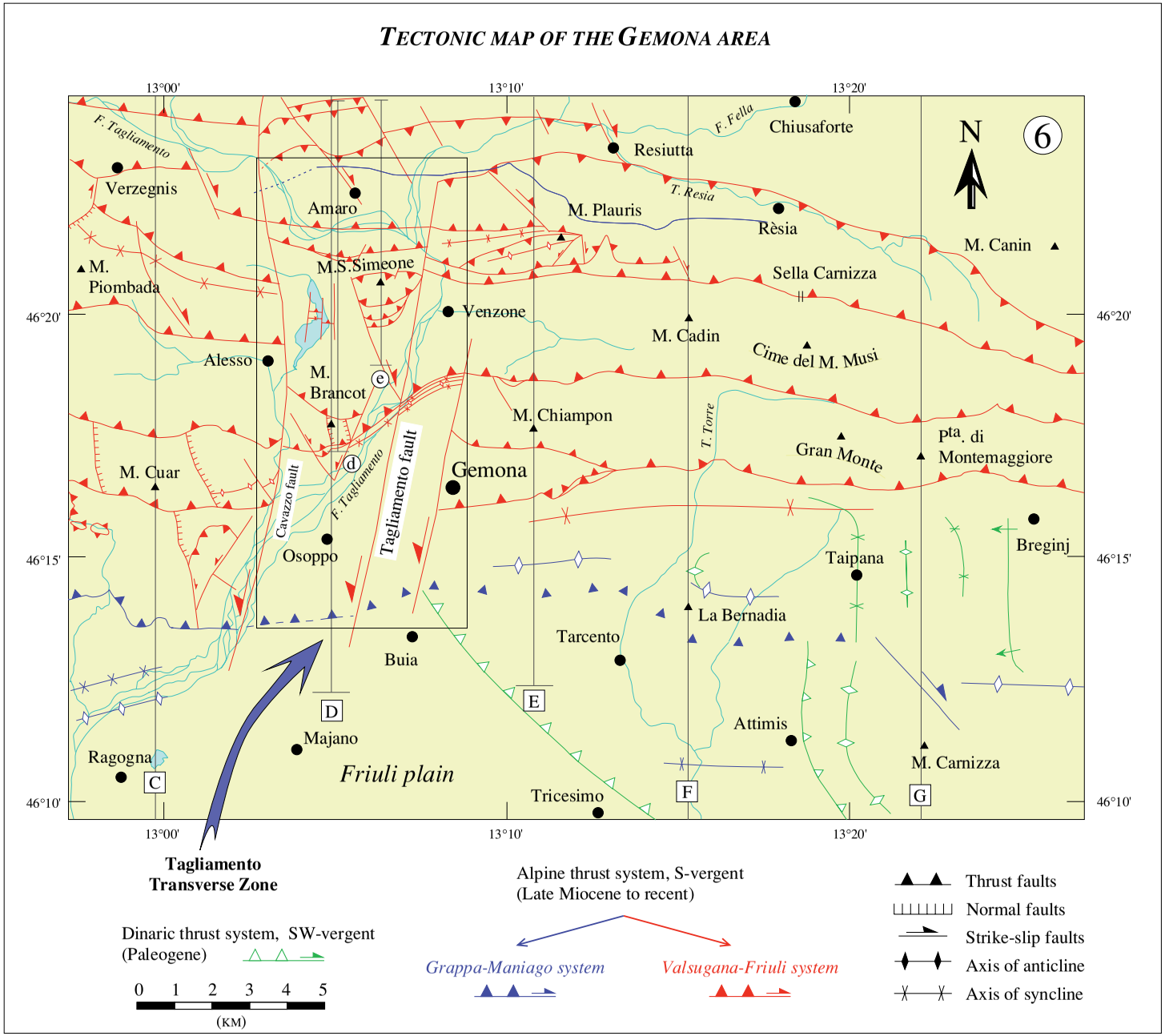

Fig. 19. Tectonic map of the Gemona area (n°6 in Figs. 2 & 3). Based on new mapping at 1: 10.000 and 1: 25.000, and on previous mapping of Feruglio (sheet 25 Udine, 1925, 1929), and Carobene *et al*. (1981). Large-scale cross-sections C, D, E, F and G refer to Figs. 25-29. In the Tagliameno transverse zone, local cross-sections (e) and (d) refer to Figs. 20 and 21.

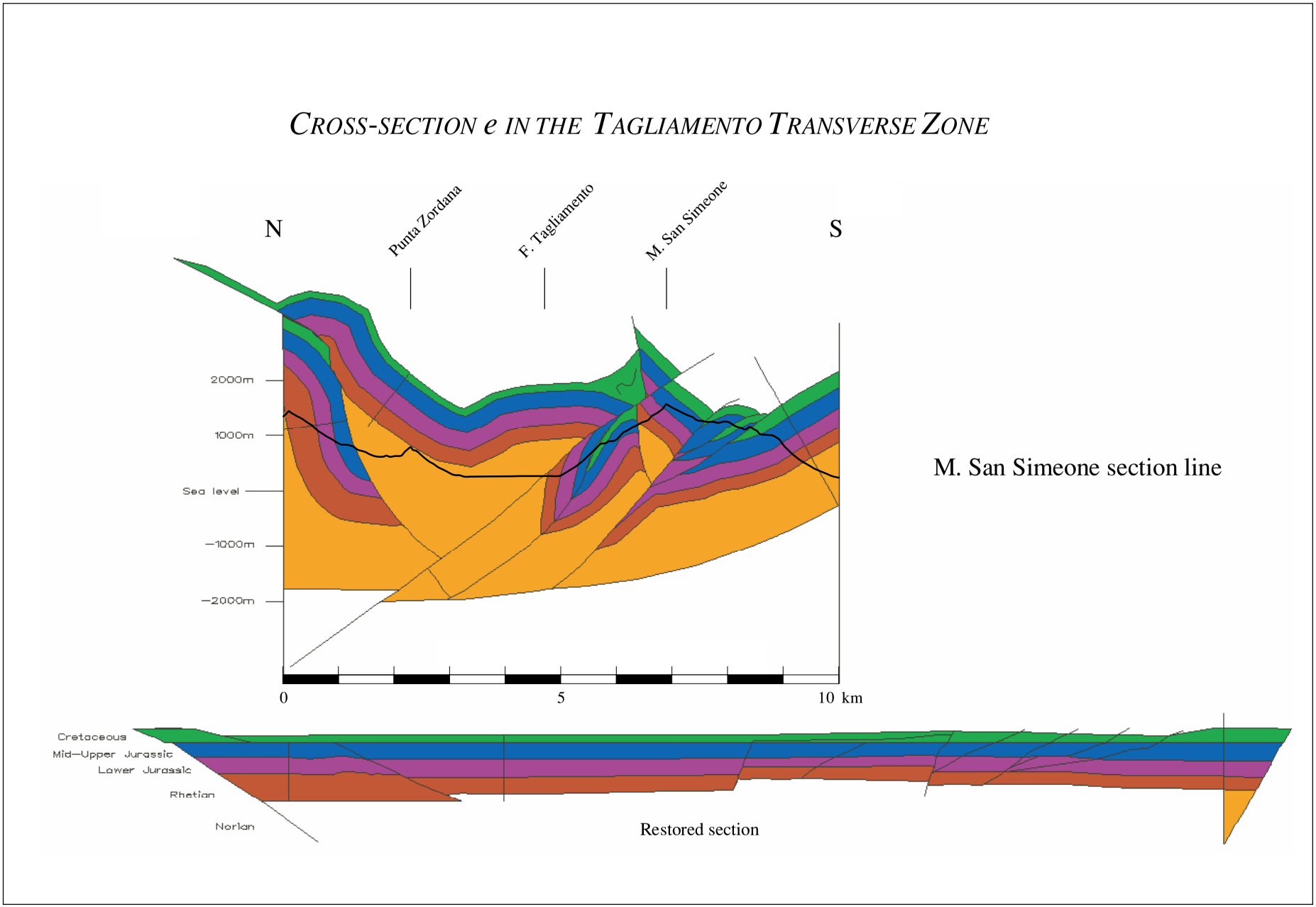

Fig. 20. Cross-section and restored section (e) through the Tagliamento transverse zone (location in Fig. 19).

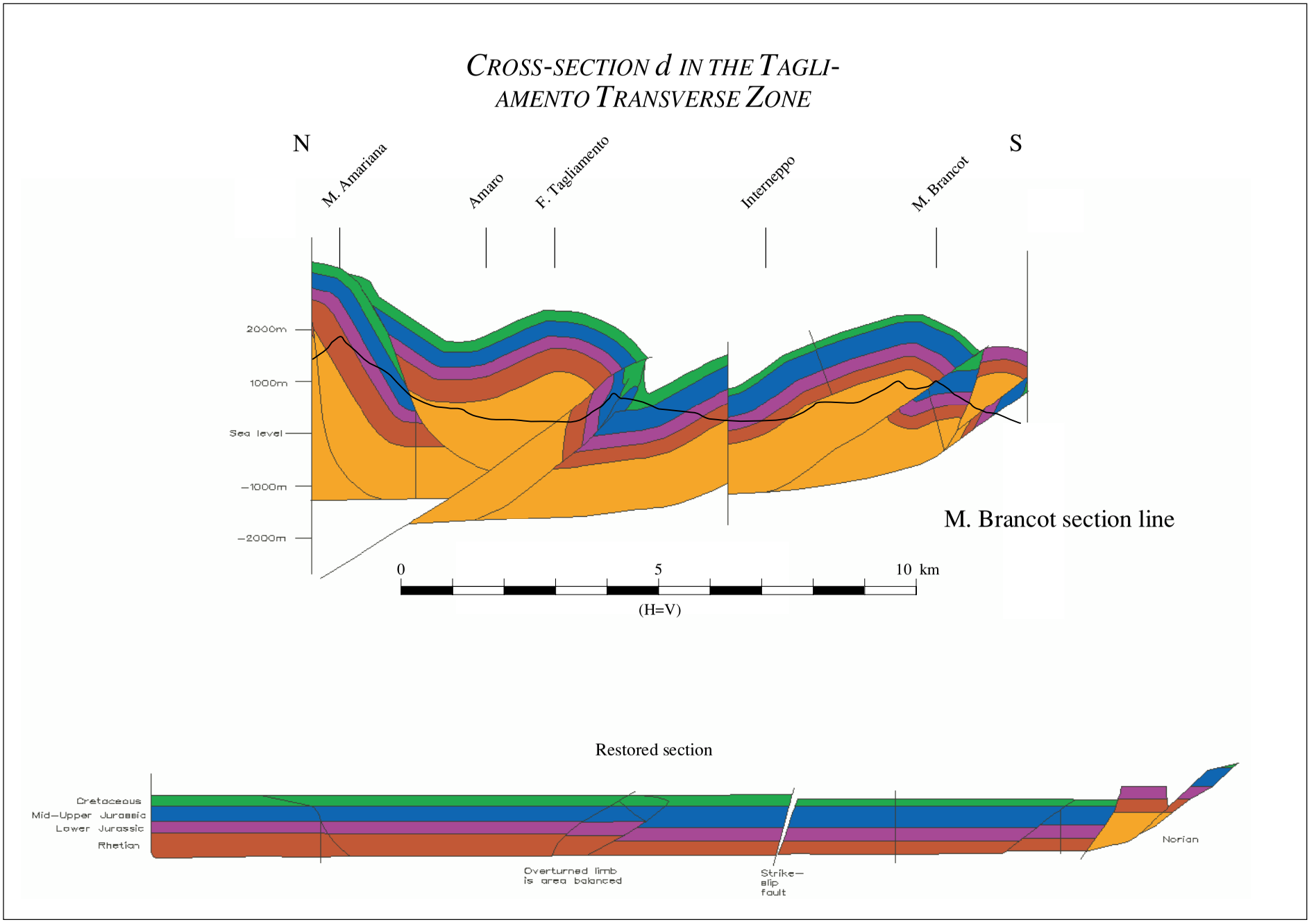

Fig. 21. Cross-section and restored section (d) through the Tagliamento transverse zone (location in Fig. 19).

synsedimentary fault, the Cavazzo fault (Fig. 19), parallel to the Tagliamento fault is suspected for the same reasons described above.

Interpretation. As the steep Tagliamento and Cavazzo inherited faults trend in an acute angle to the N-S Alpine transport direction, they gave rise to a sinistral transverse zone. During Alpine thrusting, sinistral reactivation of thsee inherited faults triggered anticlockwise rotations of blocks around their vertical axis (Fig. 19). Moreover, the combined effect of newly formed dextral strike-slip faults and sinistral reactivation of the inherited faults leads to asymmetric triangular indenters (M. S. Simeone and M. Brancot, Fig. 19). The geometry within these contractional indenters shows an intricate fold and thrust structure.

4.3 TECTONOSTRATIGRAPHY

Balancing a cross-section needs in a first step the establishment of a tectonostratigraphy (mechanichal stratigraphy) of the deformed area. Based on the stratigraphic column and observations of deformation style of different strata or rock types in the study area or analogous settings, the stratigraphic column can be divided into mechanically stiff and soft units. Thus, the tectonostratigraphy indicates the potential décollement levels within the stratigraphic wedge and serves to predict the structural style in not exposed areas. Accordingly, this mechanical stratigraphy is the most readily applied criterion for assessing what kind of structural style is expected, and in particular for the construction and extrapolation of structures at depth.

The rigid carbonate layers alternating with shales and evaporitic horizons determine the flat-ramp-flat tectonic style (Fig. 4). The large-scale structure of the eastern end of the Southern Alps is mainly controlled by two majors décollement levels. The deepest is located in the evaporitic sequence of the Upper Permian Bellerophon formation. The Middle Permian conglomerates and sandstones of the Tarvis breccia and Val Gardena formations remained attached to the crystalline basement rocks during Alpine thrusting.

The second décollement follows the Carnian Raibl horizon further up in the stratigraphic column. The thick Upper Triassic platform carbonates behaved as the most rigid layer during deformation and serve as a key-bed for the restoration. Some minor décollement horizons are located at the base and the top of Cretaceous deposits (Biancone and Scaglia horizons, respectively), and at the top of the Paleogene flysch, but none of them systematically served as a detachment. This depends presumably on the structural position and the local sedimentary facies. Between the Ladinian and Norian rigid carbonate layers, the Carnian Raibl hemipelagic and shaly sediments are intensively folded. The same can be observed in the Wengen and Livinallongo volcanodetritic sediments, located between platforms of Anisian and Ladinian ages.

The synthetic stratigraphic column in figure 4 refers to the northeastern end of the Dolomites and the Friuli Alps. In the eastern Dolomites and the western Carnic Alps, the crystalline basement consists of anisotropic epizonal micaschists and phyllites, intruded by large, homogeneous, massive and mainly acidic plutons (various authors, 1971). These heterogeneities, however, had little or no influence on Alpine tectonics. The basement thrusts cut across basement heterogeneities and formed thrust sheets with ramp-folds. Even in the central and eastern Carnic Alps where metamorphism is very low (anchizonal), internal deformation is attributed to the Variscan orogeny (Vai, 1979; Castellarin and Vai, 1981; Venturini, 1990a, 1990b; Läufer, 1996; Rantitsch, 1997; Hubich, 1999). There, faults and ramp-folds seem to be the main expression of Alpine deformation.

4.4 ALPINE THRUST SYSTEMS

The eastern South Alpine fold-and-thrust belt is built up by three major thrust systems (Fig. 2). Each system involves a pre-Upper Permian basement unit. They can be identified on various local tectonic maps (Figs. 5, 9, 12, 13, 17 & 19) as well as on an overview map (Fig. 2), and on cross-sections (Figs. 23-29). From the hinterland to the foreland these have been called the Carnia system, the Friuli system and the Maniago system. These systems are differentiated for the first time in this study and, the names

assigned to them are informal. These three thrust systems can be followed to the west into the Dolomites, where they correlate with the three systems defined by Schönborn (1999). The Carnia system extends into the Marmolada-Sorapiss system, the Friuli system is linked to the Valsugana system and the Maniago system continues into the Grappa system.

4.4.1 The Carnia thrust system

The Carnia thrust system is mainly located in the Carnic Alps. Based on structural continuation, this thrust system is interpreted in this study to be connected with the Marmolada-Sorapiss thrust system located farther west. However, the transtensive zone of Sappada is located in between (chapter 7). Slip along this system is difficult to quantify due to the absence of reliable markers in the pre-Mesozoic sequence.

4.4.2 The Friuli thrust system

The Friuli thrust system constitutes the largest part of the tectonic framework by far. It consists of several thrusts branching into different splays. The southernmost thrust of the Friuli transported the pelagic sequences of the Perifriuli domain onto the Friuli platform.

4.4.3 The Maniago thrust system

The frontal Maniago thrust splays into two branches when a basement slab was emplaced onto the undeformed authochthonous cover. The main branch followed the upper Cretaceous décollement. The splay broke through the hinge of the ramp anticline and transported Cretaceous onto Miocene. This fault is the southernmost thrust exposed. The ongoing activity along the Maniago thrust system is documented by recent earthquakes, whose hypocenters are aligned along the thrust plane (chapter 6).

4.5 TIMING OF DEFORMATION

The best constraint on timing the onset of deformation is dating the youngest sediments below thrust faults. The older bracket of the age of Alpine deformation is given by Early Miocene deposits found in the footwall of thrusts of the Marmolada-Sorapiss thrust system (Doglioni and Siorpaes, 1990) and Tortonian sandstones observed below the Valsugana thrust (Venzo, 1939). Miocene sedimentary facies of the foreland deposits (Massari, 1990; Massari *et al*., 1993) arguably point to an onset of thrusting in the easternmost Southern Alps (more exactly of the Friuli-Valsugana system) during the middle Tortonian. The ongoing activity of the deformation is documented by uplifted Quaternary terraces (Benedetti *et al*., 1995), and intense continuous seismicity (*e.g*., the recent Friuli earthquakes of 1976 and 1980, Slejko *et al*., 1987; Andersen and Jackson, 1987).

5. CROSS-SECTION BALANCING IN THE FRIULI ALPS

5.1 CONSTRUCTION OF CROSS-SECTIONS

Various problems hamper balancing in the Friuli Alps. No deep seismic reflection or well data are available to constrain the deep structure. The deep wells of the Friuli plain give a scanty information due to their excessive distance from the section lines. Additionally, tectonic difficulties such as the superposition of two nearly perpendicularly trending contractional phases, the presence of transverse zones (*e.g.*, Tagliamento and Incaroio), and abrupt thickness changes due to Mesozoic paleotectonics complicate section balancing. Nevertheless, the tectonic style of the eastern Southern Alps is favorable for the construction of balanced cross-sections for the following reasons: (i) there are prominent detachment horizons, separated by thick rigid layers with minimal internal shortening, (ii) bed thickness in the mainly chevron-type folds is largely preserved (deformation by flexural slip, no thickening or thinning of strata), (iii) the domain was deformed at very low temperatures, and (iv) large shortening. Accordingly, the balancing concept may be applied to the Friuli Alps. Based on surface data, consistent sections may be drawn thanks to kinematic balancing.

The first step consists in choosing a good line of section. An ideal section line should have at least the following qualities:

- parallel to the transport direction
- does not cut major strike-slip faults
- optimizes proximity to data, particularly for the younger deformation phase

Different indicators can be used to define the transport direction in a brittle fold-and-thrust belt. The transport direction is determined best with large-scale structures such as thrust direction, fold axes and fold vergence. Small-scale indicators such as slickensides, stylolites on the fault planes, shape fabrics or shear bands should be used only statistically

over large areas because they might be influenced by local inhomogeneities. In a seismically active thrust belt such like the Friuli Alps, earthquake focal mechanisms can be also used as kinematics indicators. In the Friuli Alps, all the kinematic indicators described above support a north-south transport direction.

Major sinistral and dextral strike-slip faults limit the Tagliamento and Incaroio transverse zones. For this reason, only one large-scale cross-section has been constructed inside these zones (section D). This section shows only the geometry inside these intricate zones since strike-slips hamper balancing and calculating the shortening. Consistent sections may be constructed west and east of these transverse zones since no other major strike-slip faults were observed.

The last point, that the best line of section should be chosen in the area with maximum information is evident, although often forgotten. Obviously, intensive fieldwork improves the choices of cross-section location.

5.1.1. Geometry of the autochthon

The depth and the dip of the undeformed autochthon under the foreland must be known in order to construct balanced sections through a frontal fold-and-thrust belt as it defines the lower boundary of the system. The best information is provided by seismic-reflection data or deep wells.

Seismic-reflection data and deep wells constrain the top of the autochthonous rocks of the foreland. There is no seismic data in the Friuli thrust belt, but seismic-reflection data of other thrust belts suggest the dip of the undeformed autochthon to be generally on the order of 1° to 4° (*e.g.*, North American Cordillera; Bally *et al.*, 1966; Oldow *et al.*, 1989, and Appalachians; Cook *et al.*, 1979). In this study, the undeformed autochthon has been drawn with an average dip of 2.5° towards the hinterland to the north. This value is

assumed to be constant on each section since the flexure of the downgoing plate in better documented cases is rather uniform and may be projected over large distances along strike.

For constructions of this study, the depth of the Mesozoic in the foreland was designed according to AGIP wells (AGIP, 1977; Pieri and Groppi, 1981; Cati *et al*., 1987b, Sartorio and Rozza, 1991; Barozzi and Colombi, 1992), shallow seismic-reflection profiles located in the Friuli-Veneto plain (Amato *et al*., 1977; Pieri and Groppi, 1981), and magnetic and gravimetric data acquired by AGIP (AGIP, 1984; Arisi-Rota and Fichera, 1985; Cassano *et al*., 1986; Cati *et al*., 1987a; Cavallin and Pirini Radrizzani, 1987). The thickness of the Mesozoic sequence was adapted to outcrops and to data from AGIP wells located in the Friuli-Veneto plain (*e.g*., S. Dona 1, Eraclea 1, Cavanella 1, Cesarolo 1, Le Grave 1, Gemona 1, Bernadia 1, Terenzano 1, Lavariano, Buttrio 1, Donà di Piave 1, Grado 1), and in the Northern Adriatic Sea (*e.g*., Assunta 1, Amanda 1 bis, Triglia 1, Amira 1, and many others located further south). The Cesarolo 1 well (T.D. 4332 m) completely drilled the southern edge of the Friuli platform (Cati *et al*., 1987b). It ends in the Upper Triassic Dolomia Principale formation. The Amanda 1 bis well (T.D. 7305 m) drilled in the Northern Adriatic Sea, about 50 km E from Venice (long. 13°00'38", 094 E; lat. 45°24'47", 063 N) reached sedimentary strata of Permian age at depth of 6840 m (Cati *et al*., 1987b; Sartorio and Rozza, 1991). This well ends in the Goggau limestones of Lower Permian age. The Middle Permian Amanda formation is directly overlain by limestones of Middle Triassic age (Latemar formation of latest Anisian-Ladinian age) in this well. The Assunta 1 well (T.D. 4747 m) drilled in the Northern Adriatic Sea reached Caledonian granites (Barozzi and Colombi, 1992). An important part of the AGIP well data was integrated in the large-scale cross-sections of Roeder and Lindsey (1992). All these published data have been used to constrain the southern part of the cross-sections (Figs. 23-29) in the Friuli plain where the regional pin-line was placed.

5.1.2 Location of section lines

The Tagliamento transverse zone in the south and the Incaroio transverse zone in the north constitute two major aligned north-south trending structures in the Friuli Alps (Fig. 22). They cut the belt into two segments of completely different structures, defining three blocks: a central block that corresponds to the transverse zones separates the western and eastern blocks. Consequently, the spatial distribution of cross-sections is organized according to these three blocks (Fig. 22). Three cross-sections A, B and C (Fig. 23, 24 and 25) have been constructed in the western block, three others sections E, F and G (Figs. 27, 28 and 29) in the eastern block, and a last one (section D) inside the central block (Fig. 26). These seven cross-sections are drawn N-S and extend from the E-Insubric line (Periadriatic line) at the north end (Austria) to the Friuli plain at the south end (Figs. 23-29). The length of section lines varies from 50 to 67 km.

5.1.3 Geometry of the western block (sections A, B and C)

Cross-sections A, B and C illustrate the geometry of the western block (map location in Fig. 22, and cross-sections in Figs. 23-25). The three sections have been constructed in the same way. The large-scale structure is made up of a superposition of the Lower-Middle Triassic unit onto another one. The same thrust produces a stack of south-vergent slices further south, detached above the Carnian décollement horizon. The three sections show a detachment between the Middle Triassic unit and the Upper Triassic unit. The basal Lower-Middle Triassic unit thrust southwards another Lower-Middle Triassic unit. Further south, the Maniago thrust transported a basement slab onto the undeformed authochtonous of the foreland. The thrust is divided further up into two branches, whith one following the décollement in the Upper Cretaceous beds. The other branch is emergent and produced an anticline formed by Cretaceous limestones. This anticline is too tight to involve Upper Triassic strata. This implies a décollement in the Lower Cretaceous Biancone horizon above the rigid Jurassic and Upper Triassic layers. As this thrust emerges in Maniago, the frontal thrust system has been called "Maniago thrust system" (informal name).

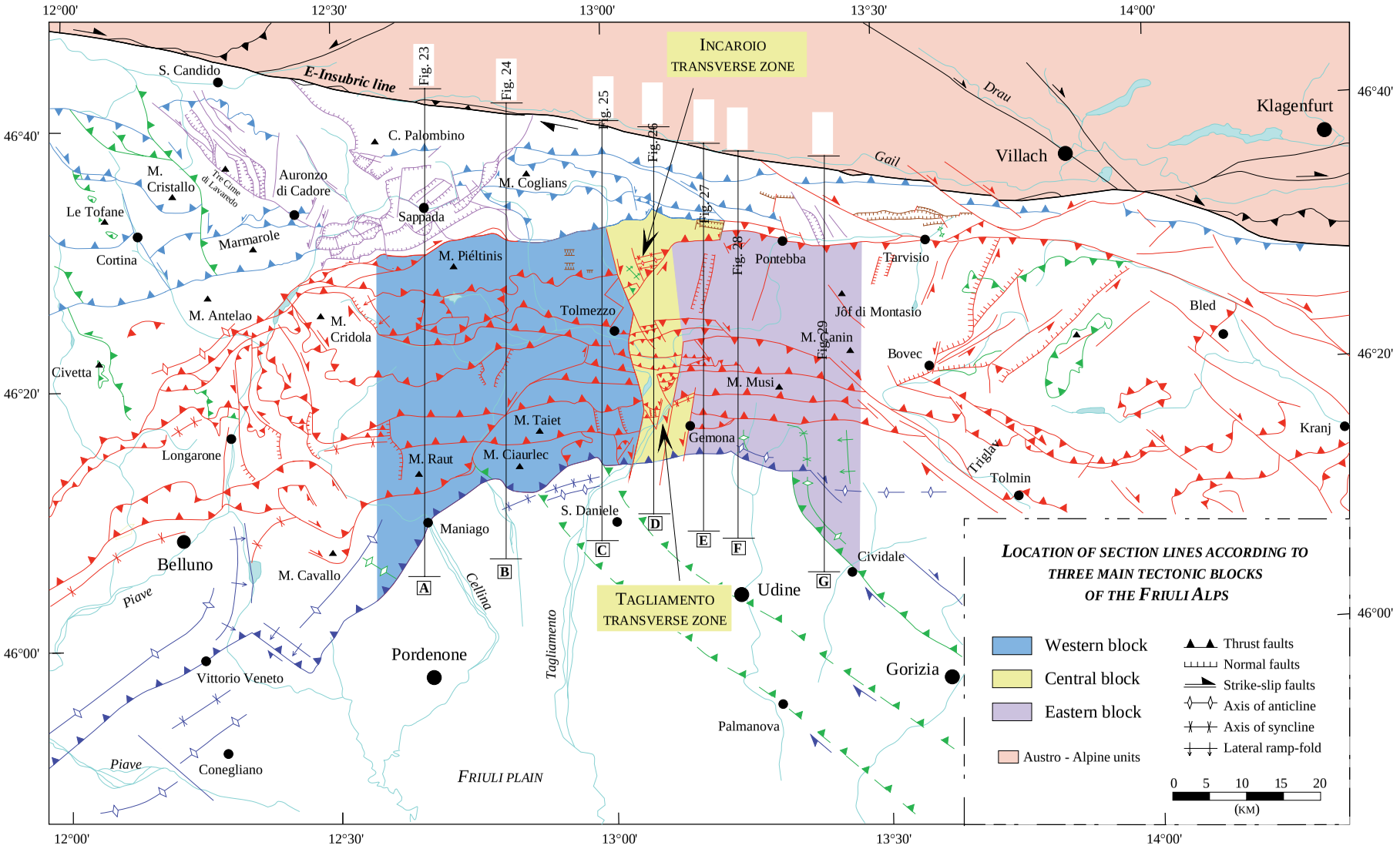

Fig. 22. Location of section lines according to three main tectonic blocks. Large-scale cross-sections A-G refer to Figs. 23-29. The Incaroio and Tagliamento transverse zones are located in the central block.

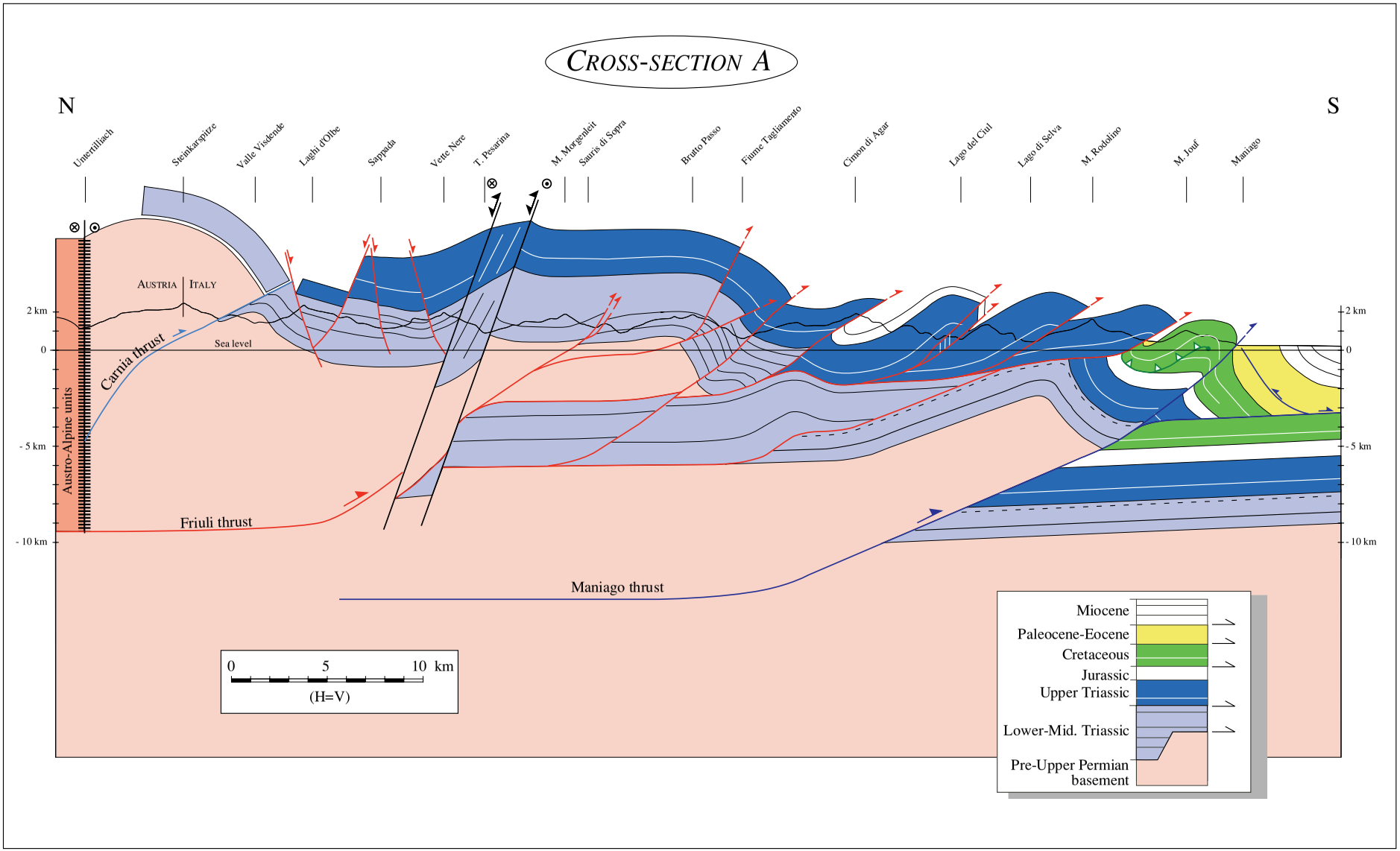

Fig. 23. Large-scale cross-section A from the E-Insubric line to the Friuli plain (location in Figs. 2, 3, 13, 17 and 22).

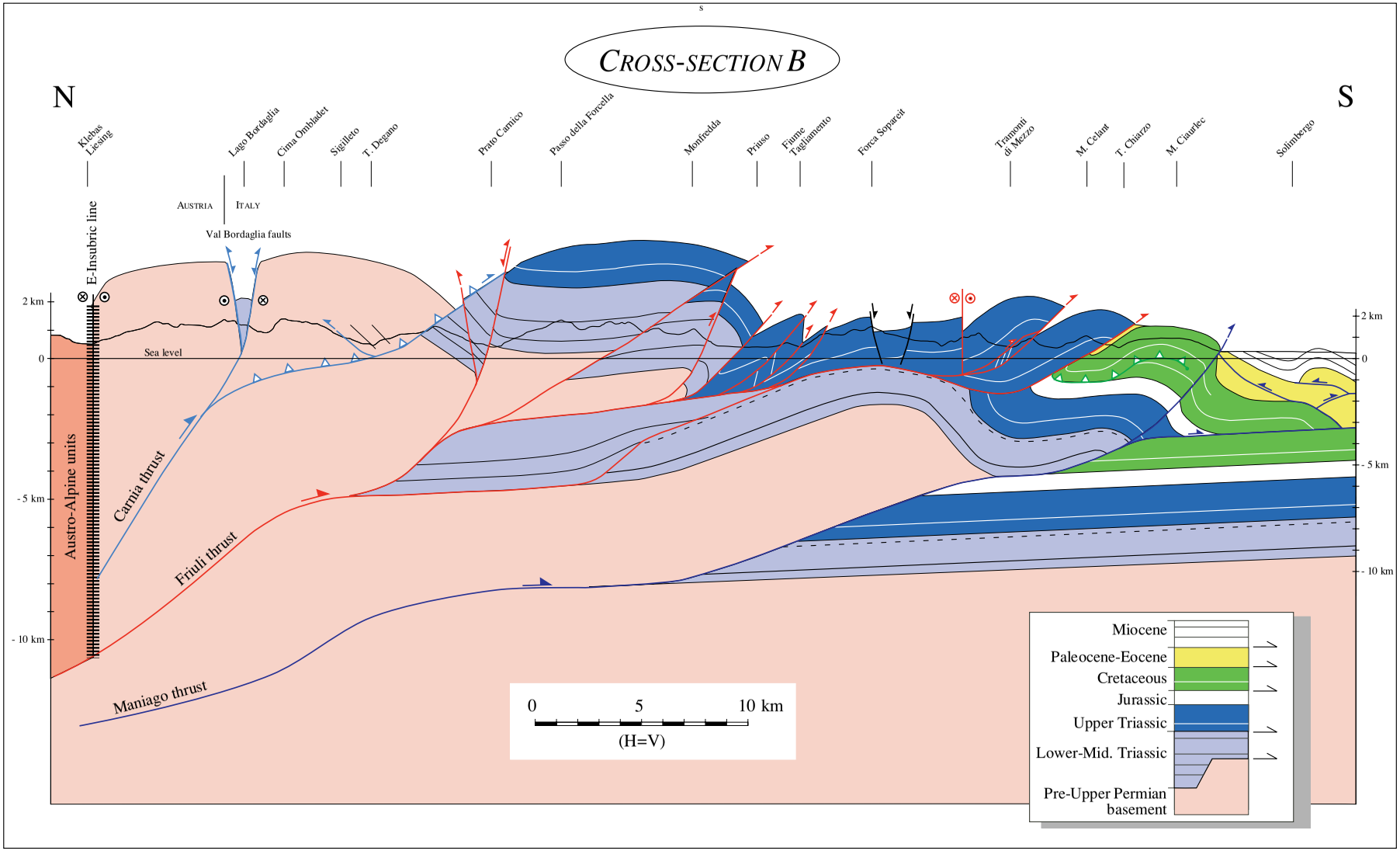

Fig. 24. Large-scale cross-section B from the E-Insubric line to the Friuli plain (location in Figs. 2, 3, 13, 17 and 22).

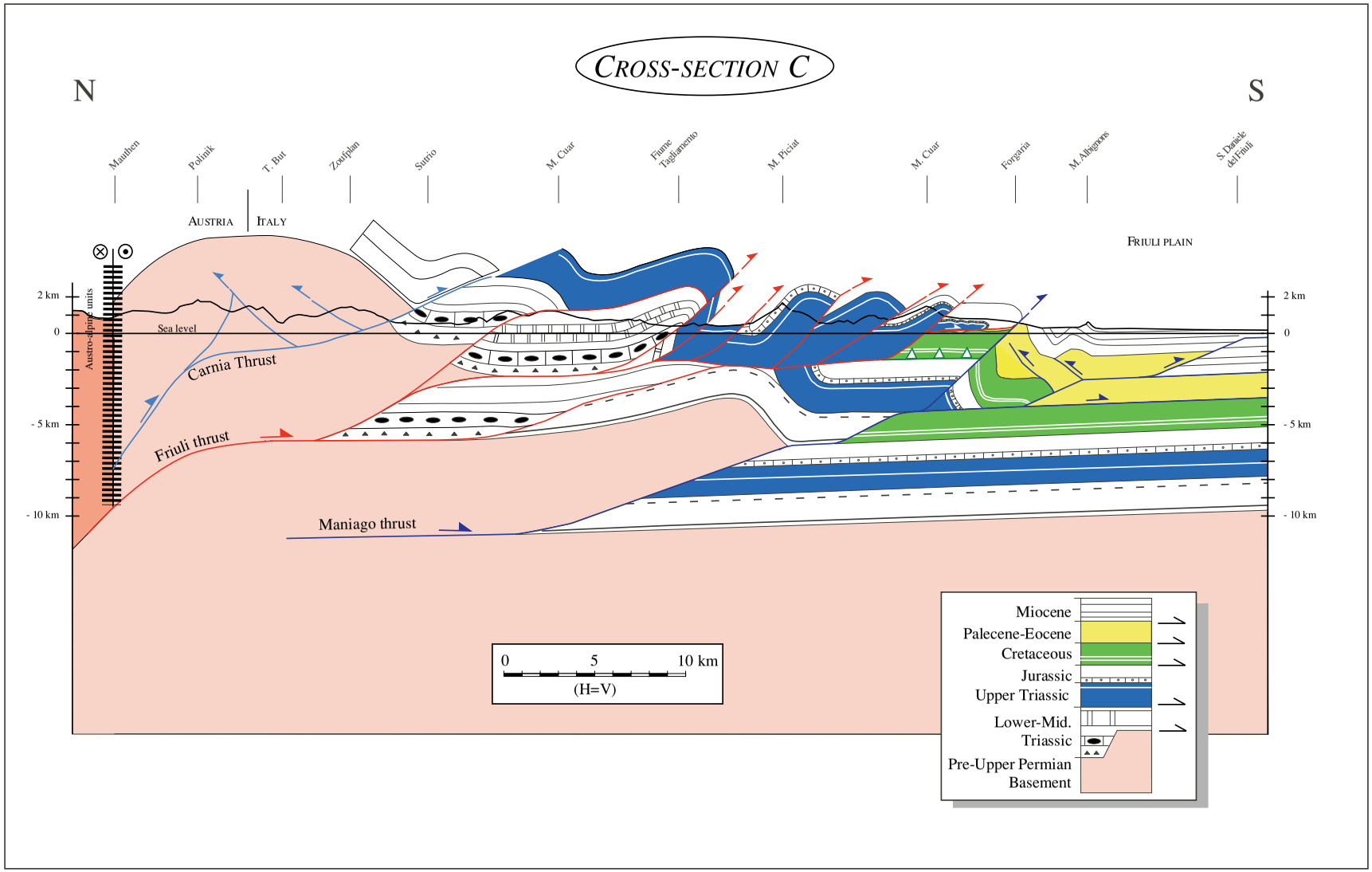

Fig. 25. Large-scale cross-section C from the E-Insubric line to the Friuli plain (location in Figs. 2, 3, 9, 19 and 22).

The Maniago thrust system produced a triangle zone at depth. This triangle zone generates a general southward dipping monocline characteristic of the Venetian and Friuli foothills between Vittorio Veneto and S. Daniele del Friuli. It is the most important structure of the foreland. Its presence is suggested by: (i) the absence of an important thrust at the base of the foothills, (ii) the necessity of a thrust at the base of the M. Albignons anticline to resolve the volume problem of the structural high, and (iii) the south-dipping monocline in the frontal part of the chain which is typical for triangle zones. This triangle zone consists of a combination of duplexes and backthrusts. As in a duplex, displacement is transferred from a lower to a higher stratigraphic horizon through a number of imbricate faults. However, once gathered into an upper detachment the displacement is once again transferred, this time into a foreland-dipping and hinterland-vergent backthrust.

In comparison with sections A and B (Figs. 23 and 24), cross-section C (Fig. 25) shows an additional splay in the frontal part of the Friuli thrust system. This splay is linked to the main thrust that transported the sequences of the intra-Friuli basin onto the Friuli platform (called Periadriatic thrust in Castellarin, 1981, or Perifriuli thrust in Cousin, 1981). However, this splay does not extend laterally; it is limited to a restricted area near the M. Pala (Fig. 13). The origin of this structure is questioned because Dinaric structures are clearly present in this area (e.g. M. Ciaurlec, M. Jouf in Figs. 13 & 14). Nevertheless, based on structural geometry and kinematic indicators, this splay is interpreted as an Alpine structure in this study. The Mesozoic strata of the hangingwall were dragged and overturned along the south-vergent thrust. Kinematic indicators such as E-W striking fold axes and slickensides on the fault planes indicate a southward transport. The thrust may have been nucleated by the presence of a Dinaric syncline at this place. In the next Dinaric syncline to the west, between the M. Jouf and M. Ciaurlec, a south-vergent Alpine thrust developed two splays linked to the frontal Friuli thrust. It can be concluded that the frontal Friuli thrust split into two or three branches when it propagated into a Dinaric syncline. This case shows that pre-existing local conditions (Dinaric folds) may have an influence on thrust topography. On the other hand, detachments are currently lower in synclines, may be

the same happened further up above the anticlines. However, we can not verify this hypothesis because the hangingwall above the anticlines is today eroded.

5.1.4 Geometry of the eastern block (sections E, F and G)

Cross-sections E, F and G (Figs. 27-29) illustrate the geometry of the eastern block (location in Fig. 22). The Carnic Alps emerged when the Carnia thrust superposed to the south two basement slabs onto each other. At the same time, the Carnia thrust inverted the Permo-Carboniferous graben of Pramollo (Fig. 9) located in the southern basement slab. The Permian normal faults near the northern rim of the graben were reactivated as transpressionnal reverse faults during Alpine compression. Similar structures have been described in the central Southern Alps (Schönborn and Schumacher, 1994). Small-scale criteria point to a dextral transpressive movement along this E-W trending upthrust. In the literature, this line is generally called the Hochwipfel line. The graben is deformed by different branches of the Carnia thrust (Figs. 27 and 28). Within the graben, slip propagated along a décollement in the Upper Carboniferous Auernig formation.

In the three cross-sections, a steep south-dipping fault separates the autochthonous cover in the north from the Lower to Middle Triassic unit further south. Based on geometric relations between fault and strata, and exposed slickensides on the faults, this fault is interpreted as a north-vergent backthrust active during folding of the Paleozoic basement in the north. This fault is called Fella-Sava line (*e.g.* Castellarin, 1981). According to some authors (Müller, 1977; Slejko *et al.*, 1987; Carulli *et al.*, 1990), recent seismicity occurred along this line. The focal mechanisms indicate dextral strike-slip movement (earthquakes in 1956 and 1976). Consequently, this fault is still active, reactivated as a strike-slip fault. This backthrust transported a thick Lower-Middle Triassic sequence (4.5 km thick) onto a sequence of the same age which was reduced (1-1.5 km) during Middle Triassic rifting phase. Additionally, the sediment type is different between the footwall (northern part) and the hangingwall (southern part). The northern part is composed of Anisian-Ladinian breccia that reworked Scythian sediments. These

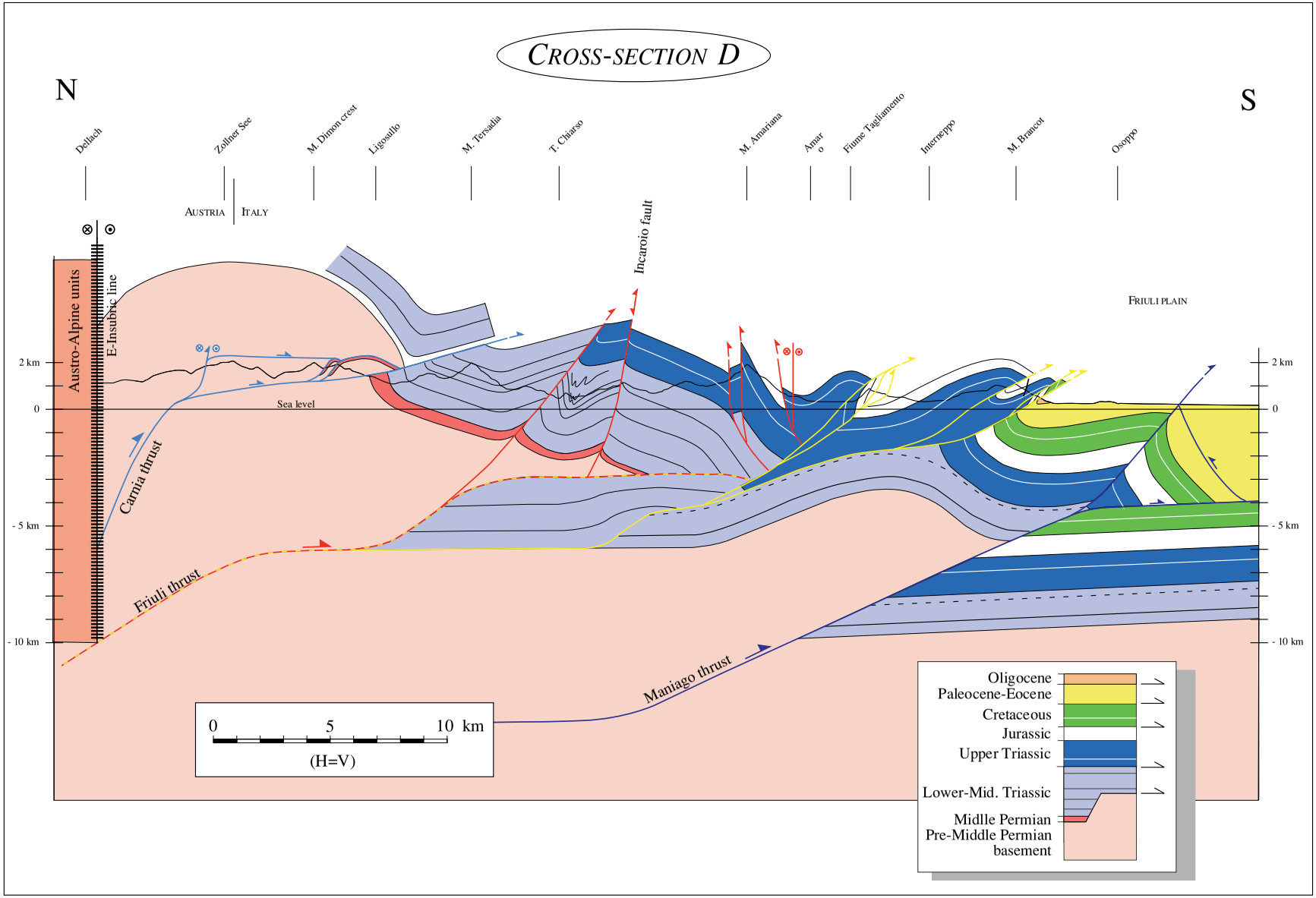

Fig. 26. Large-scale cross-section D from the E-Insubric line to the Friuli plain (location in Figs. 2, 3, 9, 19 and 22).

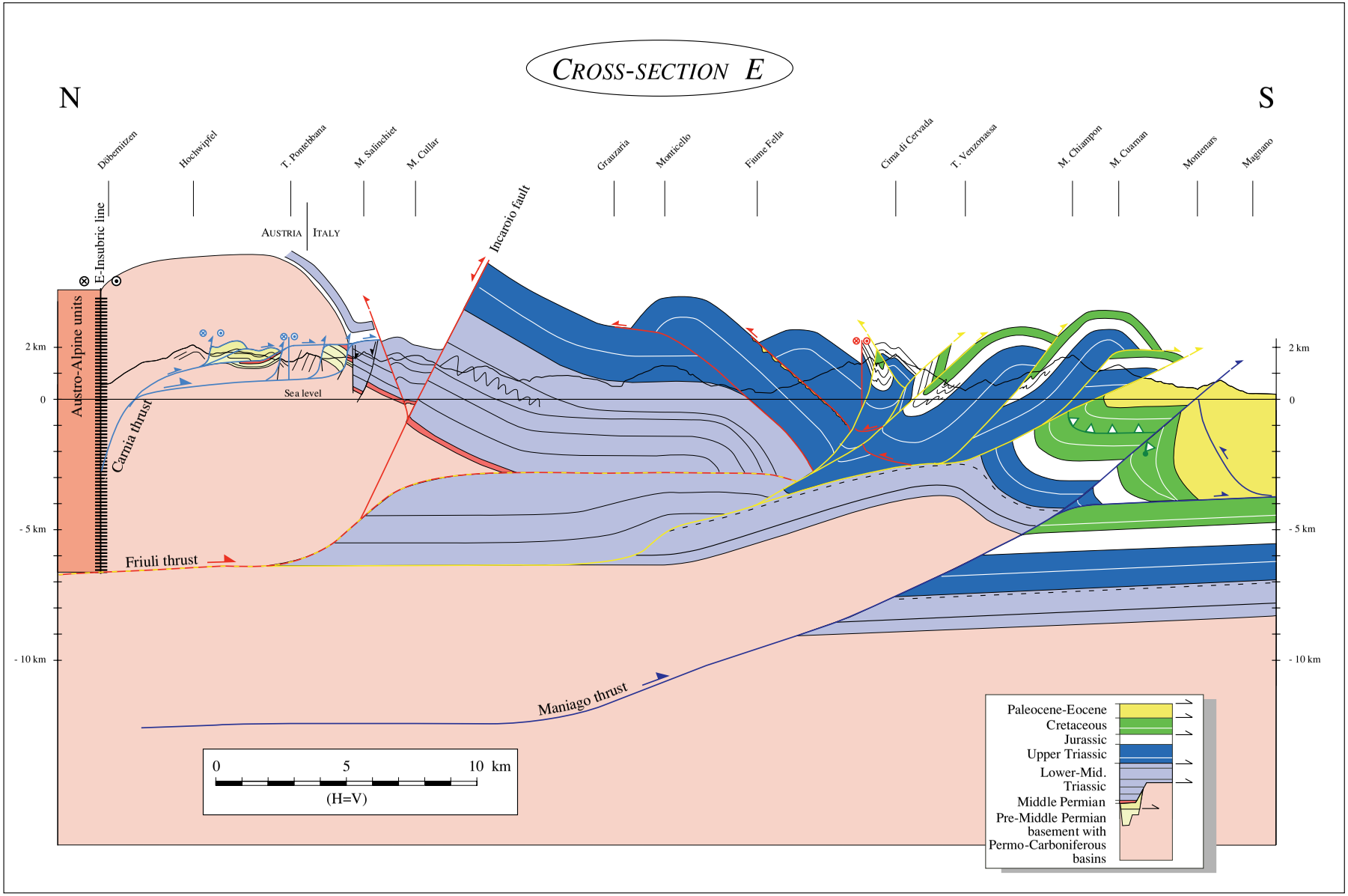

Fig. 27. Large-scale cross-section E from the E-Insubric line to the Friuli plain (location in Figs. 2, 3, 9, 19 and 22).

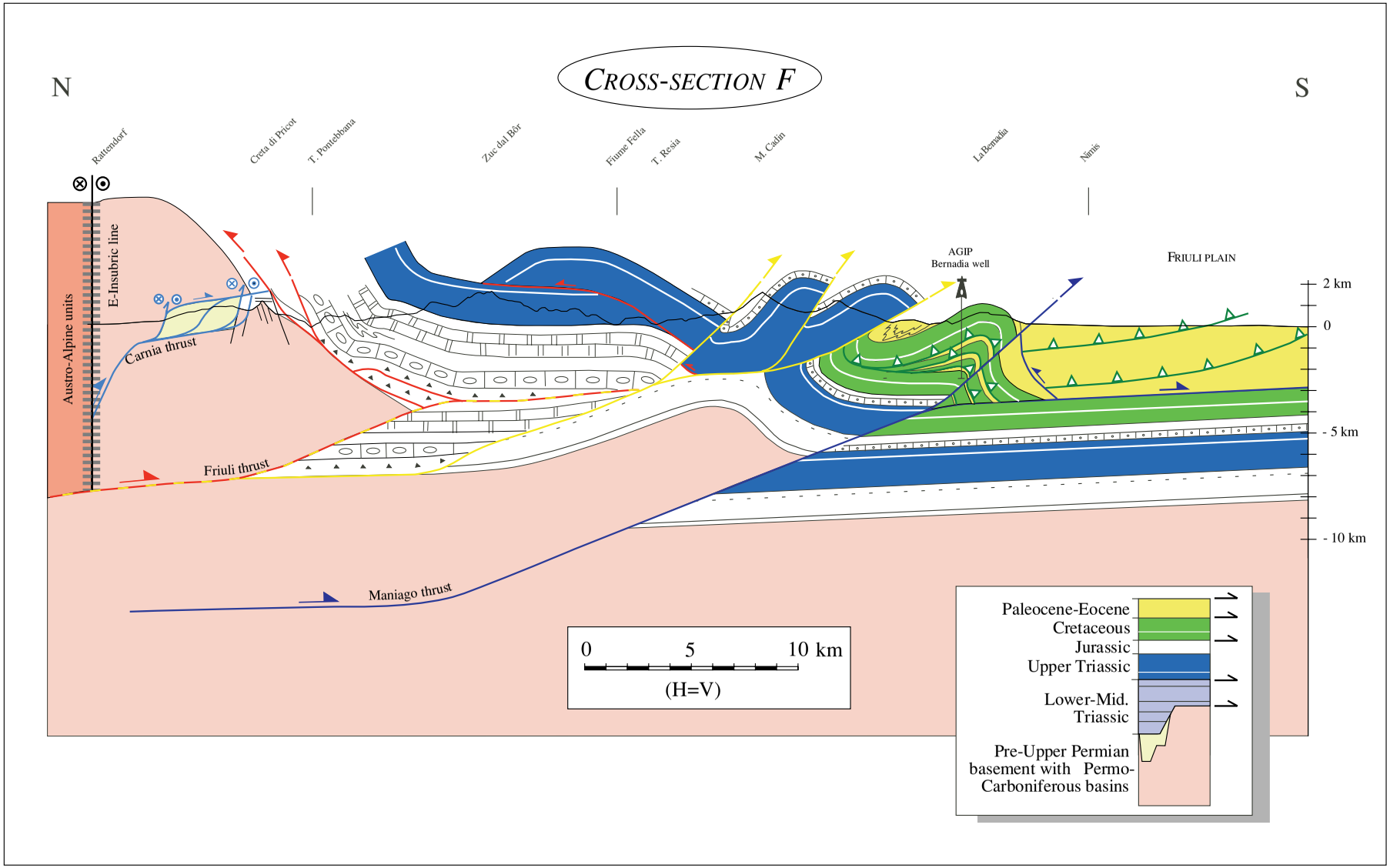

Fig. 28. Large-scale cross-section F from the E-Insubric line to the Friuli plain (location in Figs. 2, 3, 9, 19 and 22).

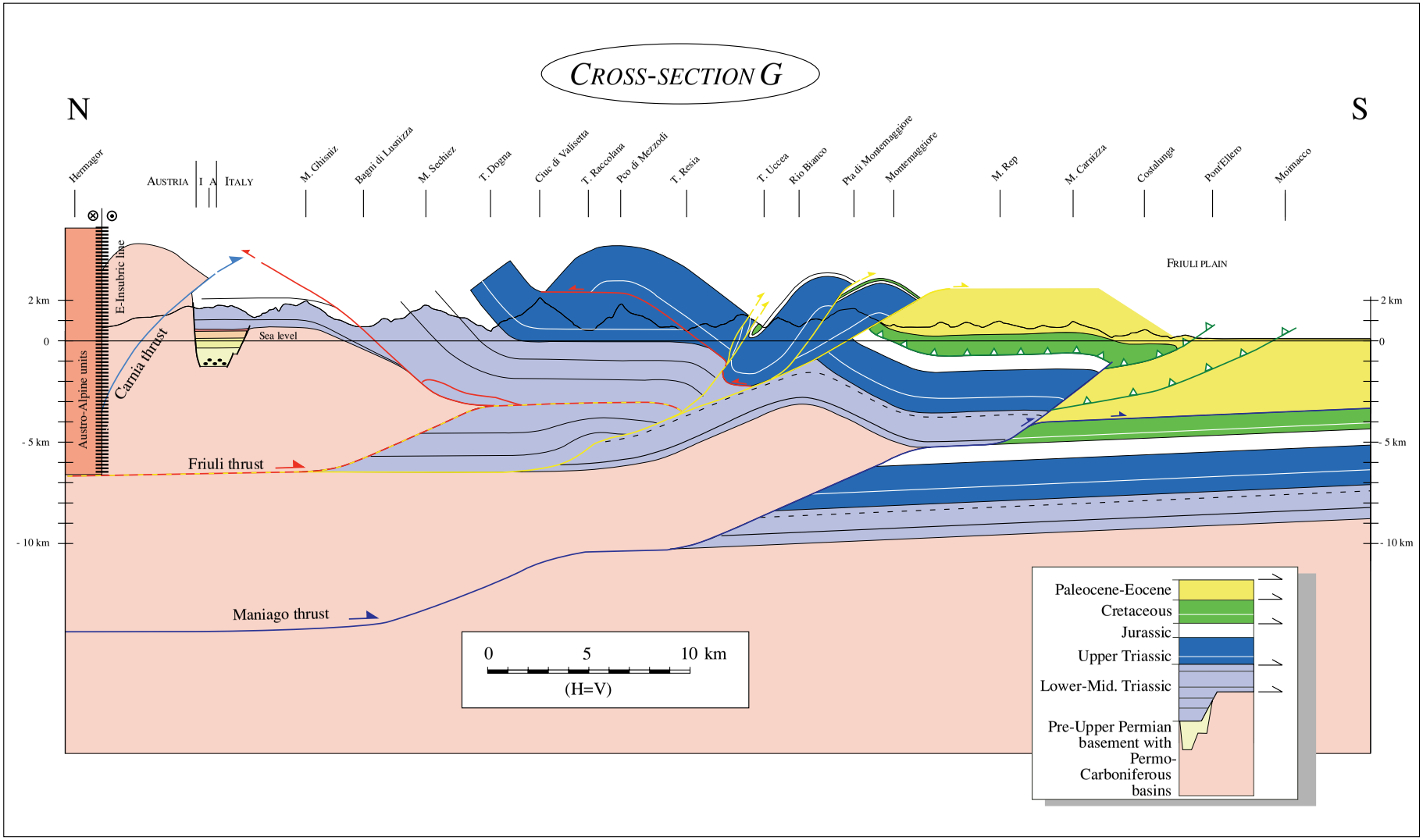

Fig. 29. Large-scale cross-section G from the E-Insubric line to the Friuli plain (location in Figs. 2, 3, 9, 19 and 22).

observations suggest the presence of a Middle-Triassic synsedimentary fault with an E-W strike and a steep south-dipping. This inherited fault figures in the restored section F (chapter 5.2, Fig. 33). The backthrust that characterizes the eastern block was initiated along this E-W trending inherited fault. It is interesting to note that the backthrust ends westward against another Middle Triassic synsedimentary fault that trends NNE-SSW. This fault plays a major role during Alpine deformation since it is sinistrally reactivated and thus transfers the shortening of the backthrust into the Incaroio transverse zone.

The frontal thrust of the Friuli system emerges at the south underneath the frontal chain (M. Chiampon-Gran Monte). This thrust has a major importance since it superposes the Upper Triassic layers onto Eocene flysch. This thrust transported the pelagic sequences of the Perifriuli domain (Cousin, 1981) onto the limestones of the Friuli platform.

Cross-section F (Fig. 28) cross-cuts the Bernadia well drilled by AGIP (1977). This drill hole reveals that the deep structure is more complex than expected from field surface data. This example illustrates well that nature is not always deformed in the simplest way possible. The well crosses three thin thrust slices of the Eocene flysch. Surface structural data around the Bernadia area indicate that the Neogene E-W trending anticline, which is due to the emplacement of the Maniago thrust, is superposed onto an older NW-SE oriented anticline that trends parallel to the Paleogene structures in the Dinarides. Consequently, these slices are interpreted as Paleogene structures, i.e. southwest-vergent thrusts. According to Martinis (1966), the tectonic slices cut by the Bernadia well are made up of Jurassic limestones and of Eocene flysch. Considering structural arguments, I think that the limestones are of Cretaceous age and not of Jurassic age (see also p. 288 of Cousin, 1981). The south-vergent anticline of La Bernadia is too tight to involve Jurassic strata. Surface control on the thickness of the Cretaceous limestones is good and allows this interpretation. This implies detachment in the Biancone horizon underneath the relatively rigid Cretaceous limestones. This interpretation is in good agreement with the Dinaric structures observed in the western frontal part of the Friuli Alps (Fig. 15). Moreover, Martinis' interpretation implies a décollement underneath or within the Jurassic limestones.

That has been never observed in field and the Upper Triassic and Jurassic beds do not favor a detachment since they are composed of thick-bedded dolomites and limestones. The succession of Eocene flysch with the Cretaceous limestones implies another detachment in the lower part of the flysch further up in the stratigraphic column.

5.1.5 Comparisons between the western and the eastern block

All cross-sections show stacking of two Lower-Middle Triassic units onto each other. The thrust causing that superposition has pushed the Upper Triassic unit towards the south, and produced a south-vergent imbricate fan, detached above the Carnian décollement horizon. In the western block, this imbricate fan is made up of three tectonic sheets, whereas in the eastern block, only two slices were developed. This difference may be explained by the backthrust of the Lower-Middle Triassic unit onto the basement in the eastern block. This major lateral change of structure probably has been initiated along the Incaroio paleofault (see chapter 4.2.2).

In each cross-section, the Maniago thrust transported a basement slab onto the autochthonous sequence. The basement slab has a thickness of some 5 km in all sections. This is in agreement with the other crystalline thrust sheets in different mountains belts, where crystalline sheets seem to be often 4-5 km thick (*e.g.*, Schönborn, 1992b, 1999; and see discussions by Hatcher and Hooper, 1992). This implies a subhorizontal intracrystalline detachment. The detachment depth may be estimated in adding the sedimentary sequence with a basement sheet. This calculation leads to a décollement located between 12 and 14 km, which would approximately correspond to the position of the brittle-ductile transition. The position of the ramp in the basement is given by the length of the detachment along the base of the Lower-Middle Triassic unit of the Maniago sheet. Filling the gap with a stack of Mesozoic thrust sheets instead of basement would imply more complex tectonics and additional shortening. Due to the lack of evidence of Mesozoic thrust sheets and the added complexity, interpretation of a basement thrust sheet is favored. See also Schönborn (1999)

for an illustrated example of three different constructions, all balanced, of an anticline further west in the Dolomites.

5.1.6 Geometry of the central block (cross-section D)

Cross-section D crosses the Incaroio transverse zone in the north and the Tagliamento transverse zone in the south (Fig. 26; location in Fig. 22). The geometry of the Incaroio transverse zone is interpreted in this study as a triangular indenter pushed southward during Alpine deformation (Fig. 16). The internal part of the indenter was deformed into a southeast-vergent anticline-syncline pair. Cross-section D shows that a splay of the Friuli thrust broke through the hinge of the anticline, whith overturning and thinning of the frontal limb (near Fiume Tagliamento in Fig. 26). The syncline is very tight and the Middle Triassic Schlern dolomites are lacking. Undoubtly, the absence of the Ladinian thick rigid layers has largely favored syncline formation. The Schlern formation forms isolated platforms and may abruptly be replaced laterally by thin shales. Another better exposed example is observed in the footwall of the Incaroio fault where the Schlern dolomites build a 500 m thick cliff that vanishes laterally. Breccias and olistolites are observed in the transition zone. The southern part of the section crosses the Tagliamento transverse zone. Geometry within this intricate zone is explained in chapter 4.2.3.

5.2 KINEMATIC EVOLUTION AND RESTORATION

The kinematic approach is an indispensable tool and probably the best way to construct balanced cross-sections in the Friuli Alps, where the deep structure is poorly constrained due to the lack of deep reflection seismic data, and complex tectonics. The deep structure is extrapolated from mainly surface information, and unexposed features are treated as simply as possible. Forward modeling allows for the understanding of the intermediate stages and therefore the kinematic evolution from the undeformed state cross-section to the deformed state cross-section. A plausible cross-section must be retrodeformable and the use of the method of line length balancing quickly shows major

errors. An accurate balancing would require a horizontal restoration of the youngest beds deposited before deformation, in this case the Eocene flysch.

5.2.1 Kinematic evolution of the western block

Cross-section C is representative of the western block. It has been chosen to illustrate the kinematic evolution from the undeformed state (Fig. 30) to the deformed state (Fig. 25). The restored section C shows the simple polygonal trajectories of the three major thrust systems (Fig. 30). The kinematic evolution according to this section is in sequence from north to south. Consequently, deformation began first with the Carnia thrust system, which transported a basement slab southward. This basement slab is exposed in the Carnic Alps. When the basement ramped up, it split first into two branches, one being a dextral transpressional reverse fault reactivating a paleofault (called Gamskofel-Polinik line by Läufer, 1996). Further up, the main branch split into two backthrusts (Fig. 25). The transpressional reverse faults and the first backthrust in the sequence produced a small triangle structure. However, the chronology between both faults is not known since the cross-cutting relations have been eroded. The Friuli thrust transported the next basement slab southward. After a flat at the base of the Lower-Middle Triassic unit it ramped up in a main branch and two splays. All three ramped up to the Raibl detachment horizon. Slip propagated southward along the décollement and ramped up three times in sequence through the Upper Triassic unit. A last splay transported the Upper Triassic-Jurassic unit onto the Eocene flysch. This thrust transported the sequences of the intra-Friuli basin onto the Friuli platform. Finally, the Maniago thrust emplaced another basement slab and formed an anticline with a thrust trajectory involving various ramps and flats within the Mesozoic sequence (décollement at the base and at the top of Cretaceous beds). A splay broke through the hinge of the ramp fold. This splay is steep and corresponds to the most external, exposed thrust of the belt. Deformation of the most external anticline (M. Albignons in Fig. 25) is currently still active. Tectonic slices of Cretaceous limestones are thrust onto Miocene molasse and upper Pliocene conglomerates (Cousin, 1981; Benedetti *et al*., 1995). These observations suggest the Maniago thrust to be still active. This ongoing

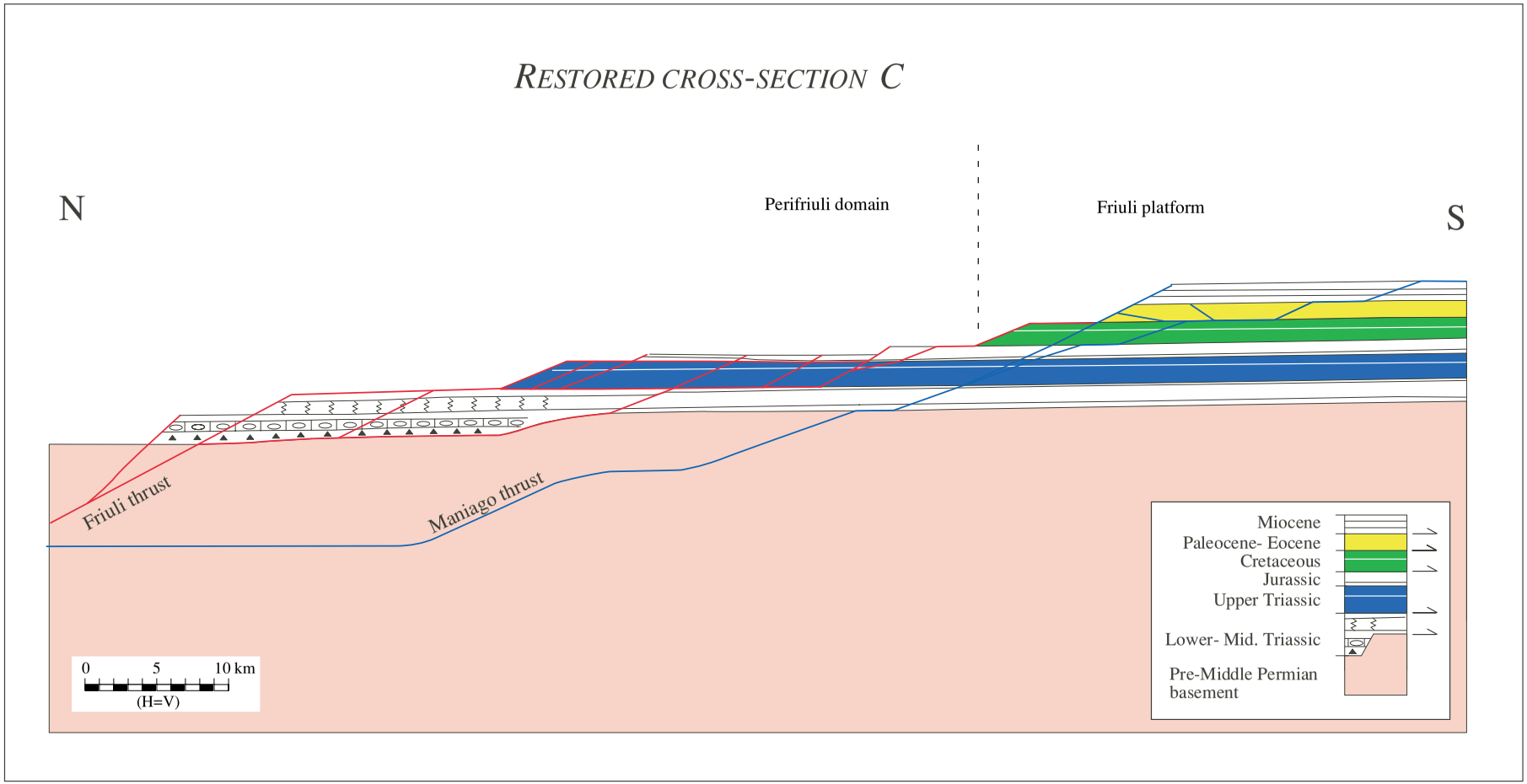

Fig. 30. Restoration of cross-section C (Fig.25). The southernmost branch of the Friuli thrust (termed Periadriatic overthrust or Perifriuli thrust in the literature) transported the Perifriuli domain located in the north onto the Friuli platform in the south The Perifriuli domain and the Friuli platform were defined by Cousin (1981).

activity is confirmed by focal mechanisms and hypocenter distribution of recent earthquakes (chapter 6).

5.2.2. Kinematic evolution of the eastern block

Cross-section F is assumed to be representative of the eastern block (defined in Fig. 22). It has been chosen to illustrate the kinematic evolution from the undeformed state (Fig. 33) to the deformed state (Fig. 28). The kinematic evolution according to this section is in sequence from north to south, except an out-of-sequence thrust within the Friuli system.

The Carnia thrust transported a basement slab onto another one and inverted the Permo-Carboniferous basin of Pramollo, located in the lower basement slab. The Permian normal faults near the northern rim of the graben were reactivated as transpressionnal reverse faults during Alpine compression. Small-scale criteria point to a dextral transpressive movement along this E-W trending upthrust. In the literature, this line is generally called the Hochwipfel line (e.g. Venturini, 1990b; Läufer, 1996). The graben is deformed by different branches linked to the Carnia thrust. In the graben, slip propagated along a décollement level located in the Upper Carboniferous Auernig formation.

The Friuli thrust transported the next basement slab southward. After a flat at the base of the Lower-Middle Triassic unit, it ramped up in a main branch that split into a backthrust and a south-vergent thrust. The backthrust superposed a Lower-Middle Triassic unit onto another one, whose thickness was strongly reduced during the Middle Triassic rifting phase. Thickness and sedimentation changes point to a synsedimentary fault. The Middle Triassic synsedimentary fault constitutes a foreland dipping normal fault which acts as an obstacle when the backthrust propagated to the north. To overcome this obstacle, the backthrust formed small duplexes in the Lower Triassic beds requiring a décollement along the Upper Permian Bellerophon horizon (Fig. 28).

The complex geometry of the M. Cadin is explained here with an out-of-sequence thrust or a truncated wedge (Fig. 31). The angular relationships between the strata in the hangingwall and in the footwall imply a structure made up of two stages (Fig. 32). During the first step, the structure evolves as a wedge bounded by a floor thrust at the base of the Upper Permian-Middle Triassic cover and a passive roof thrust at the top. This structure is termed intercutaneous wedge in the literature (Boyer and Elliott, 1982; McClay, 1992). In a second stage, the Friuli thrust system propagated to the south, the thrust ramped upward and split into two branches. One branch followed the Carnian décollement horizon, producing an imbricate fan composed of two south-vergent Upper Triassic slices. The other branch ramped through the wedge. This out-of-sequence thrust may be related to the change of thickness in the not exposed Lower-Middle Triassic sequence due to rifting. Based on field data and deep wells in the Friuli plain, thickness changes are expected to occur somewhere between the northern and the southern parts of the cross-section. As Middle Triassic normal faults are observed in filed, this thickness change is suspected to be abrupt, occurring along one or several normal faults that act as an obstacle with respect to the thrust. To overcome this obstacle, the thrust has various possibilities, one of which is the development of an out-of-sequence thrust.

A model similar to the one in figure 32 is used to explain the kinematic evolution of cross-sections D and E (Figs. 26 and 27). Figure 34 shows, however, that the fault tip propagated further southward in cross-sections D and E (Figs. 26 and 27), compared to the cross-sections F and G (Figs. 28 and 29). A double backthrust results implying more shortening related to this stage than in sections D and E.

5.2.3 Shortening calculation

Minimum shortening amounts to 50 km in both restored blocks. Slip along the Maniago thrust amounts to 18 km; along the Friuli thrust system to some 28 km, and some 3-5 km can be attributed to the Carnia thrust. Total slip along the Carnia thrust system is poorly constrained due to the absence of reliable markers, but shortening must be much

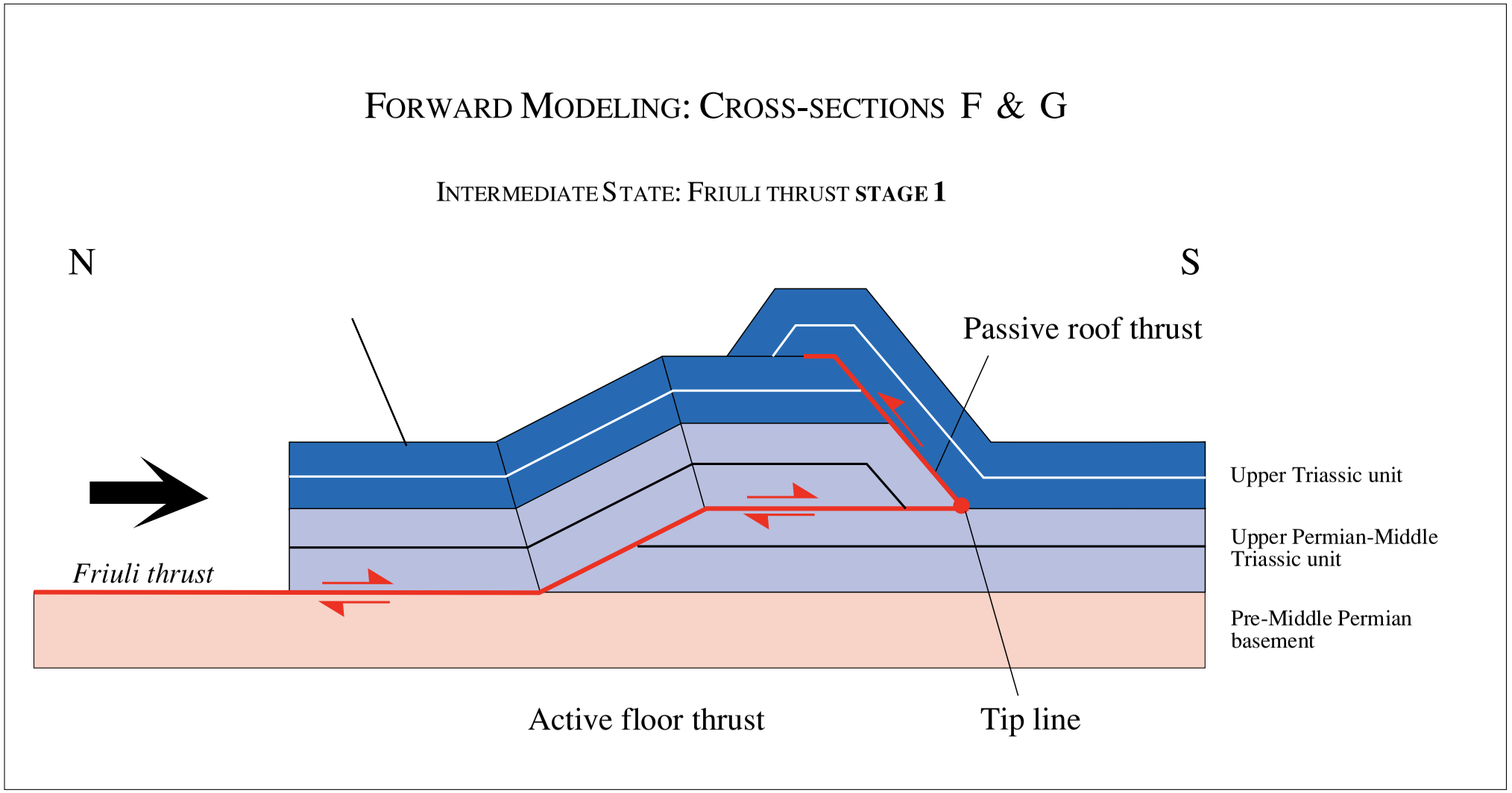

Fig. 31. Schematic forward modeling for cross-sections F and G. Intermediate stage 1 within the Friuli thrust. This intermdiate structure is a wedge bounded by a floor thrust at the base and a passive roof thrust at the top.

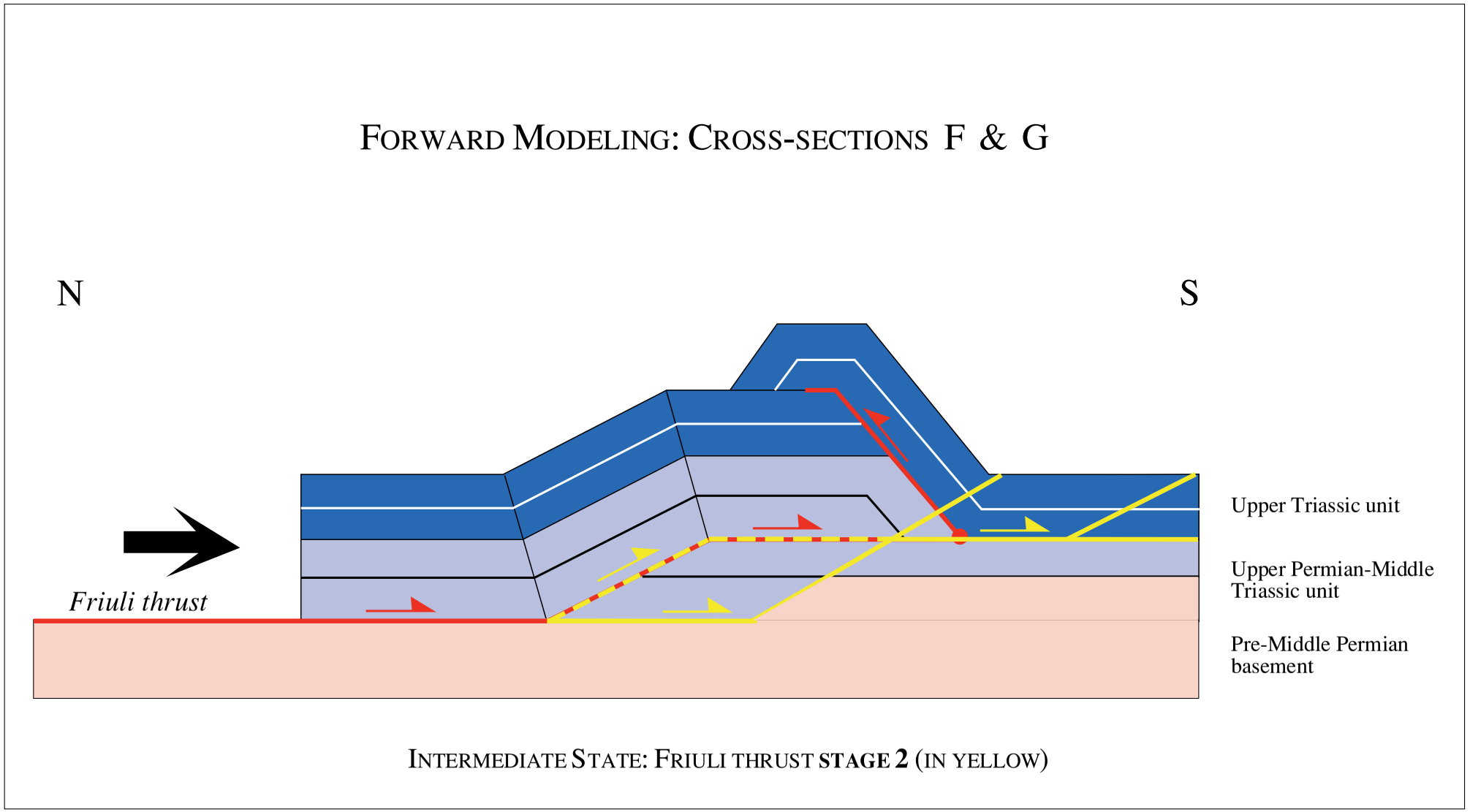

Fig. 32. Schematic forward modeling for cross-sections F and G. Intermediate stage 2 (in yellow) within the Friuli thrust. This thrust ramped upward through the bounded wedge formed during the first stage.

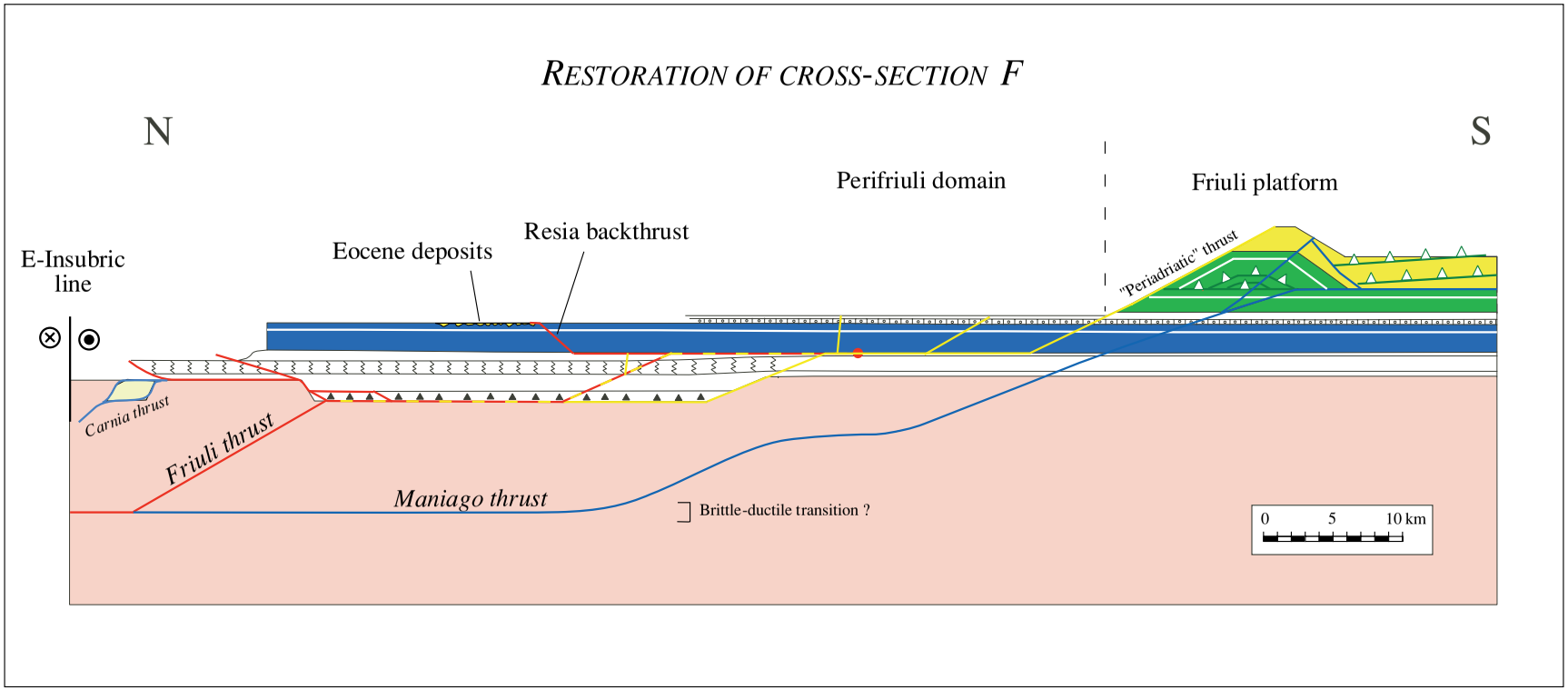

Fig. 33. Restoration of cross-section F (Fig. 28). Note the important erosion in the footwall of the Resia backthrust where Eocene deposits overly directly the Upper Triassic dolomites. The Maniago thrust system ramped upward through Paleogene Dinaric thrusts.

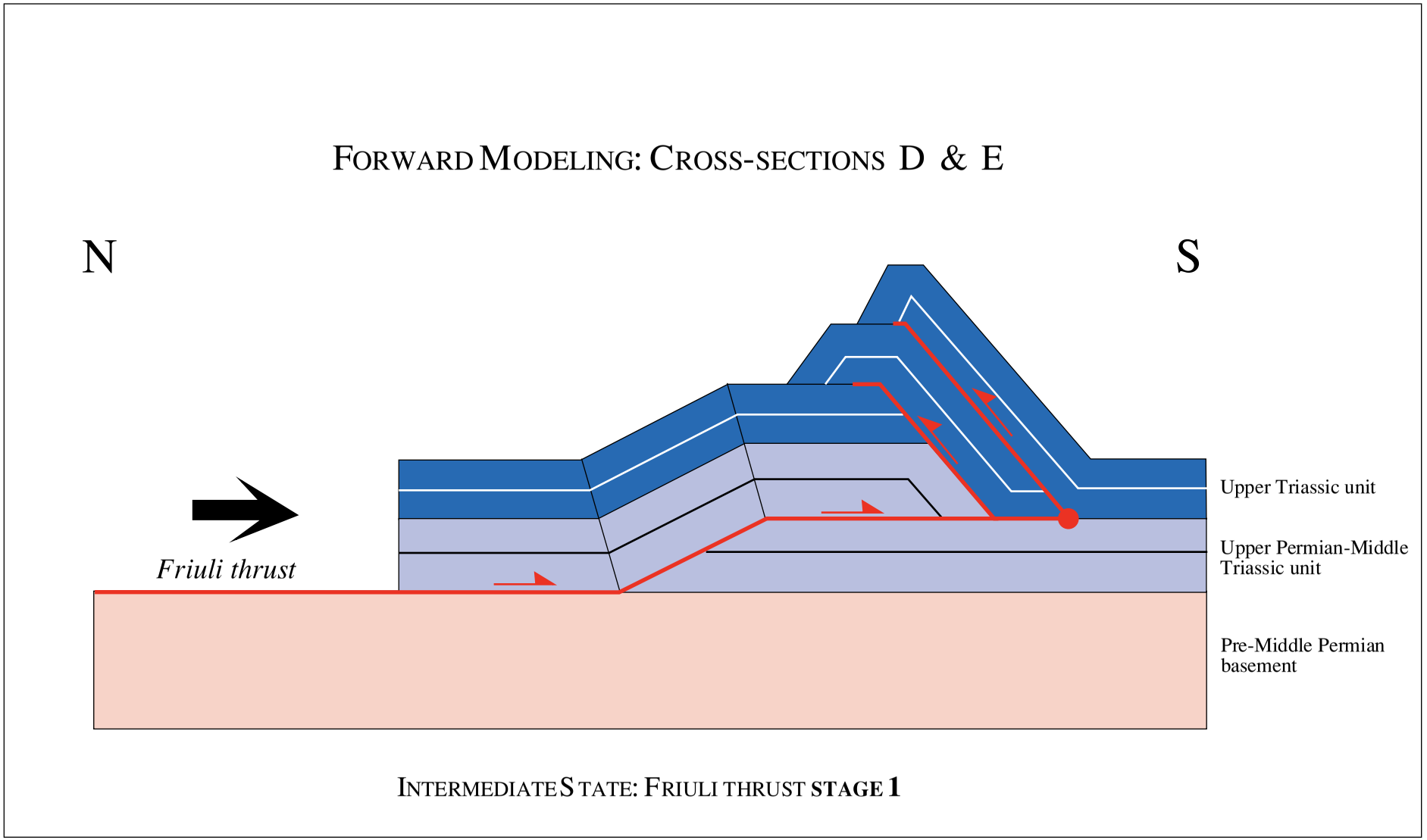

Fig. 34. Schematic forward modeling for cross-sections D and E. Intermediate stage 1 within the Friuli thrust. With respect to cross-sections F and G, the tip line propagated more southward and thus an additionnal backthrust resulted.

lower than those of the Friuli and Maniago systems. Further west in the Dolomites, the location where the Carnia system cut through the Mesozoic sequence is exposed. This renders possible the quantification of shortening along the Carnia system (see Schönborn, 1999). According to Schönborn, shortening along the Marmolada-Sorapiss thrust (the western continuation of Carnia thrust) amounts to some 3.5 km.

5.2.4 Leeway in construction

Field observations and data of deep wells indicate important lateral thickness variations of the Lower to Middle Triassic sequence. In the northern part of the Friuli Alps, the exposed transitions are abrupt, along a fault or a platform edge. Middle Triassic rifting is suspected to be responsible for these thickness changes (see chapter 2.2). The southernmost exposed Lower-Middle Triassic sequences are very consistent: 4500-5000 m. In the Friuli plain, deep wells indicate the influence of the Middle Triassic tectonics. The Lower-Middle Triassic is strongly reduced compared to sequences further north (thickness: 1500-1700 m). Between these two points (on a cross-section), there is no constraints with regards to the thickness. One or several Middle Triassic normal faults can be inferred between both points. Constructions were simplified by assuming a smooth transition.

The difference in lengths of a deformed and restored section provides the total shortening of the belt along the section. However, the shortening of a given section depends largely on the construction type. A construction without flats within the thrust trajectories leads to a minimum shortening. This style of deformation does not correspond with what is visible at the surface. Another style of construction introduces thrusts not visible at the surface and very long décollements, which lead to more intricate structures, thinner thrust slabs, and increased shortening. Roeder and Lindsay (1992) applied this style in their constructions. These two construction types can be considered as end-members and surface data suggest the more adequate solution to be in between. It is important that only thrusts visible at the surface have been used for the constructions. Fewer thrusts always

lead to thicker thrust sheets and thus give smaller shortening for a given orogenic wedge. Accordingly, all the constructions in this study can be regarded as conservative.

6. SEISMOTECTONICS OF THE FRIULI AREA

6.1. CURRENT SEISMISITY VERSUS ALPINE TECTONICS

Numerous destructive earthquakes have hit the area in northeastern Italy extending from Lake Garda in the west to the border with Slovenia and Croatia in the east. The major earthquakes occurred mainly at Lake Garda, in the Belluno region and in central Friuli. Whereas in the Garda zone, last documented strong earthquakes occurred during the first centuries AD., the Friuli area is seismically active until today. The Friuli region is characterized by the strongest seismicity of the Southern Alps (magnitude: $M_L = 6.4$ on the Richter scale). The 1976-earthquake sequence that shook the Friuli area were dramatic with its thousand fatalities.

Inside the Friuli area, the seismotectonic character is not homogeneous. Focal mechanisms are of both thrust and strike-slip type (Slejko *et al.*, 1987, 1989; Bressan *et al.*, 1992, 1998). The Tagliamento transverse zone is deformed by strike-slip mechanisms with NNW-SSE oriented P axes. The fault plane solutions of earthquakes occurring in the Tagliamento zone have systematically revealed sinistral strike-slip movements along NNE-SSW-trending faults (Fig. 35). By contrast, seismicity in the eastern block (defined in chapter 5.1.2) is mainly characterized by thrust mechanisms with P axes oriented from NNW-SSE to N-S (Fig. 35). Focal mechanisms record a rotation of $\sigma 1$ from 310° to 350°. The sinistral strike-slip Tagliamento fault deflects the main $\sigma 1$ from 350° to 310°.

Most of the strong earthquakes were located in the eastern block of the Friuli Alps (defined in Fig. 22). Hypocenters of these earthquakes can be projected into the cross-sections E and F. Figure 36 shows the structural position in the cross-section E of the 1976-earthquake hypocenters. Spatial distribution and focal mechanisms of aftershock-hypocenters following the earthquakes of May 1976 (data from Finetti *et al.*, 1979 and Carulli *et al.*, 1990) point to activity along the frontal thrust system: the Maniago thrust. The aftershocks of May (red square in Fig. 36) shows mainly thrust mechanisms, whereas

the October aftershockes are principally characterized by strike-slip mechanisms (dark blue dots). The epicentre succession from May to September 1976 shows a progressive northward migration of the contractional earthquakes. These data suggest that an earthquake sequence starts first along thrust faults before being propagating along strike-slip faults. The duality between the two types of movement can be explained in considering the local cross-cutting relationships between thrust faults and strike-slip faults. As both types of faults are oriented nearly perpendicularly, a small slip on the thrust fault induces strain incompatibilities in the proximity of the strike-slip fault. Consequently, slip along this fault is needed to accommodate the displacement on the thrust. The depth of the hypocenters are concentrated in the upper 20 km of the crust (Slejko *et al.*, 1987), but, most of hypocenters are located between 2 and 10 km depth (Fig. 36). The hypocenters are mainly located in Mesozoic sediments, and only rarely in the basement.

The Friuli area recorded two main earthquakes in 1976: the main shock occurred the May 6 (M_L = 6.4), and the main aftershock occurred the September 15 (M_L= 6.1). Focal mechanisms of these two earthquakes show thrust type (Slejko *et al.*, 1987). Hypocenters of both earthquakes are reported on cross-section F (Fig. 37). Indicative parameters of these two main destructive earthquakes were calculated by Amato *et al*. (1977). The assumed area was taken to be 200 km^2 for the May 6 earthquake, and they calculated the length of the activated fracture (19 km), and the displacement average along the fault (66.3 cm). For the September 15 aftershock, the extend of the area was taken to be 270 km^2, and they obtained 22 km for the length of the activated fracture and 17.4 cm for the displacement average along the fault.

Figure 37 indicates a good correlation between the hypocenter distribution of the strongest eartquakes showing thrust mechanisms and the construction of cross-section F. The epicenter of the strongest earthquake (M_L = 6.4; date: 06.05.1976) that shook the Friuli region is nearly exactly located on the section line. Its projection into the cross-section matches perfectly with the location of the Maniago thrust ramp.

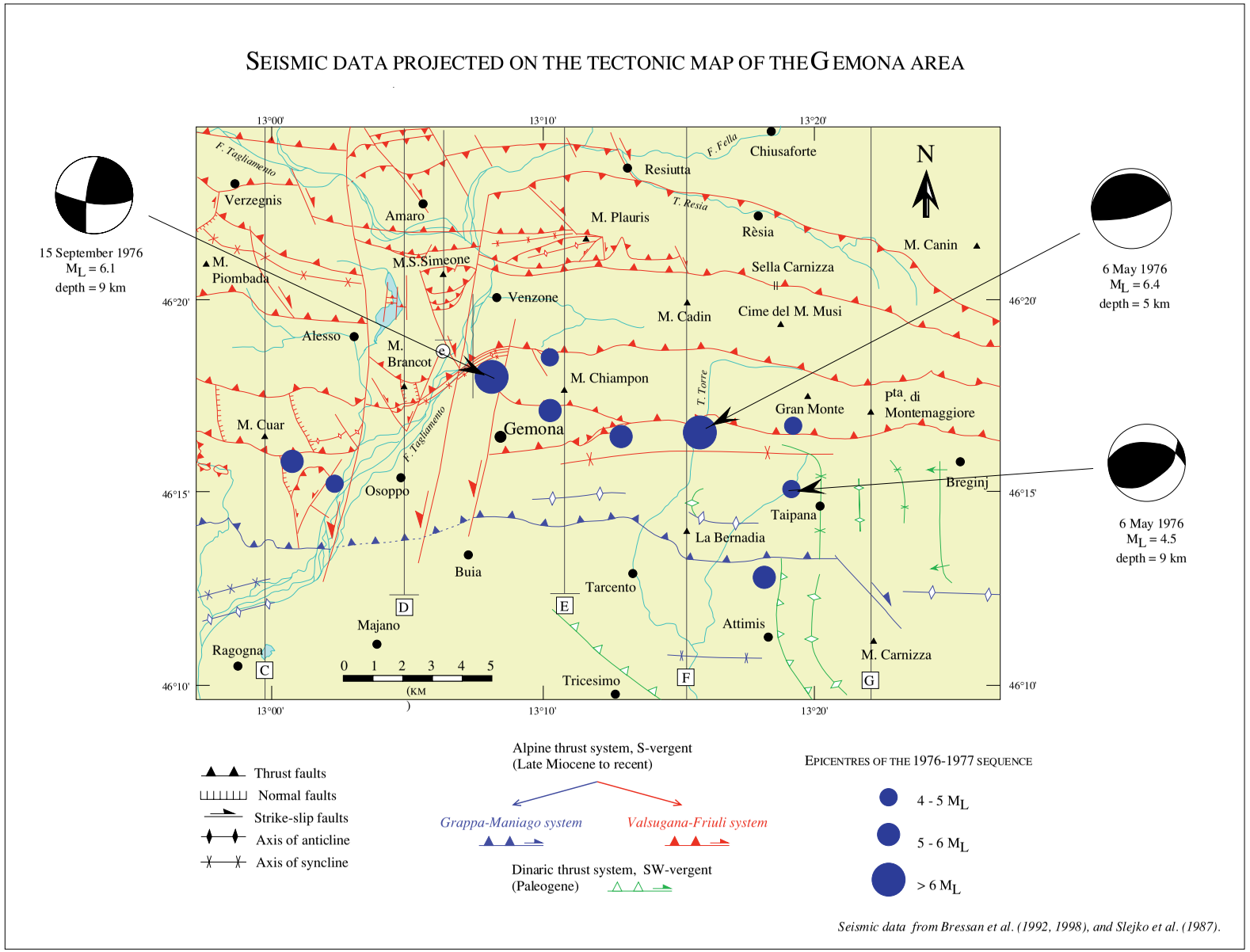

Fig. 35. Distribution of epicentres on the tectonic map of the Gemona area. Focal mechanisms, magnitude and date of the strongest earthquakes are indicated. Note that the Tagliamento transverse zone is deformed by strike-slip mechanisms, whereas the eastern block shows thrust mechanisms.

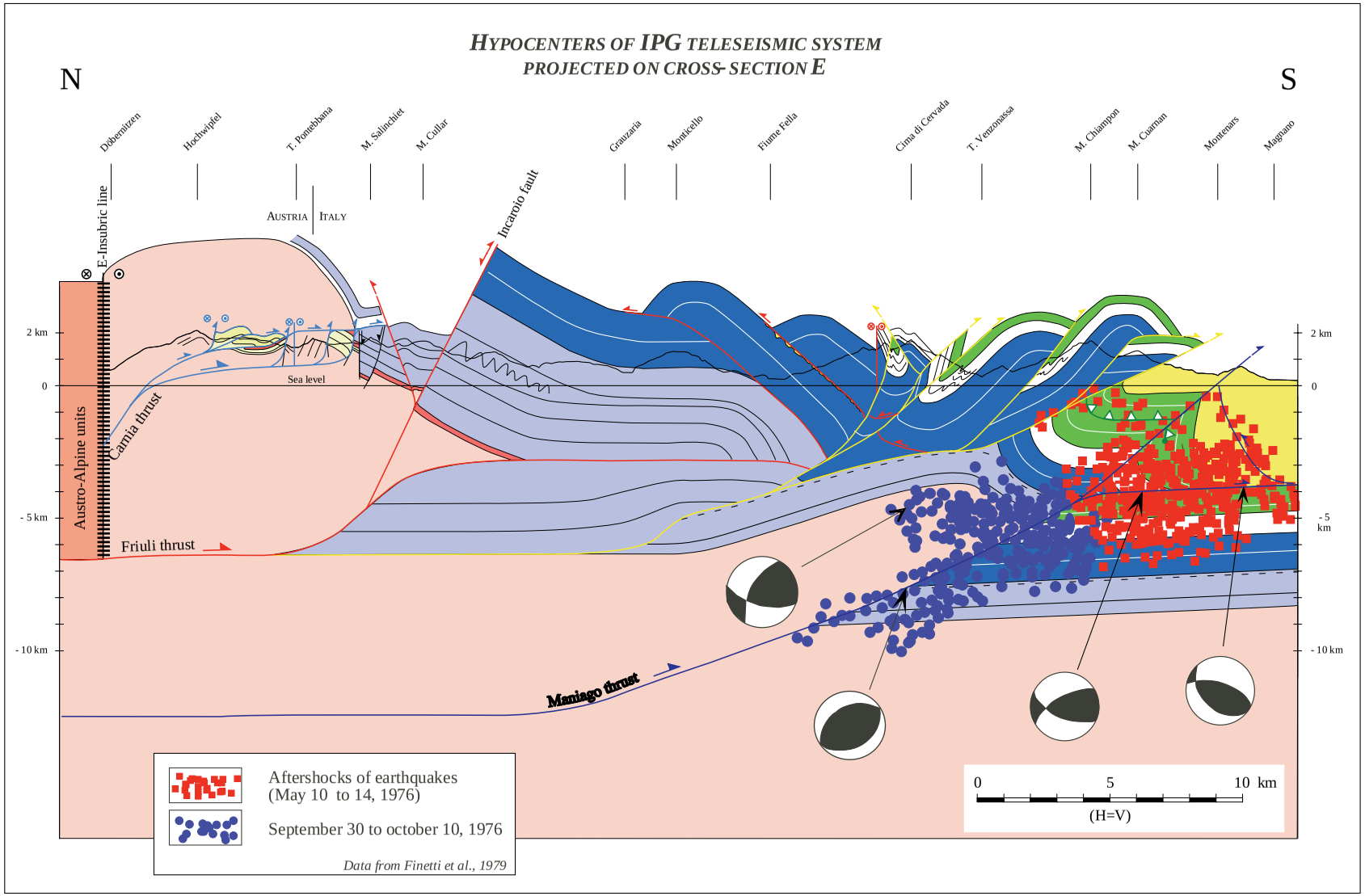

Fig. 36. Projection of some major earthquakes on cross-section F. Focal mechanisms of these earthquakes are indicated. Note the good correlation between the construction and locations of hypocenters.

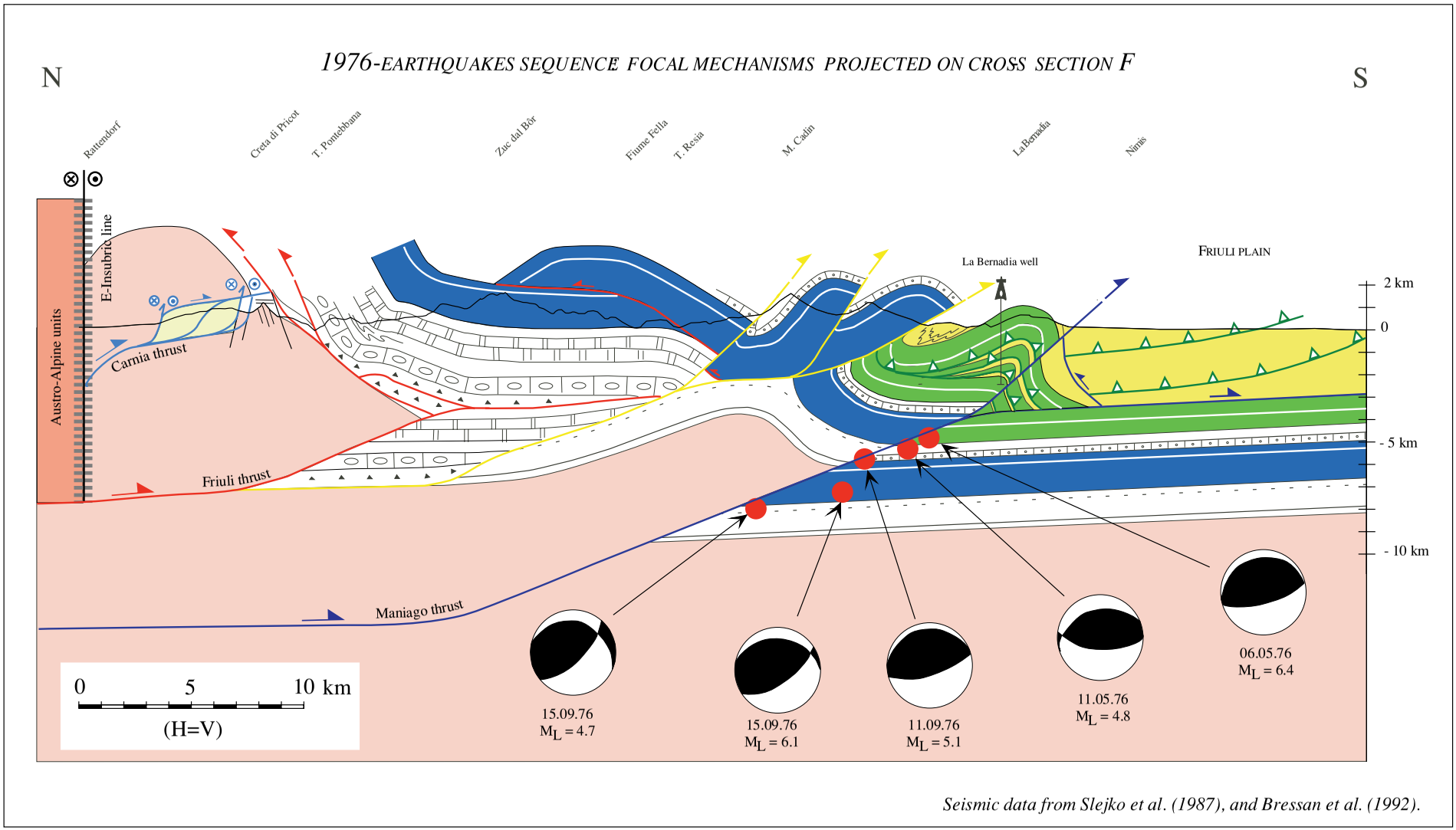

Fig. 37. Projection of hypocenter-aftershocks on cross-section E. Focal mechanisms of some major earthquakes are indicated. Spatial distribution of hypocenters points to activity along the Maniago thrust system.

6.2. COMPARISONS WITH SANDBOX MODELS

Koyi *et al.* (1999) related displacements along thrusts to the magnitude of earthquakes. He investigated two kinds of sandbox models. The first type of model shortened above a high-friction décollement and the second model shortened above a low friction (ductile) décollement. In areas where sedimentary rocks are shortened above a layer of salt or overpressurized shale, more than one thrust is active at a given time. Hence, it is expected that the entire fold and thrust belt is seismically active. However, since the bulk shortening is accommodated by slip along several thrusts across the belt, slip rate along individual thrust is expected to be low. Therefore, low magnitude earthquakes prevail in fold and thrust belt shortened above a ductile substratum (rocksalt or shale). In absence of a ductile layer, a piggy-back stack of imbricates forms with only the youngest of the thrusts at the deformation front being active. Unless erosion leads to reactivation of the older thrusts in these imbricate systems, only the frontal area of the wedge is expected to be seismically active. In these areas, since most of the bulk shortening is accommodated by slip along one thrust, the slip rate is expected to be high. Therefore, large-magnitude earthquakes (M_L= 6.4-6.8) are expected to occur in areas shortened above high-friction décollements. According to Koyi's models, the large-magnitude earthquakes recorded in the Friuli area (M_L= 6.4) indicate a high-friction décollement at the base of the wedge (high friction critical taper). This fits well to the hangingwall-ramp or footwall-ramp situation of the Maniago thrust (Fig. 37, and cross-sections A-G).

7. THE TRANSTENSIONAL ZONE OF SAPPADA

A look at the large-scale map of the eastern Southern Alps reveals the existence of an extensional faulted zone between the northeastern Dolomites and the Carnic Alps (Fig. 2). The northern thrusts of the Dolomites end to the east abruptly against a normal faulted area, 25 km long and 5-10 km wide. In this study, the graben area has been informally called "transtensional zone of Sappada" since the whole region around Sappada is located within the graben. This zone is illustrated in the tectonic map of the Sappada area (Fig. 17). This area underwent a complex Alpine tectonic evolution, including extensional, contractional and strike-slip deformations. The tectonic framework is made up of an ENE to NE-trending graben system, a SE-trending dextral fault system, and E-W striking south-vergent thrusting.

The study of the Sappada area is based on various sheets of the Italian geological map at 1: 100.000 (sheet 12 Pieve di Cadore, Castiglioni *et al.*, 1940; sheet 13 Ampezzo, Gortani *et al.*, 1933; sheet 4c-13 Monte-Cavallino-Ampezzo, various authors, 1971), two sheets of the tectonic map of the Southern Alps at 1. 200.000 edited by Castellarin in 1981 (sheet 12 Cortina d'Ampezzo, Semenza, 1981; sheet 4c-13 Monte Cavallino-Ampezzo, Frascari and Vai, 1981), and new mapping at scale 1: 10.000 and 1: 25.000.

7.1 THE SAPPADA GRABEN SYSTEM

7.7.1 Observations and data

The village of Sappada is located in the middle of a large graben striking WSW-ENE to SW-NE. According to sheets 4c-13 of the Italian geological map (various authors, 1971) and to Braga *et al.* (1971), the youngest sedimentary strata outcropping in the Sappada graben are Upper Jurassic limestones (Fig. 38). Structural relationships between the graben and the surrounding area are complex. The description of the Sappada graben goes from west to east. The tectonic map of the Auronzo di Cadore area shows the western part of the Sappada graben (Fig. 12). The western end of the Sappada graben is made up of subvertical NNE-trending faults (purple in Fig. 12) that cut two branches of the

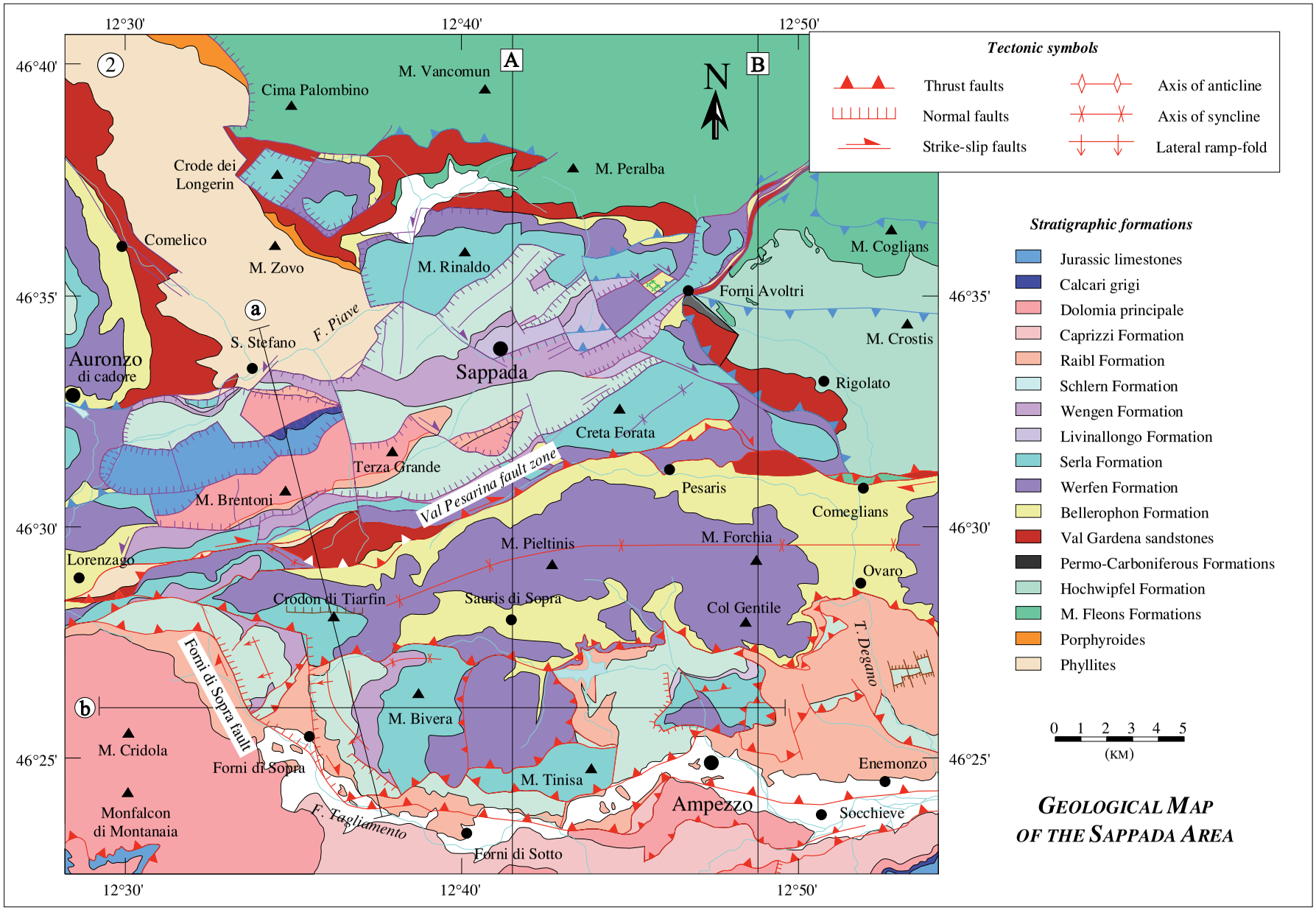

Fig. 37. Geological map of the Sappada area (n °2 in Figs. 2 & 3). Based on new mapping at 1: 10.000 and 1: 25.000, and after Gortani *et al.* (1933), and the Italian geological map at 1: 100.000 (sheets 4c-13 Monte Cavallino-Ampezzo, 1971). Large-scale cross-sections A and B refer to Figs. 22 and 23. Local cross-sections (a) and (b) refer to Figs. 38 and 39.

Marmolada-Sorapiss thrust system (blue in Fig. 12) near the locality of Cima Gogna along the Piave River. Kinematic indicators (slickensides and stylolites) related to the NNE-trending faults indicate sinsitral strike-slip displacement. Both branches of the Marmolada-Sorapiss thrust system are south-vergent, E-W trending thrusts, whose the southern one is termed Sorapiss thrust in figure 12. The southern border of the Sappada graben follows the Pesarina valley termed Val Pesarina fault zone (Figs. 17 and 38). There, geometrical relationships between the southern end of the graben and the Friuli-Valsugana thrust system are less evident (Fig. 17). This area is characterized by a complex network of steep NNW dipping faults. Map-scale and small-scale kinematic criteria such as slickensides, stylolites and fold axes indicate that the more recent movements along this faulted zone are transpressive with an important dextral component. The geological map of the Sappada area (Fig. 38) shows an alignement along the western part of the Val Pesarina fault zone of three lenses of epizonal basement rocks overlain by the Val Gardena sandstones of Middle Permian age. These lenses are strongly deformed and their sigmoidal shape points to a dextral slip component. These lenses of basement are surrounded by Lower-Middle Triassic beds and appear to have been pushed up. Various small-scale indicators (slickensides, stylolites) and meso-scale indicators such as fold axes support the kinematics inferred from map-scale structures. The Val Pesarina fault zone (Fig. 17) is connected in the west to the Valsugana thrust (Fig. 11) and in the east to the western continuation of the Fella-Sava line that separates the basement unit in the north and the Lower-Middle Triassic sequence in the south (Fig. 9).

The Val Pesarina fault zone is today seismically active. ENE-trending faults with vitrified planes are observed inside the Val Pesarina fault zone at several outcrops. These vitrified planes are located in the Schlern formation near the faulted contact between the Wengen shales in the SSE and the Schlern dolomites in the NNW (Fig. 38). Farmers of the Pesarina valley said me that important rock falls (Fig. 39) were produced by the recent earthquakes that shook the region (magnitude from 3 to 5 on the Richter'scale). The fault plane solutions of the main earthquake (1956 November 5; M_L = 4.8) that occurred near Paluzza along the Fella-Sava line (Fig. 9) indicate dextral strike-slip movements (Slejko *et*

Fig. 39. The Val Pesarina fault zone is parallel to the view (i.e. WSW-ENE strike). Mountain chain behind is made up of the Ladinian Schlern dolomites (Creton di Clap Grande). Outcrops at first plane are made up of Anisian Serla dolomites. The Val Pesarina fault zone is located between the top of the forest and the chain behind. According to farmer accounts, rock falls in the middle of the photo were produced by recent earthquakes.

al., 1987). The Val Pesarina fault zone constitutes the western continuation of the Fella-Sava line (Fig. 17). These observations and data testify to the ongoing seismic activity inside the Val Pesarina fault zone, and therefore the recent activity of the Friuli thrust system.

7.1.2 Interpretation

Timing of the Sappada graben formation may be debated. The Sappada graben is younger than Dinaric deformation since SW-vergent folds are clearly cut by steep ENE-trending faults related to the graben (Fig. 18). These cross-cutting relationships indicate that the Sappada graben is post-Eocene. What are the temporal relationships between the Sappada graben and the Friuli-Vasugana thrust system? Geometry of section (a) across the Val Pesarina fault zone suggests that the Sappada graben system and the Friuli thrust were probably contemporaneously active (Fig. 40). The dextral transpression indicated by slickensides and focal mechanisms of earthquakes postdate the Sappada graben formation. The later dextral transpression seems only to have reactivated the Val Pesarina fault zone as is suggested by the concentration of recent seismicity along this faulted zone.

7.2. THE SE-TRENDING DEXTRAL FAULT SYSTEM

7.2.1 Observations and data

The tectonic map in figure 17 shows two major, SE-trending faults at the southwestern edge and north of the Sappada graben. The northern fault is interpreted to be responsible for the tilting of the epizonal basement and its authochthonous cover toward the SW. This fault is not a straight fault but it is composed of small SSE to S-trending segments or "bridges" that link the main SE-trending fault. These "bridges" are probably contemporaneous with the small north-south trending grabens of the Croda dei Toni and M. Paterno northwest of Auronzo di Cadore (Fig. 12) reported from Caputo (1997). According to Caputo (1997), normal and transtensional kinematics were recognized only northeast of the Val Marzon line (Fig. 12). The western end of the Sappada graben, made

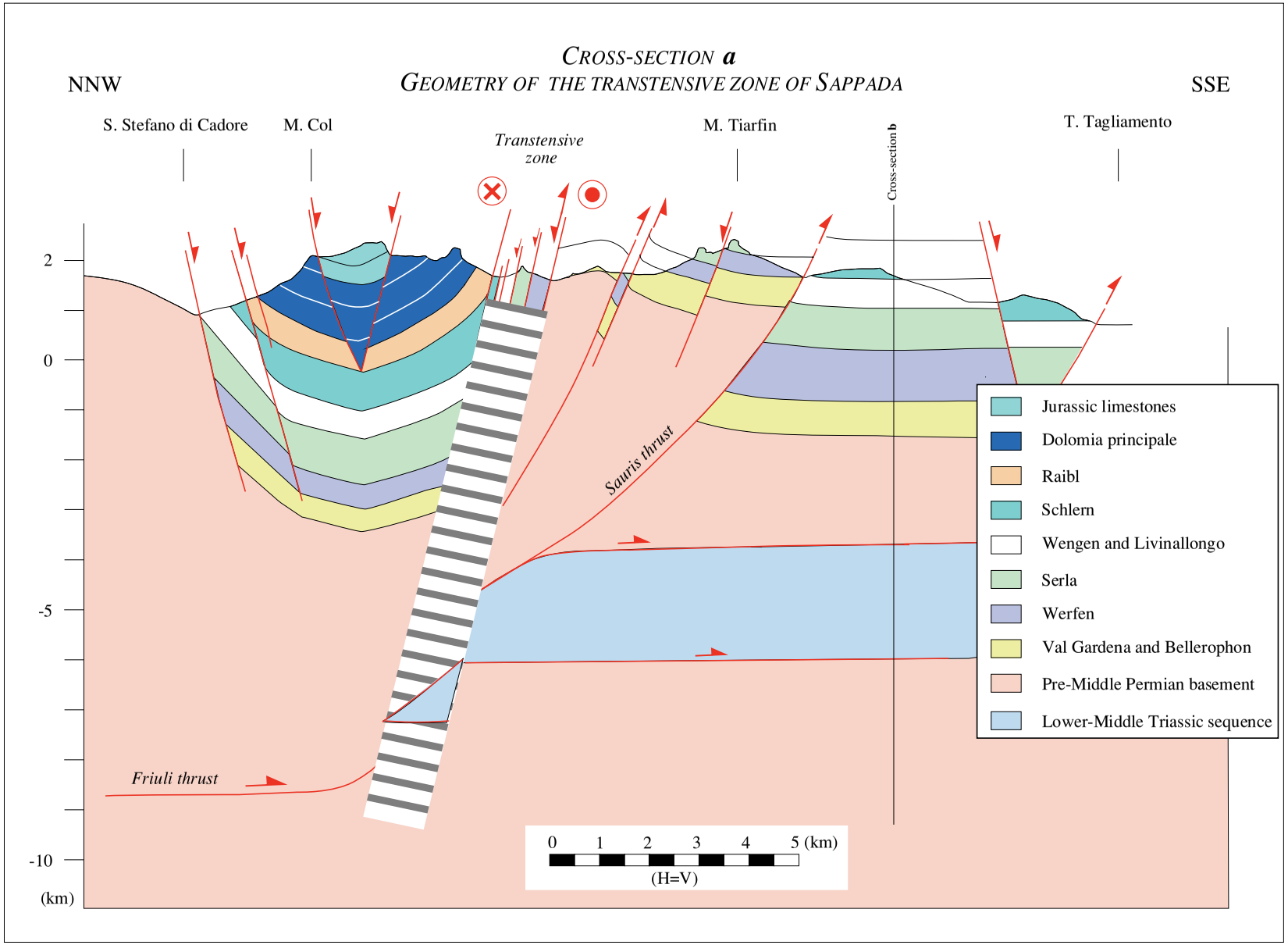

Fig. 40. Cross-section a (location in Fig. 17). Geometry of the transtensive zone of Sappada.

up of NNE-trending faults, plays the role of a transfer zone between both dextrally SE-trending, the Val Marzon line and the Forni di Sopra fault. Normal and transtensional deformations are limited into the northeastern area by these three segment faults. The geometry and kinematics of the SE-trending fault at the southwestern edge of the graben are more complex. To unravel the geometry, an east-west trending cross-section (b) was constructed through the M. Bivera-Clapsavon area (Fig. 41).

7.2.2 Interpretation

The structure drawn in figure 41 may be explained with a rollover geometry along the dextral SE-trending fault near Forni di Sopra (Fig. 17). This structure may be interpreted as a lateral ramp with a dextral slip component (indicated by striations). The tectonic map of figure 17 shows three east-vergent thrusts (termed X, Y and Z) in the footwall of the south-vergent Sauris thrust. The major thrust, in Lake Sauris, transported the Werfen formation (Scythian) onto the Raibl formation (Carnian), whereas the easternmost thrust (Z in Fig.17) superposed the Serla formation (Anisian) onto the Raibl formation. The more logical construction consists in drawing an imbricate fan of thrusts in the Lower-Middle Triassic sequence at depth. Such a construction gives an east-west shortening of about 12 km. Is this construction consistent with the surrounding structures? At which deformation phase can it be linked, Alpine or Dinaric? A Dinaric origin does not seem compatible with the overall tectonic framework. First, evidence for Dinaric thrusting is sparse, and Dinaric thrusts have a small shortening in the neighboring area. Secondly, these thrusts would be backthrusts with respect to the west-southwest Dinaric vergence and so far no Dinaric backthrust has been identified in the Southern Alps. Thirdly, these thrusts have no continuation to the north or south. Interpreted as an Alpine structure, these faults are strongly oblique with respect to the transport direction and is considerable in comparison to the total shortening along a north-south section (about 20%). This construction would lead to a prominent block rotation. No data support this interpretation. An alternative construction consists in filling the available space in depth with basement rocks (Fig. 41). This way, the east-west shortening is significantly smaller. There are north-

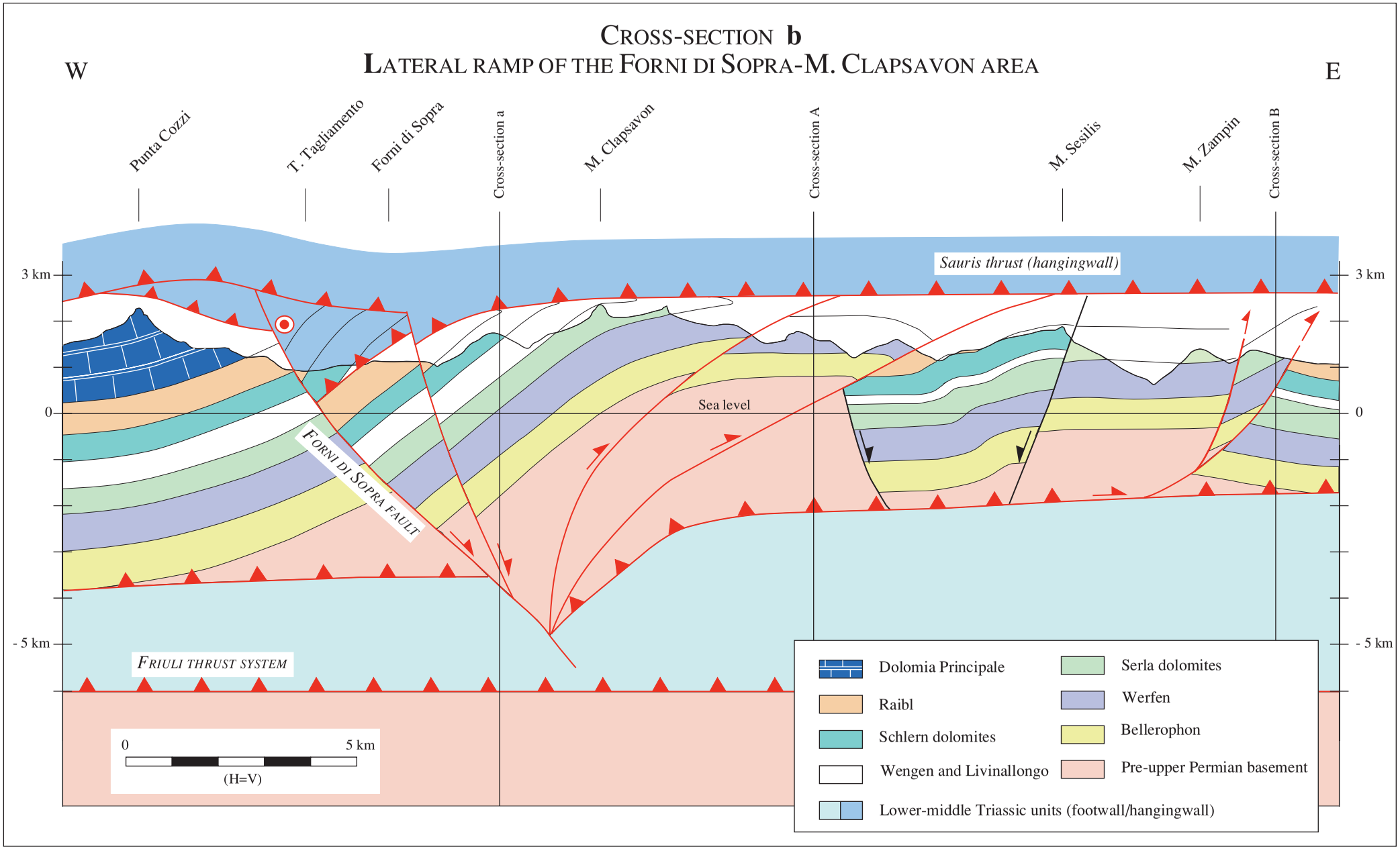

Fig. 41. Cross-section b (location in Fig. 38). Geometry in roll-over along the lateral ramp of the Forni di Sopra-M. Clapsavon area.

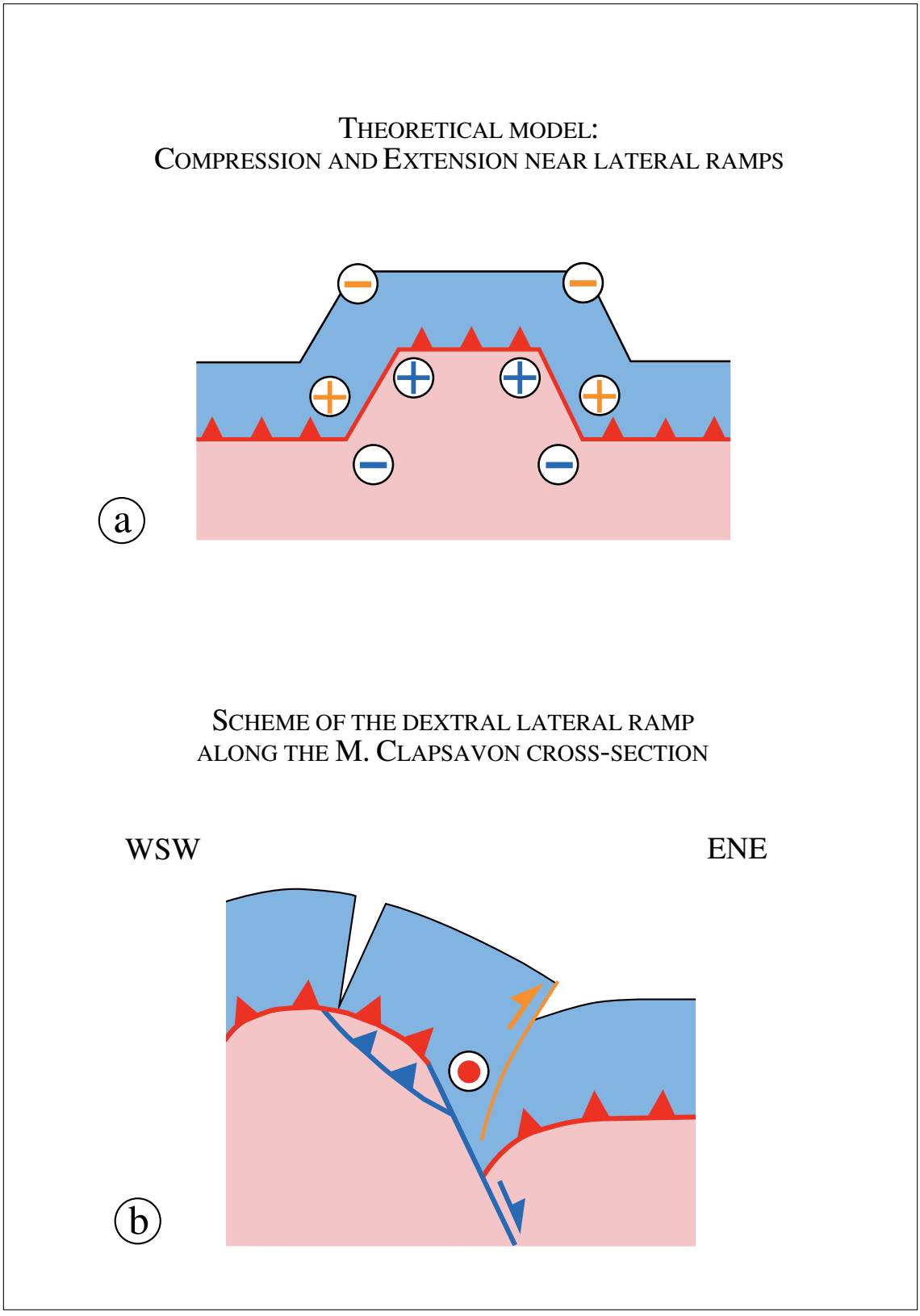

Fig. 42. (a) Theoretical model for compression and extension near lateral ramps from Apotria *et al*. (1992), and Schönborn (pers. comm.). (b) scheme of the dextral lateral ramp along the M. Clapsavon cross-section (Fig. 41).

south trending normal faults (i.e. near M. Sesilis) need to be integrated in the construction (Fig. 17). As these normal faults are cut by Alpine thrusts, they must be older. However, their age is not well constrained. Thickness changes may be observed in the Ladinian strata (westward thickening) but no breccias were observed. These observations are not convincing enough for Middle Triassic syn-sedimentary faults. Since Carnian deposits are the youngest horizons in the footwall of the Sauris thrust, there is no direct evidence of a Jurassic origin, although this hypothesis seems most likely. Jurassic normal faults are preserved south of this region (west of M. Valcalda, in Fig. 13) and their orientation is generally north-south, like near M. Sesilis. So, an Alpine age of the east-vergent thusts is assumed. These east-vergent thrusts may be linked with the dextral lateral-ramp into a model which links them kinematically. Figure 42 illustrates what is theoretically expected when compression occurs along a lateral ramp (Schönborn, pers. comm.). The hangingwall (blue) is laterally compressed in the synclines (+), and laterally expanded in the anticlines (-). The footwall (pink) deformed the opposite way; it is laterally compressed near the top of the obstacle, and laterally expanded near the foot of the obstacle. The hangingwall of the model would be represented by the footwall of the Sauris thrust and the east-vergent thrusts would be due to the space problem in the syncline. The cross-section (b) of the M. Clapsavon area (Fig. 41) withstands well the comparison with the theoretical model (Fig. 42). Nevertheless, the solution proposed in cross-section (b) must be considered only as a possible solution (or a working hypothesis for the future) but not as the definitive solution.

7.3 KINEMATIC MODEL OF THE TRANSTENSIONAL ZONE OF SAPPADA

At the eastern end of the Southern Alps, the Alpine thrusts are gradually replaced by southeast-trending dextral strike-slip faults (Palmanova, Udine, Cividale, Idrija) that follow the northeastern border of the current Adriatic plate toward the Dalmatian coast (Fig. 2). These faults branch off the dextral E-Insubric line at an angle of 30-35°, typical of Riedel faults. In the western part (northeastern end of the Dolomites), these faults do not join the E-Insubric line, but they merge into the transtensive area near the line (Fig. 2). To the west

this transtensional zone is sharply limited by the continuation of the Palmanova line toward the NW (Fig. 43). This suggests a relation between the large dextral SE-trending faults and the peculiar wedge-shaped transtensional area. Dextral displacement along the E-Insubric line must decrease toward the east since the Palmanova line takes up part of the displacement. Thus, the area where the Palmanova line branches off the E-Insubric line must be under extension as long as both faults act contemporaneously (Fig. 43, see also Schönborn, 1999). Figures 43 and 44 explain these faults as a pull-apart structure between the two dextral strike-slip faults. As this area experiences transtension in a NNW-SSE contractional regime, SSE-trending normal faults are expected. However within this area, transtension is expressed by a network of SSE to SE normal faults and E to ENE-trending normal faults which is partially incoherent with a NNW-SSE contractional regime (Fig. 44). This network of transtensional faults followed and reactivated inherited faults. As the graben system strikes ENE, inherited patterns with the same direction are suspected. Further west in the central Dolomites, the N70° trending Stava line is interpreted as a transpressional zone of Middle Triassic age (Doglioni, 1984, 1987). Additionally, the Early Jurassic paleoboundary between the Trento platform and the Belluno basin is suspected to follow the same direction further west in Valsugana (Bosellini *et al*., 1981). Permian normal faulting, expressed as ENE oriented graben and pull-aparts, is described in the literature (Massari, 1986). Paleogene southwest-vergent thrusts trending SE could have initiated the lateral ramp system. These lateral ramps were linked together with SSE-trending bridges, parallel to the main contraction direction. In conclusion, the transtensional event linked to the activity along the E-Insubric line reactivated inherited faults. Their orientation seems to have strongly controlled directions of the Alpine structures. In the Southern Alps, many Alpine faults are suspected to reflect an ancient pattern, but generally this is difficult to prove because of the lack of exposed syntectonic sediments.

This kinematic model of the Sappada zone implies synchronous activity of the Valsugana-Friuli-Palmanova-Idrija system and the E-Insubric line (Figs. 43 and 44). However, the southeast trending strike-slip faults were presumably still active after activity

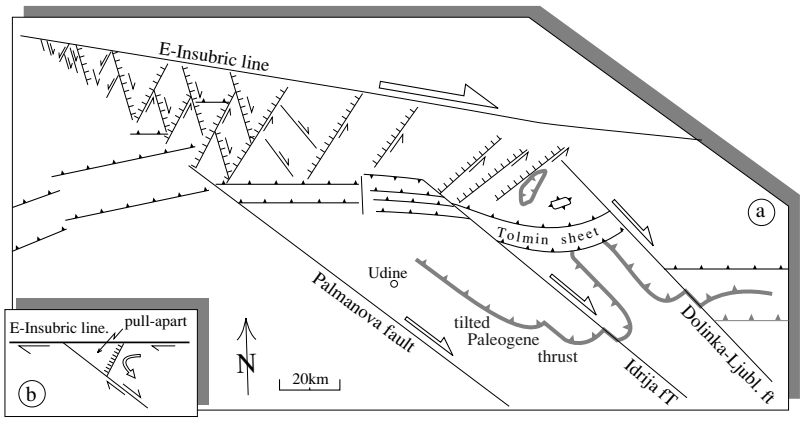

Fig. 43. Intense faulting in the Carnic and Julian Alps can be explained as a pull-apart structure between the SE-trending faults (*e.g.*, the Palmanova and Idrija faults), and the equally dextral E-Insubric line. (a) and (b) Scheme of the suggested pull-apart structure. Taken from Schönborn (1999).

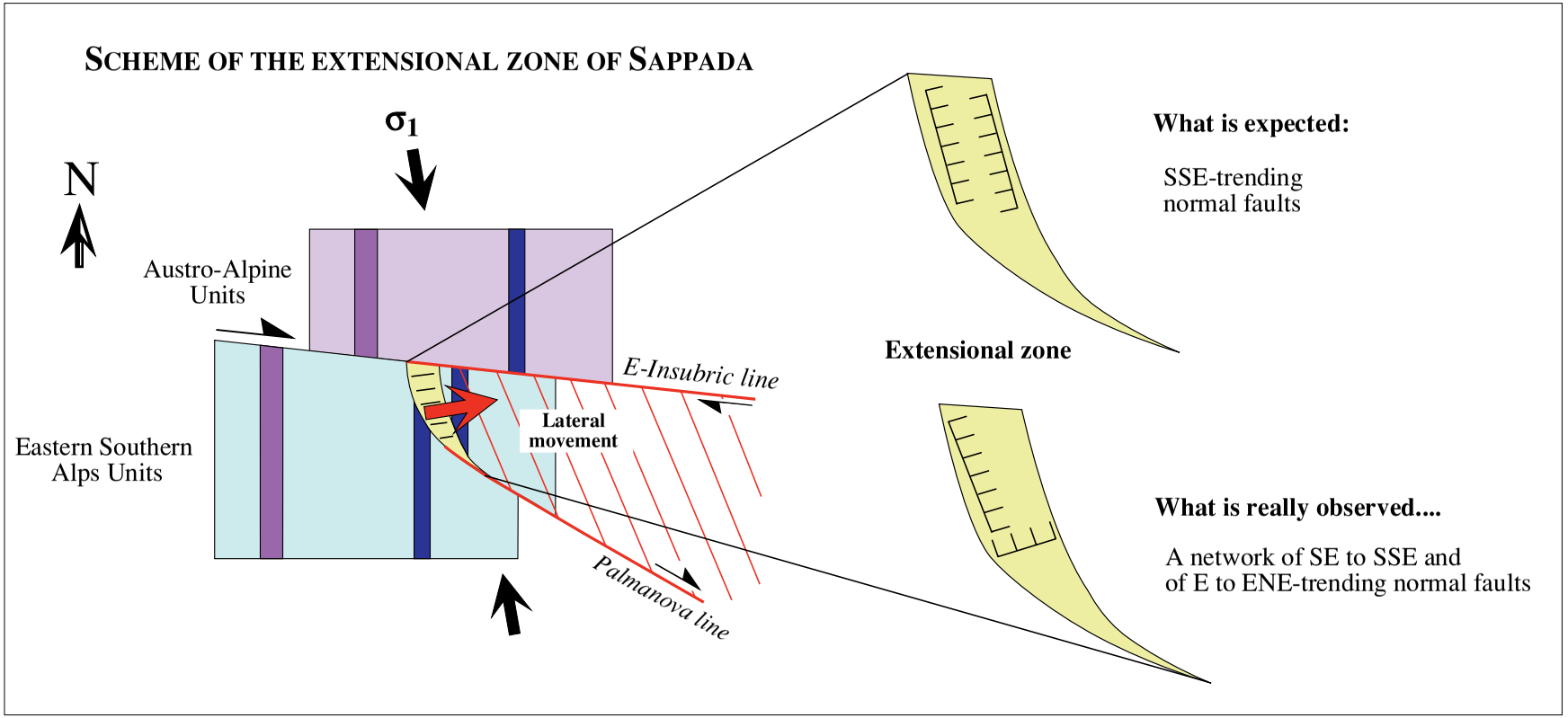

Fig. 44. Interpretation of the transtensional zone of Sappada. Scheme of the suggested pull-apart structure between the dextral E-Insubric line and the dextral Palmanova line.

along the E-Insubric line had ceased, because similarly oriented but less important faults cross-cut the E-Insubric line in the Carnic Alps (Fig. 2, see also Läufer, 1996). In the Karawanken mountains further east, the southeast trending dextral strike-slip faults link with contemporaneously active transpressional structures fringing the E-Insubric line (Polinski and Eisbacher, 1992, Fodor *et al*., 1996, 1998). Some of these faults displace and presumably postdate the E-Insubric line. Further east, close to the Pannonian basin, deep transtensional basins opened up between the E-Insubric line and southeast-trending dextral faults during the Pliocene and Quaternary (Vrabec, 1996). The Velenje basin is filled with up to 1000 m of Plio-Quaternary deposits.

8. THERMAL MATURITY OF SEDIMENTS

In this chapter, I determine the thermal maturity of rocks from the Friuli Alps. The final objective is to test whether Dinaric and/or Alpine tectonics have affected the thermal maturity or not. In other parts of the Alpine belt, various studies have tried to quantify the influence of tectonics on low-grade to very low-grade metamorphism (Burkhard, 1988; Mosar, 1988). There are many methods for quantifying the thermal maturity of diagenetic to low-grade metamorphic domains. Both organic and mineral indicators can be used to assess diagenetic or low-grade conditions. Generally, measurable indicators of thermal maturity cannot be directly converted to paleotemperatures because they depend on several parameters such as temperature, time, pressure, type of organic matter, rock and mineral composition, pH and other factors. A large set of independent indicators should be used to confirm that results are consistent.

The first step consists in mapping the indicators of thermal maturity such as vitrinite reflectance, T_{max} from Rock-Eval pyrolysis, clay mineral assemblages, illite crystallinity and the smectite to illite transformation ratio. Mapping the thermal indicators is a useful tool for testing the anomalous zones near the major thrusts.

8.1 ORGANIC THERMAL INDICATORS

8.1.1 Introduction

Organic matter in sediments is very sensitive to heat exposure. The maturation level attained by the organic matter is irreversible and depends only on a few factors such as temperature and time (Teichmüller & Teichmüller, 1986; Tissot *et al.,* 1987). This is the main reason why organic diagenesis is so important for reconstructing the thermal history of sedimentary basins. The maturation level of sedimentary organic matter is usually expressed by two kinds of indicators. The first category groups together the optical maturation indices such as vitrinite reflectance, thermal alteration index (TAI) and spectral fluorescence indicators. The second kind of indicator consists of the organic geochemistry

parameters of kerogen, such as T_{max} from Rock-Eval pyrolysis, H/C and O/C ratio from last analysis, electron paramagnetic resonance and stable carbon isotopes. Vitrinite reflectance and T_{max} from Rock-Eval pyrolysis are undoubtedly the most widely used indicators of thermal maturity. Vitrinite reflectance is also regarded as the most reliable and precise method for quantifying organic diagenesis (Bustin *et al*., 1985). Vitrinite reflectance is an optical method. The temperature index obtained from Rock-Eval pyrolysis (T_{max}) is another widely used maturation index (Tissot & Welte, 1984). In addition, Rock-Eval pyrolysis yields information on the composition and origin of the organic matter (Espitalié *et al.,* 1985a, 1985b, 1986).

A fair amount of organic matter derived from higher plants is required to use the technique with confidence. Due to the absence of organic rich horizons in the study area, we were not able to measure the vitrinite reflectance directly. The vitrinite reflectance parameter can be recalculated from Rock-Eval pyrolysis. Vitrinite reflectance and T_{max} have been correlated in an Espitalié's diagram (1985b). Knowing T_{max} values, obtained from Rock-Eval, vitrinite reflectance can be estimated with help of this diagram. This process is not as reliable as direct measurements, and both parameters - T_{max} and vitrinite reflectance - should be obtained independently if possible.

8.1.2 Rock-Eval pyrolysis

Rock-Eval pyrolysis is used to determine the petroleum potential and thermal maturity of rocks. This method provides a rapid evaluation of the type of solid organic matter. A complete Rock-Eval analysis is divided into a pyrolysis phase and oxidation phase. Pyrolysis consists in heating a sample at a pre-selected rate in an inert atmosphere and monitoring the type and amount of gases produced. The analysis simulates maturation of organic matter by progressively heating the rock samples to 850°C. This heating distils the free organic compounds, then cracks pyrolytic products from the kerogen. A detailed introduction to the Rock-Eval pyrolysis techniques and applications can be found in the literature (Espitalié *et al*., 1985, 1986; Lafargue *et al*., 1996).

Samples were analysed at the Geological Institute of the University of Neuchâtel with a Rock-Eval 6 pyrolyzer (Vinci Technologies). Samples were desiccated and ground prior to analysis. A known quantity of the sample is heated at 250°C for 3 minutes in the oven. The free hydrocarbons in the rock are vaporised and recorded as an initial peak S1. The sample is then heated to 850°C through step-wise heat increases of 25°C each minute. The remaining organic matter is then thermally cracked releasing hydrocarbons which produce a second peak S2. Maximum production of these hydrocarbons (top of peak) occurs at a temperature called T_{max}. The total organic carbon (TOC) of the sample is obtained by summing the pyrolysed carbon with that obtained by oxidation of the residual organic matter at the final temperature of 850° C. The use of the Rock-Eval 6 pyrolyzer instead of the Rock-Eval 2 pyrolyzer has several advantages. In Rock-Eval 6, the final pyrolysis temperature is 850°C instead of 600°C. As a consequence, and more specifically for type III kerogen, the petroleum potential of the samples (S2) is increased and the resulting Hydrogen Index (HI) is more representative. Another output of this high temperature pyrolysis is the possibility of measuring high T_{max} values for type III samples with vitrinite reflectance values (Ro) greater than 2. The correlation between T_{max} and Ro is extended to very mature samples which was not possible with the Rock-Eval 2 pyrolyzer.

The apparatus is calibrated by a sample used as standard after each 10 samples. The standard of the Rock-Eval 6 pyrolyzer is characterized by T_{max}: 419°C and TOC: 2.86 %. The Rock-Eval apparatus measures the following parameters: S1, S2, T_{max}, TOC and MINC, which are represented on chromatograms.

S1: This parameter quantifies the free hydrocarbons (HC) present in the sample and is expressed in mg HC per gram of sample.

S2: This parameter represents the residual petroleum potential which has not yet been used to generate hydrocarbons. S2 varies with TOC, type of organic matter and maturation level, and is expressed in mg HC per gram of sample.

T_{max}: the temperature index. T_{max} (°C) is considered as a widely used maturation index, as it increases with the maturation of organic matter (Tissot & Welte, 1984). Tmax is measured at the top of the peak S2. T_{max} varies with the type of organic matter and is more sensitive for determining the degree of maturation in organic matter of type III (Espitalié, 1986).

TOC: Total Organic Carbon. This is a measure of the quantity of organic carbon in a sample and is expressed in weight %. TOC is the sum of the pyrolysed carbon (PC) and the remaining carbon (RC). This parameter is used for source rock characterization (Espitalié *et al.,* 1986).

MINC: This parameter measures the quantity of mineral carbon in a sample, expressed in weight %.

The validity of theses parameters is subjected to the following constraint: if TOC < 0.3%, all parameters become unreliable. This restriction constrains to sample only in rich organic matter horizons.

26 outcrop samples were chosen for Rock-Eval analysis (ANNEXE 1). They were collected from the shales of the Auernig formation (Upper Carboniferous), from the marls of the Livinallongo (lower Ladinian), Wengen (upper Ladinian), and Raibl (Carnian) formations, from the bituminous limestones of Caprizzi (Norian), and from the Eocene flysch. According to the chromatograms (signal and geometry of the peak S2) and TOC values, 20 samples provided reliable values and can be correlated with others indicators. All samples have been plotted in the van Krevelen diagram (H/C versus O/C; Tissot & Welte, 1984). Results indicate that the organic matter in all samples is mainly composed of type III kerogen. This type of organic matter is derived from terrestrial higher plants. The type III kerogen is the only source of organic matter that can be directly correlated with the vitrinite reflectance (Espitalié *et al.*, 1985b). Accordingly, Tmax values obtained from Rock-Eval can be transformed into vitrinite reflectance values (Ro%).

8.2 MINERAL THERMAL INDICATORS

8.2.1 Methodology

Many maturation indices based on the diagenesis of the mineral fraction have been developed. The clay mineral analysis and the fluid inclusion analysis provide the main mineral thermic indicators. The equilibrium of clay minerals and their mutual transformations probably provided the most used mineral indicators in the past. Clay mineral assemblages in general and the smectite to illite transformation in particular have been used by many investigators as indicators of thermal history (Kübler, 1964, 1984; Burst 1959, 1969 and many others). The following methods were applied in this study:

Identification of clay mineral assemblages
Calculation of percentage illite in mixed-layered illite/smectite
Illite crystallinity (IC) measurement.

These three methods are based on X-ray diffraction analysis (XRD). All XRD analysis were performed by T. Adatte at the laboratory of geochemistry, mineralogy and sedimentology (University of Neuchâtel), using a SCINTAG's XRD diffractometer. This X-ray powder diffractometer (model: SCINTAG XDS 2000) has the following characteristics:

The fixed (routine) analytical conditions are:

- the spectral counter (KEVEX PSI1,PELTIER cooled silicon detector)
- wave length: 1.5406 A Cu Kα1
- generator power: 45 kV and 40 mA
- goniometer type: θ/θ
- goniometer radius: 250 mm
- emitting slits: 2 mm, 4 mm
- receiving slits: 0.5 mm, 0.3 mm
- continuous scan

- round (ϕ25 mm) glass plates

The variable analytical conditions are:

- goniometer speed (range from 1°/min to 10°/min.)
- acquisition step size (chopper increment: .03 or .05 °2θ)
- sample spinning or not

The files generated with SCINTAG are raw data (.RD), that are transformed by the software (DMS program, v. 2.63, graphic-normal display) into calculated (.NI) files. The calculations are the following: Fast Fourier noise filter, background subtraction and Kα2 stripping. The Scherrer width (SW) measurements are usually made on calculated files. As an instrumental error can occur due to the fluctuation of the X-ray source, detection and amplification, the same sample is tested 6 times under the same conditions: goniometer speed of 1°/min., step size of .03 and spinning round glass plate. The mean SW error is < 3% and the mean intensity error is < 1%.

Whole rock samples were prepared following the method of Kübler (1987). For each rock sample, approximately 20 g were ground to obtain small rock chips (1 to 5mm). Of these, 5 g were dried at a temperature of 60°C and then ground again to a homogenous powder with particle size <40µm. 800 mg of this powder was compressed (20 bars) in a powder holder and analyzed by XRD. Whole rock composition was determined using external standards based on the methods described by Ferrero (1965, 1966), Klug & Alexander (1974), Kübler (1983), and Moore & Reynolds (1989).

Clay mineral analyses were based on the Kübler's methods (1987). Ground chips were mixed with de-ionized water (pH 7-8) and agitated. The carbonate fraction was removed with 10% HCl (1.25N) at room temperature for 20 minutes or more until all the carbonate was dissolved. Ultrasonic disaggregation was performed for 3 minutes. The insoluble residue was washed and centrifuged (5-6 times) until a neutral (pH 7) suspension was obtained. Separation of different grain size fractions (<2µm and 2-16µm) was obtained

by the timed settling method based on Stokes law. The selected fraction was then pipetted onto a glass plate and air-dried at room temperature. XRD analyses of oriented clay samples were made after air-drying in ethylen-glycol solvated conditions for the fraction <2μm. The intensities of selected XRD peaks characterizing each clay mineral (e.g., chlorite, mica, kaolinite, chlorite-smectite and illite-smectite mixed-layers) were measured for semi-quantitative estimates of the proportion of clay minerals present in the size-fractions <2μm and 2-16μm. Therefore, clay minerals are given in percent abundance and in counts per minute without correction factors. The clay mineral ratios are calculated from XRD mineral peak data in counts per minute.

8.2.2 Identification of clay mineral assemblages

The clay mineral assemblages were qualitatively determined on the < 2 μm and 2-16 mm size-fractions. X-ray identification of clay minerals is based essentially on the recognition of structural characteristics, the most important one being layer spacing. Oriented samples of most clay minerals show almost exclusively the 00L diffractions from which the layer spacings are obtained by means of the Bragg law. Clay minerals diffraction patterns are characterized by the peak position, intensity, shape and breadth. Four basic groups of clay minerals can be distinguished (Eslinger & Pevear, 1988) according to the first order reflection near:

i) 7 Å (1:1 minerals, e.g. kaolinite, serpentinite)
ii) 10 Å (non-swelling 2:1 minerals, e.g. mica)
iii) 14 Å (swelling 2:1 minerals, e.g. smectite and non-swelling chlorite)
iv) Sepiolite and palygorskite

X-ray identification of clay minerals has been performed on 90 samples collected from different stratigraphic horizons and tectonic units. The clay mineral assemblages are summarized in Table 1, where they are compared with different indicators of thermal maturity.

8.2.3 Percentage of illite in mixed-layered illite-smectite

Illite/smectite is the most abundant, diverse, and widespread of the mixed-layered clay minerals in sedimentary rocks. The transformation of smectite to illite is probably the volumetrically most important clay mineral reaction in sedimentary rocks and is linked to burial diagenesis. Smectite illitization is a forward reaction that is favored by temperature, time and K concentration. It is generally accepted that the percentage of smectite layers in illite/smectite (%S in I/S) invariably decreases with increasing temperature. Therefore, the mineral is a potential, sensitive indicator of thermal transformation (Moore and Reynolds, 1989). Illite forms from smectite under diagenetic conditions according to the reaction:

K-feldspar + smectite —> illite + chlorite + quartz

Srodon & Eberl (1984) compiled temperature data for the conversion of smectite percentage in mixed-layered I/S in the North Sea, the Gulf Coast and the Douala basin. They reported the following temperature ranges for a fixed I/S composition: 80% S in I/S: 50 - 80°C, 60% S in I/S: 60 - 90°C, 40% S in I/S: 80 - 110°C, 20% S in I/S: 120 - 200°C. Theses paleotemperatures estimations have been used in this study to calculate the burial depths. Assuming a paleogeothermal gradient of 25°C/km and a mean annual surface temperature of 15°C, the following approximated burial depths may be calculated:

- 80% S in I/S: 1.4 - 2.6 km
- 60% S in I/S: 1.8 - 3.0 km
- 40% S in I/S: 2.6 - 3.8 km
- 20% S in I/S: 4.2 - 7.4 km

These values are only approximate and give a rough idea about the burial depth according to the percentage of smectite in I/S.

The structure of mixed-layered illite-smectite is complex. Illites/smectites exhibit a sequence of interlayering schemes that begins with random interstratification (Reichweite

R=0), proceeds to short range ordering (R=1, rectorite) and then to long range ordering (R=3) of the illite and smectite layers. Virtually all mixed-layers containing 40 to 100% smectite layers are randomly interstratified; in the case of less than 40% smectite layers, ordered interstratification is the general rule. The relation between the percentage of illite or smectite in mixed-layered illite-smectite and the degree of ordering allows to define the "Reichweite" of a sample. The percentage of illite in mixed-layered illite-smectite was mesured on 72 samples (ANNEXE 2). All values have been transformed into a "Reichweite" value in order to compare them with thermal maturity data obtained from other methods. Locations of samples can be found in Table 1.

8.2.4 Illite crystallinity (IC) measurement

Weaver observed in 1960 that illite peaks vary considerably in shape and in width. He proposed the "sharpness ratio" to quantify this phenomenon and found that peak sharpness increased with increasing diagenetic and metamorphic grades. Kübler (1964, 1967, 1968) developed a more convenient parameter for the quantitative evaluation of peak sharpness. Kübler introduced the "illite crystallinity index" (IC) that consists in measuring in mm or in degrees 2θ, the full width at the half height of the first diffraction peak of the mica group. This measurement is also named Scherrer width (SW). The Scherrer width (SW) and peak measurements were done on the first (10Å) mica reflection of < 2µm air-dried, < 2µm glycolated and 2-16µm air-dried, oriented clays. IC is considered as an useful parameter of incipient metamorphism in shales and marls. IC has been calibrated with mineralogical associations and compared with the potential oil window and vitrinite reflectance data (Kübler, 1968, Héroux *et al.*, 1979). Major problems in the use of this parameter are related to the sensivity of IC to an increase of Mg or Na activities versus K and the widening of the (001) peak due to the neoformation of clay minerals (Kübler, 1990).

The SCINTAG XDS 2000 diffractometer defines the limits between diagenesis, anchizone and epizone as follows:

- 0.22 °2θ for the limit between anchizone and epizone
- 0.33 °2θ for the limit between diagenesis and anchizone

The corresponding temperatures for these limits may be obtained with fluid inclusion data. The diagenesis-anchizone boundary is estimated at 235±10 °C (Mullis, 1995; Mullis *et al.,* 1995), whereas the anchi-epizone boundary is fixed to about 300°C (Frey, 1986).

IC is mainly a function of temperature and has therefore been widely applied to determine diagenetic and very low-grade conditions. An increase in temperature leads to increased crystallinities and sharper and more symmetric peaks. However, the following factors may also influence illite crystallinities: fluid pressure, strain, time, lithology, illite chemistry, varying geothermal gradients, interferences with other peaks on the diffractogram and laboratory conditions.

Besides temperature, lithology plays the most important role. This is often underestimated and may lead to erroneous interpretations. To avoid this problem, samples should be taken from fine-grained pelitic rocks with almost constant mineralogy. In other sedimentary rocks as sandstones or limestones, illite is often of detrital origin. A mixture of detrital and authigenic micas would therefore lead to artificially higher crystallinities (lower IC values) and would be not any more indicative for the thermal conditions. In this case, IC values give some information on the freshness of detritism. The influence of the lithology decreases strongly with increasing maturation. After the diagenesis-anchizone boundary, lithologic effects become negligible and data are reliable.

The occurrence of certain minerals may influence the measurement of IC by increasing the width of the illite first basal reflection near 10 Å. Examples for minerals which interfere with illite are paragonite (9.66 Å), the mixed-layered paragonite/phengite, allevardite (corrensite, 10.9 Å) and pyrophyllite (9.14 Å). As a consequence, the IC seems to be lower and so does the metamorphic grade. The presence and the amount of these

minerals must be determined in order to correct the IC. Their contents in the measured samples are extremely low, their influence on the illite peak can be neglected.

IC measurement was performed on 90 samples collected from different stratigraphic layers and tectonic units in the study area (ANNEXE 3). A representative sampling was achieved including samples from the Variscan basement as well as from the post-Variscan sequence and the different Alpine sequences. IC values should must be compared with other indicators before determining the thermal conditions (see chapter 8.3).

8.3 ZONEOGRAPHY OF VERY LOW-GRADE METAMORPHISM

8.3.1 Methodology and terminology

Thermal maturity of 90 samples taken in different tectonic and stratigraphic horizons was determined using both mineral and organic indicators. The following indicators were applied in this study:

- Clay mineral assemblages
- Mixed-layered illite/smectite ratio —> Reichweite
- Illite crystallinity (IC)
- Rock-Eval pyrolysis —> Vitrinite reflectance (Ro%)

Results obtained from the different methods were compared before classing the samples in different diagenetic stages (Table 1). The zoneography used in Table 1 is based on the zones by Kübler (1980, and Kübler *et al*., 1979a, 1979b) who divided the domain of diagenesis and very low-grade metamorphism into 6 zones, called Kübler zones. Kübler zones 5 and 6 correspond to anchizone and epizone respectively. For lower thermal conditions, Kübler has split the diagenetic domain into four zones (from 1 to 4). This subdivision within the domain of diagenesis is very useful for determining very low-grade conditions with precision. According to the present-day study, the domain of diagenesis

was divided into three parts since the Kübler zones 1 and 2 were not distinguishable. Therefore, the zoneography of diagenesis has been defined as follows:

- Superficial diagenesis corresponding to the Kübler zones 1 and 2
- Middle diagenesis -> zone 3
- Deep diagenesis -> zone 4

8.3.2 Data representation in map and cross-section

Sappada area. The distribution of samples in map reveals no influence of tectonics on thermal maturity (Fig. 45). All samples of the Lower-Middle Triassic sequence indicate middle diagenetic conditions. Both samples from siltstones of the Middle Permian and Upper Permian reveal deep diagenetic conditions. In addition, the occurrence of a Variscan epizonal basement in the north and a Variscan anchizonal basement in the northeast of the map is confirmed by our data. These two basement units with different metamorphic grade are separated by the Bordaglia fault zone represented in figure 45. Based on structural and sedimentological data, these two Paleozoic sequences are interpreted by Hubich *et al*., (1999) as two different Variscan nappes (Fleons and Cellon-Kellerwand nappes), explaining the difference in the metamorphic grade. The Bordaglia inherited fault has been reactivated during Alpine deformation as a sinistral transpressive fault. All data may be best visualized in cross-section (Fig. 46).

Tolmezzo and Gemona areas. Samples of various stratigraphic horizons and different tectonic units were mapped in both areas (Figs. 47 & 48) and placed in a large-scale cross-section (Fig. 49) as well as in a restored section (Fig. 50). All data from the Alpine sequence, except the samples of Carnian age, indicate diagenetic conditions. Pre-Middle Permian basement is characterized by anchizonal to epizonal conditions, mainly inherited from Variscan deformation (Menegazzi *et al.*, 1991; Rantitsch, 1997; Läufer, 1996, Hubisch, 1999). The Middle Permian to Miocene sedimentary cover reveals diagenetic conditions. Superficial diagenetic conditions in Cretaceous limestones and Paleogene

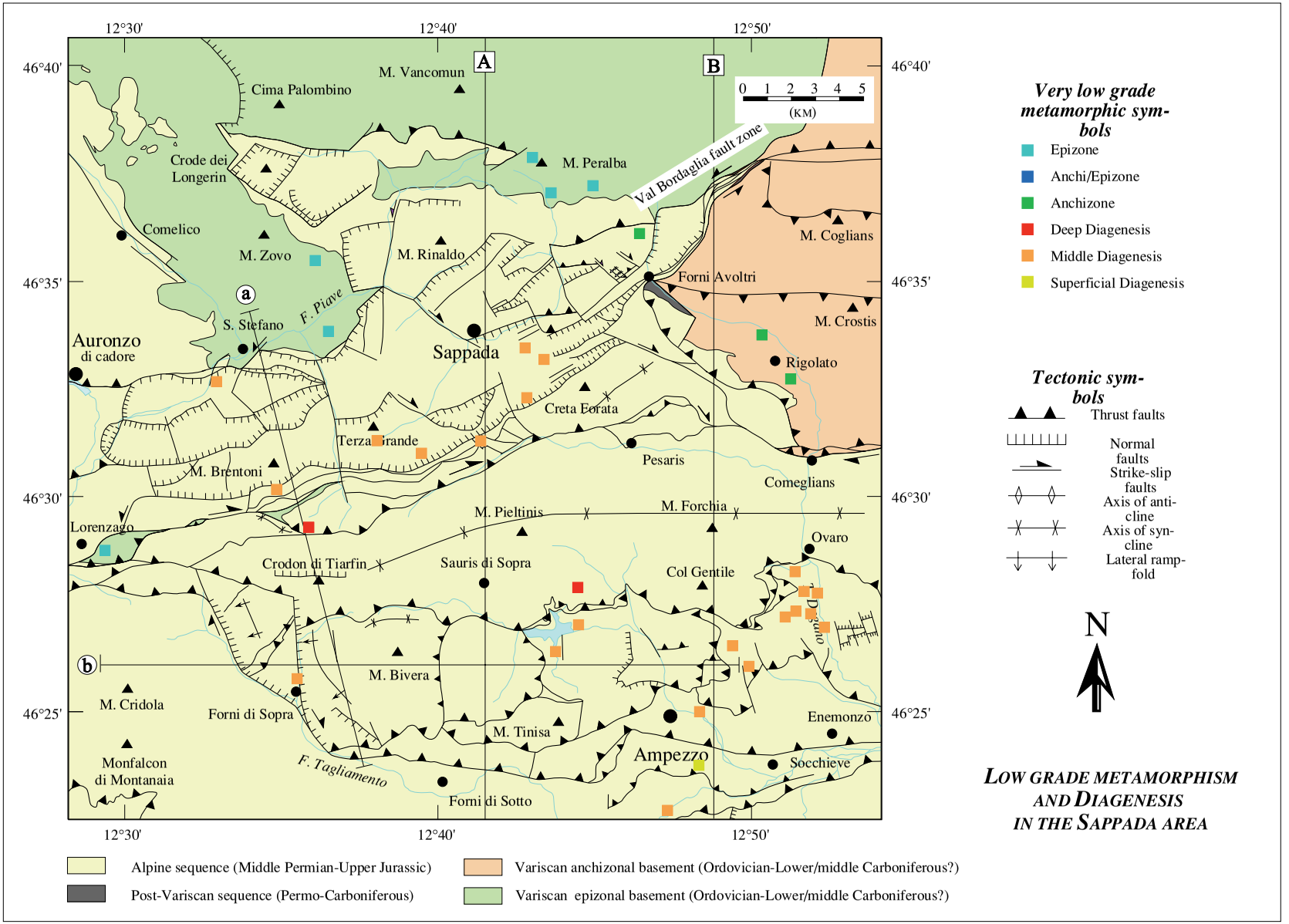

Fig. 45. Map of diagenetic to very low grade metamorphic indices in the Sapadda area. The Val Bordaglia fault zone separates the Variscan epizonal basement rocks in the northwest from the Variscan anchizonal basement rocks in the southeast. See explanations in text.

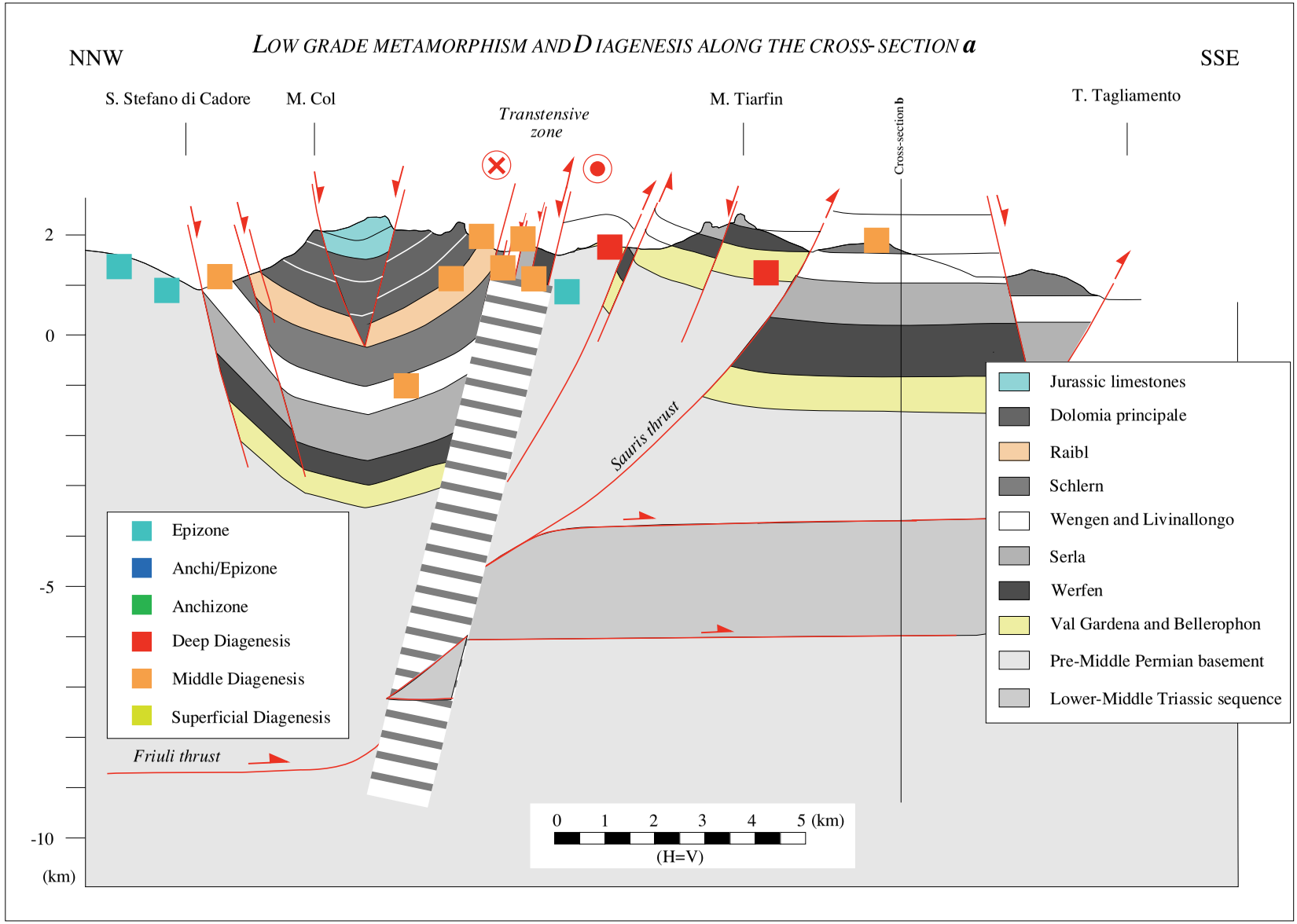

Fig. 46. Diagenesis to very low grade metamorphism along the cross-section (a) across the Sappada zone (Fig. 41). See explanations in text.

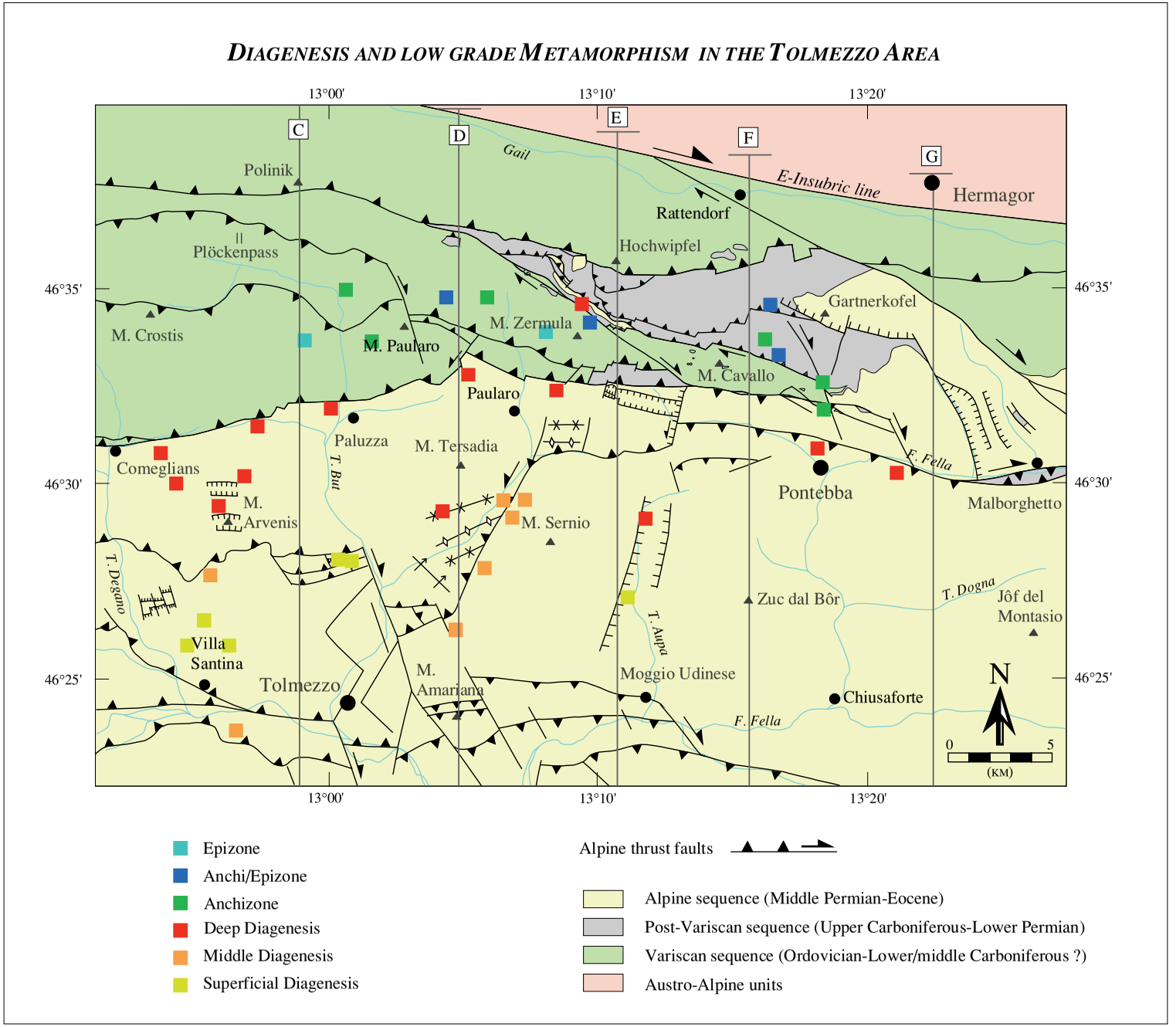

Fig. 47. Map of diagenetic to very low grade metamorphic indices in the Tolmezzo area.

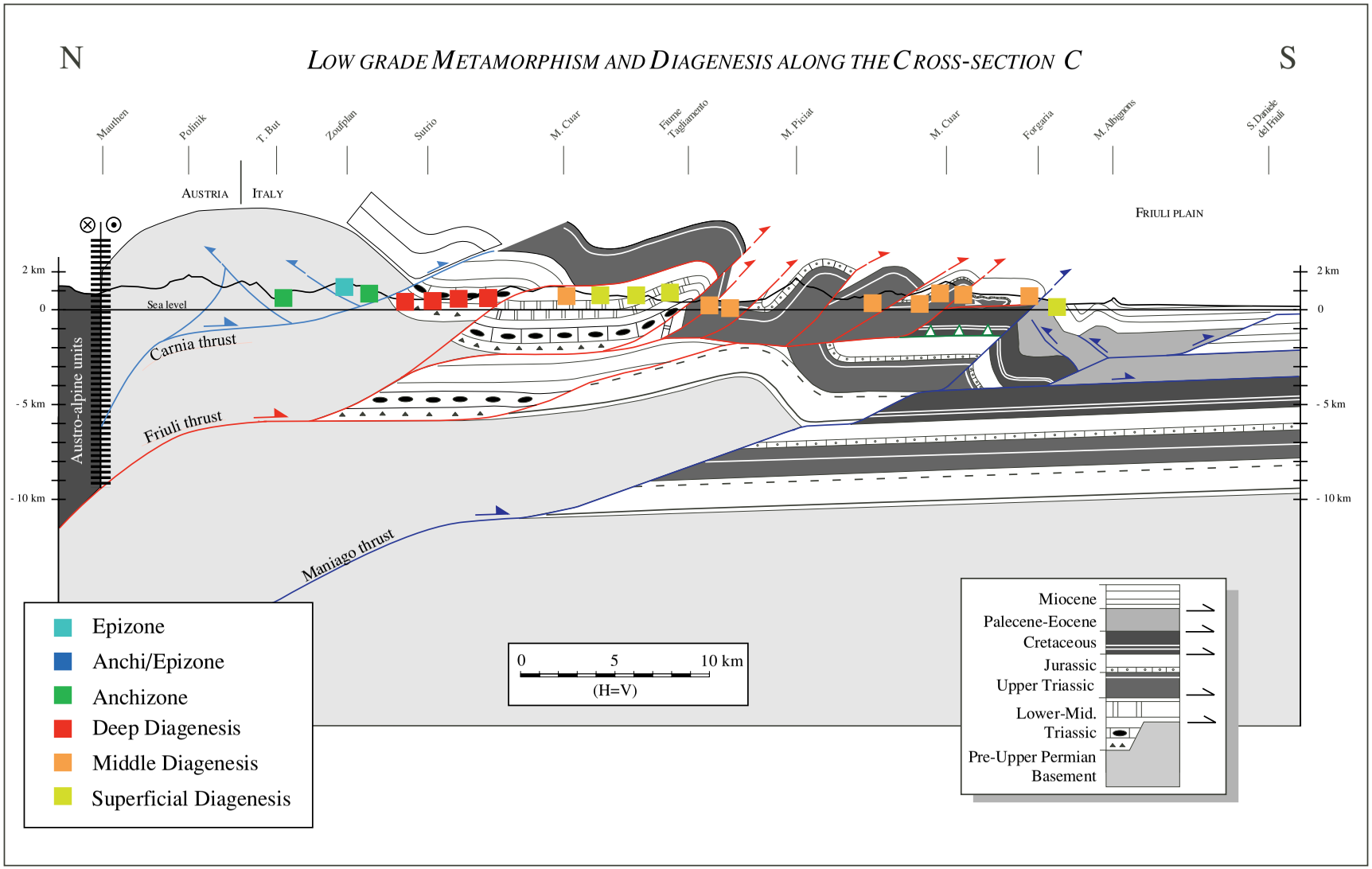

Fig. 49. Diagenesis to very low grade metamorphism along the cross-section C (Fig. 25). See explanations in text.

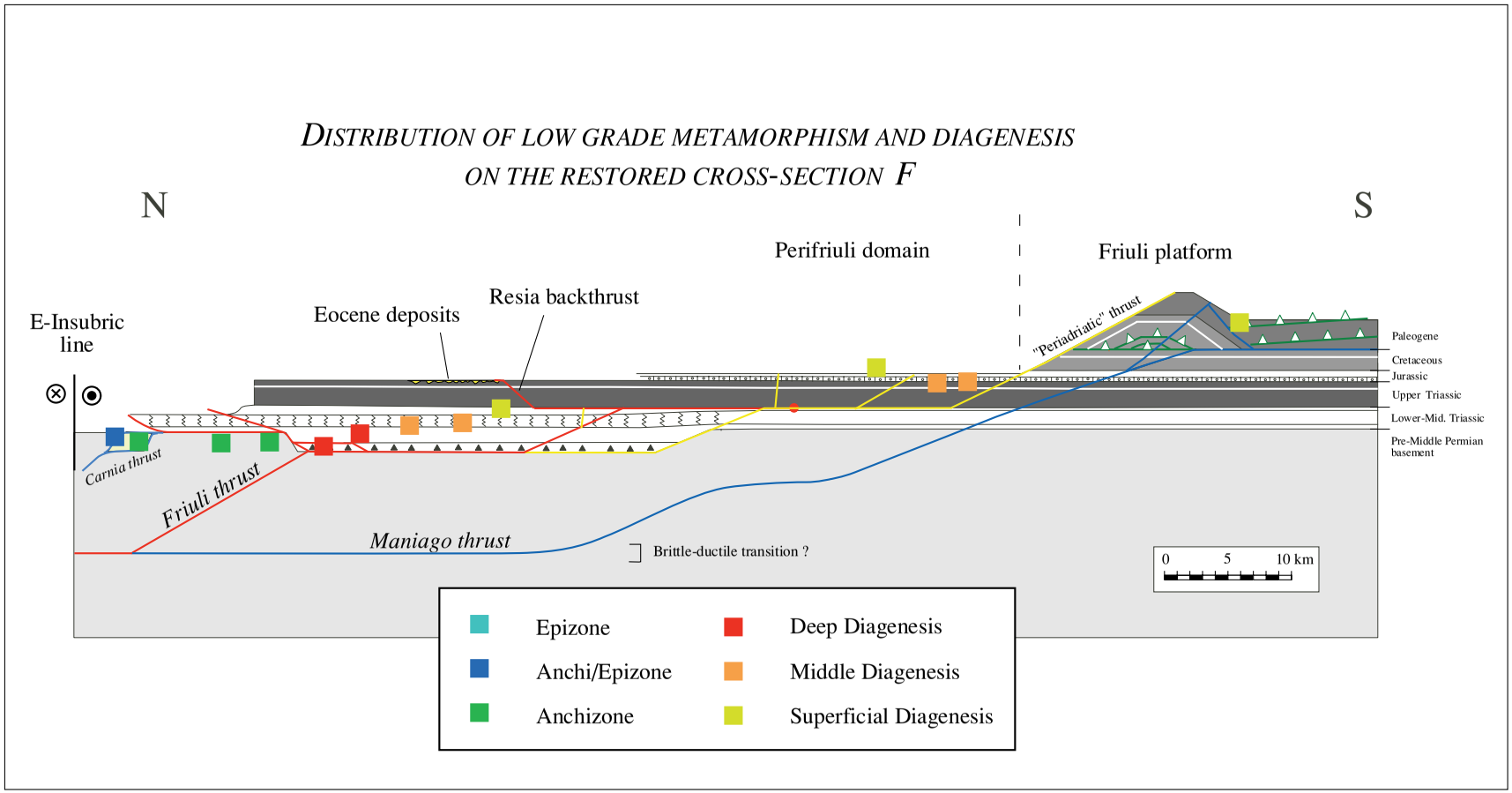

Fig. 50. Distribution of low grade metamorphism and diagenesis on the restored cross-section F (Fig. 33). Except for Carnian samples, thermal conditions of each rock in the Upper Permian-Quaternary cover correspond to its burial depth. Pre-Middle basement shows anchizonal metamorphism, which was inherited during Variscan deformations.

flysch and deep diagenetic conditions found in the red siltstones of the Middle Permian indicate a gradual increase of diagenesis towards depth (Fig. 50). Except for samples of Carnian age, thermal maturity of each sample can be explained by diagenetic burial, independently of the tectonic setting.

8.3.3 The Carnian anomaly

Various samples of the Carnian hemipelagic sediments have recorded "only" superficial diagenetic conditions (Fig. 50 and Table 1). The IC Scherrer width distribution of all collected samples versus a “stratigraphic time “ points to a Carnian anomaly (Fig. 51). In fact, the spreading of IC values in the Carnian does not fit with the general trend. This anomaly may be best understood when the paleotectonic evolution is considered. During Middle Triassic times continued differential subsidence of the basement to the east produced local basins, like the Truogolo Cadorino (Viel, 1979), within the larger Carnico-Bellunese basin. Within this large basin, minor horsts and grabens broke the upper crust into several N-S striking blocks. On the other hand, in the eastern Friuli Alps, a reduced, pelagic sedimentation occurred during Mesozoic times and locally strong erosion affected the sedimentary pile as deep as the Upper Triassic carbonates (Cousin, 1981). As an example, in Val Uccea, an erosive contact separates the Maastrichian Flysch from the Rhetian carbonates, and in Val Resia, the same carbonates are directly overlain by Eocene conglomerates (chapter 2.4). These observations indicate that there, Mesozoic sedimentation was condensed and deposed sediments were strongly eroded before the deposition of the Maastrichtian flysch. Consequently, the thickness of sediments overlying the Carnian deposits should not have exceeded 2 km. This thickness corresponds approximately to the Upper Triassic sequence. In conclusion, the "Carnian anomaly" may be explained by differential subsidence rates within the Carnico-Bellunese basin and by an overlying sedimentary pile of reduced thickness due to condensed sedimentation and important erosion.

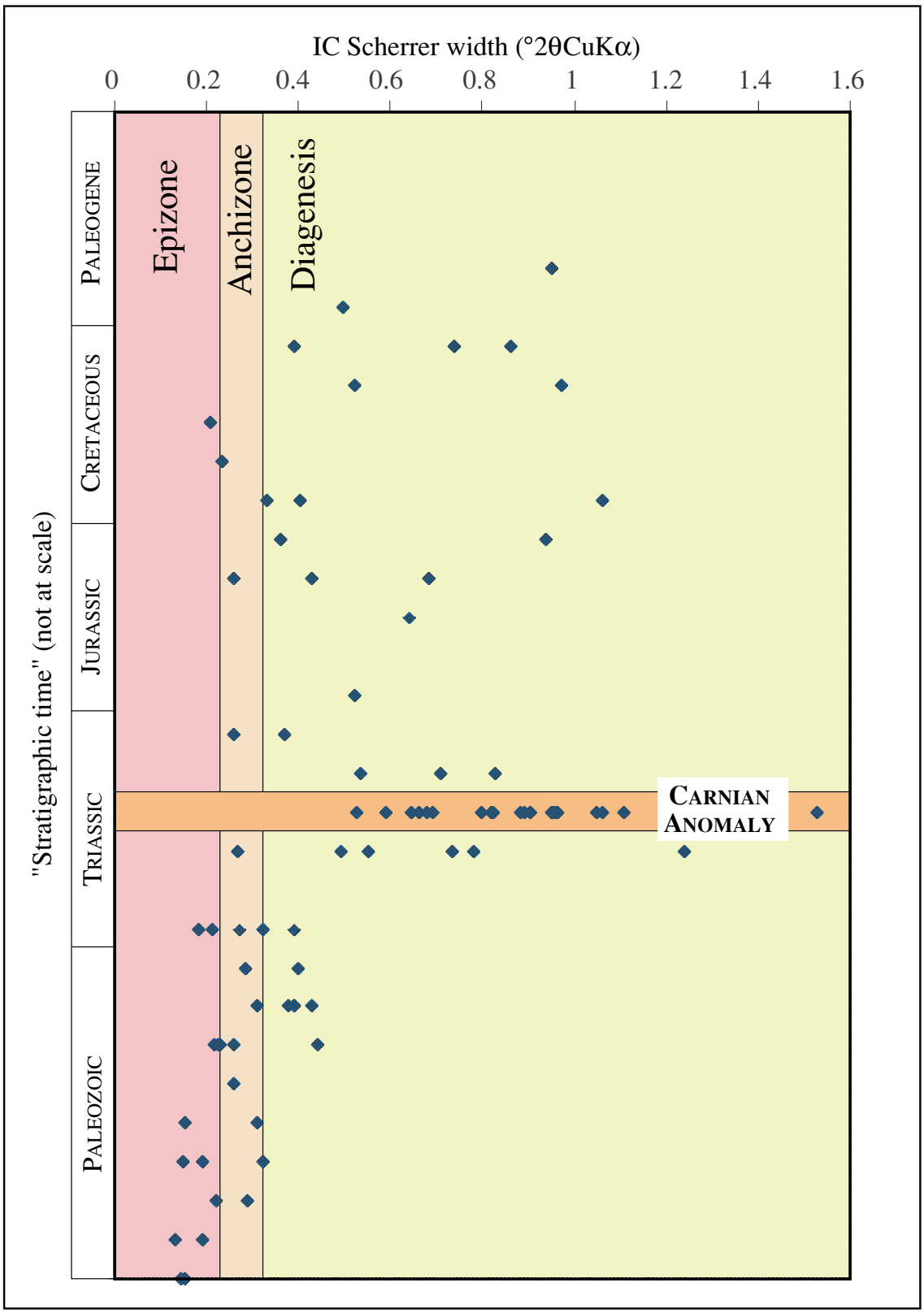

Fig. 51. Illite crystallinity (IC Scherrer width) versus "Stratigraphic time". Distribution shows a wide spreading of values in Carnian samples.

9. GEODYNAMICS OF THE FRONTAL PART OF THE THRUST BELT

In this chapter, I discuss the interference between the regional subsidence of the eastern South Alpine foredeep (Veneto basin), the thrust uplift rate (vertical motion), and the thrust advance rate (horizontal motion) of the frontal part of the easternmost part of the South Alpine orogenic wedge.

9.1 TEMPORAL EVOLUTION OF THE THRUST BELT

The onset of the Alpine, Valsugana-Carnia thrust system may be assumed as Tortonian thanks to the presence of Tortonian sediments found below the Valsugana thrust (Venzo, 1939). But has the thrust belt grown southward in a regular continuous fashion or was it generated step by step? The temporal evolution of the orogenic wedge may be reconstructed with the help of unconformities. However, how do the unconformities within the Neogene molasse and Plio-Quaternary sediments have to be interpreted? Do they record moments of sea level fall (lowstands) or do they mark phases of tectonic activity? The different interpretations of the unconformitites and conglomeratic supply in the molassic sequence allow for different tectonic reconstructions. In general, plates move with a regular velocity suggesting that in areas of deformation the tectonic evolution should follow a line of almost constant activity. If the unconformities recorded moments of general lowstand, e.g. related to the salinity crisis in the Mediterranean area, the thrust belt developed more gradually and sea-level oscillations orchestrated the arrangement of the syntectonic sedimentary sequences. With the sea level change interpretation, the chain is rising constantly from Late Miocene. But if we assume the unconformities and conglomeratic supply to be related to tectonics, then episodic tectonic activity alternates with quiet periods.

9.2 SUBSIDENCE IN THE SOUTH ALPINE FOREDEEP

The Southern Alps foredeep underwent a slightly different evolution in its western and eastern parts. The western Southern Alps foredeep is more strongly influenced by the Apenninic flexure than the eastern Southern Alps foredeep. In the eastern part of the South Alpine foredeep, the Dinaric foredeep interferes with its effects of subsidence at least between the Paleocene and the middle Miocene. Rates of subsidence lower or similar to those of the Southern Alps are calculated from the entire thickness of the Dinaric foredeep deposits. After the Late Cretaceous, the shallow Dinaric foredeep prograded into a west-southwest directions. The Southern Alps foredeep was partly involved in thrusting. Subsidence rates have been low, rarely exceeding 0.3 mm /year.

The published data from two AGIP wells (Cati *et al*., 1987b) have been used to draw burial curves for the Adriatic sea (Amanda 1 bis, Fig. 52) and the Friuli plain (Cesarolo 1, Fig. 53). Both locations are experiencing ongoing subsidence, as is indicated by the thick sequence of Quaternary deposits (822 m in Amanda 1 bis). The Amanda well (Fig. 52) has been drilled in an area which was located in a basinal setting during the Jurassic. This area is located between the Belluno basin in the west and the southwestern Friuli platform in the east (Fig. 10). Data from the Amanda well indicate three periods of time with high sedimentation rates (Fig. 52). They are related to (i) the Middle Triassic rifting and the following thermal subsidence, (ii) the Paleogene flysch being deposited during the Dinaric phase and (iii) the filling of the Alpine foredeep. This well reveals a minimum Alpine burial of about 7.5 km. According to data taken in this well, we calculate a subsidence rate of 0.25 mm/year for the last 5 million years. The Cesarolo well has been drilled into the southwestern Friuli platform (Fig. 53). This well shows a high sedimentation rate in Late Jurassic related to the building of reefs consisting of the Ellipsactinia limestones. In this area, the Dinaric phase is not documented since a hiatus occurs from the early Late Cretaceous to the beginning of the Neogene. As this well has not reached the pre-Middle Permian basement, it is not possible to calculate the Alpine burial rate on the southwestern Friuli platform.

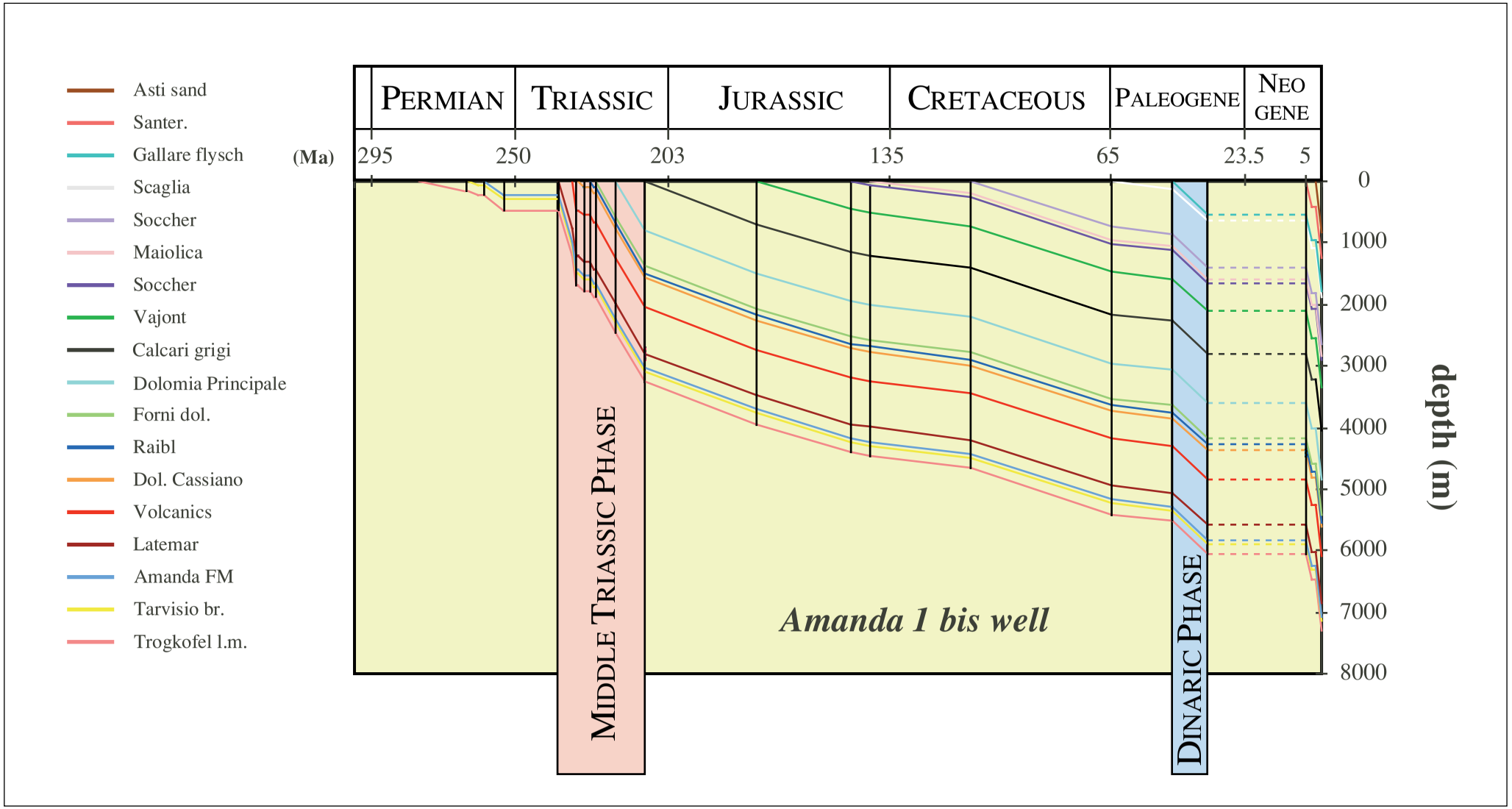

Fig. 52. Burial curves in the Adriatic sea (Amanda 1 bis, AGIP well), Curves are constructed for the period between Early Permian and today after data from Cati *et al*. (1987b).

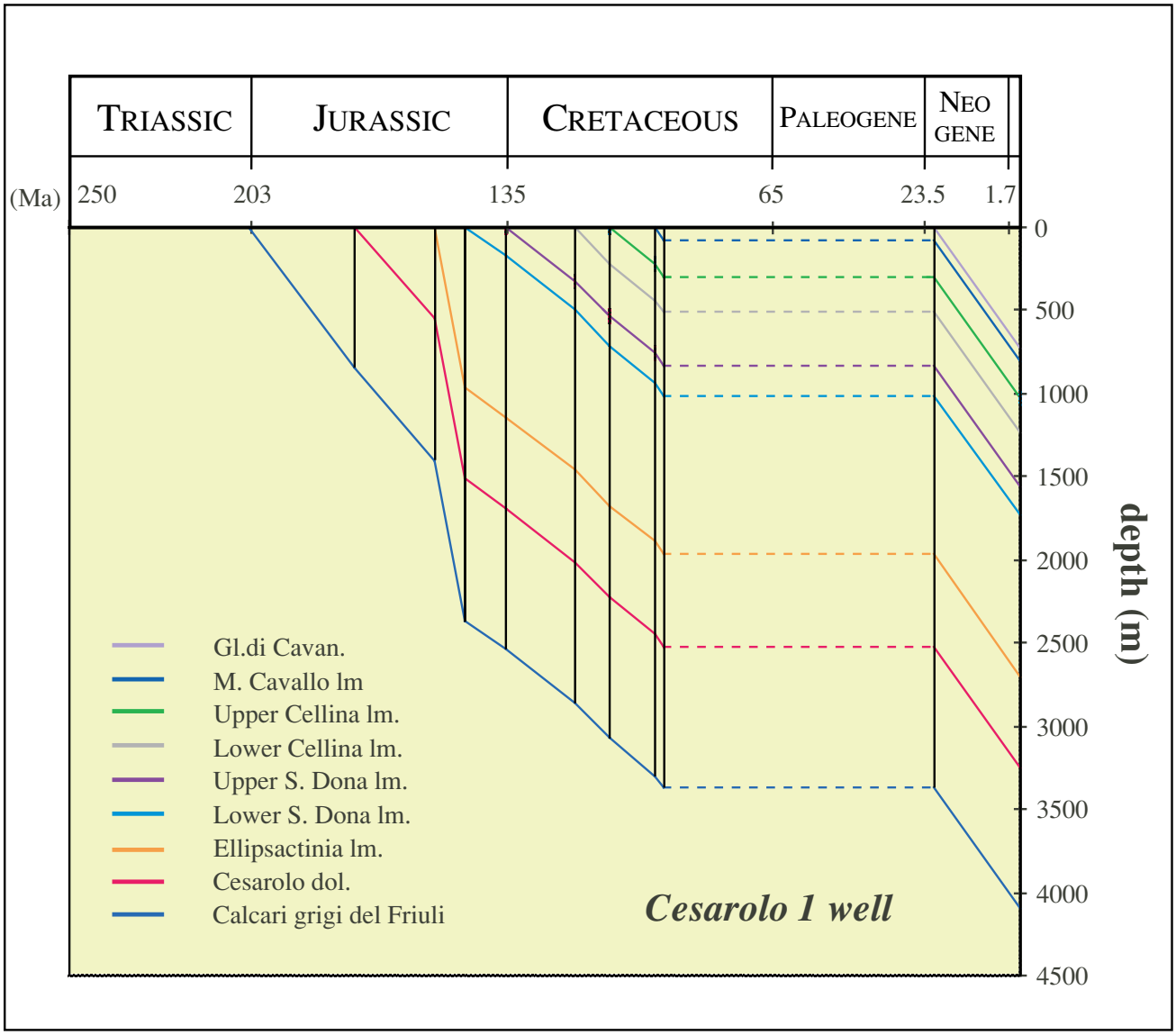

Fig. 53. Burial curves in the Friuli-Veneto plain (Cesarolo 1, AGIP well). The curves are drawn from the beginning of Early Jurassic (deposition of the Calcari grigi del Friuli) after data from Cati *et al*. (1987b).

9.3 THRUST UPLIFT RATE VERSUS THRUST ADVANCE RATE

In this section, the uplift rate is compared with the thrust advance rate (vertical versus horizontal motions in the Alpine orogenic thrust wedge).

9.3.1 Calculation of the uplift rate

The structure of the Friuli frontal belt allows the construction of subsidence curves involving the Friuli and Maniago thrust systems. The southernmost branch of the Friuli thrust system transported Upper Triassic dolomites onto the Eocene flysch. This fault has the greatest throw among all exposed thrusts in the Friuli Alps. This major fault has transported the pelagic sequences of Jurassic-Cretaceous age onto the thick Friuli carbonate platform. Therefore, the Jurassic-Cretaceous sequence does not have the same thickness in the hangingwall and the footwall of the frontal Friuli thrust. These thickness changes prevent a direct calculation of the thrust uplift rate. For that reason, two subsidence curves have been constructed: (i) in the Friuli platform (Fig. 54) and (ii) in the basin (Perifriuli domain, Fig. 55). The reference level is taken at the base of the Upper Triassic dolomites since this horizon has been detached above the Carnian décollement by the Friuli thrust (see Fig. 28).

The thrust uplift rate may be roughly calculated by integrating the thrusts in subsidence curves. The beginning of thrusting must be known (c. 10 Ma, see chapter 4.5). The calculation of the uplift rate is based on a geometric construction and depends on two crucial points: the depth of the initial point (base of the Upper Triassic beds at 10 Ma) and the height of the current point (base of the Upper Triassic beds on a present-day cross-section).

- Leeway for the current point (t=0): the hangingwall of the thrust is in a flat position, that means that the ending of the fold must be projected into the sky. This leeway is partially reduced by cross-section balancing. The uncertainty concerns the height

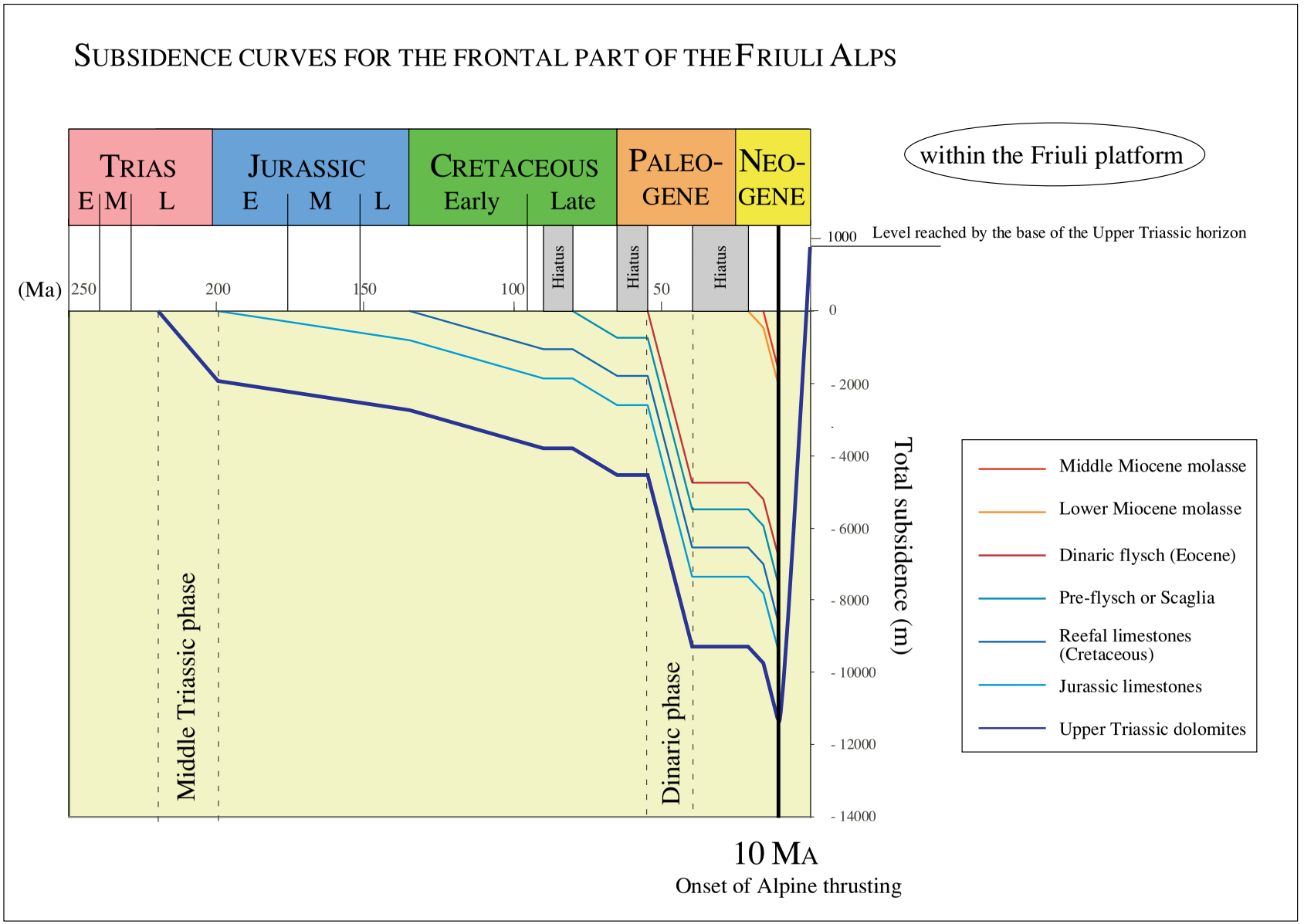

Fig. 54. Subsidence curves for the frontal part of the Friuli Alps (in the Friuli platform). Data are in Table 2.

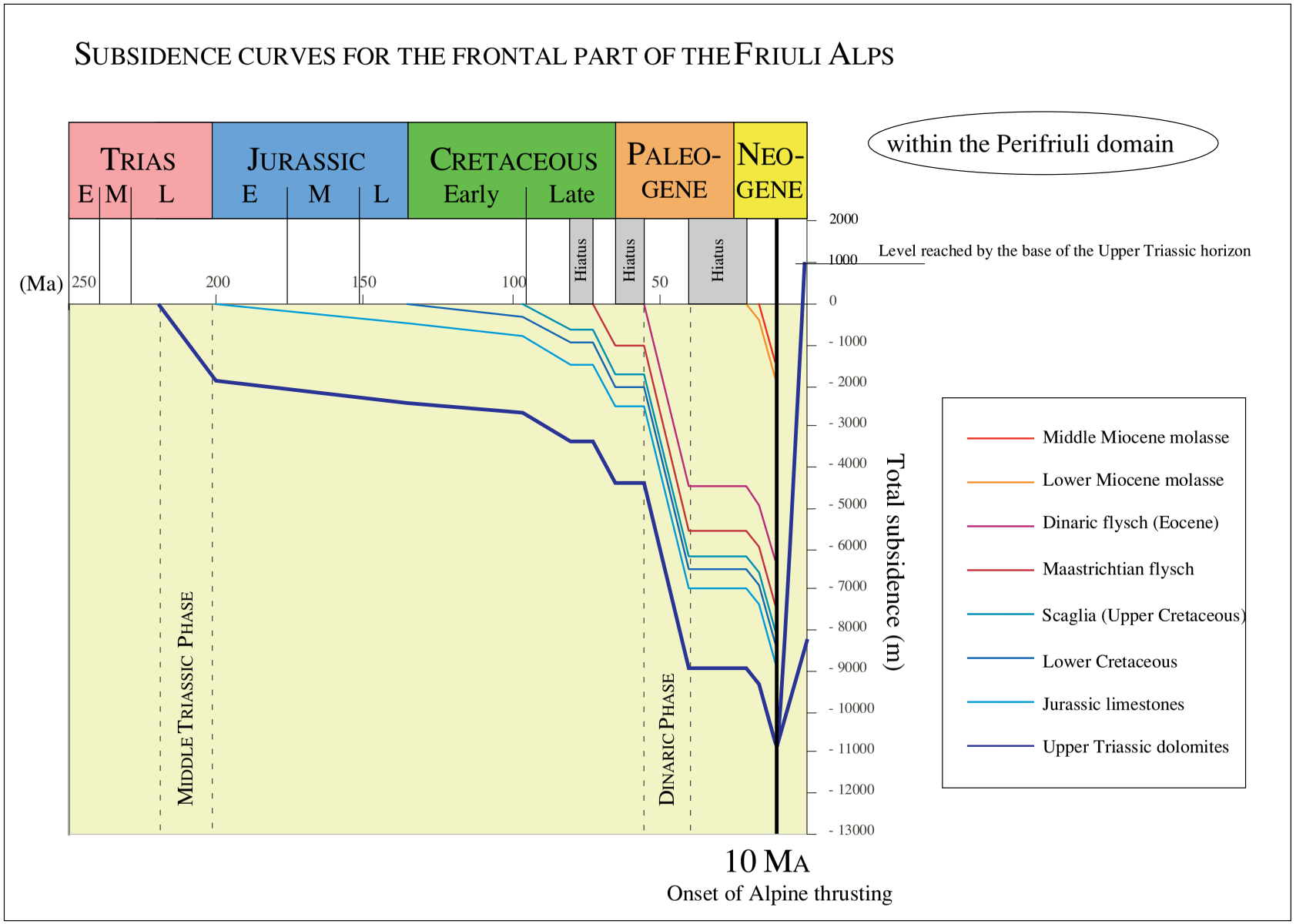

Fig. 55. Subsidence curves for the frontal part of the Friuli Alps (in the Perifriuli domain). Data are in Table 2.

reached by the Upper Triassic beds when they were thrust onto the Eocene flysch. The error margin is very low on the uplift rate, estimated at less than ±2 %.

- Leeway for the initial point (t =10 Ma): the depth of the base of the Dolomia Principale level before the onset of thrusting depends on the thickness and the paleo-water depths of each formation of the sedimentary pile deposed from the Late Triassic until 10 Ma. The information is available back to the Upper Cretaceous deposits. Unfortunately, the Tertiary sediments of the hangingwall were eroded during uplift and therefore their original thickness is not known and must be extrapolated from the foredeep. The nature of sediments, flysch and molasse, increases the uncertainty on both thickness and paleo-water depths. Table 2 indicates the values used for the subsidence curves. The error range of this point is estimated at ±7%.

The uplift rate is calculated by taking the difference of height between the original and final points, and dividing by the time interval. The calculated thrust uplift rate amounts to 1.24 mm/year assuming a continuous uplift during 10 Ma, without tectonic break. According to the uncertainties about sediment thickness, paleo-water depths and erosion quantifications, the extreme values spread from 1.15 to 1.33 mm/year. This range of values fits well with the regional data for the Southern Alps (0.5-2 mm/year; Doglioni, 1993; Doglioni and Prosser 1997).

Between the initial point and the current point, the used path is not known. The proposition of a continuous uplift without break is the easier solution.

9.3.2 Thrust advance rate

Considering the entire South Alpine belt, we obtain an average rate of thrust tip displacement of about 5 mm/year, assuming a thrusting period of 10 Ma and a total shortening of 50 km. A calculation of vertical versus horizontal motions in the South Alpine orogenic wedge indicate that the thrust advance rate is about 4 times greater than the thrust uplift rate.

Thermal data did not indicate an influence of tectonics on the thermal maturity of overthrust sediments. These results can be interpreted as follows: the time interval (10 Ma) is too short to produce a transfer of heat from the Upper Triassic carbonates of the hangingwall into the Paleogene flysch of the footwall. In addition, the time interval is also too short to equilibrate a perturbed temperature profile. As a consequence, timing of thrusting is probably the main reason why the Ceno-Mesozoic cover remained in the diagenetic domain, independently of the tectonic setting. In the eastern Southern Alps, one of the main factors controlling the paleotemperature regime, and hence the thermal maturity of sediments, is burial via sedimentary loading.

10. CONCLUSIONS

Based mainly on extensive fieldwork, this study has resulted in:

- construction of a consistent tectonic map of the easternmost Southern Alps. The tectonic setting consists of three thrust systems that are geometrically and kinematically linked.
- characterization of the geometry of the deep structures of the Friuli Alps. This information was lacking so far since no seismic reflection data exist in the fold-and-thrust belt.
- development of a model for the kinematic evolution involving three thrust systems (Carnia, Friuli and Maniago systems). Deformation propagated in sequence towards the foreland from north to south, except in the eastern part of the Friuli Alps where an out-of–sequence thrust is needed by field data. Retrodeformation indicates a minimum shortening of 50 km for the entire studied area.
- interpretation of the tectonic style for the external Dinarides belt. Based on Alpine/Dinaric superposed structures, a low critical taper is demanded. Long detachments in the evaporites of the Upper Permian and the absence of metamorphism support this interpretation.
- confirmation of the strong influence of inherited faults on Alpine and Dinaric structures. Transverse zones resulted from these inherited structures. They cut the belt into several segments of different structures. Examples from the study area are the Tagliamento and Incaroio transverse zones and the transtensional zone of Sappada. Ages of the inherited faults may be suspected by thickness changes in sediments or by the sedimentation type (breccia). However, geological evidence is not always exposed or may be eroded. Reliable indicators support the existence of Middle Triassic and Early Jurassic normal faults in the eastern Southern Alps.
- demonstration of a good correlation between the intense ongoing seismicity of the Friuli region and the geometry of the thrust belt. The hypocenter distribution

points to activity of the most frontal thrust of the belt which is in agreement with in sequence thrusting.

- confirmation that the sediments of the Alpine cycle (Late Permian-Quaternary) were deformed under diagenetic conditions, implying that tectonics had no influence on the thermal conditions. The diagenetic conditions are related to burial via sedimentary loading. Timing is probably the reason why tectonics had no influence (10 My is too short). Until now, no thermal studies at large-scale were carried out in the Alpine sediments of the easternmost Southern Alps.
- discussion of the geodynamics of the South Alpine orogenic wedge. This discussion is based on:
    - subsidence rate -> based on thickness and paleowater depth
    - thust uplift rate -> based on subsidence curves
    - thrust advance rate -> calculated with shortening

Calculations indicate that the Alpine orogenic wedge grows four times faster horizontally than vertically.

REFERENCES

AGIP, 1977. Temperature sotterranee. Inventario dei dati raccolti durante la ricerca e la produzione di idrocarburi in Italia. *Edited by AGIP*, 1930 p.

AGIP, 1984. Aeromagnetic map of Italy and surrounding seas. *Boll. Geof. Teor. Appl.*, **26**, 152 p.

AMADESI, E., 1968. La geologia dei gruppi di M. Brancot e di M. S. Simeone (Friuli udinese). *Giorn. Geol*., ser. 2, **36/1**, 24 p.

AMADESI, E. AND LENARDUZZI, G., 1973. Geologia del gruppo del M. Festa (Friuli udinese). *Mem. Museo Trid. Sc. Nat.*, **1 9** (2), 1-28.

AMATO, A., BARNABA, P.F., FINETTI, I., GROPPI, G., MARTINIS, B. AND MUZZIN, A., 1977. Geodynamic outline and seismicity of the Friuli-Venetia-Julia region. *Boll. Geof. Teor. Appl.*, **72**, 217-256.

AMATO, A., DE FRANCO, R. AND MALAGNINI, L., 1990. Local source tomography: applications to Italian areas. *Terra Nova*, **2**, 596-608.

AMBROSETTI, P., BARTOLINI, C., BOSI, C., CARRARO, F., CIARANFI, N., GHISETTI, F., PAPANI, G., VEZZANI, L., ZANFERRARI, A. AND ZITELLI, N., 1983. Neotectonic Map of Italy, 1:500'000. *CNR, Quad. Ric. Scient*., 4.

ANDERSEN, H. AND JACKSON, J., 1987. Active tectonics in the Adriatic region. *Geophys. J. R. Astron. Soc*., **91**, 937-983.

ARISI-ROTA, F. AND FICHERA, R., 1985. Magnetic interpretation connected to "geomagnetic provinces": the Italian case history. 47th Meeting E.A.E.G., *AGIP*, Milano, 30 p.

ARTHAUD, F. AND MATTE, P., 1977. Late Paleozoic strike-slip faulting in southern Europe and northern Africa: Result of a right-lateral shear zone between the Appalachians and the Urals. *Geol. Soc. Amer. Bull*., **88**, 1305-1320.

ASSERETO, R., 1963. La geologia della valle di Ugovizza (Alpi Carniche*). Boll. Serv. Geol. It.*, **82**, 109-148.

ASSERETO, R., DESIO, A., COMIZZOLI, G. AND PASSERI, L.D., 1967. Carta Geologica d'Italia). Foglio 14a, Tarvisio (II ed.). Scala 1:100.000. *Serv. Geol. d'Italia*, Roma.

ASSERETO, R., DESIO, A., DI COLBERTALDO, D. AND PASSERI, L.D., 1968. Note illustrative della Carta Geologica d'Italia. Foglio 14a Tarvisio. *Serv. Geol. d'Italia*, 70 p., Roma.

ASSERETO, R., BOSELLINI, A., FANTINI-SESTINI, N. AND SWEET, W.C., 1973. The Permian-Triassic boundary in the Southern Alps (Italy). In: Logan, A. and Hills, L.V. (Eds), the Permian and Triassic systems and their mutual boundary. *Can. Soc. Petrol. Geol. Mem*., **2**, 176-199.

BALLY, A.W., GORDY, P.L. AND STEWART, G.A., 1966. Structure, seismic data, and orogenic evolution of southern Canadian Rocky Mountains. *Bull. Can. Petroleum Geology*, **14/3**, 337-381.

BARABANO, M.S., KIND, R. AND ZONNO, G., 1985. Focal parameters of some Friuli earthquakes (1976-1979) using complete theoretical seismograms. *J. Geophys*., **58**, 175-182.

BAROZZI, P. AND COLOMBI, L., 1992. Profilo CROP-01/01A, sezioni sismiche e geologiche e ipotesi di tracciato del profilo nella pianura Padana. *Studi Geologici Camerti, volume speciale* (1992/2), CROP 1-1A, 161-170.

BENEDETTI, L. TAPPONIER, P., MEYER, B. AND GAUDEMER, Y., 1995. Active folding in the Veneto-Friuli region (northern Italy). *Terra Abstr*. 7, **36**.

BERNOULLI, D., BERTOTTI, G. AND FROITZHEIM, N., 1992. Mesozoic faults and associated sediments in the Austroalpine-South Alpine passive continental margin. *Mem. Soc. Geol. It.*, **45**, 25-38.

BERTOTTI, G., PICOTTI, V., BERNOULLI, D., AND CASTELLARIN, A., 1993. From rifting to drifting: tectonic evolution of the South-Alpine upper crust from the Triassic to the Early Cretaceous. *Sediment. Geol.* **86**, 53-76.

BIANCHIN, G., CARULLI, G.B., FRIZZO, P., LONGO SALVADOR, G., MANTOVANI, F., MASÈ G., MEZZACASA, G. AND SEMENZA, E., 1980. Carta geologica della zona compressa tra il T. Chiarzò e il F. Fella (Alpi Carniche). Scala 1:20'000. *Grafica Ferrarese.*

BIGI, G., COSENTINO, D., PAROTTO, M., SARTORI, R. AND SCANDONE, P., 1992. Structural model of Italy, map scale 1:500'000, *Prog. Fin. Geodyn., Quad. Ric. Scient. Cons. Naz. delle Ric.*, Rome, 114-3.

BOSELLINI, A. AND SARTI, M., 1978. Geologia del gruppo M. Cuar – M. Covria (Prealpi carniche). *Giorn. Geol.*, **43**, 47-88.

BOSELLINI, A., 1984. Progradation geometries of carbonate platforms: example from the Triassic of the Dolomites, northern Italy. *Sedimentology*, **31**, 1-24.

BOSELLINI, A., MASETTI, D. AND SARTI, M., 1981. A Jurassic "Tongue of the Ocean" infilled with oolithic sands: the Belluno through, Venetian Alps, Italy. *Marine Geol.*, **44**, 59-95.

BOSELLINI, A., CASTELLARIN, A., DOGLIONI., C., GUY., T., LUCCHINI, F., PERRI, M.C., ROSSI., P.L., SIMBOLI, G. AND SOMMAVILLA, E., 1982. Magmatismo e tettonica nel Trias delle Dolomiti. In: *Guida alla Geologia del Sudalpino centro-orientale (edited by Castellarin, A. & Vai, G.B.). Soc. geol. It.*, 189-210.

BOSSELINI, A. AND DOGLIONI, C., 1986. Inherited structures in the hangingwall of the Valsugana Overthrust (Southern Alps, Northern Italy). *J. Struct. Geol.*, **8/5**, 581-583.

BOYER, S.E. AND ELLIOTT, D., 1982. Thrust systems. *Am. Assoc. Petr. Geol. Bull.*, **66**, 1196-1230.

BRAGA, G.P., CARLONI, G.C., COLANTONI, P., CORSI, M., CREMONINI, G., FRASCARI, F., LOCATELLI, D., MONESI, A., PISA, G., SASSI, F.P., SELLI, R., VAI, G.B. AND ZIRPOLI, G., 1971. Note illustrative della Carta Geologica d'Italia. Fogli 4c-13 Monte Cavallino-Ampezzo. *Ser. Geol. d'Italia*, 108 p., Roma.

BRANDNER, R., 1988. The Permian-Triassic boundary in the Dolomites (Southern Alps, Italy), San Antono section. *Ber. Geol. Bundesanst., 15 rare events in geology, IGCP 199*, 49-56.

BRANDNER, R., DONOFRIO, D.A., KRAINER, K., MOSTLER, H., RESCH, W. AND STINGL, V., 1984. Correlation of transgressional and regressional events in the Lower Triassic of the Northern and Southern Alps (Bundsandstein-, Servino-, Werfen Formation). 5th Eur. Regional Meet. Sedimentol (IAS), Marseille, April 1984.

BRESSAN, G. DE FRANCO, R. AND GENTILE, G.F., 1992. Seismotectonic study of the Friuli (Italy) area based on tomographic inversion and geophysical data. *Tectonophysics*, **207**, 383-400.

BRESSAN, G. SNIDARCIG, A. AND VENTURINI, C., 1998. Present state of tectonic stress of the Friuli area (eastern Southern Alps). *Tectonophysics*, **292**, 211-227.

BRUSCA, C., GAETANI, M., JADOUL, F. AND VIEL, G., 1981. Paleogeografia Ladino-Carnica e metallogenesi del Sudalpino. *Mem. Soc. Geol. It.* **22**, 65-82.

BUGGISCH, W. AND NOÈ, S., 1986. Upper Permian and Permian-Triassic boundary of the Carnia (Bellerophon Formation, Tesero horizon, Northern Italy). *Mem. Soc. Geol. It.*, **34**, 91-106.

BURKHARD, M., 1988. L'Hélvétique de la bordure occidentale du massif de l'Aar (évolution tectonique et métamorphique). *Eclogae geol. Helv.*, **83**, 559-583.

BURST, J.F., 1959. Postdiagenetic clay mineral environmental relationships in the Gulf Coast Eocene. *Clays and clay Min.*, **6**, 327-341.

BURST, J.F., 1969. Diagenesis of Gulf Coast clayed sediments and its possible relation to petroleum migration. *Bull. Amer. Assoc. Petroleum. Geol.*, **53**, 73-93.

BUSER, S., 1987. Development of the Dinaric and the Julian carbonate platforms and of the intermediate Slovenian basin (NW Yugoslavia). *Mem. Soc. Geol. It.*, **40**, 313-320.

BUSTIN, R.M., BARNES, M.A. AND BARNES, W.C., 1985. Diagenesis 10. Quantification and modelling of organic diagenesis. *Geoscience Canada*, **12**, 4-21.

BUXTORF, A., 1916. Prognosen und Befunde beim Hauensteinbasis- und Grenchenbergtunnel und die bedeutung der letzteren für die Geologie des Juragebirges. *Verh. Naturforsch. Ges. Basel*, **27**, 195-254.

CAPUTO, R., 1996. The polyphased tectonics of Eastern Dolomites, Italy. *Mem. Sci. Geol.*, Padova, **48**, 93-106.

CAPUTO, R., 1997. The puzzling regmatic system of Eastern Dolomites, Italy. *Mem. Sci. Geol.*, Padova, **49**, 27-36.

CAROBENE, L., CARULLI, G.B. AND VAIA F., 1981. Foglio 25 Udine. In: Castellarin, A. (a cura di). Carta tettonica delle Alpi Meridionali (alla scala 1:200.000). *Prog. Fin. Geodinamica C.N.R.*, Pubbl. 441, 39-45.

CARULLI, G.B., CAROBENE, L., CAVALLIN, A., MARTINIS, B. AND ONOFRI, R., 1980. Evoluzione strutturale Plio-quaternaria del Friuli della Venezia Giulia. In: Contributi preliminari alla realizzazione della carta neotettonica d'Italia. Pubbl. n. 356 P.F. *Geodinamica*, 489-545.

CARULLI, G.B., ZUCCHI STOLFA, M.L. AND PIRINI RADRIZZANI, C., 1982a. L'eocene di Monte Forcella (Gruppo del Monte Amariana-Carnia orientale). *Mem. Soc. Geol. It.*, **24**, 65-70.

CARULLI, G.B., FRASCARI, F. AND SEMENZA, E., 1982b. Geologia delle Alpi Tolmezzine (Carnia). In: A. Castellarin & G.B. Vai (a cura di). *Guida alla geologia del Sudalpino centro-orientale. Guide geol. reg. S.G.I.*, Bologna, 337-348.

CARULLI, G.B., GIORGETTI, F., NICOLICH, R. AND SLEJKO, D., 1982c. Friuli zona sismica: sintesi di dati sismologici, strutturali e geofisici. In: A. Castellarin & G.B. Vai (a cura di): *Guida alla geologia del Sudalpino centro-orientale. Guide geol. reg. S.G.I.*, Bologna, 361-370.

CARULLI, G.B., PIRINI RADRIZZANI, C. AND PONTON, M., 1986. The Permian-Triassic boundary in the Paularo area (Carnia). *Mem. Soc. Geol. It.*, **34**, 107-120.

CARULLI, G.B., SEMENZA, A., BIANCHIN, G. AND MANTOVANI, G., 1987. La geologia della zona tra il T. Chiarzò e il F. Fella (Alpi Carniche). *Giorn. Geol.*, **49/1**, 1-32.

CARULLI, G.B., NICOLICH, R., REBEZ, A. AND SLEJKO, D. 1990. Seismotectonics of the Northwest External Dinarides. *Tectonophysics*, **179**, 11-25.

CARULLI, G.B., AND PONTON, M., 1992. Interpretazione strutturale profonda del settore centrale carnico-friulio. *Studi Geologici Camerti, volume speciale* (1992/2), CROP 1-1A, 275-284.

CASSANO, E., ANELLI, L., FICHERA, R. AND CAPPELLI, V., 1986. Pianura Padana. Interpretazione integrata di dati geologici e geofisici. 73° Congresso Società Geologica Italiana, Roma.

CASTELLARIN, A., 1979. Il problema dei raccorciamenti crostali nel Sudalpino. *Rend. Soc. geol. It.*, **1**, 21-23.

CASTELLARIN, A. (ed.), 1981. Carta tettonica delle Alpi Meridionali (alla scala 1:200'000). *Prog. Fin. Geodinamica CNR*, Publ. 441, 220 p.

CASTELLARIN, A., FRASCARI, F. AND VAI, G.B., 1980. Problemi di interpretazione geologica profonda del Sudalpino orientale. *Rend. Soc. Geol. It.*, **2** (1979), 55-60.

CASTELLARIN, A. AND VAI, G.B., 1981. Importance of Hercynian tectonics in the framework of the Southern Alps. *J. Struct. Geol.*, **3**, 377-386.

CASTELLARIN, A. AND VAI, G.B., 1982. Introduzione alla geologia strutturale del Sudalpino. In: A. Castellarin & G.B. Vai (a cura di): *Guida alla geologia del Sudalpino centro-orientale. Guide geol. reg. S.G.I.*, Bologna, 1-22.

CASTELLARIN, A., LUCCHINI, F., ROSSI, P.L., SARTORI, R., SIMBOLI, G. AND SOMMAVILLA, E., 1982. Note geologiche sulle intrusioni di Predazzo e dei M. Monzoni. In: A. Castellarin & G.B. Vai (a cura di): *Guida alla geologia del Sudalpino centro-orientale. Guide geol. reg. S.G.I.*, Bologna, 211-219.

CASTELLARIN, A., CANTELLI, L., FESCE, A.M., MERCIER, J.L., PICOTTI, V., PINI, G.A, PROSSER, G. AND SELLI, L., 1992. Alpine compressional tectonics in the Southern Alps. Relationships with the N-Apennines. *Ann. Tec.*, Firenze, **6** (1), 62-94.

CASTIGLIONI, B., LEONARDI, P., MERLA, G., TREVISAN, L. AND ZENARI, S., 1940. Foglio 12 Pieve di Cadore, della Carta Geologica delle Tre Venezie alla scala 1: 100.000. *Uff. Idrogr. Mag. Acque*, Venezia.

CATI, A., FICHERA, R. AND CAPELLI, V., 1987a. Northeastern Italy. Integrated processing of geophysical and geological data. *Mem. Soc. Geol. It.*, **40**, 273-288.

CATI, A., SARTORIO D. AND VENTURINI, S., 1987b. Carbonate platforms in the subsurface of the northern Adriatic area. *Mem. Soc. Geol. It.*, **40**, 295-308.

CAVALLIN, A., 1976. Osservazioni sulla tettonica nella Conca di Tramonti (Prealpi Carniche). *Riv. Ital. Paleont. Strat.*, **82**, 285-292.

CAVALLIN, A., 1981. Fogli 24 Maniago e 39 Pordenone. In: Castellarin, A. (a cura di). Carta tettonica delle Alpi Meridionali (alla scala 1:200'000). *Prog. Fin. Geodinamica C.N.R.*, Pubbl. 441, 46-50.

CAVALLIN, A. AND MARTINIS, B., 1982. Gli scorrimenti del margine settentrionale della piattaforma carbonatica adriatica. In: A. Castellarin & G.B. Vai (a cura di): *Guida alla geologia del Sudalpino centro-orientale. Guide geol. reg. S.G.I.*, Bologna, 349-359.

CAVALLIN, A. AND PIRINI RADRIZZANI C., 1987. Geodynamic evolution of Friuli region (Northern sector of African promontory). *Mem. Soc. Geol. It.*, **40**, 345-354.

CERETTI, E., 1965. La geologia del gruppo del M. Plauris (Carnia). *Giorn. Geol.*, Ser. 2. **33/1**, 1-50.

CHAMBERLIN, R.T., 1910. The Appalachian folds of central Pennsylvania. *J. Geol.*, **18**, 228-251.

CHANNELL, J.E.T., DOGLIONI, C. AND STONER, J.S., 1992. Jurassic and Cretaceous paleomagnetic data from the Southern Alps (Italy). *Tectonics*, **11**, 811-822.

CHANNELL, J.E.T. AND DOGLIONI, C., 1994. Early Triassic paleomagnetic data from the Dolomites (Italy). *Tectonics*, **13/1**, 157-166.

CHAPPLE, W.M., 1978. Mechanics of thin-skinned fold-and-thrust belts. *Geol. Soc. Am. Bull.*, **89**, 1189-1198.

COMEL, A. AND FERASIN, F., 1956. Carta Geologica delle Tre Venezie. Foglio 39 Pordenone. *Uff. Idrogr. Mag. Acque*, Venezia.

CONSOLE, R., 1977. Focal mechanism of some Frioul earthquakes. *Boll. Geof. Teor. Appl.*, **72**, 549-558.

COOK, F.A., ALBAUGH, D.S., BROWN, L.D., KAUFMAN, S., OLIVER, J.E. AND HATCHER, JR., 1979. Thin-skinned tectonics in the crystalline southern Appalachians: COCORP seismic-reflection profiling of the Blue Ridge and Piedmont. *Geology*, **7**, 563-567.

COUSIN, M., 1981. Les rapports Alpes-Dinarides. Les confins de l'Italie et de la Yougoslavie. *Soc. Géol. du Nord, Publ. 5*, **1**, 1-521, **2**, 1-521.

DAHLEN, F.A., SUPPE, J. AND DAVIS, D., 1984. Mechanics of fold-and-thrust belts and accretionary wedges: Cohesives Coulomb theory. *J. Geophys. Res.*, **89**, 10087-10101.

DAHLSTROM, C.D.A., 1969. Balanced cross sections. *Can. J. Earth Sci.*, **6**, 743-757.

DAHLSTROM, C.D.A., 1970. Structural geology in the eastern margin of Canadian Rocky Mountains. *Bull. Can. Petroleum Geology*, **18/3**, 332-406.

DALLA VECCHIA, F.M. AND RUSTIONI M., 1996. Mammalian trackways in the Conglomerato di Osoppo (Udine, NE Italy) and their contribution to its age determination. *Mem. Sci. Geol.*, **48**, 221-232.

DAVIS, D., SUPPE, J. AND DAHLEN, F.A., 1983. Mechanics of folds-and-thrust belts and accretionary wedges. *J. Geophys. Res.*, **88**, 1153-1172.

DE ZANCHE, V., 1990. A review of Triassic stratigraphy and paleogeography in the Eastern Southern Alps. *Boll. Soc. Geol. It.*, **109**, 59-71.

DOGLIONI, C., 1983. Duomo Medio-Triassico nelle Dolomiti. *Rend. Soc. Geol. It.* **6**, 13-16.

DOGLIONI, C., 1984. Tettonica triassica transpressiva nelle Dolomiti. *Giorn. Geol.* Ser. 3, **46**, 47-60.

DOGLIONI, C., 1985. The overthrusts in the Dolomites: ramp-flat systems. *Eclogae geol. Helv.*, **78**, 335-350.

DOGLIONI, C., 1987. Tectonics of the Dolomites, *J. Struct. Geol.*, **9**, 181-193.

DOGLIONI, C., 1992a. The Venetian Alps thrust belt. In: K. McClay (Ed.), *Thrust tectonics, Chapman & Hall, London*, 319-324.

DOGLIONI, C., 1992b. Relationships between Mesozoic extensional tectonics, stratigraphy and Alpine inversion in the Southern Alps. *Eclogae geol. Helv.*, **85/1**, 105-126.

DOGLIONI, C., 1993. Some remarks on the origin of foredeeps. *Tectonophysics*, **228**, 1-22.

DOGLIONI, C. AND CASTELLARIN, A., 1985. A geologic schematic cross-section of the Southern Alps. *Rend. Soc. Geol. It.*, **8**, 35-36.

DOGLIONI, C. AND BOSELLINI, A., 1987. Eoalpine and mesoalpine tectonics in the Southern Alps. *Geol. Rundschau*, **76**, 735-754.

DOGLIONI, C. AND SIORPAES, C., 1990. Polyphase deformation in the Col Bechei area (Dolomites-Northern Italy). *Eclogae geol. Helv.*, **83/3**, 701-710.

DOGLIONI, C. AND PROSSER G., 1997. Fold uplift versus regional subsidence and sedimentation rate. *Marine and Petroleum Geology*, **14/2**, 179-190.

EBBLIN, C., 1977. Orientation of stresses and strains in the Piedmont area of eastern Friuli, NE Italy. *Boll. Geof. Teor. Appl.*, **72**, 559-579.

ELLIOTT, D., 1983. The construction of balanced cross sections. *J. Struct. Geol.*, **5**, 101.

ESLINGER, E. AND PEVEAR, D., 1988. Clay minerals. *SEPM* Short Course 22.

ESPITALIÉ, J., 1986. Use of Tmax as a maturation index for different types of organic matter. Comparison with vitrinite reflectance. In: *Burrus, J. (Editor): Thermal Modeling in Sedimentary Basins. 1st IFP Exploration Research Conference*, Carcans, France, June 3-7 1985, Editions Technip-Paris, 475-496.

ESPITALIÉ, J., DEROO, G. AND MARQUIS, F., 1985a. La pyrolyse rock-eval et ses applications, première partie. *Rev. Inst. Franç. Pétrole*, **40**, 563-579.

ESPITALIÉ, J., DEROO, G. AND MARQUIS, F., 1985b. La pyrolyse rock-eval et ses applications, deuxième partie. *Rev. Inst. Franç. Pétrole*, **40**, 755-784.

ESPITALIÉ, J., DEROO, G. AND MARQUIS, F., 1986. La pyrolyse rock-eval et ses applications, troisième partie. *Rev. Inst. Franç. Pétrole*, **41**, 73-89.

FERASIN, F., 1958. Ricerche geologiche sulle Prealpi Carniche. *La ricerca scientifica*, **28/11**, 2279-2285.

FERASIN, F., BRAGA, G.P., CORSI, M. AND LOCATELLI, D., 1969. La linea dell'alto Tagliamento fra la Val Cimoliana ed il gruppo del M. Verzegnis in Carnia. *Mem. Ist. Geol. Min. Univ. Padova*, **27**, 1-15.

FERUGLIO, E., 1925. Carta Geologica delle Tre Venezie. Foglio 25, Udine. *Uff. Idrogr. Mag. Acque*, Venezia, Firenze.

FERUGLIO, E., 1929. Note illustrative della Carta Geologica delle Tre Venezie. Foglio Udine. *Uff. Idrogr. Mag. Acque*, Venezia.

FERRERO, J., 1965. Dosage des principaux minéraux des roches par diffraction de rayon X. *Rapport C.F.P (Bordeaux)*, inédit.

FERRERO, J., 1966. Nouvelle méthode empirique pour le dosage des minéraux par diffraction R.X. *Rapport C.F.P* (Bordeaux), inédit, 26.

FINETTI, I., RUSSI, M. AND SLEJKO, D., 1979. The Friuli earthquake (1976-1977). *Tectonophysics*, **53**, 261-272.

FINETTI, I., BRICCHI, G., DEL BEN, A., PIPAN M. AND XUAN Z., 1987. Geophysical study of the Adria plate. *Mem. Soc. Geol. It.*, **40**, 335-344.

FODOR, L., BOGOMIR, J., MARTON, E., SKABERNE, D., CAR, J. AND VRABEC, M., 1996. Miocene tectonic evolution of the Periadriatic zone and surrounding area in Slovenia: Repeated dextral transpression. *Mitt. Ges. Geol. Bergbaustud. Oesterr.*, **41**, 106.

FODOR, L., JELEN, B., MARTON, E., SKABERNE, D., CAR, J. AND VRABEC, M., 1998. Miocene-Pliocene tectonic evolution of the Slovenian Periadriatic fault: Implications for Alpine-Carpathian extrusion models. *Tectonics*, **17/5**, 690-709.

FRASCARI, F., 1968. Ricerche tettoniche nel gruppo montuoso dell'Arvenis (Carnia). *Giorn. Geol.*, Ser. 2, **34/1**, 1-20.

FRASCARI, F., 1982. Stratigrafia, paleotettonica e assetto strutturale della zona mediana carnica. In: A. Castellarin & G.B. Vai (a cura di): *Guida alla geologia del Sudalpino centro-orientale. Guide geol. reg. S.G.I.*, Bologna, 329-335.

FRASCARI, F., VAI, G.B. AND ZANFERRARI, A., 1979. Profilo Carnico Centrale. Nota illustrativa sommaria. *Rend. Soc. Geol. It.*, **1** (1978), 15-17.

FRASCARI, F., SEMENZA, E., SPALLETTA, C., VAI, G.B. AND VENTURINI, C., 1980. Profilo Carnico B: Gailtal-M. S. Simeone. Nota illustrativa sommaria. *Rend. Soc. Geol. It.*, **2** (1979), 17-20.

FRASCARI, F., SPALLETTA, C., VAI, G.B. AND VENTURINI, C., 1981. Foglio 14 Pontebba. In: Castellarin A. (a cura di), Carta tettonica delle Alpi Meridionali (alla scala 1:200'000). Pubbl. n. 441, *Prog. Fin. Geodinamica* (S.P.5) C.N.R., Tecnoprint, Bologna, 23-30.

FRASCARI, F. AND VAI, G.B., 1981. Fogli 4c – 13 Monte Cavallino-Ampezzo. In: Castellarin A. (a cura di), Carta tettonica delle Alpi Meridionali (alla scala 1:200.000). Pubbl. n. 441, *Prog. Fin. Geodinamica* (S.P.5) C.N.R., Tecnoprint, Bologna, 31-38.

FREY, M., 1986. Very low-grade metamorphism of the Alps – an introduction. *Schweiz. Mineral. Petrogr. Mitt.*, **66**, 13-27.

GEISER, P.A., 1988. The role of kinematics in the construction and analysis of geological cross sections in deformed terranes. *Spec. Pap. Geol. Soc. Am.*, **222**, 47-76.

GIANOLLA, P., 1992. Evoluzione Mediotriassica del vulcanismo di Rio Freddo (Alpi Giulie, Italia). *Mem. Sci. Geol.*, **44**, 193-209.

GILLCRIST, R., COWARD, M. AND MUGNIER, J.-L., 1987. Structural inversion and its controls: examples from the Alpine foreland and the French Alps. *Geodinamica Acta*, **1/1**, 5-34.

GOGUEL, J., 1962. Tectonics. Freeman, San Francisco, 347 p.

GORTANI, M. AND DESIO, A., 1925. Carta Geologica delle Tre Venezie. Foglio 14 Pontebba. Scala 1: 100.000. *Uff. Idr. Mag. Acque*, Venezia, Firenze.

GORTANI, M. AND DESIO, A., 1927. Note illustrative della Carta Geologica delle Tre Venezie. Foglio "Pontebba". *Uff. Idr. Mag. Acque*, Venezia, 86 p., Padova

GORTANI, M., DE TONI, A. AND ZENARI, S., 1933. Carta Geologica delle Tre Venezie. Foglio 13 Ampezzo. Scala 1:100'000. *Uff. Idr. Mag. Acque*, Venezia, Firenze.

GORTANI, M., DI COLBERTALDO, D. AND SELLI, R., 1949. Carta Geologica delle Tre Venezie. Foglio 14a Tarvisio. Scala 1:100'000. *Uff. Idr. Mag. Acque*, Venezia, Padova.

GRANDESSO, P., MASSARI, F. AND STEFANI, C., 1992. Flysh e molassa nell'area veneto-friulana: rapporti con l'evoluzione tettonica dei sistemi dinarico e sudalpino. *Studi Geologici Camerti, volume speciale* (1992/2), CROP 1-1A, 259.

HAAS, J., KOVACS, S., KRYSTYN, L. AND LEIN, R., 1995. Significance of Late Permian-Triassic facies zones in terrane reconstructions in the Alpine-North Pannonian domain. *Tectonophysics*, **242**, 19-40.

HALLAM, A., 1983. Supposed Permo-Triassic megashear between Laurasia and Gondwana. *Nature*, **301**, 499-502.

HATCHER, R.D. AND HOOPER, R.J., 1992 Evolution of crystalline thrust sheets in the internal parts of the mountain chains. In: *Thrust Tectonics*, edited by K. McClay, Chapman and Hall, London, 217-234.

HÉROUX, Y., CHAGNON, A. AND BERTRAND, R., 1979. Compilation and correlation of major thermal maturation indicators. *Bull. Amer. Assoc. Petroleum Geol.*, **63**, 2128-2144.

HUBICH, D. AND LÄUFER, A.L., 1997. Variscan kinematics and nappe tectonics in the Carnic Alps (Southern Alps). *Terra Abstracts*, EUG 9, 37/5P16, 348.

HUBICH, D., LÄUFER, A.L. AND LOESCHKE, F.A., 1999. Geodynamic evolution of the Carnic Alps: Plate tectonic interpretation of the southern margin of the European Variscides. *4th Workshop on Alpine Geological Studies, Tübingen, TGA, Series A*, **52**, 2-4.

ITALIAN IGCP 203 GROUP (Ed.), 1986. Permian and Permian-Triassic boundary in the South-Alpine segment of the western Tethys. Field guidebook. 182 p. SGI & IGCP proj. 203Mtg, July 1986.

JADOUL, F. AND NICORA, A., 1979. L'assetto stratigrafico-paleogeografico del Trias medio-superiore della Val d'Aupa (Carnia orientale). *Riv. Ital. paleont. Strat.*, mem. **XIV**, 11-140.

KLUG, H.P. & ALEXANDER, L. 1974. X-ray Diffraction Procedures for Polycrystalline and Amorphous Materials. *(Ed. by John WILEY and Sons, Inc.). New York.*

KOYI, H., HESSAMI, K., TEIXELL, A. AND SANS, M., 1999. Determination of life cycle of thrust faults in sandbox models. *Thrust Tectonics Conference, April 26-29 1999. Royal Holloway, University of London.*

KRAINER, K., 1992. Fazies, Sedimentations prozesse und Paläogeographie im Karbon der Ost- ind Südalpen. *Jahrb. Geol. Bundesanst.*, **135/1**, 99-193.

KRAINER, K., 1993. Late-and Post-Variscan Sediments of the Eastern and Southern Alps. In: *Pre-Mesozoic geology in the Alps*, edited by J.F. von Raumer and F. Neubauer, 537-564, Springer Verlag Berlin.

KREUTZER, L.H., 1990. Mikrofazies, Stratigraphie und Paläogeographie des Zentralkarnischen Hauptkammes zwischen Seewarte und Cellon. *Jahrb. Geol. Bundesanst.*, **133**, 275-343.

KÜBLER, B., 1964. Les argiles indicateurs de métamorphisme. *Rev. Inst. Fr. Pét.*, **19**, 1093-1112.

KÜBLER, B., 1967. La cristallinité de l'illite et les zones tout à fait supérieur du métamorphisme. *Etages tectoniques, Colloque de Neuchâtel*, 105-122.

KÜBLER, B., 1968. Evaluation quantitative du métamorphisme par la cristallinité de l'illite, *Bull. Centre. Rech. Pau –S.N.P.A.*, **2**, 385-397.

KÜBLER, B., 1980. Les premiers stades de la diagenèse organique et de la diagenèse minérale. Deuxième partie: Zonéographie par les transformations minéralogiques,

comparaison avec la réflectance de la vitrinite, les extraits organiques et les gazs absorbés. *Bull. Ver. Schweiz. Petroleum-Geol. u. –Ing.*, **46/110**, 1-22.

KÜBLER, B., 1983. Dosage quantitatif des minéraux majeurs des roches sédimentaires par diffraction X. *Cahier de l'institut de Géologie de Neuchâtel*. Série AX N°1.1 & 1.2.

KÜBLER, B., 1984: Les indicateurs des transformations physiques et chimiques dans la diagenèse, température et calorimétrie. In: *Lagache, M. (Editor), Thermométrie et barométrie géologiques. Soc. Franç. Mineral. Cristallogr., Paris*, **2**, 489-596.

KÜBLER, B., 1987. Cristallinité de l'illite, méthodes normalisées de préparations, méthodes normalisées de mesures. *Cahiers de l'Institut de Géologie de Neuchâtel.* Série ADX, 1-8.

KÜBLER, B., 1990. "Cristallinité" de l'illite et mixed-layers: brève révision. *Schweiz. Mineral. Petrogr. Mitt.*, **70**, 89-93.

KÜBLER, B., BETRIX, M.A. AND MONNIER, F., 1979a. Les premiers stades de la diagenèse organique et de la diagenèse minérale. Première partie: Zonéographie par la maturation de la matière organique. *Bull. Ver. Schweiz. Petroleum-Geol. u. –Ing.* **45/108**, 1-22.

KÜBLER, B., PITTION, J.L., HÉROUX, Y., CHAROLLAIS, J. AND WEIDMANN, M., 1979b. Sur le pouvoir réflecteur de la vitrinite dans quelques roches du Jura, de la molasse et des nappes préalpines, helvétiques et penniques (Suisse occidentale et Haute-savoie). *Eclogae geol. Helv.*, **72/2**, 347-373.

LAFARGUE, E., ESPITALIÉ, J., MARQUIS, F. AND PILLOT, D., 1996. ROCK EVAL 6 applications in hydrocarbon exploration, production and in soil contamination studies. *IFP*, 5th Latin American Congress on Organic Geochemistry, Cancun, October 6-10, 1996.

LAUBSCHER, H.P., 1965. Ein kinematisches Modell der Jurafaltung. *Eclogae Geol. Helv.*, **58**, 323-318.

LAUBSCHER, H.P., 1971a. The large-scale kinematics of the western Alps and the northern Apennines and its palinspastic implications, *Am. J. Sci*., **271**, 193-226.

LAUBSCHER, H.P., 1971b. Das Alpen-Dinariden Problem und die Palinspastik der suedlichen Tethys. *Geol. Rundsch*., **60**, 813-833.

LAUBSCHER, H.P., 1985a. The Late Alpine (Periadriatic) intrusions and the Insubric Line. *Mem. Soc. Geol. It.*, **26**, 21-30.

LAUBSCHER, H.P., 1985b. Large-scale, thin-skinned thrusting in the Southern Alp: kinematic models. *Geol. Soc. Amer. Bull*., Boulder, **96**, 710-718.

LAUBSCHER, H.P., 1988. Material balance in Alpine orogeny. *Geol. Soc. Amer. Bull*., Boulder, **100**, 1313-1328.

LAUBSCHER, H.P., 1990. The problem of the deep structure of the Southern Alps: 3-D material balance considerations and regional consequences. *Tectonophysics*, **176**, 103-121.

LÄUFER, A.L., 1996. Variscan and Alpine tectonometamorphic evolution of the Carnic Alps (Southern Alps) - structural analysis, illite crystallinity, K-Ar and Ar-Ar geochronology. *Tübinger Geowissenschaftliche Arbeiten (TGA), Reihe A, Band 26*, 102 p.

LEONARDI, P., 1967. Le Dolomiti. Manfrini, Rovereto, Italy, 1019 p.

MANZONI, M., VENTURINI, C. AND VIGLIOTTI, L., 1989. Paleomagnetism of Upper Carboniferous limestones from the Carnic Alps. *Tectonophysics*, **165**, 73-80.

MARSHAK, S. AND WOODWARD, N., 1985. Introduction to cross section balancing. In: S. Marshak and G. Mitra (Eds.), Basic methods of structural geology, Prentice hall, New jersey, 303-332.

MARTINIS, B., 1966. Prove di ampi sovrascorrimenti nelle Prealpe Friulane e

Venete. *Mem. Ist. Geol. Min.,*. Padova, **25**, 31 p.

MARTINIS, B., 1975. The Friulian and Julian Alps and pre-Alps. In: Structural model of Italy. *Quad. Ric. Sc*., **90**, Roma.

MARTINIS, B., 1979. La struttura del M. Jouf: un nuovo elemento sovrascorso delle Prealpi Carniche. *Acc. Lincei, Rend. I Cl. di Sc. fis. mat. e nat*., **65**, 313-393.

MASSARI, F., 1986. Some thoughts on the Permo-Triassic evolution of the South-Alpine area (Italy). *Mem. Soc. Geol. It.,* **34**, 179-188.

MASSARI, F., 1990. The foredeeps of the northern Adriatic margin: Evidence of diachroneity in deformation of the Southern Alps. *Riv. Ital. Paleont. Strat*., **96**, 351-380.

MASSARI, F., GRANDESSO, P., STEFANI, C. AND ZANFERRARI, A., 1986a. The Oligo-Miocene molasse of the Veneto-Friuli region, Southern Alps. *Giorn. Geol.*, **48**/1-2, 235-255.

MASSARI, F., GRANDESSO, P., STEFANI, C. AND JOBSTRAIBIZER,P.G., 1986b. A small polyhistory foreland basin evolving in a context of oblique convergence: the Venetian basin (Chattian to Recent, Southern Alps, Italy). In Allen P.A. and Homewood P. (Eds.). Foreland basins. *Spec. Publ. Int. Ass. Sediment*., Blackwell Scientific Publ., Oxford, **8**, 141-168

MASSARI, F., PESAVENTO, M. AND VENTURINI, C., 1991. The Permian-Carboniferous cyclothems of the Pramollo basin sequence (Carnic Alps). *Giorn. Geol*., ser. 3, **53/1**, 171-185.

MASSARI, F., MELLERE, D. AND DOGLIONI, C., 1993. Cyclicity in non-marine foreland-basin sedimentary fill: The Messinian conglomerate-bearing succession of the Venetian Alps (Italy). *Spec. Publ. Int. Assoc. Sedimentol*., **17**, 501-520.

MASSARI, F. AND NERI, C., 1997. The infill of a supradetachment (?) basin: the continental to shallow-marine Upper Permian succession in the Dolomites and Carnia (Italy). *Sedimentary Geology*, **110**, 181-221.

MATTE, P., 1986. Tectonics and plate tectonics model for the Variscan belt of Europe. *Tectonophysics*, **126**, 329-374.

MCCLAY, K.R., 1992. Glossary of thrust tectonics terms. In: *Thrust tectonics, edited by K. McClay, Chapman & Hall*, 419-433.

MENEGAZZI, R., PILI, M. AND VENTURINI, C., 1991. Preliminary data and hypothesis about the very-low metamorphic Hercynian sequence of the western Palaeocarnic Chain. *Giorn. Geol.*, ser. 3a, **53/1**, 139-150.

MOORE, D. and REYNOLDS, R., 1989. X-Ray-diffraction and the identification and analysis of clay-minerals. *Oxford University Press*, 332 p.

MORLEY, C.K., 1988. Out-of-sequence thrusts. *Tectonics*, **7**, 539-561.

MORRIS, A., FERRILL, D.A. AND HENDERSON, D.B., 1996. Slip-tendency analysis and fault reactivation. *Geology*, **24/3**, 275-278.

MOSAR, J., 1988. Métamorphisme transporté dans les Préalpes. *Schweiz. Mineral. Petrogr. Mitt.*, **68**, 77-94.

MÜLLER, G., 1977. Fault plane solution of the earthquake in Northern Italy. *J. Geophys*., **42**, 343-349.

MULLIS, J., 1995. Evolution and significance of fluids during neo-Alpine tectono-metamorphic events in the Central Alps, inferred by fluid inclusion investigations. - A review, *2nd workshop on Alpine geology*, Basel, 134-135.

MULLIS, J., RAHN, M., DE CAPITANI, C. STERN, W.B. AND FREY, M., 1995. How useful is illite "crystallinity" as a geothermometer ?, *Terra Nova Abstr. Supplem*., **1**, 128-129.

OLDOW, J.S., BALLY, A.W., AVÉ LALLEMANT, H.G. AND LEEMAN, W.P., 1989. Structural cross sections across the Cordillera. In: The Geology of North America, vol. A. *The Geology of North America - An overview*, plate 7, *Geol. Soc. of Am.*, Boulder.

PICOTTI, V. AND PROSSER, G., 1987. Studio geologico dell'area compressa tra Lozzo di Cadore e il gruppo delle Marmarole (Dolomiti, Alpi Meridionali). *G. Geol.*, **49**, 33-50.

PIERI, M. AND GROPPI, G., 1981. Subsurface geological structure of the Po plain, Italy. *Pubbl. 414 Prog. Fin. Geodin., AGIP*, Roma.

PISA, G., 1972. Geologia dei Monti a N di Forni di Sotto (Carnia occidentale). *Giorn. Geol.*, 2, **38**, II, 543-688.

PISA, G., CASTELLARIN, A., LUCCHINI, F., ROSSI, P.L., SIMBOLI, G., BOSELLINI, A. AND SOMMAVILLA, E., 1979. Middle-Triassic Magmatism in the Southern Alps: a review of general data in the Dolomites. *Riv. It. Paleont. Strat.* **85**, 1093-1110.

PLATT, J.P., 1988. The mechanics of frontal imbrication: a first-order analysis. *Geol. Rundschau*, **77/2**, 577-589.

POLI, M.E., 1996. Analisi strutturale del Monte di Medea (Friuli): tettonica polifasica nell'avampaese sudalpino orientale. *Atti Tic. Sc. Terra (Serie speciale)*, **4**, 103-113.

POLINSKI, R.K. AND EISBACHER, G., 1992. Deformation partitioning during polyphase oblique convergence in the Karawanken Mountains, Southeastern Alps. *J. Struct. Geol.*, **14**, 1203-1213.

RAMSAY, J.G., 1992. Some geometric problems of ramp flat thrust models. In: *Thrust Tectonics*, edited by K. McClay, Chapman and Hall, London, 191-200.

RANTITSCH, G., 1997. Thermal history of the Carnic Alps (Southern Alps, Austria) and its palaeogeographic implications. *Tectonophysics*, **272**, 213-232.

RATHORE, J.S. AND BECKE, M., 1980. Magnetic fabric analyses in the Gail valley (Carinthia, Austria) for the determination of the sense of movements along this region of the Periadriatic line. *Tectonophysics*, **69**, 349-368.

RATSCHBACHER, L., FRISCH, W., NEUBAUER, F., SCHMID S.M. AND NEUGEBAUER J., 1989. Extension in compressional belts: The Eastern Alps. *Geology*, **17**, 404-407.

RATSCHBACHER, L., FRISCH, W., LINZER, H.G. AND MERLE O., 1991. Extrusion in the Eastern Alps, Part 2: Structural analysis. *Tectonics*, **10/2**, 257-271.

ROEDER, D. AND LINDSEY, D., 1992. Barcis area (Veneto, Friuli, Slovenia): Architecture and geodynamics, *NAFTA*, **43**, 509-548.

SACHSENHOFER, R.F., 1992. Coalification and thermal histories of Teriary basins in relation to late Alpidic evolution of the Eastern Alps. *Geol. Rundsch.*, **81/2**, 291-308.

SARTI, M., 1979. Il Paleogene della Val Tremugna (Prealpi Carniche). *Boll. Soc. Geol. It.*, **98**, 87-108.

SARTI, M., 1982. Evoluzione strutturale del Gruppo M. Cuar-M. Covria e rilievi circostanti (Pealpi Carniche meridionali). In: A. Castellarin & G.B. Vai (a cura di): *Guida alla geologia del Sudalpino centro-orientale. Guide geol. reg. S.G.I.*, Bologna, 321-328.

SARTORIO, D. AND ROZZA, R., 1991. The Permian of Amanda 1 bis well (Northern Adriatic Sea). *Giorn. Geol*, ser. 3a, **53/1**, 187-196.

SCHMID, S.M., AEBLI, H.R., HELLER, F. AND ZINGG, A., 1989. The role of the Periadriatic line in the tectonic evolution of the Alps, in Alpine Tectonics, edited by M.P. Coward, D. Dietrich and R.G. Park, *Geol. Soc. Spec. Publ. London*, **45**, 153-171.

SCHÖNBORN G., 1992a. Kinematics of a transverse zone in the Southern Alps, Italy. In: *Thrust tectonics, edited by K. McClay, Chapman & Hall*, 299-310.

SCHÖNBORN, G., 1992b. Alpine tectonics and kinematic models of the central Southern Alps. *Mem. Sci. Geol.*, **44**, 229-393.

SCHÖNBORN, G., 1994. Evolution and Deep Structure of Val Brembana based on surface data (Southern Alps, Italy). In: Proceedings of Symposium CROP-Alpi Centrali, edited by A. Montrasio and E.

Sciesa, *Quad. Geodin. Alp. Quat*., 197-212.

SCHÖNBORN, G. 1999: Balancing cross sections with kinematics constraints: The Dolomites (northern Italy). *Tectonics*, **18/3**, 527-545.

SCHÖNBORN, G., AND SCHUMACHER, M. 1994. Controls on thrust tectonics along basement-cover detachment. *Schweiz. Mineral. Petrogr. Mitt*, **74**, 421-436.

SCHÖNLAUB, H.P. AND HEINISCH, H., 1993. The classic fossiliferous Paleozoic units of the Eastern and Southern Alps. In *Pre-Mesozoic geology in the Alps*, edited by J.F. von Raumer and F. Neubauer, 395-422, Springer Verlag Berlin.

SCHÖNLAUB, H.P., 1979. Das Paläozoikum in Österreich. *Abh. Geol. Bundesanst*., **33**, 124p.

SELLI, R., 1963. Schema geologico delle Alpi Carniche e Giulie occidentali. *Giorn. Geol*., Ser 2, **30**, 1-136.

SEMENZA, E., 1974. La fase giudicariense nel quadro di una nuova ipotesi sull'orogensi alpina nell'area italo-dinarica. *Mem. Soc. Geol. Ital.*, **13**, 178-226.

SEMENZA, E., 1981. Foglio 12, Cortina d'Ampezzo, ex-Pieve di Cadore. In Castellarin, A. (a cura di). Carta tettonica delle Alpi meridionali (alla scala 1: 200.000). *Prog. Fin. Geodinamica C.N.R.*. Pubbl. 441, 55-59.

SIRO, L. AND SLEJKO, D., 1982. Space-time evolution of the 1977-1980 seismicity in the Friuli area and its seismo-tectonic implications. *Boll. Geof. Teor. Appl*., **24**, 67-77.

SLEJIKO, D., CARULLI, G.B., CARRARO, F., CASTALDINI, D., CAVALLIN, A., DOGLIONI, C., ILLICETO, V., NICOLICH, R., REBEZ, A., SEMENZA, E., ZANFERRARI, A. AND ZANOLLA, C., 1987. Modello sismotettonico dell'Italia nord-orientale. *Cons. Naz. Ric., Terremoti, Rend.*, **1**, Trieste, 1-82.

SLEJIKO, D., CARULLI, G.B., NICOLICH, R., REBEZ, A., ZANFERRARI, A., CAVALLIN, A., DOGLIONI, C., CARRARO, F., CASTALDINI, D., ILLICETO, V., SEMENZA, E. AND ZANOLLA, C., 1989. Seismotectonics of the Eastern Southern-Alps: a review. *Boll. Geof. Teor. Appl.*, **31**, 122, 109-136.

SLEJIKO, D. AND KIJKO, A., 1990. Seismic hazard assessment for the main seismogenic zones in the Eastern Alps. *Tectonophysics*, **191**, 165-183.

SRODON, J. AND EBERL, D.D., 1984. Illite. In: *Bailey, S.W. (Editor): Micas. Min. Soc. Amer., Reviews in Mineralogy* , **13**, 495-544.

STAMPFLI, G., 1996. The Intra-Alpine terrain: A Paleotethyan remnant in the Alpine Variscides. *Eclogae geol. Helv.* **89/1**, 13-42.

STAMPFLI, G., MARCOUX, J. AND BAUD A., 1991. Tethyan margins in space and time. *Paleogeogr., Paleoecol., Paleoclim.*, **87**, 373-409.

STEFANI, C., 1984. Sedimentologia della molassa delle Prealpi Carniche occidentali. *Mem. Sc. Geol*., **36**, 427-442.

SUPPE, J., 1983. Geometry and kinematics of fault-bend folding. *Am. J. Sci*., **283**, 684-721.

SUPPE, J., 1985. Principles of Structural Geology. *Prentice-Hall, Englewood Cliffs, N.J.* 537 p.

SUPPE, J. AND MEDWEDEFF, D.A., 1990. Geometry and kinematics of fault-propagation folding. *Eclogae geol. Helv*., **83**, 409-454.

TEICHMÜLLER, M. AND TEICHMÜLLER, R., 1986. Relations between coalification and paleogeothermics in Variscan and Alpidic foredeeps of Western Europe. In: *Buntebarth, G. and Stegena, L. (Editors); Lecture Notes in Earth Sciences 5: Paleogeothermics*. Springer-verlag, Berlin, Heidelberg, London, Paris, New-York, Tokyo, 53-78.

THOMAS, W.A., 1990. Controls on locations of transverse zones in thrust belts. *Eclogae geol. Helv.*, **83/3**, 727-744.

TISSOT, B.P., PELET, R. AND UNGERER, PH., 1987. Thermal history of sedimentary basins, maturation indices and kinetics of oil and gas generation. *Bull. Amer. Assoc. Petrol. Geol*., **71**, 1445-1466.

TISSOT, B.P. AND WELTE, D.H., 1984. Petroleum formation and occurrence. 2th edition, 699 p., Springer-verlag, Berlin-Heidelberg-New-York-Tokyo.

TOLMANN, A., 1985. Geologie von Österreich, Band 2, Ausserzentralalpiner Anteil. Deuticke Verlag, Wien, 766 p.

VAI, G.B, 1979. Una palinspastica permiana della Catena Paleocarnica. *Rend. Soc. Geol. Ital.*, **1**, 25-27.

VARIOUS AUTHORS. 1971. Carta Geologica d'Italia. Fogli 4c-13 Monte Cavallino-Ampezzo. Scala 1:100.000 (II ed.). *Ser. Geol. d'Italia*, Roma.

VENTURINI, C., 1981. Foglio 14a Tarvisio. In Castellarin, A. (a cura di). Carta tettonica delle Alpi meridionali (alla scala 1: 200.000). *Prog. Fin. Geodinamica (S.P.5) C.N.R.*. Pubbl. 441, 19-22.

VENTURINI, C., 1982. Il bacino tardoercinico di Pramollo (Alpi Carniche): un'evoluzione regolata dalla tettonica sinsedimentaria. *Mem. Soc. Geol. It.* **24**, 23-42.

VENTURINI, C. (Ed), 1990a. Field workshop on Carboniferous to Permian sequence of the Pramollo-Nassfeld basin (Carnic Alps). Guidebook Pramollo 1990. *Arti Grafiche Friulani, Udine*, 1-159.

VENTURINI, C., 1990b. Geologia delle Alpi Carniche centro-orientali. *Mus. Friul. St. Nat.*, Udine, **36**, 1-222.

VENTURINI, C., 1990c. Cinematica neogenico-quaternaria del sudalpino orientale (settore friulano). *Studi Geologici Camerti, volume speciale*, 109-116.

VENTURINI, C., 1991. Introduction to the geology of the Pramollo Basin (Carnic Alps) and its surroundings. *Giorn. Geol.*, **53/1**, 13-47.

VENTURINI, C., 1992. Il conglomerato di Osoppo. *Gortania - Atti Museo Friul. St. Nat.*, **13** (1991), Udine, 31-49.

VENTURINI, C., FERRARI, A., SPALLETTA, C. AND VAI, G.B., 1982. La discordanza ercinica, il tardorogeno e il postorogeno nella geologia del Passo di Pramollo. In: A. Castellarin & G.B. Vai (a cura di): *Guida alla geologia del Sudalpino centro-orientale. Guide geol. reg. S.G.I.*, Bologna, 305-319.

VENTURINI, C. AND FONTANA, C., 1992. The Neoalpine phase in the Carnic Alps: secondary E-W compressions. *Studi Geologici Camerti, volume speciale (1992/2)*, CROP 1-1A, 271-274.

VENTURINI, C. AND D ELZOTTO, S., 1992. Evoluzione deformativa delle Alpi Carniche centro occidentali: paleotettonica e tettonica neoalpina. *Studi Geologici Camerti, volume speciale (1992/2)*, CROP 1-1A, 261-270.

VENTURINI, S. AND TUNIS, G., 1991. Segnalazione di depositi miocenici nella Val Tremugna e presso Ossopo (Friuli). *Atti Tic. Sc. Terra*, **34**, 39-42.

VENTURINI, S. AND TUNIS, G., 1992. La composizione dei conglomerati Cenozoic del Friuli: dati preliminari *Studi Geologici Camerti, volume speciale* (1992/2), CROP 1-1A, 285-295.

VENZO, S., 1939. Nuovo lembo tortoniano strizzato tra le filladi ed il permiano a Stringo di Valsugana (Trentino meridionale orientale), *Bull. Soc. Geol. Ital.*, **58**, 175-185.

VIAGGI, M. AND VENTURINI, S., 1995. Dati biostratigrafici preliminari sui depositi salmastro-dulcioli neogenici delle Prealpi Veneto-friulane. *Natura Nascosta*, Monfalcone, **13**, 32-33.

VIEL, G., 1979. Litostratigrafia Ladinica: una revisione. Ricostruzione paleogeographica e paleostrutturale dell'area Dolomitico-Cadorina (Alpi Meridionali); I e II parte. *Riv. It. Paleont. Strat.* **85**, 85-125; **85**, 297-352.

VRABEC, M., 1996. Style of postsedimentary deformation in Plio-Quaternary Velenje

basin, NE Slovenia, *Mitt. Ges. Geol. Bergbaustud. Oesterr.*, **41**, 140 p.

WEAVER, C.E., 1960. Possible use of clay minerals in search of oil. *Am. Assoc. Pet. Geol. Bull.*, **44**, 1505-1518.

WINTERER, E.L. AND BOSELLINI, A., 1981. Subsidence and Sedimentation on Jurassic Passive Continental Margin, Southern Alps, Italy. *Amer. Assoc. Petr. Geol. Bull.*, **65**, 394-421.

WOODWARD, N.B., 1987. Geological applicability of critical-wedge thrust-belt models, *Geol. Soc. Amer. Bull.*, **99**, 827-832.

WOODWARD, N.B., BOYER, S.E. AND SUPPE, J., 1989. Balanced geological cross sections: an essential technique in geological research and exploration. *American Geophysical Union Short Course in Geology*, **6**, 132 p.

ZANFERRARI, A., 1974. Sulla terminazione occidentale del sovrascorrimento periadriatico (piega faglia periadriatica auct.) nelle Prealpi Carniche. *Boll. Soc. Geol. Ital.*, **93**, 33-46.

ZANFERRARI, A., BOLLETTINARI, G., CAROBENE, L., CARTON, A., CARULLI, G.B., CASTALDINI, D., CAVALLIN, A., PANIZZA, M., PELLEGRINI, G.B., PIANETTI, F. AND SAURO, U., 1982. Evoluzione neotettonica dell'Italia nord-orientale. *Mem. Sci. Geol.*, **35**, 355-376.

ZENARI, S., 1927. Carta Geologica delle Tre Venezie. Foglio 24 Maniago. *Uff. Idrogr. Mag. Acque Venezia*, Venezia.

ZIEGLER, P.A., 1989. Post-Hercynian plate reorganisation in the Tethys and Arctic-North Atlantic. In: Manspeizer, W., (Editor), *Triassic-Jurassic rifting, continental break-up and the origin of the Atlantic ocean and passive margins, Dev. Geotecton.*, **22**, 1-27, Elsevier, Amsterdam.

TABLES AND ANNEXES

(2 Tables, 3 Annexes)

Table 1 Zoneography of diagenesis to very low grade metamorphism using organic and mineral indicators

Sample N°	Location	Lithology	Formation	Age	clay minerals	IC ° 2ϑCuKα	Reich-weite	Ro (%)	Kübler's zones	Zoneography (data)	interpr.
CN15	Stli Pra da Forca	marl	Flysch	Oligocene	I/S + mica + chl+ sm	0.95	0		2	sup. diagenesis	
sin67	Navarons	marl	Flysch	Eocene	I/S + mica + chl +sm	0.497	0	0.5 - 0.7	2	sup. diagenesis	
CN46	Valle di Uccea	marl	Flysch	Maastrichian	I/S + mica + ch + ka	0.737	1		3	mid. diagenesis	
CN47	Valle di Uccea	limestone	Flysch	Maastrichian	I/S + mica + chl	0.391	3		4	deep diagenesis	mid. dia
CN45	Valle di Uccea	marl	Flysch	Maastrichian	I/S + mica + chl	0.862	1		3	mid. diagenesis	
CN17	Braulins	marl	Scaglia	Campanian	I/S + mica + chl + sm	0.523	0		1 or 2	sup. diagenesis	
CN34	Malga Confin (Val Venzonassa)	marl	Scaglia	Campanian	I/S+mica+chl+ka+sm	0.973	0		1 or 2	sup. diagenesis	
CN23	M. San Simeone	marl	Scaglia	Turonian-Coniacian	I/S+mica+chl+sm+hl	0.206 dis.	0		1 or 2	sup. diagenesis	
CN40	M. San Simeone	marl	Scaglia	Cenomanian	I/S+mica+chl+ka+sm	0.235 dis.	0		1 or 2	sup. diagenesis	
CN35	Ospedalleto	marl	Soccher	Lower Cretaceous	I/S + mica + chl + sm	1.061	1		3	mid. diagenesis	
CN37	Avasinis	limestone	Soccher	Lower Cretaceous	I/S + mica + chl	0.404	3		4	deep diagenesis	mid. dia
CN43	Cercenaz (Avasinis)	limestone	Soccher	Lower Cretaceous	I/S + mica + chl + ka	0.332 dis.	3		4	deep diagenesis	mid. dia
CN16	Ledrania	limestone	Soccher	Tithonian	I/S + mica + chl + ka	0.361	3		4	deep diagenesis	mid. dia
CN36	M. Cumelli	marly lim.	Soccher	Kimmeridgian-Tith.	I/S + mica + chl + ka	0.936	1		3	mid. diagenesis	
CN44	Casera Nische	limestone	Soccher	Upper Jurassic	I/S + mica + chl	0.428	3		4	deep diagenesis	mid. dia
CN52	Stli Gnivizza	marly lim.	Soccher	Upper Jurassic	I/S + mica + chl + ka	0.685	3		4	deep diagenesis	mid. dia
CN54	Stli Gnivizza	marly lim.	Soccher	Upper Jurassic	I/S + mica + chl	0.257 dis.	1		3	mid. diagenesis	
CN41	M. San Simeone W	limestone	Vajont	Middle Jurassic	I/S + mica + chl	0.642	1		3	mid. diagenesis	
CN19	Valle del Torre (Rist. Sorgenti)	marl	Calcari grigi	Rhaetian-Hettangian	I/S + mica + chl + ka	0.523	3		4	deep diagenesis	mid. dia
CN49	Cuel di Forchia	dolostone	Dol. Principale	Norian- Rhaetian	I/S + mica + chl + ka	0.368	3		4	deep diagenesis	mid. dia
CN51	Nimbriu (Alesso)	dolostone	Dol. Principale	Norian- Rhaetian	I/S + mica + chl	0.258	3		4	deep diagenesis	mid. dia
sin38	Plan di Sieas (Villa)	limestone	Caprizzi	Norian	I/S + mica + ka	0.534	3		4	deep diagenesis	mid. dia
sin51	Caprizzi	marly lim.	Caprizzi	Norian	I/S + mica	0.827	??? 3	0.65 - 0.85	3	mid. diagenesis	
sin66	Madonna del Vergon (Priuso)	marly lim.	Caprizzi	Norian	I/S + mica + chl +sm	0.708	0		1 or 2	sup. diagenesis	
sin5	ex Miniera (Val di Gorto)	marl	Raibl	Carnian	I/S + mica + chl + ka	0.818	1	0.8 - 1.0	3	mid. diagenesis	
sin6	Muina	marl	Raibl	Carnian	I/S + mica + chl + ka	0.95	1		3	mid. diagenesis	
sin7	between Muina and Agrons	marl	Raibl	Carnian	rec + mica + ka	0.662	1	1.0 - 1.2	3	mid. diagenesis	
sin8	Agrons	marly lim.	Raibl	Carnian	rec + mica + chl	0.644	1		3	mid. diagenesis	
sin23	Muina	marl	Raibl	Carnian	rec+ mica + chl	0.958	1	1.2 - 1.4	3	mid. diagenesis	
sin24	Muina	marl	Raibl	Carnian	I/S + mica + chl	0.892	1		3	mid. diagenesis	
sin25	C. se Codem (Raveo)	marl	Raibl	Carnian	rec + mica + ka + chl	0.8	1		3	mid. diagenesis	
sin26	St. O Cervias (Raveo)	marl	Raibl	Carnian	I/S + mica + chl + ka	0.69	1		3	mid. diagenesis	
sin34	Trichiamps	marl	Raibl	Carnian	I/S + mica + ka + chl		1		3	mid. diagenesis	
sin35	between Val and Vinaio	marl	Raibl	Carnian	rec + mica + ka	0.965	1	0.6 - 0.8	2 or 3	sup. diagenesis	
sin36	between Val and Vinaio	marly lim.	Raibl	Carnian	mica+chl+ka+hl+paly		0		2	sup. diagenesis	
sin37	Plugna	marl	Raibl	Carnian	I/S + mica + smec	0.956	0		2	sup. diagenesis	
sin40	Casera Zums (Illegio)	marl	Raibl	Carnian	I/S + mica	1.526	1		3	mid. diagenesis	
sin42	Chiampees (Lovea)	limestone	Raibl	Carnian	I/S + mica + ka	0.525	???		3 ?	mid. diagenesis	
sin45	Fielis	marl	Raibl	Carnian	I/S + mica + chl + ka	0.883	1	1.05 - 1.25	3	mid. diagenesis	
sin63	Forni di Sopra	marl	Raibl	Carnian	I/S + mica	1.048	1	0.75 - 0.95	3	mid. diagenesis	
CN1	Lago di Sauris	marl	Raibl	Carnian	I/S + mica + chl	0.95	1		3	mid. diagenesis	
CN3	Col Sarenede	marl	Raibl	Carnian	I/S + mica + chl	0.906	1		3	mid. diagenesis	
CN5	Passo Oberenghe	marl	Raibl	Carnian	I/S + mica + chl + ka	0.678	1		3	mid. diagenesis	
CN6	Voltois	marl	Raibl	Carnian	I/S + mica + chl	0.59	1		3	mid. diagenesis	
CN11	Grauzaria	marl	Raibl	Carnian	I/S + mica + ka	0.905	??? 3	< 0.5	1 or 2	sup. diagenesis	
CN21	T. Degano/ Muina	marl	Raibl	Carnian	I/S + mica +hl ?	1.062	??? 1	1.0 - 1.2	3	mid. diagenesis	
CN24	Chiampees (Lovea)	limestone	Raibl	Carnian	I/S + mica + chl	0.825	1		3	mid. diagenesis	
CN48	Fielis	marl	Raibl	Carnian	mica + chl + ka + paly	1.106	0		1 or 2	sup. diagenesis	
CN50	Fielis	dolostone	Schlern	Upper Ladinian	I/S + mica + chl	0.266 dis.	3		5	anchizone	sup. dia
sin11	Sent. Corbellini (Clap Grande)	marl	Wengen	Upper Ladinian	I/S + mica + chl + ka	0.491	3 ?	1.1 - 1.3	3	mid. diagenesis	
sin12	Sent. Corbellini (Clap Grande)	marl	Wengen	Upper Ladinian	rec + mica + ka + chl	0.736	1	1.1 - 1.3	3	mid. diagenesis	
sin27	Rifugio M. Siera	marl	Wengen	Upper Ladinian	rec + mica + chl		1		3	mid. diagenesis	
sin28	Rifugio M. Siera	marl	Wengen	Upper Ladinian	I/S + mica + ka + chl	0.781	1	1.25 - 1.45	3 or 4	mid. diagenesis	
sin43	Chiampees (Lovea)	marl	Wengen	Upper Ladinian	I/S + mica + chl + ka	1.241	1	0.75 - 0.95	3	mid. diagenesis	
CN22	Galizzis	marl	Wengen	Upper Ladinian	I/S + mica + chl	0.552	3		4	deep diagenesis	
sin54	Col Trondo	marl	Livinallongo	Lower Ladinian	I/S + mica + chl		1	0.8 - 1.0	3	mid. diagenesis	
sin46	M. Zoncolan (Pian di Val)	sandstone	Werfen	Scythian	mica + chl + ka	0.184	3		6	epizone	deep dia
sin47	M. Zoncolan (Scaletona)	sandstone	Werfen	Scythian	mica	0.212	3		5	anchi/epizone	deep dia
sin64	Pontebba	marl	Werfen	Scythian	mica + chl	0.322	3		4 or 5	diag./anchizone	
CN20	M. Palis	siltstone	Werfen	Scythian	mica + chl	0.39	3		4	deep diagenesis	
CN28	M. Tamai	sandstone	Werfen	Scythian	mica + chl	0.272	3		5	anchizone	deep dia
sin30	Pierabech	siltstone	Bellerophon	Upper Permian	mica + chl	0.286	3		5	anchizone	
CN2	Lateis	siltstone	Bellerophon	Upper Permian	mica	0.398	3		4	deep diagenesis	
CN18	Zovello	siltstone	Val Gardena	Middle Permian	mica + ka	0.376	3		4	deep diagenesis	
CN25	Cercivento	siltstone	Val Gardena	Middle Permian	mica + chl	0.391	3		4	deep diagenesis	
CN31	Ravinis	siltstone	Val Gardena	Middle Permian	mica + chl	0.427	3		4	deep diagenesis	
CN39	St Salinis	siltstone	Val Gardena	Middle Permian	mica + chl	0.391	3		4	deep diagenesis	
CN4	Sella Ciampigotto	siltstone	Val Gardena	Middle Permian	mica + chl	0.31	3		4 or 5	diag./anchizone	
sin55	Passo Cason di Lanza	argillite	Auernig	Up. Carboniferous	mica + chl + ka + pa	0.23	3	> 3	5 or 6	anchi/epizone	
sin58	Sonnenalpe Naßfeld	argillite	Auernig	Up. Carboniferous	mica + chl + ka + pa	0.216	3	> 3	5 or 6	anchi/epizone	
sin59	Naßfeld Pass (Pas. di Pramollo)	sandstone	Auernig	Up. Carboniferous	mica + chl + ka + pa	0.261	3	> 3	5	anchizone	
sin60	Stausee (Naßfeld Pass)	siltstone	Auernig	Up. Carboniferous	mica + chl + ka + pa	0.225	3		5 or 6	anchi/epizone	
CN26	Passo del Cason di Lanza	sandstone	Auernig	Up. Carboniferous	mica + chl + ka	0.442	3		4	deep diagenesis	
sin61	along Rio Bombaso pt. 1400m	siltstone	Bombaso	Up.-Mid. Carbon.	mica + chl + ka + pa	0.258	3		5	anchizone	
CN29	Lago M. Dimon	siltstone	Dimon	Low. Carboniferous	mica + chl	0.31	3		4 or 5	diag./anchizone	
CN33	Zoufplan	siltstone	Dimon	Low. Carboniferous	mica + chl	0.154	3		6	epizone	
sin62	Malvueric Basso	limestone	Hochwipfel	Devonian	mica + chl + ka	0.322	3		4 or 5	diag./anchizone	

Table 1 Zoneography of diagenesis to very low grade metamorphism using organic and mineral indicators

CN14	M. Peralba	marble	Hochwipfel	Devonian	mica + chl + ka	0.147	3		6	epizone	
CN27	M. Zermula	marble	Hochwipfel	Devonian	mica + chl + ka	0.192	3		6	epizone	
CN30	Ramaz	marble	Hochwipfel	Up. Silurian-Devon.	mica + chl + ka	0.221	3		5 or 6	anchi/epizone	
CN42	Meledis Bassa	limestone	Hochwipfel	Up. Silurian-Devon.	mica + chl	0.287	3		5	anchizone	
CN8	Passo di Avanza	schist	Val Visdende	Low. Ordovician ?	mica + chl	0.132	3		6	epizone	
CN10	Passo dei Cacciatori	schist	Val Visdende	Low. Ordovician ?	mica + chl	0.191	3		6	epizone	
CN7	Lorenzago	schist	Phyllites	???	mica + ka	0.144	3		6	epizone	
CN9	Passo Zovo	schist	Phyllites	???	mica + chl	0.154	3		6	epizone	

Table 2 Data used for the subsidence curves

Friuli platform

Lithology	Age (Ma)	Thickness (m)	Water depth (m)	Tectonic subsidence (m)	Total subsidence (m)
Upper Miocene Molasse	5 to 11	1000	50	2783-3200	11450-13300
Middle Miocene Molasse	11 to 16	900-1100	500	2900-3317	10400-12250
Lower Miocene Molasse	16-21	200-300	200	2300-2650	9000-10650
hiatus	21-40				
Eocene Dinaric flysch	40-55	2500-3000	2000	4033-4350	8600-10150
hiatus	55-65				
Pre-flysch or Scaglia	65-80	0-50	500-1000	1700-2350	4100-5050
hiatus	80-90				
Reefal limestones (Cret.)	90-135	950-1150	0	1200-1333	3600-4000
Jurassic limestones	135-200	750-850	0	883-950	2650-2850
Upper Triassic	200-220	1900-2000	0	633-667	1900-2000

Perifriuli domain (Friuli basin)

Lithology	Age (Ma)	Thickness (m)	Water depth (m)	Tectonic subsidence (m)	Total subsidence (m)
Upper Miocene Molasse	5 to 11	1000	50	2467-2783	11750-12650
Middle Miocene Molasse	11 to 16	900-1100	500	2583-2900	10700-11600
Lower Miocene Molasse	16-21	200-300	200	1983-2233	9300-10000
hiatus	21-40				
Eocene Dinaric flysch	40-55	2500-3000	2000	3717-3933	8900-9500
hiatus	55-65				
Maastrichtian flysch	65-72	0-50	1000	1883-1933	4400-4500
hiatus	72-80				
Scaglia (Up. Cretaceous)	80-96	150	500	1383-1417	3350-3450
Lower Cretaceous	96-135	100	200	1033-1067	2700-2800
Jurassic limestones	135-200	500	0	800-833	2400-2500
Upper Triassic	200-220	1900-2000	0	633-667	1900-2000

ANNEXE 1

Vitrinite reflectance values (Ro%)
calculated from Tmax (Rock-Eval 6)

Sample	Location	Formation	Age	TOC (%)	T max (°C)	S2 Intensity mg/g	S2 peak signal	Ro (%)	Degree of maturation
sin5	ex miniera (Val di Gorto)	Raibl	Carnian	0.45	471	392	good	0.8 - 1.0	mature
sin6	Muina	Raibl	Carnian	0.3	526	134	bad	1.4 - 1.7	
sin7	Between Muina and Agrons	Raibl	Carnian	1.01	487	779	good	1.0 - 1.2	mature
sin11	Sent. Corbellini (Clap Grande)	Wengen	Ladinian	0.32	498	101	tolerable	1.1 - 1.3	mature
sin12	Sent. Corbellini (Clap Grande)	Wengen	Ladinian	0.82	497	98	tolerable	1.1 - 1.3	mature
sin23	Muina	Raibl	Carnian	0.32	505	135	tolerable	1.2 - 1.4	mature
sin28	Rifugio M. Siera	Wengen	Ladinian	1.16	508	538	good	1.25 - 1.45	mature
sin35	between Val and Vinaio	Raibl	Carnian	0.32	443	246	good	0.6 - 0.8	mature
sin43	Chiampees (Lovea)	Wengen	Ladinian	0.23	464	162	tolerable	0.75 - 0.95	mature
sin45	Fielis	Raibl	Carnian	0.53	495	114	bad	1.05 - 1.25	
sin51	Caprizzi	Caprizzi	Norian	0.94	454	2241	very good	0.65 - 0.85	mature
sin54	Col Trondo	Livinallongo	Ladinian	1.07	470	2453	very good	0.8 - 1.0	mature
sin55	Passo Cason di Lanza	Auernig 1	U. Carboniferous	0.94	601	109	distorted	> 3	overmature
sin58	Sonnenalpe Naßfeld	Auernig 3	U. Carboniferous	1.68	600	234	distorted	> 3	overmature
sin59	Naßfeld Pass (Passo di Pramollo)	Auernig 3	U. Carboniferous	0.58	604	145	distorted	> 3	overmature
sin63	Forni di Sopra	Raibl	Carnian	0.5	466	291	good	0.75 - 0.95	mature
sin67	Navarons	Flysch	Eocene	0.38	433	640	very good	0.5 - 0.7	mature
CN1	Lago di Sauris (Sud)	Raibl	Carnian	0.68	525	131	bad	1.4 - 1.7	
CN11	Grauzaria	Raibl	Carnian	0.81	405	1577	very good	< 0.5	immature
CN21	T. Degano (Mulina)	Raibl	Carnian	0.48	490	155	tolerable	1.0 - 1.2	mature
sin25	C. se Codem (Raveo)	Raibl	Carnian	0.22	392	493	very good	< 0.4	immature
sin36	between Val and Vinaio	Raibl	Carnian	0.16	449	340	very good	0.65 - 0.85	mature
sin37	Plugna	Raibl	Carnian	0.19	461	283	very good	0.75 - 0.95	mature
sin38	Plan di Sieas (Villa)	Caprizzi	norian	0.25	425	286	very good	0.4 - 0.6	immature
sin40	Casera Zums (Illegio)	Raibl	Carnian	0.15	434	905	very good	0.5 - 0.7	immature
sin42	Chiampees (Lovea)	Raibl	Carnian	0.24	422	354	very good	0.4 - 0.6	immature

ANNEXE 2

Calculation of percentage illite in mixed-layered illite-smectite

References:

MOORE, D.M. & REYNOLDS, R.C. Jr. (1989) "X-ray diffraction and the identification and analysis of clay minerals. Ed: Oxford University Press.

Equation: $\% sm = 4.7198605006 * \Delta^2 - 91.843364241 * \Delta + 449.63133345$

(Rolli 1993, after datas from Reynolds 1989)

Sample N°	Pos IS 002	Pos IS 003	Δ (003-002)	%Sm in IS	%ill. in IS	Reichweite
CN1	9.1870	17.2024	8.0154	17	83	1
CN2	9.1961	17.4165	8.2204	14	86	3
CN3	9.1821	17.3886	8.2065	14	86	
CN3	9.4337	16.9437	7.5100	26	74	1
CN4	9.0927	17.5715	8.4788	10	90	3
CN5	9.3405	17.3357	7.9952	17	83	1
CN6	9.1207	17.5807	8.4600	10	90	
CN6	9.4313	17.2652	7.8339	20	80	1
CN11	9.0632	17.3219	8.2587	13	87	3
CN12	9.1770	17.6055	8.4285	11	89	3
CN15	9.4749	16.0225	6.5476	51	49	0
CN16	9.1442	17.5181	8.3739	12	88	3
CN17	10.2968	16.1172	5.8204	75	25	1
CN19	9.0763	17.5192	8.4429	11	89	3
CN20	9.2816	17.5488	8.2672	13	87	3
CN22	9.2256	17.6294	8.4038	11	89	3
CN23	10.5453	15.8751	5.3298	94	6	0
CN24	9.1346	17.2571	8.1225	15	85	1
CN25	9.2396	17.6984	8.4588	10	90	3
CN26	9.1823	17.6865	8.5042	10	90	3
CN28	9.1397	17.5336	8.3939	11	89	3
CN31	9.2056	17.6935	8.4879	10	90	3
CN34	9.6148	16.0023	6.3875	56	44	0
CN35	9.7405	16.8136	7.0731	36	64	1
CN36	9.2328	17.3124	8.0796	16	84	1
CN37	9.2463	17.6479	8.4016	11	89	3
CN39	9.1703	17.7287	8.5584	9	91	3
CN40	9.9644	15.8381	5.8737	73	27	0
CN41	9.1070	17.0484	7.9414	18	82	1
CN43	9.1175	17.3718	8.2543	13	87	3
CN44	9.2088	17.5169	8.3081	12	88	3
CN45	9.3145	17.2455	7.9310	18	82	1
CN46	9.2927	17.5087	8.2160	14	86	3
CN47	9.0665	17.5908	8.5243	10	90	3
CN49	9.2211	17.7579	8.5368	10	90	3
CN50	9.2581	17.6977	8.4396	11	89	3
CN51	9.2456	17.1374	7.8918	19	81	1
CN51	8.9466	17.4075	8.4609	10	90	
CN52	9.1697	17.6313	8.4616	10	90	3
CN54	9.2029	17.2838	8.0809	16	84	
CN54	9.4758	16.7621	7.2863	31	69	1
sin5	9.2665	17.6534	8.3869	11	89	
sin5	9.4944	17.0713	7.5769	25	75	1
sin6	9.2210	17.5192	8.2982	13	87	
sin6	9.5088	17.0041	7.4953	26	74	1
sin7				30	70	1
sin8				30	70	1
sin11	9.2627	17.5731	8.3104	12	88	3
sin12				30	70	1

sin23					30	70	1
sin24		9.3184	17.4071	8.0887	16	84	
sin24		9.6045	16.8708	7.2663	31	69	1
sin25					30	70	1
sin26		9.1037	16.6554	7.5517	25	75	1
sin27					30	70	1
sin34					30	70	1
sin35					30	70	1
sin37					>40		0
sin38		9.1302	17.3388	8.2086	14	86	3
sin40		9.3481	17.3153	7.9672	17	83	
sin40		9.7353	16.7680	7.0327	37	63	1
sin43		9.2876	17.2088	7.9212	18	82	1
sin45		9.0513	17.4566	8.4053	11	89	
sin45		9.3561	17.1810	7.8249	20	80	1
sin46		9.1383	17.7784	8.6401	8	92	3
sin47		9.1968	17.8174	8.6206	9	91	3
sin51		9.1436	17.4747	8.3311	12	88	3
sin62		9.2138	17.5543	8.3405	12	88	3
sin63		9.2476	17.2983	8.0507	16	84	1
sin64		9.1942	17.7919	8.5977	9	91	3
sin66		10.3141	15.5780	5.2639	97	3	0
sin67		9.5496	16.0954	6.5458	51	49	0

ANNEXE 3 Illite crystallinity (IC) values

Sample	Location	Formation	Age	I (CPS)	SW° 2JCuKa
sin5 2n	ex Miniera (Val di Gorto)	Raibl	Carnian	270	0.818
sin5 2g				117	failed
sin6 2n	Muina	Raibl	Carnian	227	0.95
sin6 2g				270	0.391
sin7 2n	between Muina and Agrons	Raibl	Carnian	150	0.662
sin7 2g				failed	failed
sin8 2n	Agrons	Raibl	Carnian	168	0.644
sin8 2g				178	0.652
sin11 2n	Sentiero Corbellini (Clap Grande)	Wengen	Ladinian	438	0.491
sin11 2g				354	0.52
sin12 2n	Sentiero Corbellini (Clap Grande)	Wengen	Ladinian	618	0.736
sin12 2g				313	0.759
sin23 2n	Muina	Raibl	Carnian	358	0.958
sin23 2g				263	1.002
sin24 2n	Muina	Raibl	Carnian	417	0.892
sin24 2g				190	0.782
sin25 2n	C. se Codem (Raveo)	Raibl	Carnian	615	0.8
sin25 2g				532	0.855
sin26 2n	St. O Cervias (Raveo)	Raibl	Carnian	248	0.69
sin26 2g				246	0.631
sin27 2n	Rifugio M. Siera	Wengen	Ladinian	99	failed
sin27 2g				88	failed
sin28 2n	Rifugio M. Siera	Wengen	Ladinian	258	0.781
sin28 2g				failed	failed
sin30 2n	Pierabech	Bellerophon	upper Permian	1459	0.286
sin30 2g				1819	0.253
sin34 2n	Trichiamps	Raibl	Carnian	145	failed
sin34 2g				failed	failed
sin35 2g	between Val and Vinaio	Raibl	Carnian	206	0.965
sin35 2g				111	failed
sin36 2n	between Val and Vinaio	Raibl	Carnian	85	failed
sin36 2g				70	failed
sin37 2n	Plugna	Raibl	Carnian	253	0.956
sin37 2g				135	failed
sin38 2n	Plan di Sieas (Villa)	Caprizzi	Norian	143	0.534
sin38 2g				176	0.451
sin40 2n	Casera Zums (Illegio)	Raibl	Carnian	314	1.526

sin40 2g				186	failed
sin42 2n	Chiampees (Lovea)	Raibl	Carnian	117	0.525
sin42 2g				failed	failed
sin43 2n	Chiampees (Lovea)	Wengen	Ladinian	223	1.241
sin43 2g				failed	failed
sin45 2n	Fielis	Raibl	Carnian	1260	0.883
sin45 2g				618	1.057
sin46 2n	M. Zoncolan (Pian di Val)	Werfen	Scythian	1302	0.184
sin46 2g				1275	0.175
sin 47 2n	M. Zoncolan (Scaletona)	Werfen	Scythian	714	0.212
sin 47 2g				628	0.184
sin51 2n	Caprizzi	Caprizzi	Norian	154	0.827
sin51 2g				120	0.506
sin55 2n	Passo Cason di Lanza	Auernig	Up. Carboniferous	228	0.23
sin55 2g				210	0.202
sin58 2n	Sonnenalpe Naßfeld	Auernig	Up. Carboniferous	538	0.216
sin58 2g				461	0.198
sin59 2n	Naßfeld Pass (Passo di Pramollo)	Auernig	Up. Carboniferous	428	0.261
sin59 2g				368	0.248
sin60 2n	Stausee (Naßfeld Pass)	Auernig	Up. Carboniferous	487	0.225
sin60 2g				440	0.235
sin61 2n	along Rio Bombaso pt. 1400m	Bombaso	Up. Carboniferous	317	0.258
sin61 2g				279	0.235
sin62 2n	Malvueric Basso		Devonian	477	0.322
sin62 2g				380	0.322
sin63 2n	Forni di Sopra	Raibl	Carnian	411	1.048
sin63 2g				263	1.132
sin64 2n	Pontebba	Werfen	Scythian	1200	0.322
sin64 2g				1077	0.23
sin66 2n	Madonna del Vergon (Priuso)	Caprizzi	Norian	173	0.708
sin66 2g				142	0.469
sin67 2n	Navarons	Flysch	Eocene	1028	0.497
sin67 2g				932	0.459
CN1 2n	Lago di Sauris	Raibl	Carnian	1610	0.95
CN1 2g				953	0.633
CN2 2n	Lateis	Bellerophon	upper Permian	2097	0.398
CN2 2g				2388	0.316
CN3 2n	Col Sarenede	Raibl	Carnian	282	0.906

CN3 2g				205	0.619
CN4 2n	Sella Ciampigotto	Val Gardena	middle Permian	1555	0.31
CN4 2g				1387	0.287
CN5 2n	Passo Oberenghe	Raibl	Carnian	541	0.678
CN5 2g				408	0.633
CN6 2n	Voltois	Raibl	Carnian	497	0.59
CN6 2g				380	0.573
CN7 2g	Lorenzago	Val Visdende	Ordovician	8646	0.144
CN7 2g				8205	0.124
CN8 2n	Passo di Avanza	Val Visdende	Ordovician	3079	0.132
CN8 2g				2984	0.132
CN9 2n	Passo Zovo	Val Visdende	Ordovician	4286	0.154
CN9 2g				4920	0.125
CN10 2n	Passo dei Cacciatori	Val Visdende	Ordovician	3111	0.191
CN10 2g				2906	0.169
CN11 2n	Grauzaria	Raibl	Carnian	496	0.905
CN11 2g				227	0.802
CN14 2n	M. Peralba	Hochwipfel	Devonian	5198	0.147
CN14 2g				5196	0.133
CN15 2n	Stli Pra da Forca	Flysch	Oligocene	1020	0.95
CN15 2g				670	0.641
CN16 2n	Ledrania		Tithonian	867	0.361
CN16 2g				654	0.257
CN17 2n	Braulins		Campanian	729	0.523
CN17 2g				622	0.316
CN18 2n	Zovello	Val Gardena	middle Permian	1452	0.376
CN18 2g				absent	
CN19 2n	Valle del Torre	Scaglia	upper Cretaceous	439	0.523
CN19 2g				286	0.368
CN20 2n	M. Palis	Werfen	Scythian	1004	0.39
CN20 2g				785	0.31
CN21 2n	T. Degano/ Mulina	Raibl	Carnian	647	1.062
CN21 2g				311	0.788
CN22 2n	Galizzis	Wengen	Ladinian	1774	0.552
CN22 2g				1415	0.428
CN23 2n	M. San Simeone	Scaglia rossa	Turon.-Coniacian	450	0.206
CN23 2g				443	0.162
CN24 2n	Chiampees	Raibl	Carnian	700	0.825
CN24 2g				372	0.92

CN25 2n	Cercivento	Val Gardena	middle Permian	2101	0.391
CN25 2g				1932	0.369
CN26 2n	Passo del Cason di Lanza	Auernig	Up. Carboniferous	465	0.442
CN26 2g				383	0.427
CN27 2n	M. Zermula	Hochwipfel	Devonian	1929	0.192
CN27 2g				1701	0.184
CN28 2n	M. Tamai	Werfen	Scythian	1013	0.272
CN28 2g				903	0.221
CN29 2n	Lago M. Dimon	Dimon	low. Carboniferous	2444	0.31
CN29 2g				2213	0.294
CN30 2n	Ramaz	Hochwipfel	upper Silurian-	2575	0.221
CN30 2g			lower Devonian	2354	0.206
CN31 2n	Ravinis	Val Gardena	middle Permian	1475	0.427
CN31 2g				1245	0.397
CN33 2n	Zoufplan	Dimon	low.Carboniferous	2064	0.154
CN33 2g				2094	0.133
CN34 2n	Malga Confin	Scaglia rossa	Maastrichtian	855	0.973
CN34 2g				652	0.545
CN35 2n	Ospedalleto	Soccher	Lower Cretaceous	463	1.061
CN35 2g				365	0.663
CN36 2n	M. Cumelli		Kimmeridgian	653	0.936
CN36 2g			lower Tithonian	488	0.317
CN37 2n	Avasinis	Soccher	lower Cretaceous	606	0.404
CN37 2g				505	0.317
CN39 2n	St Salinis	Val Gardena	middle Permian	501	0.391
CN39 2g				433	0.346
CN40 2n	M. San Simeone	Scaglia rossa	Cenomanian	413	0.235
CN40 2g				393	0.155
CN41 2n	M. San Simeone W	Vajont	middle Jurassic	904	0.642
CN41 2g				583	0.574
CN42 2n	Meledis Bassa	Hochwipfel	upper Silurian-	550	0.287
CN42 2g			lower Devonian	700	0.288
CN43 2n	Cercenaz (Avasinis)	Soccher	lower Cretaceous	631	0.332
CN43 2g				509	0.214
CN44 2n	Casera Nische	Ammonitico ros.	upper Jurassic	461	0.428
CN44 2g				390	0.294
CN45 2n	Valle di Uccea	Scaglia rossa	Maastrichtian	1052	0.862
CN45 2g				925	0.67

CN46 2n	Valle di Uccea		Jurassic	534	0.737
CN46 2g				414	0.31
CN47 2n	Valle di Uccea		up. Triassic	749	0.391
CN47 2g				656	0.228
CN48 2n	Fielis	Raibl	Carnian	161	1.106
CN48 2g				136	failed
CN49 2n	Cuel di Forchia	Dolomia Princip.	Norian	752	0.368
CN49 2g				648	0.317
CN50 2n	Fielis	Schlern	upper Ladinian	357	0.266
CN50 2g				283	0.295
CN51 2n	Nimbriu (Alesso)	Dolomia Princip.	Norian	131	0.258
CN51 2g				112	0.243
CN52 2n	Stli Gnivizza	Soccher	upper Jurassic	638	0.685
CN52 2g				586	0.633
CN54 2n	Stli Gnivizza	Soccher	upper Jurassic	171	0.257
CN54 2g				144	0.183